

Glial dysfunction in the pathology of temporal lobe epilepsy

Dissertation

zur

Erlangung des Doktorgrades (Dr. rer. nat.)

der

Mathematisch-Naturwissenschaftlichen Fakultät

der

Rheinischen Friedrich-Wilhelms-Universität Bonn

vorgelegt von

Lukas Paul Henning

aus

Wuppertal, Deutschland

Bonn, 2022

Angefertigt mit Genehmigung der Mathematisch-Naturwissenschaftlichen Fakultät der
Rheinischen Friedrich-Wilhelms-Universität Bonn

- 1. Gutachter:** **Prof. Dr. Christian Steinhäuser**
Institut für Zelluläre Neurowissenschaften
- 2. Gutachterin:** **Prof. Dr. Christa E. Müller**
Pharmazeutisches Institut

Tag der Promotion: 17.04.2023

Erscheinungsjahr: 2023

This dissertation is based on the following published articles:

Henning, L., Antony, H., Breuer, A., Müller, J., Seifert, G., Audinat, E., Singh, P., Brosseron, F., Heneka, M. T., Steinhäuser, C., & Bedner, P. (2022). Reactive microglia are the major source of tumor necrosis factor alpha and contribute to astrocyte dysfunction and acute seizures in experimental temporal lobe epilepsy. *Glia*. Advance online publication. <https://doi.org/10.1002/glia.24265>

Henning, L., Steinhäuser, C., & Bedner, P. (2021). Initiation of Experimental Temporal Lobe Epilepsy by Early Astrocyte Uncoupling Is Independent of TGF β R1/ALK5 Signaling. *Frontiers in Neurology*, 12, 660591. <https://doi.org/10.3389/fneur.2021.660591>

Deshpande, T., Li, T., **Henning, L.**, Wu, Z., Müller, J., Seifert, G., Steinhäuser, C., Bedner, P. (2020). Constitutive deletion of astrocytic connexins aggravates kainate-induced epilepsy. *Glia*. <https://doi.org/10.1002/glia.23832>

Acknowledgments

First of all, I would like to thank Prof. Dr. Christian Steinhäuser for providing me with the opportunity to work on these interesting projects over the last five years. Without his supervision and support, this work would not have been possible.

I am grateful to Prof. Dr. Christa Müller, Prof. Dr. Frank Kirchhoff, Prof. Dr. Evi Kostenis and Prof. Dr. Karl Schilling for accepting my request to be part of the examination committee and for their time and efforts in reviewing my doctoral thesis.

In particular, I would like to thank Dr. Peter Bedner for his excellent support and outstanding mentoring during my time here at the IZN. Together we have spent countless hours performing animal surgeries, having scientific discussions, harvesting cells, writing papers and supervising students. It's always been fun! Not forgotten will be the similar number of Schnitzel every Wednesday at 11.30 a.m. sharp!

I would like to thank PD Dr. Seifert for performing all the semi quantitative RT-PCRs, supervision of students involved in my project, as well as the genotyping and breeding of the different mouse lines used in this doctoral thesis and in other projects. Moreover, I would also like to thank PD Dr. Ronald Jabs for his valuable methodological and technical support regarding all kinds of questions and problems, especially in the fields of electrophysiology, microscopy and statistics.

Special thanks go to Dr. Julia Müller, who introduced me to the various techniques required to complete this project. Without her and Dr. Tushar Deshpande's previous work on the epilepsy project, this PhD thesis would not have been possible. Similarly, I want to thank Thomas Erdmann and Dr. Silke Künzel for their technical and administrative support.

Of course, I would like to thank all colleagues and former PhD students of the IZN for the pleasant working atmosphere and great time together: Alberto, Aline, Björn, Camille, Catia, Daniel, Dario, Dmitry, Jessica, Kamjab, Kirsten, Linda, Nehal, Oussama, Paula, Petr, Stefan H., Stefan P. and Zhou. Further I would like to thank Prof. Dr. Christian Henneberger for fruitful scientific collaboration and many interesting discussions during our weekly lab seminars.

My deepest appreciation goes to my family and friends, especially my parents, for their unconditional support and understanding and the fact that they made it possible for me to pursue a university education. Finally, I want to thank my wife, Almuth, for her love, patience and understanding and a beautiful time together here in Bonn.

Table of contents

List of abbreviations	iii
1. Introduction	1
1.1 Epilepsy	1
1.1.1 MTLE-HS.....	2
1.1.2 The role of inflammation and tumor necrosis factor alpha in epilepsy	4
1.2 Astrocytes	7
1.2.1 Physiology of astrocytes.....	9
1.2.2 Astroglial networks and gap junctions	10
1.2.3 Reactive astrocytes and epilepsy	13
1.3 Microglia	15
1.3.1 Physiology of microglia	16
1.3.2 Microglia in epilepsy.....	17
1.4 The blood-brain barrier.....	19
1.4.1 Structural and functional properties of the BBB	20
1.4.2 BBB dysfunction in epilepsy.....	21
2. Aims of this thesis	24
3. Reactive microglia are the major source of tumor necrosis factor alpha and contribute to astrocyte dysfunction and acute seizures in experimental temporal lobe epilepsy	26
3.1 Summary of the publication	26
3.2 Statement of contribution	28
3.3 Publication.....	29
4. Initiation of experimental temporal lobe epilepsy by early astrocyte uncoupling is independent of TGFβR1/ALK5 signaling	54
4.1 Summary of the publication	54
4.2 Statement of contribution	56
4.3 Publication.....	56
5. Constitutive deletion of astrocytic connexins aggravates kainate-induced epilepsy	70
5.1 Summary of the publication	70
5.2 Statement of contribution	72
5.3 Publication.....	72
6. Discussion	87

7. Conclusions	92
8. Perspective	93
Summary of the thesis.....	95
References	96
List of figures	136

List of abbreviations

[K ⁺] _o	extracellular K ⁺ concentration
A ₁ R	adenosine ₁ -receptor
ADK	adenosine-kinase
AED	antiepileptic drugs
ALK	activin-like kinase
AMPA	α-amino-3-hydroxy-5-methyl-4-isoxazolepropionic acid
AQP4	aquaporin-4
ATP	adenosine triphosphate
BBB	blood-brain barrier
BDNF	brain-derived neurotrophic factor
CA	cornu ammonis
cAMP	cyclic adenosine monophosphate
CNS	central nervous system
COOH	cytosolic C-terminus
CSF1R	colony-stimulating factor 1 receptor
Cx	connexin
DKO	double knock-out mice lacking the astroglial gap junction-forming proteins Cx30 and C43
E _K	K ⁺ equilibrium potential
EAAT	excitatory amino acid transporter
EC	endothelial cell
EEG	electroencephalography

eGFP	enhanced green fluorescent protein
ELISA	enzyme-linked immunosorbent assay
EMP	erythro-myeloid progenitor
GCD	granule cell dispersion
GFAP	glial fibrillary acidic protein
GJ	gap junction
GJC	gap junction channel
GS	glutamine synthetase
HC	hemichannel
HS	hippocampal sclerosis
IL	interleukin
ILAE	international league against epilepsy
IP3	inositol triphosphate
KA	kainic acid
Kir	inwardly rectifying K ⁺ channel
LTP	long-term potentiation
MTLE-HS	mesial temporal lobe epilepsy with hippocampal sclerosis
NCX	Na ⁺ /Ca ²⁺ exchanger
NF- κB	nuclear factor-κB
NKA	Na ⁺ /K ⁺ -ATPases
NKCC1	N ⁺ /K ⁺ /Cl ⁻ co-transporter
NMDA	N-methyl-D-aspartate receptor
NVU	neurovascular unit

PTZ	pentylenetetrazole
qPCR	quantitative polymerase chain reaction
SE	status epilepticus
SGS	spontaneously generalized seizure
solTNF	soluble tumor necrosis factor
TACE	TNF α converting enzyme
TBI	traumatic brain injury
TGF β	transforming growth factor β
TJ	tight junction
TLE	temporal lobe epilepsy
TMEV	Theiler's murine encephalomyelitis virus
tmTNF	transmembrane tumor necrosis factor
TNF α	tumor necrosis factor α
TNFR1 (p55TNFR)	tumor necrosis factor receptor 1
TNFR2 (p75TNFR)	tumor necrosis factor receptor 2
TRADD	tumor necrosis factor receptor 1-associated intracellular death domain
V _m	membrane potential
WT	wild-type

1. Introduction

Epilepsy is a disorder of the central nervous system (CNS) characterized by the occurrence of unprovoked recurrent seizures (Fisher et al., 2014). More than 1 % of the world population suffer from epilepsy but despite intense research into the underlying mechanisms, still about one third of patients remains refractory to pharmacological treatment (Löscher et al., 2013; Patel et al., 2019). Most of the currently available antiepileptic drugs (AEDs) act as seizure suppressors but fail to modulate the underlying process of epileptogenesis (the process by which a previously healthy brain develops into an epileptic one) (Löscher et al., 2013). The development of most AEDs has been based on a neurocentric approach, which assumes that ‘epileptic neurons’ (Janigro & Walker, 2014, p.254) are at the center of an imbalance between excitatory and inhibitory neurotransmission causing epilepsy (Janigro & Walker, 2014; Patel et al., 2019). However, the fact that the therapeutic efficacy of AEDs has not improved during the last decades (Perucca et al., 2020) indicates the need for novel strategies in anti-epileptic drug development (Löscher et al., 2013). Research over the last decades demonstrates that glial cells are crucial for CNS functioning, both indirectly supporting and actively modulating neuronal information processing (Santello et al., 2019; Sierra et al., 2019). Due to their ability to become rapidly reactive in response to injury, astrocytes and microglia are increasingly being recognized as key players in neurological diseases and disorders, including epilepsy (Devinsky et al., 2013; Eyo et al., 2017; Heneka et al., 2014). Moreover, a plethora of research indicates that neuroinflammatory processes could play a major role in epileptogenesis (Aronica et al., 2017; Vezzani et al., 2011). The purpose of this work was to uncover the contribution of astrocyte dysfunction and microglia-mediated immunity to epileptogenesis in mesial temporal lobe epilepsy with hippocampal sclerosis (MTLE-HS). More specifically, this PhD thesis includes three publications that cover different aspects of glial and neuroinflammatory mechanisms and their contribution to the pathogenesis of epilepsy.

The following section provides an introduction into various aspects relevant to the understanding of this work.

1.1 Epilepsy

According to the current report of the International League Against Epilepsy (ILAE) classification of the epilepsies is based on three levels, including seizure type (focal vs. generalized vs. unknown), epilepsy type (focal vs. generalized vs. combined generalized & focal vs. unknown) and epilepsy syndrome (a group of traits or symptoms that correlate and

occur together including, for example, the type of seizure and its triggers, electroencephalography (EEG) patterns as well as structural abnormalities) (Scheffer et al., 2017). In addition, the classification of epilepsy should incorporate the identification of its etiology (idiopathic vs. structural/metabolic/genetic/infectious or immune). In focal epilepsy, seizures originate from a specific region in one hemisphere of the brain (Kanner & Bicchi, 2022). Temporal lobe epilepsy (TLE) is the most common form of focal epilepsy (Tatum, 2012). Although the etiology of TLE is often unknown, in about 40% of cases it can be linked to a precipitating injury such as febrile seizures, head trauma, infection, brain tumors or *status epilepticus* (SE) (Löscher & Brandt, 2010). These preceding brain lesions are followed by a 'latent period' that varies in length from weeks to years before the first spontaneous recurrent seizures start to emerge (Becker, 2018). The most common types of seizures in TLE are focal awareness seizures (localized seizure onset in a specific area of the brain with no loss of consciousness; formerly known as simple partial) and focal impaired awareness seizures (localized seizure onset but propagation to other cortical and subcortical areas with loss of consciousness and the potential to progress into focal to bilateral tonic-clonic seizures; previously called complex partial) (Kanner & Bicchi, 2022; Tatum, 2012). In the majority of TLE cases, seizures originate in the hippocampus, in which case it is hence classified as mesial temporal lobe epilepsy (MTLE) (Tatum, 2012). Approximately 56 % of MTLE patients are characterized by a condition known as hippocampal sclerosis (HS), which refers to a number of structural abnormalities including hippocampal atrophy and astrogliosis (section 1.2.3) (Thom, 2014).

1.1.1 MTLE-HS

The ILAE developed a classification scheme, which distinguishes three types of HS: ILAE HS type I ('classical HS'; about 60-80% of all MTLE cases): extensive neuronal cell loss and astrogliosis in *cornu ammonis* (CA) 1, CA4 and CA3, but not CA2; ILAE HS type II (atypical, 5-10% of cases): neuronal cell loss and astrogliosis predominantly in the CA1 subfield; ILAE type III (atypical, 3-7.4% of cases): neuronal cell loss and astrogliosis primarily in the CA4 subfield (Blümcke et al., 2013; Thom, 2014). Although the current classification scheme relies exclusively on neuronal loss and astrogliosis to classify HS, the pathology includes other frequently observed alterations such as granule cell dispersion (GCD), mossy fibre sprouting and interneuron loss (Thom, 2014). For example, GCD, which refers to a pathological widening of the granule cell layer either due to ectopic migration of dentate granule cells or aberrant seizure-induced neurogenesis, can be found in about 50% of ILAE HS Type I cases (Liu et al., 2020). Various AEDs with differing modes of action are available for the treatment of MTLE-

HS, with levetiracetam, lamotrigine and carbamazepine being among the group of the most widely prescribed AEDs (Androsova et al., 2017). However, AED resistance is common in MTLE-HS and surgical removal of the seizure onset zone is sometimes the only way to achieve seizure freedom in patients (Androsova et al., 2017).

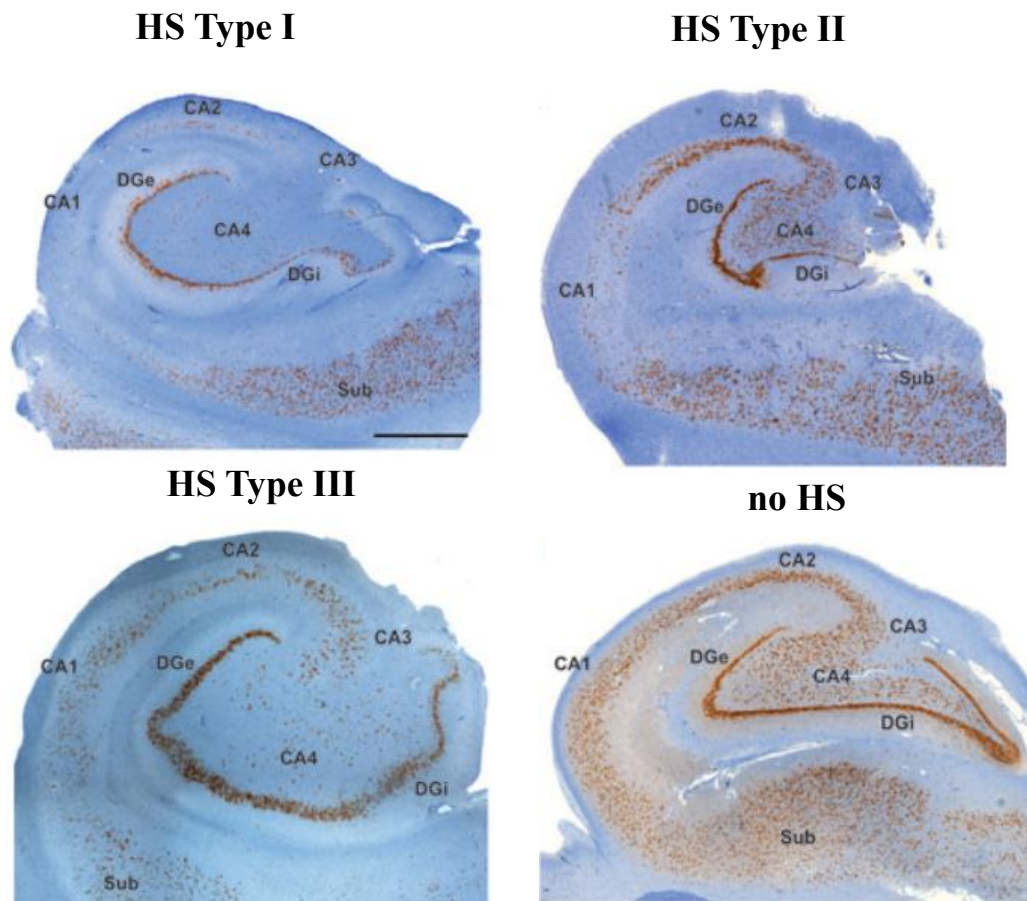


Figure 1. Different subtypes of MTLE-HS according to the ILAE consensus classification. Images depict a combined NeuN and hematoxylin staining in surgically resected human hippocampi of MTLE-HS patients. *Upper left:* HS Type I is characterized by extensive neuronal cell loss particularly in CA1 and 4 but less pronounced so in CA2 and 3. *Upper right:* In HS Type II cell loss occurs primarily in CA1 whereas in HS Type III (*lower left*) cell loss is restricted to CA4. Both HS Type II and III represent atypical cases of HS. All HS types are characterized by astrogliosis in the affected subfields. *Lower right:* Control tissue without HS. Scale bar = 1mm. Used with permission of John Wiley & Sons, Inc., from International consensus classification of hippocampal sclerosis in temporal lobe epilepsy: A Task Force report from the ILAE Commission on Diagnostic Methods, Blümcke et al., 54(7) ©2013; permission conveyed through Copyright Clearance Center, Inc.

Epileptogenesis refers to “the development and extension of tissue capable of generating spontaneous seizures, resulting in a) development of an epileptic condition and/or b) progression of the epilepsy after it is established” (Pitkänen & Engel, 2014, p. 233). However, studying the mechanisms of epileptogenesis in human MTLE-HS specimens is difficult, as most biopsies are obtained from patients at late stages of the disorder and the availability of non-

epileptic control tissue is low, rendering interpretation of the data difficult (Becker, 2018). Therefore, an understanding of the mechanisms of epileptogenesis in MTLE-HS critically relies on experimental models that mimic key aspects of the condition. Several animal models of MTLE-HS have been developed based on different types of epilepsy-induction, including models of chemoconvulsant-induced SE, traumatic brain injury (TBI), electrical kindling, or CNS infection (Becker, 2018). The administration of kainic acid (KA) either systemically or into different brain regions is one of the most commonly used models of MTLE (Rusina et al., 2021). KA is an analog of glutamate, which binds to ionotropic KA (as well as to α -amino-3-hydroxy-5-methyl-4-isoxazolepropionic acid (AMPA)) receptors expressed throughout the CNS, but which are particularly abundant in the hippocampus (Ben-Ari & Cossart, 2000; Rusina et al., 2021). The administration of KA leads to the development of SE, which is followed by a seizure-free latent period of variable length and the emergence of spontaneous generalized seizures (SGS) (Rusina et al., 2021). Previously, we have introduced the *intracortical* (sometimes also referred to as *supprahippocampal* (Rusina et al., 2021)) KA-injection model (Bedner et al., 2015). In this model, KA is unilaterally injected into the cortical area just above the right dorsal hippocampus using a blunt injection cannula (Bedner et al., 2015; Rusina et al., 2021). Compared to the *intrahippocampal* KA model (Bouilleret et al., 1999), *intracortical* KA injection provides the advantage that it prevents mechanical damage to the hippocampus. Importantly, the *intracortical* KA model reliably induces SE and reproduces key features of MTLE-HS, including the development of SGS, loss of CA1 pyramidal neurons, GCD and astrogliosis (Bedner et al., 2015; Jefferys et al., 2016; Pitsch et al., 2019). In addition, a recent transcriptomic analysis revealed substantial overlap between genes that are differentially regulated in KA-induced and human pharmaco-resistant TLE, indicating successful replication of key molecular alterations in human TLE by KA injection (Conte et al., 2020).

1.1.2 The role of inflammation and tumor necrosis factor alpha in epilepsy

Despite intense research the precise mechanisms of epileptogenesis that culminate in the development of TLE remain largely unknown (Galanopoulou et al., 2021; Vezzani et al., 2011). Importantly, however, mounting clinical and experimental evidence suggests that neuroinflammatory processes causally contribute to the genesis of epilepsy (Aronica et al., 2017; Devinsky et al., 2013; Löscher et al., 2020; Rana & Musto, 2018). For example, it has long been recognized that focal febrile seizures during early childhood carry an increased risk of developing TLE later in life (Dubé et al., 2007; French et al., 1993). Moreover, several studies provide evidence for immune activation, including increased cytokine production and

complement activation, in human MTLE-HS (Aronica et al., 2007; Aulická et al., 2022; Crespel et al., 2002; Gershen et al., 2015; van Gassen et al., 2008). For example, pro-inflammatory cytokines are upregulated in human MTLE-HS specimens with a history of a recent seizure, and induction of epileptiform activity in human MTLE-HS tissue leads to upregulation of several of these cytokines (Morin-Brureau et al., 2018). Moreover, seizure frequency correlates with the expression of several inflammatory markers in patients with pharmaco-resistant MTLE (Pernhorst et al., 2013). Similarly, increased cytokine production and immune cell activation has been demonstrated in experimental models of TLE (Aronica et al., 2017; Avignone et al., 2008; Benson et al., 2015; Broekaart et al., 2018; Sano et al., 2021; Vezzani et al., 2002). Pro-inflammatory cytokines represent a promising target for the treatment of epilepsy as they do not only orchestrate inflammation but also directly influence neuronal excitability and modulate seizures (Prinz et al., 2019; Vezzani et al., 1999, 2011). Of particular interest for the study of epilepsy is the cytokine tumor necrosis factor alpha (TNF α), as it exerts various neuromodulatory functions in the CNS (McCoy & Tansey, 2008; Santello & Volterra, 2012). TNF α is a pleiotropic cytokine that exists as a transmembrane bound (tmTNF) and a soluble form (solTNF), both of which are biologically active and signal *via* two different receptors, TNF receptor 1 (TNFR1 or p55TNFR) and TNFR2 (p75TNFR) (Brenner et al., 2015; McCoy & Tansey, 2008; Santello & Volterra, 2012) (Figure 2). Cleavage of tmTNF by the enzyme matrix metalloprotease TNF alpha converting enzyme (TACE or ADAM17) generates the 51 kDa homotrimer solTNF (Santello & Volterra, 2012). Although solTNF and tmTNF can bind to both TNFR1 and TNFR2, solTNF preferentially signals *via* TNFR1, while tmTNF exerts its biological effects primarily through binding to TNFR2 (Brambilla et al., 2011; McCoy & Tansey, 2008). TNFR1 is expressed on most cell types of the CNS, while TNFR2 expression is restricted to microglia and endothelial cells (Santello & Volterra, 2012). The latter is controversial, however, as TNFR2 expression has also been documented in hippocampal neurons (Balosso et al., 2005). TNFR1 contains an intracellular death domain (TRADD) which promotes the formation of a signaling complex that activates nuclear factor- κ B (NF- κ B)-dependent transcription, which in turn stimulates pro-survival signaling, proliferation and inflammation (McCoy & Tansey, 2008; Santello & Volterra, 2012). Alternatively, TNFR1 activation can trigger a cascade leading to apoptosis (Brenner et al., 2015; Faustman & Davis, 2010). TNFR2 signaling similarly relies on NF- κ B-mediated transcription but lacks a cytosolic death domain, which is why it is primarily associated with pro-survival and pro-inflammatory effects (Faustman & Davis, 2010; McCoy & Tansey, 2008; Santello & Volterra, 2012). However, it should be noted that TNF signaling is complex and depends to a great degree on

the context in which signaling occurs (Faustman & Davis, 2010). Moreover, anticipating the outcome of TNF-signaling is challenging, as considerable crosstalk between TNFR1 and TNFR2 pathways has been documented (Brenner et al., 2015; McCoy & Tansey, 2008).

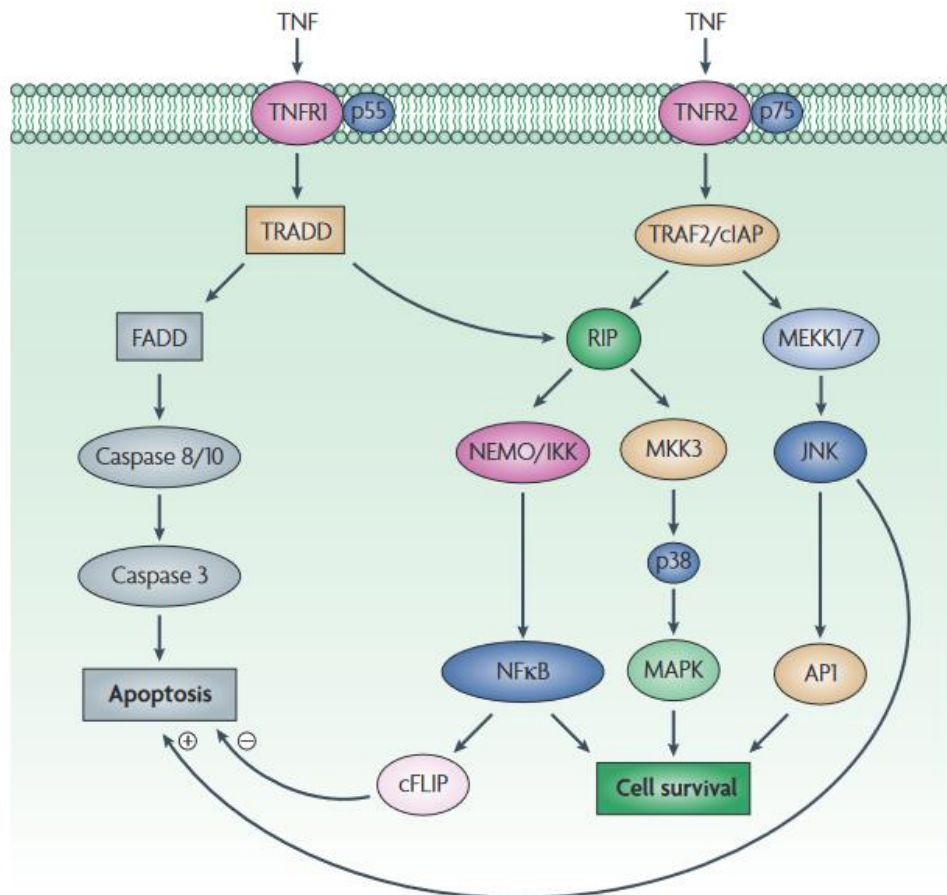


Figure 2. Overview of TNFR1 (p55) and TNFR2 (p75) signaling pathways. TNFR1 activation can induce different downstream signaling pathways depending on the context in which signaling occurs. Generally, binding of TNF α to TNFR1 activates TRADD. TRADD in turn interacts with various downstream adaptor proteins such as RIPK1, which leads to activation of NF- κ B-dependent transcription to promote cell survival and inflammation. Alternatively, TRADD can recruit FADD to induce apoptosis. In contrast, TNFR2 lacks a cytosolic death domain but instead activates the adaptor protein TRAF1/2, which induces several downstream signaling cascades including NF- κ B to initiate pro-survival effects. Arrows indicate possible interactions between TNFR1 and 2 signaling. Please note that the TNF signaling pathways depicted here refer to signaling in T cells. API: activator protein 1; cFLIP: cellular FLICE-like inhibitory protein; cIAP: cellular inhibitor of apoptosis protein; FADD: Fas-associated death domain; IKK: inhibitor of κ B kinase; JNK: Jun N-terminal kinase; MAPK: mitogen-activated protein kinase; MEKK: mitogen-activated protein kinase kinase kinase; MKK3: dual specificity mitogen-activated protein kinase kinase 3; NEMO: nuclear factor- κ B (NF- κ B) essential modulator; RIP: receptor interacting protein (also known as RIPK1); TRADD: TNFR1-associated death domain; TRAF: TNF receptor-associated factor. Reprinted by permission from Springer Nature, Nature Reviews Drug Discovery, TNF receptor 2 pathway: drug target for autoimmune diseases, Denise Faustman et al, ©2010.

Several studies report elevated TNF α transcript and protein levels in both human and experimental MTLN-HS (Benson et al., 2015; Conte et al., 2020; De Simoni et al., 2000; Lachos

et al., 2011; Lehtimäki et al., 2003; Minami et al., 1991; Nikolic et al., 2018; Sano et al., 2021; Vezzani et al., 2002). For example, previous data from our lab demonstrates elevated ipsilateral hippocampal TNF α concentrations in mice 4 and 24 h post *intracortical* KA injection (Müller, 2018). Moreover, evidence for increased TNFR1 signaling has been found in hippocampal tissue from human MTLE (Yamamoto et al., 2006). Importantly, TNF α signaling has been implicated in the development and progression of epilepsy (Balosso et al., 2005; Kirkman et al., 2010; Kramer et al., 2012; Patel et al., 2017; Probert et al., 1995; Rana & Musto, 2018; Weinberg et al., 2013). For example, TNF α knock-out has been shown to attenuate Theiler's murine encephalomyelitis virus (TMEV)-induced acute seizures (Patel et al., 2017). Interestingly, in the same study knock-out of TNFR2 exacerbated seizure severity while combined TNFR1/TNFR2 knock-out had no effect on TMEV-induced seizures (Patel et al., 2017). In line with this, mice deficient in TNFR1 were found to be less susceptible to develop seizures after TMEV infection (Kirkman et al., 2010). A similar observation was made in chemoconvulsant-induced epilepsy, showing that deletion of TNFR1 decreased, whereas lack of TNFR2 increased acute seizure severity after KA injection (Balosso et al., 2005). Finally, selective activation of TNFR1 using human TNF α exacerbated KA-induced acute seizures, while co-activation of both TNFR1 and TNFR2 using rat TNF α did not affect seizure susceptibility (Weinberg et al., 2013). Together, these data indicate antagonistic effects of TNFR1 vs. TNFR2 signaling in experimental MTLE.

Conclusively, there is convincing evidence that neuroinflammation contributes to epileptogenesis. Pro-inflammatory cytokines, in particular TNF α , are upregulated in experimental and human MTLE and possess neuromodulatory functions, suggesting that they are potentially disease-modifying factors. Chronic activation of innate immune cells and glia in response to an epileptogenic brain insult could lead to sustained cytokine production and disturbed CNS homeostasis promoting the development of epilepsy. In the following paragraphs, the major immunocompetent CNS cells, astrocytes and microglia, and their contribution to epilepsy and neuroinflammation will be introduced.

1.2 Astrocytes

Astrocytes are a class of non-neuronal cell of ectodermal origin belonging to the family of glial cells in the CNS (Verkhratsky et al., 2019). Glial cells, also known as neuroglia, account for about half of the total volume of the human brain (Verkhratsky et al., 2019). However, estimates of astrocyte numbers vary widely and depend on the species, with previous reports in rodents suggesting an astrocyte to neuron ratio of about 0.3 to 0.4 (Nedergaard et al., 2003) and more

recent numbers showing that astrocytes account for 10 – 20 % of all cells in most regions of the rodent CNS (Sun et al., 2017). Initially, neuroglia, including astrocytes, were thought to merely form a connective tissue providing structural support to neurons (Virchow, 1856/2013, 1858/2010). Nowadays, however, it is known that astrocytes have a plethora of functions, including the maintenance of ionic and metabolic homeostasis in the CNS as well as the direct modulation of neuronal activity as part of the ‘tripartite synapse’ (Araque et al., 1999; Perea et al., 2009; Verkhratsky & Nedergaard, 2018). Unlike neurons, astrocytes exhibit passive electrophysiological properties, incapable of generating action potentials and are characterized by a hyperpolarized membrane potential due to a high K^+ permeability (Dallérac et al., 2018; Verkhratsky & Nedergaard, 2018). Moreover, astrocytes constitute a highly heterogeneous cell population with respect to both morphology and function (Khakh & Sofroniew, 2015; Zhang & Barres, 2010). Anatomical studies dating back more than a century (Andriezen, 1893; Kölliker, 1889 as cited in Oberheim, Goldman & Nedergaard, 2012) already revealed the distinction between protoplasmic and fibrous astrocytes, which refers to the structural and functional differences of gray and white matter astrocytes, respectively (Khakh & Sofroniew, 2015). Additionally, astrocytes have a complex spongiform morphology, occupying non-overlapping territories, and their extensive ramifications are estimated to contact ~140 000 synapses in the hippocampal CA1 of rats (Bushong et al., 2002) (Figure 3). Together, these unique properties enable astrocytes to exert tight control over the extracellular milieu and neuronal activity. In the following paragraph, some of the physiological functions of astrocytes in the CNS will be discussed.

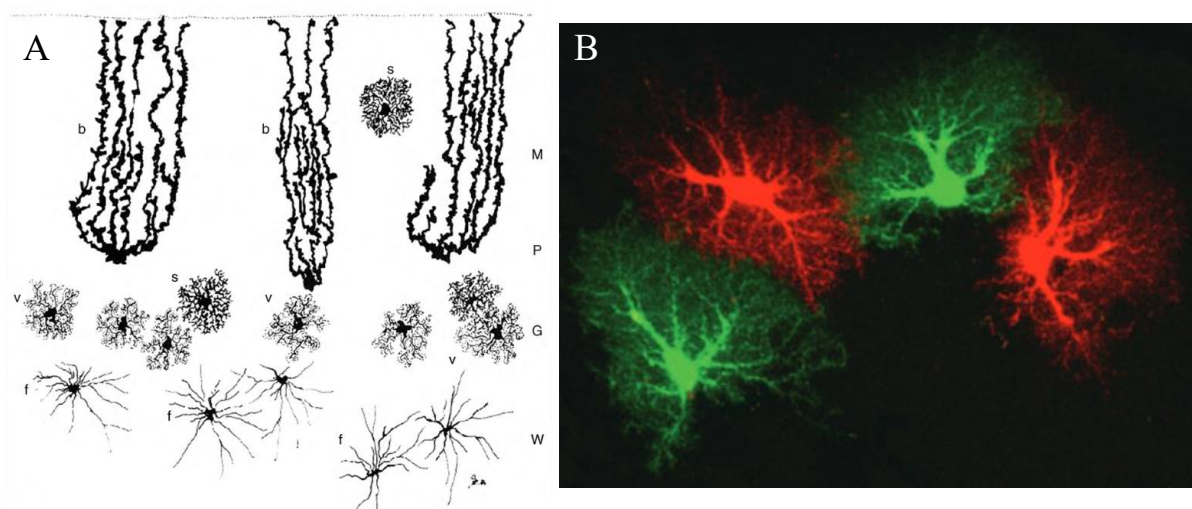


Figure 3. Astrocytes are characterized by morphological heterogeneity and occupy distinct non-overlapping territories. A) Golgi staining of astrocytes in the human cerebellum, indicating the various shapes of astrocyte morphology. Reprinted from *Current Opinion in Neurobiology*, 20(5), Zhang and Barres, Astrocyte heterogeneity: an underappreciated topic in neurobiology, 588-594, ©2010, with

permission from Elsevier. **B)** Dye-injected mouse hippocampal astrocytes characterized by a typical spongiform morphology and non-overlapping territories. Used with permission of Springer, from Handbook of neurochemistry and molecular neurobiology. Neuroactive proteins and peptides. GFAP and Astrocyte Intermediate Filaments. Chapter 14, Milos Pekny and Ulrike Wilhelmsson, ©2006; permission conveyed through Copyright Clearance Center, Inc. (Pekny & Wilhelmsson, 2006).

1.2.1 Physiology of astrocytes

Astrocytes control the extracellular milieu of the CNS as they play a major role in ion and water homeostasis, regulation of the extracellular space volume, neurotransmitter uptake and turnover as well as energy supply (Verkhratsky & Nedergaard, 2018). Under physiological conditions, glutamate uptake is primarily mediated by specialized astrocytic membrane transporters called excitatory amino acid transporter (EAAT) 1 and 2 (GLAST and GLT-1 in rodents) (Passlick et al., 2021). Glutamate uptake reduces the spread of glutamate from the synaptic cleft, ensuring the efficacy of synaptic transmission and prevention of excitotoxicity (Passlick et al., 2021). Moreover, astrocytes convert glutamate taken up from the synapse into glutamine and shuttle it back to neurons for the production of glutamate, a process known as the glutamate-glutamine cycle (Cheung et al., 2022; Verkhratsky & Nedergaard, 2018). Further, astrocytic endfeet enwrap blood vessels allowing uptake of glucose from the circulation, which is metabolized into lactate in the process of glycolysis and transported into neurons as an energy substrate (Philippot et al., 2021). In fact, glutamate uptake and lactate production are interlinked, as uptake of glutamate increases the intracellular Na^+ concentration which drives aerobic glycolysis (Verkhratsky & Nedergaard, 2018). Together, this model is referred to as the astrocyte-neuron lactate shuttle (Pellerin & Magistretti, 1994). Additionally, astrocytes maintain water, ion and pH homeostasis of the extracellular space by a multitude of channels and transporters expressed on their membranes (Verkhratsky & Nedergaard, 2018). For example, astrocytes maintain K^+ homeostasis *via* different uptake mechanisms including active transport by Na^+/K^+ -ATPases (NKA), passive diffusion through inwardly-rectifying K^+ channels or, during high extracellular K^+ concentrations ($[\text{K}^+]_o$), secondarily active transport *via* $\text{N}^+/\text{K}^+/\text{Cl}^-$ (NKCC1) co-transporters (Hertz et al., 2013; Kofuji & Newman, 2004; Verkhratsky & Nedergaard, 2018). Astrocytic control of $[\text{K}^+]_o$ has further been shown to depend on ‘spatial K^+ buffering’ (Kofuji & Newman, 2004), a concept that will be described in more detail in the following section. Finally, astrocytes actively shape neuronal activity through Ca^{2+} -dependent release of various neuroactive substances, collectively known as ‘gliotransmitters’ (Araque et al., 2014). For example, the induction of long-term potentiation (LTP) at hippocampal synapses has been shown to depend on the release of the N-methyl-D-aspartate receptor (NMDAR) co-agonist D-serine from astrocytes (Henneberger et al., 2010). Moreover, glutamate released from astrocytes modulates basal synaptic transmission in hippocampal

granule cells, an effect that is both TNF α and P2Y₁R-dependent (Nikolic et al., 2018; Santello et al., 2011).

In sum, astrocytes are vital to CNS function. On the one hand, they sustain CNS homeostasis by controlling extracellular glutamate and K⁺ levels as well as by providing energy metabolites to neurons. On the other hand, they actively control synaptic transmission and plasticity through gliotransmitter release. A failure to fulfill these functions could promote hyperexcitability and might even culminate in the development of epilepsy.

1.2.2 Astroglial networks and gap junctions

Astrocytes are interconnected and form large functional syncytia *via* structures called gap junctions (GJs) (Giaume et al., 2021) (Figure 4). The formation of gap junction channels (GJCs) allows for the direct exchange of low-molecular-weight molecules (< 1.5 kDa) between the cytoplasm of neighboring astrocytes. GJCs are composed of a family of proteins called connexins (Cxs) which oligomerize into a hexameric protein structure, the connexon. The docking of two opposing connexons leads to the formation of a GJC. A connexon consisting of identical Cxs is called homomeric, whereas connexons composed of different Cxs are referred to as heteromeric. Similarly, a GJC can be composed of connexons of the same isotype (homotypic), or of different isotypes (heterotypic) (Giaume et al., 2021) (Figure 4). In astrocytes of the adult brain, Cx43 and Cx30 are the primary GJC-forming Cxs (Giaume et al., 2010). Connexons that do not assemble to form a GJC are called hemichannels (HCs) and allow bidirectional exchange of small molecules between the cytoplasm and the extracellular space (Cheung et al., 2014; Giaume et al., 2021). Importantly, Cx43 function is partially regulated by phosphorylation of the cytosolic C-terminus (COOH) (Márquez-Rosado et al., 2012). The Cx43 COOH-terminus contains more than a dozen known phosphorylation sites that can be modified by several kinases thereby regulating their assembly, stability and conductance (Solan & Lampe, 2020). Indeed, targeting Cx43 phosphorylation has been employed as a treatment strategy in CNS pathology, such as stroke (Freitas-Andrade et al., 2019) and altered phosphorylation of the Cx43 COOH-terminus was found in human and experimental MTLT-HS (Deshpande et al., 2017).

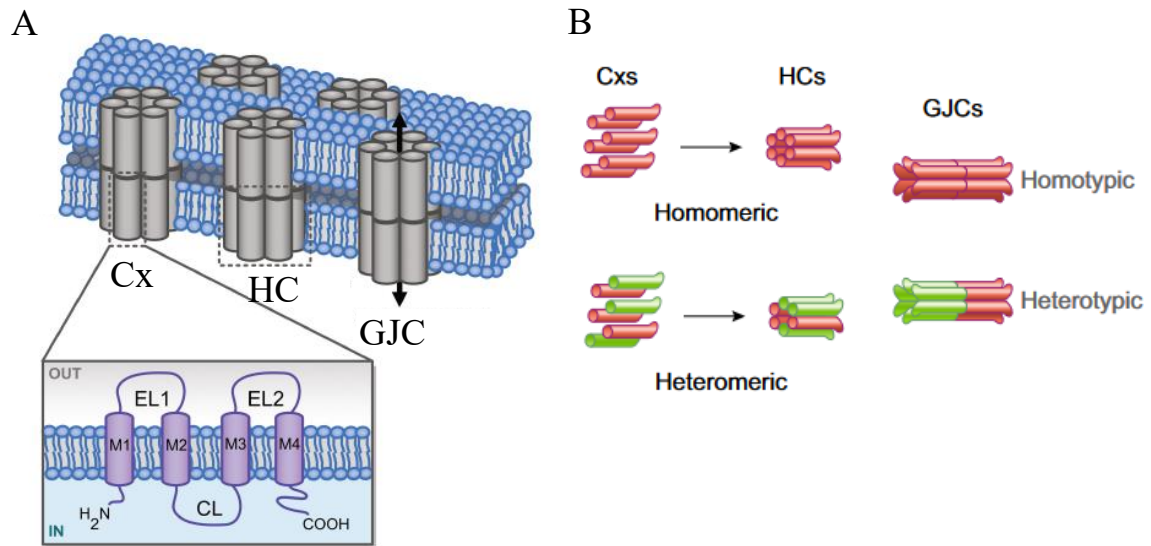


Figure 4. Structural composition of gap junction channels. **A)** A single connexin (Cx) molecule consists of four transmembrane domains (M1 – 4), which are connected by two extracellular loops (EL1 and 2) and one cytosolic loop (CL). Moreover, an N- (H_2N) and C-terminal (COOH) side reside within the cytoplasm. Six connexins oligomerize to form a hemichannel (HC) or connexon. Two opposing HCs assemble to form a gap junction (GJ) channel, allowing diffusion of small molecular weight molecules through its pore (arrow). The image has been modified from Stephan et al., 2021. © 2021 Stephan, Eitelmann and Zhou. **B)** Connexin HCs can assemble as homo- or heteromeric structures. Similarly, two opposing HCs combine to form either a homo- or heterotypic GJCs. Image modified with permission from Giaume et al., 2021. © The American Physiological Society (APS).

Various molecules can diffuse through astrocytic GJCs ranging from ions such as K^+ , Na^+ and Ca^{2+} , to second messengers including cyclic adenosine monophosphate (cAMP) and inositol triphosphate (IP3), as well as energy metabolites such as glucose and lactate (Pannasch & Rouach, 2013). In the mouse hippocampus, interastrocytic coupling primarily depends on Cx43 and to a lesser extent on Cx30 (Gosejacob et al., 2011). Importantly, astrocytes spatially redistribute K^+ through their GJ coupled network (Kofuji & Newman, 2004; Steinhäuser et al., 2012). The theoretical concept of spatial K^+ buffering has initially been proposed by Richard Orkand and colleagues (Orkand et al., 1966) and was first demonstrated experimentally in Müller cells, an astrocyte-like glial cell in the retina (Newman et al., 1984). In Orkand's model, the difference between the local K^+ equilibrium potential (E_K) and the membrane potential (V_m) of an astrocyte exposed to an increased $[K^+]_o$ creates a driving force for K^+ influx into the cell (Breithausen, 2020). Importantly, due to electrical coupling within the astroglial network, the astrocytic V_m remains more hyperpolarized than E_K at sites of high $[K^+]_o$, ensuring a constant flow of K^+ into the cell (Ma et al., 2016). K^+ is subsequently redistributed through the astrocytic network along the K^+ concentration gradient from sites of elevated to sites with a lower $[K^+]_o$, where V_m is more depolarized than E_K leading to K^+ efflux (Steinhäuser et al., 2012) (Figure

5). Impairments in astrocytic GJ coupling are therefore expected to lead to ineffective clearance of locally increased extracellular K^+ (Breithausen et al., 2020). Indeed, experimental evidence from both genetic and pharmacological studies reveals the importance of astroglial GJ coupling for the maintenance of K^+ homeostasis (Bazzigaluppi et al., 2017; EbrahimAmini et al., 2021; Pannasch et al., 2011; Wallraff et al., 2006). Based on these findings, it has been hypothesized that loss of astrocyte GJ coupling promotes neuronal excitability, as increased $[K^+]_o$ would shift the neuronal membrane potential closer to the threshold to generate action potentials (Kofuji & Newman, 2004) (section 1.2.3). Several techniques are available to investigate the extent of GJC in astrocytes (Stephan et al., 2021), but the most commonly used method makes use of small tracers ($< 1 - 1.2$ kDa) injected into individual astrocytes, which are capable to diffuse through the astrocytic GJ coupled network. For example, N-biotinyl-L-lysine (biocytin) can be injected into individual astrocytes and subsequently immunostained and visualized using streptavidin-conjugated fluorescent antibodies (Bedner et al., 2015; Wallraff et al., 2006). Alternatively, astrocytes can be filled with fluorescent dyes, allowing direct visualization of dye spread through the astrocytic network, for example using a two-photon microscope (Anders et al., 2014).

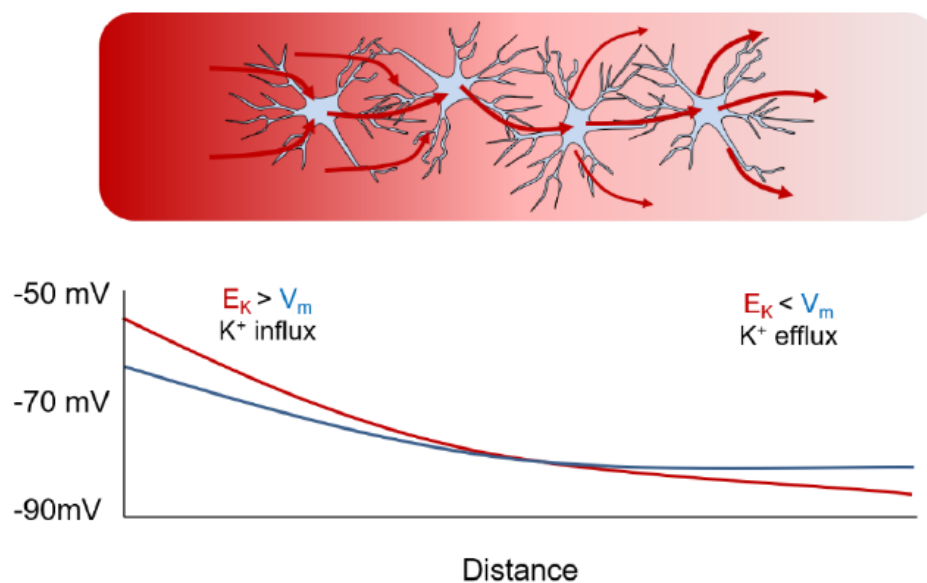


Figure 5. Spatial K^+ buffering in astroglial networks. At sites of high $[K^+]_o$, the difference between the local E_K and the astrocytic V_m leads to K^+ influx into the astrocyte. As a result of electrical coupling within the astrocytic network, depolarization of an astrocyte exposed to high $[K^+]_o$ remains limited, maintaining a hyperpolarized V_m close to that of adjacent astrocytes and ensuring a constant driving force for K^+ to enter the cell (Ma et al., 2016). At distant sites with a lower $[K^+]_o$, K^+ is released into the extracellular space, effectively resulting in redistribution of K^+ from sites of high to sites of lower $[K^+]_o$. The red intensity gradient in the top panel indicates the K^+ concentration gradient. The image is taken from Breithausen, 2020.

1.2.3 Reactive astrocytes and epilepsy

Astrocytes rapidly respond to various types of injury and noxious stimuli with alterations in their morphology, molecular signature, function and number (Escartin et al., 2019, 2021). Astrocytes that undergo such a transformational process in response to CNS injury are commonly referred to as ‘reactive astrocytes’ (while the process is also known as ‘astrogliosis’). Reactive astrocytes are found in a variety of CNS pathologies ranging from neurodegenerative and demyelinating diseases to ischemia, infection, traumatic head injury, and epilepsy (Escartin et al., 2019; Hol & Pekny, 2015). Although simplifying nomenclatures such as ‘neurotoxic’ and ‘neuroprotective’ have been proposed to classify reactive astrocytes (Escartin et al., 2019; Liddelow et al., 2017), these cells are characterized by a high degree of heterogeneity whose phenotype likely depends on the specific disease in question (Escartin et al., 2019, 2021). The most commonly employed marker of reactive astrocytes is glial fibrillary acidic protein (GFAP), an intermediate filament protein that is typically upregulated in response to injury (Hol & Pekny, 2015; Liddelow & Barres, 2017) (Figure 6). It should be noted, however, that reactive astrocytes are characterized by a plethora of molecular and functional changes that go far beyond changes in GFAP expression (Escartin et al., 2019).

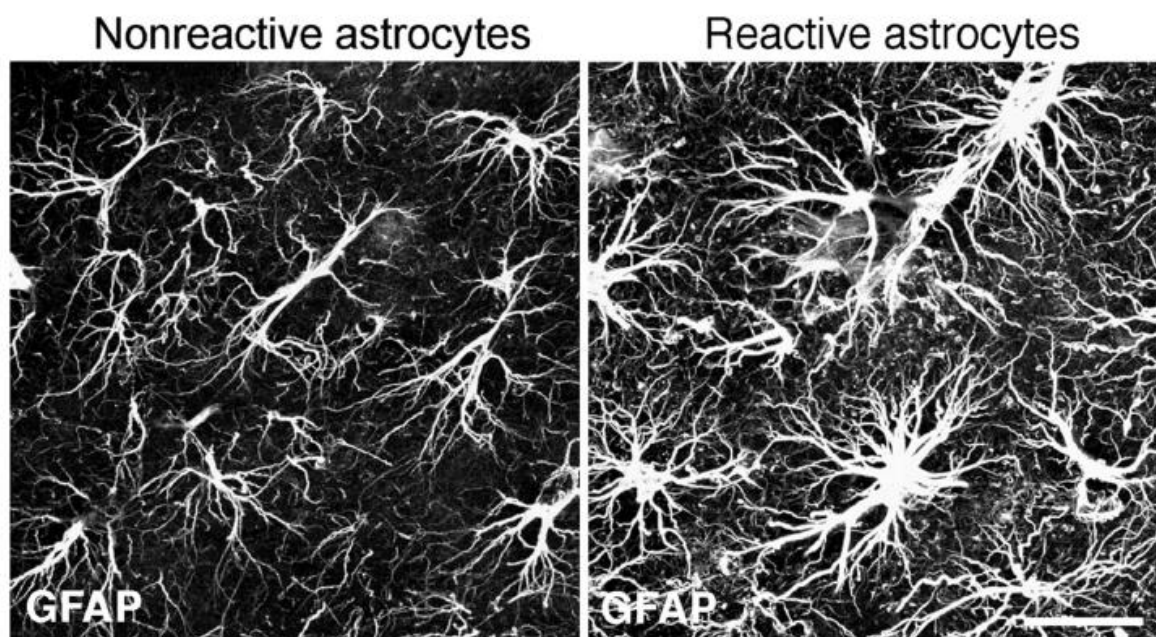


Figure 6. Reactive hippocampal astrocytes. GFAP staining of astrocytes in the molecular layer of the dentate gyrus (DG) four days after entorhinal cortex lesion, demonstrating a typical increase in GFAP immunoreactivity of reactive astrocytes. GFAP staining reveals a thickening of GFAP-positive astrocyte processes, indicative of cellular hypertrophy in reactive vs. non-reactive astrocytes. Image has been modified with permission from Wilhelmsson et al., 2006. Copyright (2006) National Academy of Sciences, U.S.A.

Reactive astrocytes are a well described phenomenon in both human and animal models of epilepsy (Bedner et al., 2015; Binder & Steinhäuser, 2006; Blümcke et al., 2013; Briellmann et al., 2002; Sano et al., 2021). Experimental evidence further suggests that reactive astrocytes are causally involved in epileptogenesis. For example, virally overexpressing enhanced green fluorescent protein (eGFP) in astrocytes induces astrogliosis and has been shown to promote hippocampal hyperexcitability, possibly due to downregulation of glutamine synthetase (GS) (Ortinski et al., 2010). Similarly, astrocyte-specific deletion of $\beta 1$ -integrin induces a reactive phenotype in astrocytes that is sufficient for the development of epilepsy (Robel et al., 2015). Moreover, reactive astrocytes in human and animal models of TLE are characterized by impaired homeostatic functions, including defective glutamate and K^+ clearance (Bedner et al., 2015; Clarkson et al., 2020; Hinterkeuser et al., 2000; Proper et al., 2002), but also dysregulated GS (Eid et al., 2004; Hammer et al., 2008; Swamy et al., 2011), adenosine-kinase (ADK) (Aronica et al., 2011; Gouder, 2004) and aquaporin-4 (AQP4) (Alvestad et al., 2013; Eid et al., 2005) expression and function. Intriguingly, astrocytes completely lose their ability to form GJ coupled networks in human MTLE-HS and loss of functional coupling between astrocytes could be recapitulated in a mouse model of MTLE-HS where it was shown to be accompanied by impaired K^+ clearance and to precede neuronal cell death (Bedner et al., 2015). Together, these data indicate a potentially causative role for loss of astrocytic GJ coupling in epileptogenesis. Interestingly, astrocyte uncoupling depends on subcellular reorganization and altered phosphorylation, rather than decreased expression of the GJ-forming Cx43 (Deshpande et al., 2017). More specifically, in the *intracortical* MTLE-HS model, the phosphorylation status of Cx43 is rapidly altered in the injected vs. non-injected hippocampus, most likely due to increased phosphorylation at the serine residue 262, which reduces the opening probability of the GJ channel (Deshpande, 2017; Thévenin et al., 2013). Further evidence for the importance of GJ coupling in epilepsy comes from a study showing that hippocampal slices from mice constitutively lacking both astroglial Cxs (DKO) are characterized by spontaneous epileptiform events and an increased sensitivity to epileptic stimuli (Wallraff et al., 2006). Moreover, genetic deletion of astroglial Cxs induces reactive astrocytes, impairs glutamate and K^+ clearance and increases basal excitatory neurotransmission and synaptic release probability (Pannasch et al., 2011). However, the role of astrocyte coupling in epilepsy is still controversial, as astrocyte networks not only control K^+ and glutamate homeostasis, but also maintain the activity-dependent supply of energy metabolites to neurons (Philippot et al., 2021; Rouach et al., 2008). Thus, in principle, changes in functional coupling between astrocytes could exert both pro- and anti-epileptic effects, making it difficult to predict their contribution to the

development of epilepsy (Deshpande et al., 2020). A study by Chever and colleagues (2016) illustrates the complex relationship between loss of astrocyte coupling and the development and maintenance of seizure activity. In this study it was shown that although DKO mice are characterized by an increased number of seizures in response to pentylentetrazole (PTZ) injection, the duration and severity of these seizures was reduced (Chever et al., 2016). Moreover, experimental evidence examining the impact of astrocyte uncoupling in models of chronic epilepsy, such as the KA model of MTLE-HS, is lacking.

Conclusively, more data is required to elucidate the precise role of astroglial networks in the pathogenesis of epilepsy. Moreover, the signaling pathways that contribute to loss of GJ coupling in astrocytes in MTLE remain ill-defined and require further investigations.

1.3 Microglia

Microglia are the resident immune cells of the CNS (Prinz et al., 2019). First described by Pío del Río-Hortega in 1919 and long considered as passive bystanders of the CNS, microglia today are recognized as multifunctional cells with important roles in immune regulation, brain development, homeostasis and synaptic plasticity (Prinz et al., 2019; Sierra et al., 2019; Wu et al., 2015). Microglia are mononuclear phagocytes that arise from erythro-myeloid progenitors (EMPs) in the yolk-sac during primitive hematopoiesis (Li & Barres, 2018). They are long-lived cells characterized by low turnover and self-renewal, whose survival depends on colony-stimulating factor 1 receptor (CSF1R) signaling (Green et al., 2020; Li & Barres, 2018). Already 100 years ago microglia have been recognized to acquire an ‘activated’ or ‘reactive’ phenotype in response to brain injury and disease, often recognized by their characteristic amoeboid morphology (Río-Hortega, 1919 as cited in Sierra et al., 2019). However, the classification of microglia transitioning from a ‘resting’ into an ‘activated’ state is nowadays considered to be too simplistic, since microglial responses vary widely depending on the specific pathological context (Hanisch & Kettenmann, 2007). Today, it is known that microglial processes constantly monitor their surrounding microenvironment allowing a rapid immunological response to pathological stimuli (Davalos et al., 2005; Nimmerjahn et al., 2005). It is therefore not surprising that a number of studies found evidence for microglia contributing to various CNS pathologies such as Alzheimer’s disease (AD) (Heneka et al., 2013; Zhang et al., 2013) and Parkinson’s disease (PD) (Harms et al., 2013; Rayaprolu et al., 2013) but also neurological disorders such as epilepsy (Broekaart et al., 2018; Morin-Brureau et al., 2018). During disease or injury, microglia coordinate the inflammatory response by proliferation, the

release of cytokines and chemokines as well as by phagocytosis of cellular debris (Prinz et al., 2019).

The following paragraph will provide an overview of some of the physiological functions of microglia in the CNS. Thereafter, the role of microglia in epilepsy will be discussed.

1.3.1 Physiology of microglia

In addition to their prominent role in immune modulation, microglia fulfill various functions in the healthy CNS (Prinz et al., 2019; Sierra et al., 2019). During CNS development, microglia contribute to synaptic pruning. For example, complement-mediated synaptic pruning by microglia has been demonstrated in the retinogeniculate system and is essential for its proper maturation (Schafer et al., 2012; Stevens et al., 2007). Impaired microglial synapse pruning has further been shown to lead to an excess of dendritic spines and immature synapses in the developing hippocampus, with concomitant increases in excitability and susceptibility to seizures (Paolicelli et al., 2011). Interestingly, astrocyte-derived soluble factors, such as interleukin (IL)-33 and members of the complement system, regulate microglial synapse pruning in the developing CNS (Stevens et al., 2007; Vainchtein et al., 2018). Besides their important contribution to brain development, microglia directly modulate information processing in the mature brain. For example, microglia actively remodel synapses in response to altered sensory experience and neuronal activity in the visual cortex of juvenile mice (Tremblay et al., 2010). Additionally, microglial brain-derived neurotrophic factor (BDNF) has been shown to affect synaptic plasticity as well as motor- and fear-learning (Parkhurst et al., 2013) and microglia-depletion impairs glutamatergic transmission in the hippocampus leading to impaired object-recognition memory in adult mice (Basilico et al., 2022). Microglial control over CNS functioning largely depends on their ability to constantly survey their surroundings with their highly motile processes. The factors that guide motility of microglial processes are not fully understood, but some studies demonstrate a role for purinergic and ion signaling (Prinz et al., 2019). For example, adenosine triphosphate (ATP) released from neurons in response to repetitive NMDAR activation has been shown to trigger rapid microglial process outgrowth (Dissing-Olesen et al., 2014). Moreover, microglial process extension to local sites of injury has been shown to depend on ATP and P2Y₁₂ signaling *in vivo* (Davalos et al., 2005; Haynes et al., 2006). Recently, however, it was shown that directed movement of microglial processes towards sites of injury depends on P2Y₁₂ signaling, whereas basal microglial surveillance requires tonic activation of the two-pore K⁺ channel THIK-1 (Madry et al., 2018).

Conclusively, microglia are crucial regulators of CNS development and are increasingly being recognized to play an equally important role in information processing in the brain. Moreover, the expression of a variety of receptors on their membrane called the ‘microglial sensome’ (Hickman et al., 2013) together with their highly motile processes, enables microglia to rapidly sense and react to potentially dangerous stimuli, placing them at the forefront of CNS defense.

1.3.2 Microglia in epilepsy

Microglia are highly reactive to any type of brain insult, including TBI, infection, ischemia and neurodegeneration (Eyo et al., 2014; Hanisch & Kettenmann, 2007; Heneka et al., 2014; Qin et al., 2019; Rock et al., 2004; Therajaran et al., 2020). Microglia undergo a transformative process in response to injury or disease that includes morphological, transcriptomic and functional adaptations, which enables the now ‘reactive microglia’ to orchestrate an inflammatory response (Prinz et al., 2019). Similar to macrophages in other tissues, microglia can acquire different activation states or polarizations, known as M1 and M2 (Mantovani et al., 2005; Therajaran et al., 2020). M1-like microglia are considered to promote inflammation, expressing several pro-inflammatory cytokines like TNF α and IL1 β , as well as phagocytic markers. M2-like microglia in turn have been suggested to release anti-inflammatory cytokines and to promote tissue recovery and repair (Benson et al., 2015; Therajaran et al., 2020). Typically, reactive microglia can be differentiated from their highly ramified non-pathological counterparts by their characteristic spherical, or amoeboid morphology (Boche et al., 2013). Indeed, multiple studies found evidence for reactive microglia in human and animal models of epilepsy (Broekaart et al., 2018; Feng et al., 2019; Morin-Brureau et al., 2018; Zattoni et al., 2011) (Figure 7). Moreover, gene expression studies have identified genetic variants affecting microglial functions as potentially disease-modifying factors in epilepsy and predictive of structural changes in the epileptic brain (Altmann et al., 2022; Srivastava et al., 2018). In human MTLE-HS, Morin-Brureau et al. (2018) show that microglia acquire an amoeboid shape particularly in the sclerotic CA1 and CA3, and demonstrate that the frequency of amoeboid microglia correlates negatively with neuronal density. Reactive amoeboid-shaped microglia have also been reported in experimental models of MTLE (De Simoni et al., 2000; Wyatt-Johnson et al., 2021). However, microglial morphology in epilepsy is heterogeneous, as hyper-ramified microglia have also been described following SE-induction (Eyo et al., 2014; Rappold et al., 2006; Shapiro et al., 2008), and probably depends on the time point and brain area examined (Morin-Brureau et al., 2018). In addition to morphological changes, reactive microglia in experimental MTLE produce several M1-associated pro-inflammatory cytokines (Aronica et al., 2007; Benson et al., 2015; Sano et al., 2021; Varvel et al., 2016) and exhibit

increased proliferation and K^+ conductance (Avignone et al., 2008; Feng et al., 2019). Experimental evidence further suggests that microglia play an active role in seizure generation. For example, microglial inhibition using CSF1R blockers has been shown to attenuate seizure activity (Di Nunzio et al., 2021; Sano et al., 2021; Srivastava et al., 2018) and to be neuroprotective in epileptic mice (Di Nunzio et al., 2021). Likewise, treatment with the tetracycline antibiotic minocycline, a potent suppressor of microglial M1 activation (Kobayashi et al., 2013), alleviates chronic seizures and neurodegeneration after pilocarpine-induced SE (Wang et al., 2015). Finally, genetic overactivation of mTOR signaling leads to a non-inflammatory reactive state in microglia sufficient to induce epilepsy (Zhao et al., 2018). However, mechanistically the contribution of microglia to the pathophysiology of epilepsy is still not fully understood. As mentioned previously, microglia regulate neuroinflammation by releasing soluble mediators, such as the pro-inflammatory cytokines IL1 β , IL6 and TNF α (Prinz et al., 2019). Intriguingly, pro-inflammatory cytokines released from microglia, including TNF α , have been shown to induce reactive astrocytes (Liddel et al., 2017). Importantly, increased microglial TNF α mRNA expression has been demonstrated during the acute/early latent phase following SE-induction (Benson et al., 2015; Sano et al., 2021). Moreover, inhibiting microglia activation attenuates SE-induced increases in TNF α protein levels (Wang et al., 2015). In line with this, TNF α incubation *in vitro* as well as co-culturing of astrocytes with activated microglia has been shown to impair astrocytic GJ coupling, an essential homeostatic function of these cells (Faustmann et al., 2003; Haghikia et al., 2008; M \hat{e} me et al., 2006). Thus, microglia-derived soluble factors may contribute to epileptogenesis indirectly, by impairing astrocyte-dependent K^+ and glutamate homeostasis (Henning et al., 2022). However, at present, the cellular source of TNF α in experimental TLE has not unequivocally been determined, as many immunocompetent CNS cells, like astrocytes and microglia but also infiltrating monocytes, have been shown to produce the cytokine (Beattie et al., 2002; Lieberman et al., 1989; Varvel et al., 2016). Moreover, inhibition or depletion of microglia using minocycline or CSF1R inhibitors is unspecific, as considerable overlap in surface marker expression between microglia and peripheral macrophages exists and these drugs have been shown to influence both cell populations (Garrido-Mesa et al., 2013; Jurga et al., 2020; Li & Barres, 2018; Merry et al., 2020). Indeed, infiltration of peripheral immune cells has been well described in human and experimental MTLE (Broekaart et al., 2018; Feng et al., 2019; Walzl, K \ddot{a} ufer, Br \ddot{o} er, et al., 2018), and infiltrating monocytes contribute to neurodegeneration, seizure severity and inflammation in TLE models (K \ddot{a} ufer et al., 2018; Varvel et al., 2016; Walzl, K \ddot{a} ufer, Br \ddot{o} er, et al., 2018).

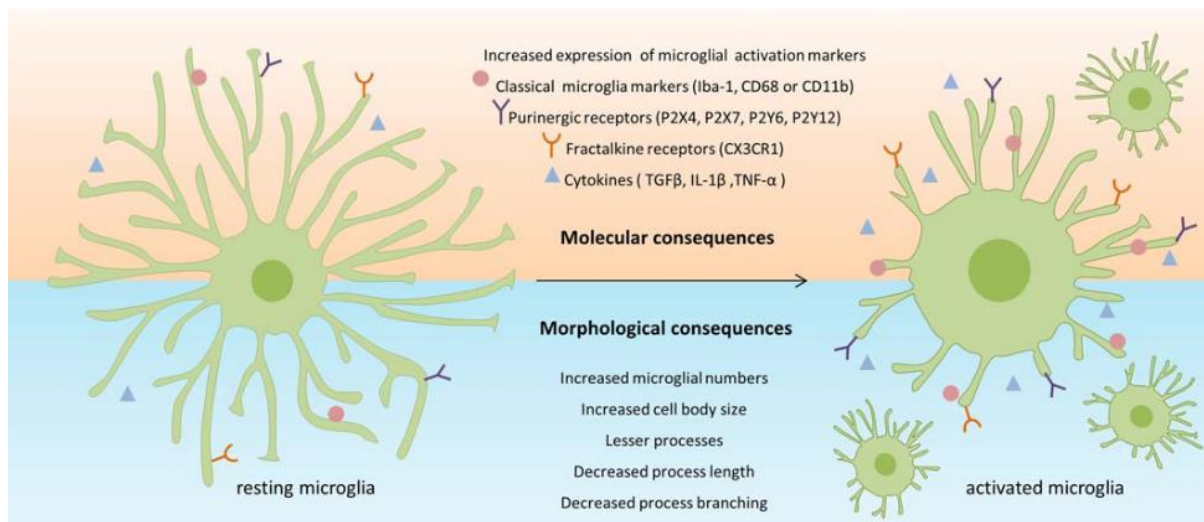


Figure 7. Morphological and molecular alterations of microglia in response to seizure activity. A number of molecular and morphological changes have been described in microglia following seizures including, upregulation of cytokines and altered marker expression as well as proliferation and changes in cell body size, process length and overall ramification. Used with permission of John Wiley & Sons, Inc., from *Microglia–Neuron Communication in Epilepsy*, Eyo, Murugan and Wu, 65(1) ©2017; permission conveyed through Copyright Clearance Center, Inc.

To summarize, microglia are important immune-regulators of the CNS. Numerous reports have identified reactive microglia as orchestrators of inflammation in epilepsy and indicate the potential to target microglia for the treatment of epilepsy. However, the exact mechanisms by which microglia influence the pathophysiology of epilepsy remain elusive and require further investigations.

1.4 The blood-brain barrier

As an integral part of the neurovascular unit (NVU), the blood-brain barrier (BBB) is an anatomical barrier composed of endothelial cells (ECs) extending along the CNS microvasculature, which tightly controls the entry of ions, metabolites and macromolecules from the blood stream into the brain (Löscher & Friedman, 2020; Obermeier et al., 2013; Sweeney et al., 2019). Additionally, the BBB prevents infiltration of pathogens, blood cells and other potentially neurotoxic components into the brain parenchyma (Sweeney et al., 2019; Zhao et al., 2015). Overall, preserving the structural integrity of the BBB is therefore essential to maintain CNS homeostasis. Indeed, loss of BBB integrity has been associated with a number of CNS pathologies, including stroke, multiple sclerosis, epilepsy, TBI and neurodegenerative disorders (Daneman & Prat, 2015; Löscher & Friedman, 2020; Parker et al., 2022; Shlosberg et al., 2010). Importantly, several human and experimental studies report a compromised BBB in epilepsy (Deshpande et al., 2017; Frigerio et al., 2012; Greene et al., 2022; Ivens et al., 2007;

van Vliet et al., 2007). BBB breakdown leads to extravasation of blood-derived factors into the CNS, which have been shown to promote epileptiform activity (Bar-Klein et al., 2014; Ivens et al., 2007; Seiffert, 2004; Weissberg et al., 2015). Therefore, an understanding of the time course and mechanisms that lead to BBB disruption as well as the factors that are subsequently released into the CNS could help to improve epilepsy treatment.

The following paragraphs will provide an overview about the structural and functional properties of the BBB as well as the role of BBB breakdown for the pathophysiology of epilepsy.

1.4.1 Structural and functional properties of the BBB

The NVU comprises various cellular components that contribute to BBB integrity including ECs, pericytes, smooth muscle cells, glial cells including astrocytes, oligodendrocytes and microglia, as well as neurons (Sweeney et al., 2019). The structural composition of the BBB varies depending on whether one examines the arteriole or capillary level of the cerebrovascular system (Sweeney et al., 2019) (Figure 8). Generally, the BBB is formed by ECs that form a layer surrounding blood vessels. ECs are connected by cellular junction proteins including tight junctions (TJs), which contribute to the physical barrier of the BBB by acting as a seal between adjacent endothelia (Greene et al., 2022; Sweeney et al., 2019). Moreover, several other endothelial connections including adherens junctions and other junctional adhesion molecules contribute to the tight structural composition of ECs at the BBB (Sweeney et al., 2019). At the capillary level, ECs are surrounded by the basement membrane, which is an extracellular matrix comprised of, for example, type IV collagens, laminin, nidogen, elastin, fibronectin and heparin sulfate proteoglycans (Löscher & Friedman, 2020; Sweeney et al., 2019). Additionally, the basement membrane harbors pericytes, which are contractile cells that control capillary diameter (Daneman & Prat, 2015; Hall et al., 2014). In contrast, smooth muscle cells surround larger arterioles but not capillaries, and regulate arteriole contraction (Iadecola, 2004). Astrocytic endfeet ensheath both capillary and arteriole vessels, forming the glia limitans (Sweeney et al., 2019). Importantly, astrocytes have been shown to contribute to neurovascular coupling, the process by which changes in neuronal activity alter cerebral blood flow to adjust energy supply to the brain (Zonta et al., 2003). However, more recent data indicates that astrocytic control of cerebral blood flow is restricted to capillaries and does not involve arterioles (Mishra et al., 2016). Membrane transporters, such as solute carrier transporters, in ECs allow for bidirectional transport of metabolites, amino acids, nucleotides and ions across the BBB (Zhao et al., 2015). Small lipophilic (< 400 Da) molecules, in turn, can passively

diffuse through the BBB (Zhao et al., 2015). In addition, endothelial efflux transporters actively shuttle potentially toxic compounds and drugs out of the brain into the blood (Löscher & Friedman, 2020; Sweeney et al., 2019).

1.4.2 BBB dysfunction in epilepsy

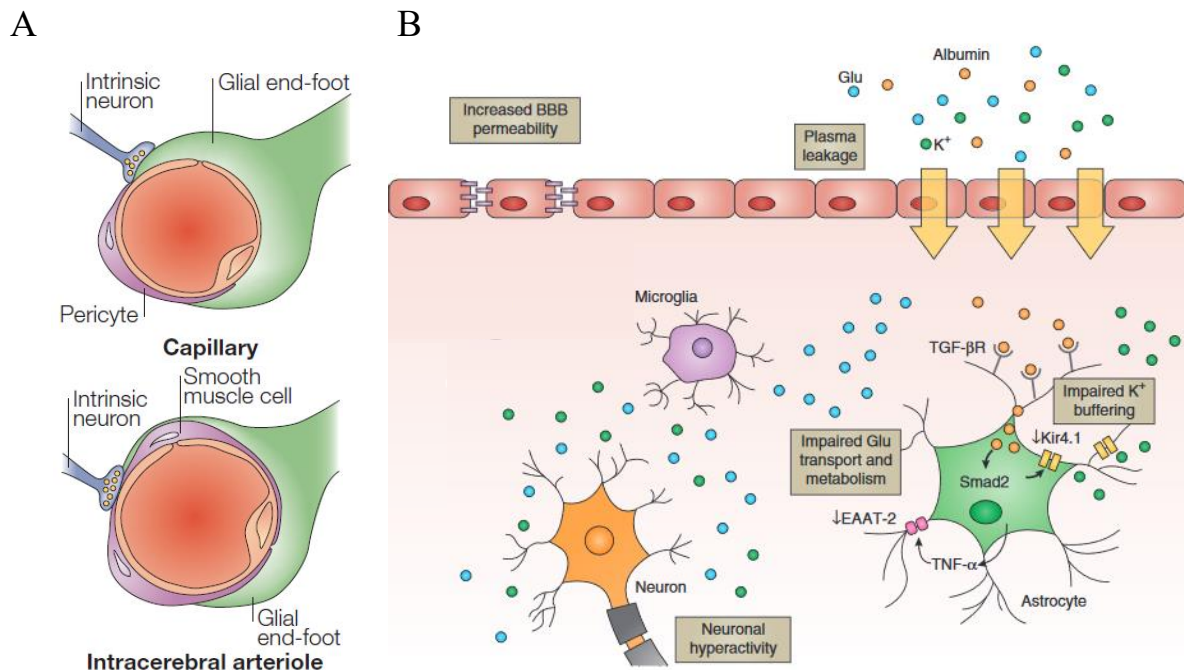


Figure 8. Structural components and epilepsy-associated alterations of the BBB. **A)** Structural composition of the BBB at the capillary and at the arteriole level. Note that smooth muscle cells cover intracerebral arterioles, whereas pericytes surround capillaries, each controlling the corresponding vessel diameter. Astrocytic end-feet cover both arterioles and capillaries, forming the glia limitans. Reprinted by permission from Springer Nature, Nature Reviews Neuroscience, Neurovascular regulation in the normal brain and in Alzheimer's disease, Costantino Iadecola, ©2004. **B)** In epilepsy, a dysfunctional BBB allows entry of serum-derived factors such as albumin into the brain parenchyma, which is supposed to be taken up via TGFβ receptors on astrocytes and to perturb K⁺ and glutamate homeostasis. Additionally, plasma-derived K⁺ and glutamate permeate through a compromised BBB contributing to neuronal excitability. Reprinted by permission from Springer Nature, Nature Medicine, Development, maintenance and disruption of the blood-brain barrier, Birgit Obermeier et al., ©2013.

The association between a compromised BBB and seizures has been known for decades (Löscher & Friedman, 2020). Indeed, already in the middle of the last century animal studies using the pro-convulsive agent PTZ and the macromolecular dye Evans Blue have provided evidence for seizure-induced BBB dysfunction (Bauer & Leonhardt, 1955, 1956). Later, a leaky BBB, as indicated by intracerebral serum albumin immunoreactivity, was demonstrated in the hippocampus of epilepsy patients and following experimentally-induced seizures (Mihály & Bozóky, 1984; Nitsch & Klatzo, 1983). Since then, several observations found evidence for BBB breakdown in human and experimental epilepsy, including MTLE-HS (Deshpande et al.,

2017; Frigerio et al., 2012; Greene et al., 2022; Milikovsky et al., 2019; van Vliet et al., 2007). Moreover, BBB disruption is common among patients with drug-resistant epilepsy and experimental evidence indicates that it contributes to pharmacoresistance and seizure frequency (Al Rihani et al., 2021; Greene et al., 2022; Marchi et al., 2009; Salar et al., 2014; van Vliet et al., 2007, 2015). However, the precise mechanisms that lead to BBB breakdown in epilepsy are ill-defined (Löscher & Friedman, 2020). Combined imaging and biomarker expression data from human epilepsy patients demonstrates a temporal correlation between seizure activity and BBB opening, indicating that seizure activity *per se* is sufficient to cause BBB disruption (Rüber et al., 2018). Indeed, glutamate released during seizure activity has been shown to increase matrix metalloproteinase expression, leading to degradation of TJ proteins and increased BBB permeability (Rempe et al., 2018). In line with this, significant downregulation of the TJ protein claudin-5 has recently been reported in both human and experimental TLE (Greene et al., 2022). Finally, several other factors, including the pro-inflammatory cytokine TNF α , reactive oxygen species and pericyte dysfunction, also promote BBB breakdown (Huang et al., 2022; Löscher & Friedman, 2020; Nishioku et al., 2010; Prager et al., 2019). How a compromised BBB in turn contributes to the development and progression of epilepsy is not fully understood. A positive-feedback loop has been suggested in which seizures lead to BBB opening, in turn causing more seizures (Löscher & Friedman, 2020). Experimental opening of the BBB as well as chemoconvulsant-induced SE lead to extravasation of serum albumin into the brain parenchyma (Bankstahl et al., 2018; Deshpande et al., 2017; Frigerio et al., 2012; Ivens et al., 2007; Seiffert, 2004) (Figure 8). Similarly, albumin immunoreactivity was found in human TLE tissue and from patients that died after SE (van Vliet et al., 2007). Serum albumin is a protein abundantly present in blood plasma of all vertebrates and is important for maintaining osmotic pressure in blood vessels and for transporting various molecules including ions, fatty acids, and amino acids throughout the body (Merlot et al., 2014). In contrast to its homeostatic functions in the blood, albumin has been shown to induce epileptiform activity through activation of transforming growth factor beta (TGF β) signaling upon penetration into the brain (Bar-Klein et al., 2014; Cacheaux et al., 2009; Weissberg et al., 2015). Intriguingly, several studies demonstrate that extravasated albumin is taken up by astrocytes (Braganza et al., 2012; Mihály & Bozóky, 1984; Senatorov et al., 2019; van Vliet et al., 2007) *via* TGF β receptors (Bar-Klein et al., 2014; Cacheaux et al., 2009; Ivens et al., 2007). Albumin uptake induces functional adaptations in astrocytes that play a role in the pathophysiology of epilepsy, including excitatory synaptogenesis, impaired K⁺ buffering, and production of pro-inflammatory cytokines (David et al., 2009; Frigerio et al., 2012; Ivens et al., 2007; Weissberg

et al., 2015). Of particular relevance for this thesis is a finding showing that *intraventricularly* injected albumin is taken up by hippocampal astrocytes decreasing coupling efficiency in these cells 24 h post injection (Braganza et al., 2012). Accordingly, TGF β signaling-dependent transcriptional downregulation of astrocytic Cxs and Kir4.1 has been demonstrated in the murine brain 24 h after albumin application (Cacheaux et al., 2009; David et al., 2009; Ivens et al., 2007). Together, these data suggest that albumin-induced TGF β signaling disrupts astrocytic spatial K⁺ buffering to promote hyperexcitability (Henning et al., 2021). So far, however, no study has examined this hypothesis in experimental TLE. Indirect evidence for this hypothesis comes from two studies showing that inhibition of TGF β 1 signaling attenuates not only KA-induced acute seizures but also astrogliosis (Zhang et al., 2019, 2020). Similarly, in a recent study inhibition of the TGF β R1/activin-like kinase (ALK)-5 has been demonstrated to mitigate KA-induced acute seizures (Greene et al., 2022).

In conclusion, accumulating evidence suggests a role of BBB dysfunction and albumin extravasation for the development of human and experimental epilepsy. Interestingly, the pro-convulsive effects of albumin appear to be mediated by TGF β -signaling dependent impairments of essential astrocyte functions, particularly loss of GJ coupling. However, direct experimental evidence for this hypothesis is currently lacking.

2. Aims of this thesis

As outlined in the previous introduction, ample evidence suggests a causal relationship between inflammation, glial reactivity and the pathophysiology of MTLE-HS (Aronica et al., 2017; Vezzani et al., 2011). In particular, loss of functional astrocyte GJ coupled networks constitutes a hallmark of MTLE-HS and could play a key role in epileptogenesis (Bedner et al., 2015; Pannasch et al., 2011; Wallraff et al., 2006). At present, however, little is known about the molecular mechanisms that lead to impaired astrocyte GJ coupling in epilepsy. Above all, the pathophysiological significance of a dysfunctional astrocyte network for the development and progression of epilepsy has not yet been adequately addressed. For this reason, the main objective of this PhD thesis is to identify the mechanisms and consequences of astrocyte GJ uncoupling in the pathology of MTLE-HS. To this end, this work is divided into three chapters, each represented by an individual publication, dealing with the following aspects:

(I) *To define the contribution of reactive microglia to astrocyte dysfunction and epileptogenesis as well as to determine the cellular source of the pro-inflammatory cytokine TNF α in MTLE-HS:* Although neuroinflammation and microglial reactivity are well-described phenomena in both experimental and human epilepsy, the contribution of both factors to epileptogenesis is less well understood (Aronica et al., 2017; Vezzani et al., 2011). Hence, in chapter three the impact of microglia-mediated neuroinflammation on astrocyte dysfunction and epilepsy development in KA-induced MTLE-HS was examined. In particular, we sought to identify whether microglia constitute the primary source of the pro-inflammatory cytokine TNF α , which we have previously shown to be rapidly upregulated and to promote epileptogenesis in the *intracortical* KA model (Müller, 2018). We hypothesized that reactive microglia are major producers of pro-inflammatory TNF α and act as drivers of epileptogenesis following *intracortical* KA injection.

(II) *To examine the consequences of seizure-induced BBB dysfunction and albumin extravasation for astrocyte network functioning and epileptogenesis in MTLE-HS.* Previous data demonstrate a correlation between BBB dysfunction and epilepsy development (Greene et al., 2022; Löscher & Friedman, 2020). A leaky BBB has been shown to lead to extravasation of serum albumin into the brain, which is thought to exert a pro-convulsive effect by impairing essential astrocyte functions in a TGF β -signaling dependent manner (David et al., 2009; Frigerio et al., 2012; Ivens et al., 2007; Weissberg et al., 2015). Therefore, chapter four of this doctoral thesis investigates the hypothesis that BBB impairments and concomitant albumin-

induced TGF β -signaling in astrocytes are crucially involved in astrocyte dysfunction and epileptogenesis.

(III) *To evaluate the role of the astroglial gap junction-coupled network in the development and progression of MTLE-HS.* The contribution of astroglial syncytia to the pathophysiology of epilepsy is controversially discussed, as these networks possess both anti- as well as pro-epileptic properties (Deshpande et al., 2020). However, previously published data from this lab suggest that the pro-epileptic aspects of dysfunctional interastrocytic GJ coupling may predominate (Wallraff et al., 2006), but conclusive evidence regarding the impact of impaired GJ coupling on epilepsy development is lacking. To resolve this conflict, chapter five of this study examines the consequences of genetic deletion of Cx30 and Cx43 in mouse astrocytes on the susceptibility to KA-induced MTLE-HS. More specifically, we hypothesized that a dysfunctional astrocyte GJ-coupled network would aggravate epilepsy pathology in response to *intracortical* KA-injection.

Taken together, the data of my PhD thesis will help to improve our understanding of the contribution of the astroglial GJ-coupled network to the development of epilepsy and will shed light on the mechanisms that lead to astrocyte uncoupling during early epileptogenesis.

3. Reactive microglia are the major source of tumor necrosis factor alpha and contribute to astrocyte dysfunction and acute seizures in experimental temporal lobe epilepsy

Lukas Henning, Henrike Antony, Annika Breuer, Julia Müller, Gerald Seifert, Etienne Audinat, Parmveer Singh, Frederic Brosseron, Michael T. Heneka, Christian Steinhäuser, Peter Bedner

The following chapter summarizes a research article that was published on September, 8th, 2022 in the journal GLIA under the terms of the Creative Commons Attribution-NonCommercial-NoDerivatives 4.0 International License (CC BY-NC-ND 4.0; <https://creativecommons.org/licenses/by-nc-nd/4.0/>). No changes to the original publication provided here were made. © 2022 The Authors. GLIA published by Wiley Periodicals LLC. <https://doi.org/10.1002/glia.24265>

3.1 Summary of the publication

Neuroinflammation is nowadays considered a hallmark of epilepsy (Aronica et al., 2017; Vezzani et al., 2011). Microglia, the innate immune cells of the brain, are the key regulatory element responsible for a coordinated immunological response to injury and disease in the CNS (Prinz et al., 2019). This coordinated response requires the transformation of ‘resting’ or ‘surveying’ microglia (Hanisch & Kettenmann, 2007) into immunologically activated or reactive microglia, characterized by a multitude of morphological, molecular and functional phenotypic adaptations (Prinz et al., 2019). Although reactive microglia have been well described in human and experimental epilepsy, their precise role in the pathology of MTLE-HS remains incompletely understood (Altmann et al., 2022; Avignone et al., 2008; Eyo et al., 2017; Morin-Brureau et al., 2018; Srivastava et al., 2018). Importantly, reactive microglia release several pro-inflammatory cytokines following epileptogenic brain insults that potentially influence the course of disease (Benson et al., 2015; Sano et al., 2021; Wang et al., 2015). In particular, the pro-inflammatory cytokine TNF α is thought to play a key role in the development of MTLE-HS, as it possesses various neuromodulatory and seizure-promoting properties (Patel et al., 2017; Santello & Volterra, 2012; Weinberg et al., 2013). However, the cellular source of TNF α in epilepsy is not well described, as several CNS-resident and infiltrating cells are capable to produce and release the cytokine (Beattie et al., 2002; Lieberman et al., 1989; Varvel et al., 2016). Moreover, the mechanism by which pro-inflammatory TNF α contributes to

epileptogenesis has not been adequately investigated. Loss of astrocyte GJ coupling occurs rapidly in experimental MTLE-HS and can be induced *in vitro* by application of TNF α (Bedner et al., 2015; Haghikia et al., 2008), highlighting dysfunctional coupling and concomitant impairments in ion homeostasis as potential mediators of the pro-epileptic effects of TNF α . To shed light on these clinically relevant questions, we combined genetic and pharmacological manipulations of microglia to study their contribution to TNF α production, astrocyte GJ uncoupling and epileptogenesis in a mouse model of MTLE-HS (Henning et al., 2022). First, we utilized immunohistochemistry and confocal microscopy to delineate the time course of microglia activation and monocyte infiltration after KA-induced SE. Enzyme-linked immunosorbent assay (ELISA) and quantitative polymerase chain reaction (qPCR) further enabled us to examine TNF α production and TNF receptor expression during the early and latent stages of epilepsy. Finally, telemetric EEG recordings and immunohistochemistry were employed to assess the chronic seizure burden and epilepsy-induced morphological alterations in microglia-specific TNF α knock-out and microglia-depleted mice.

Stereological analyses revealed profound and persistent morphological microglial reactivity developing rapidly (4 h) after *intracortical* KA injection. Reactive microglia further exhibited increased expression of the macrophage activation marker CD68 and were accompanied ipsilaterally by CD169-positive infiltrating monocytes during the latent and early chronic phases of epilepsy. Partial microglia depletion using the CSF1R inhibitor PLX5622 prevented seizure-induced astrocyte GJ uncoupling but only slightly affected astrocytic morphological changes in response to SE. Importantly, PLX treatment attenuated KA-induced acute seizures but simultaneously increased mortality in mice, indicating the need for more targeted microglial manipulation in epilepsy. Importantly, inducible microglia-specific TNF α knock-out almost completely prevented KA-induced elevations in hippocampal TNF α tissue concentrations as well as astrocyte GJ uncoupling. Combined gene expression analysis and immunohistochemistry further revealed upregulation of TNFR1 in astrocytes, indicating that microglia-derived TNF α acts *via* TNFR1 signaling to compromise astrocyte homeostatic functions during SE. However, microglia-specific TNF α knock-out did neither affect acute or chronic seizure burden nor neurodegeneration in experimental MTLE-HS. In contrast, astro- as well as microgliosis were significantly attenuated during the chronic phase of epileptogenesis in mice lacking microglial TNF α (Henning et al., 2022).

Collectively, this study illustrates the important role of reactive microglia and microglia-derived TNF α for astrocyte dysfunction and epileptogenesis. By combining microglia-specific

genetic manipulation with biochemical analyses we could identify microglia as the source of pro-inflammatory TNF α during early epileptogenesis. Both pharmacological depletion of microglia as well as genetic deletion of TNF α in microglia prevented early seizure-induced astrocyte GJ uncoupling, suggesting dysfunctional microglia-astrocyte communication as a potential disease-modifying factor in epilepsy. Moreover, the PLX-induced increase in mortality after KA injection underscores the need for highly specific microglia manipulation and reprogramming in epilepsy, as microglia also appear to exert protective effects in the pathology (Fumagalli et al., 2018; Wu et al., 2020). To our surprise, microglia-specific TNF α deletion did not affect acute or chronic seizure severity in our model. Previously, TNF α has been shown to exert primarily pro-epileptic effects *via* TNFR1, but to possess anti-epileptic properties when signaling through TNFR2 (Balosso et al., 2005; Weinberg et al., 2013). Hence, the lack of effect of TNF α deletion in microglia in our model could stem from the antithetical effects of TNFR1 vs TNFR2 signaling. The upregulation of TNFR1 in astrocytes further suggests that activation of the TNF α /TNFR1 axis plays a pivotal role in astrocyte dysfunction and underlies the pro-epileptic effects of aberrant TNF α signaling in experimental epilepsy, described previously (Müller, 2018). Therefore, future studies should investigate in more detail the role of astrocyte TNFR1 signaling for the genesis of epilepsy.

3.2 Statement of contribution



Christian Steinhäuser, Peter Bedner and Michael T. Heneka conceived the project. Lukas Henning, Julia Müller and Peter Bedner performed all surgical procedures necessary for the experimental induction of epilepsy and EEG transmitter transplantation. Lukas Henning and Julia Müller performed tracer diffusion experiments. Harvesting of cells for gene expression studies was done by Henrike Antony, Lukas Henning and Peter Bedner. Acquisition and analysis of gene expression data was performed by Henrike Antony, Annika Breuer and Gerald Seifert. Immunohistochemical staining and image acquisition were conducted by Lukas Henning, Henrike Antony and Annika Breuer. ELISA was performed by Lukas Henning under supervision of Frederic Brosseron. All statistical analyses and visualizations were conducted by Lukas Henning. Microglia-specific TNF α knock-out mice were kindly provided by Etienne Audinat. Gerald Seifert took care of the breeding and genotyping of the animals. Parmveer Singh kindly provided the PLX5622 compound as part of a material transfer agreement. Lukas Henning, Christian Steinhäuser and Peter Bedner wrote the manuscript.

3.3 Publication

Henning, L., Antony, H., Breuer, A., Müller, J., Seifert, G., Audinat, E., Singh, P., Brosseron, F., Heneka, M. T., Steinhäuser, C., & Bedner, P. (2022). Reactive microglia are the major source of tumor necrosis factor alpha and contribute to astrocyte dysfunction and acute seizures in experimental temporal lobe epilepsy. *Glia*. Advance online publication. <https://doi.org/10.1002/glia.24265>

RESEARCH ARTICLE

Reactive microglia are the major source of tumor necrosis factor alpha and contribute to astrocyte dysfunction and acute seizures in experimental temporal lobe epilepsy

Lukas Henning¹ | Henrike Antony¹ | Annika Breuer¹ | Julia Müller¹ |
Gerald Seifert¹ | Etienne Audinat² | Parmveer Singh³ | Frederic Brosseron⁴ |
Michael T. Heneka⁵ | Christian Steinhäuser¹  | Peter Bedner¹ 

¹Institute of Cellular Neurosciences, Medical Faculty, University of Bonn, Bonn, Germany

²Institute of Functional Genomics, University of Montpellier, CNRS, INSERM, Montpellier, France

³Plexxikon Inc., Berkeley, California, USA

⁴German Center for Neurodegenerative Diseases (DZNE), Bonn, Germany

⁵Université du Luxembourg, Esch-sur-Alzette, Luxembourg

Correspondence

Christian Steinhäuser, Institute of Cellular Neurosciences, Medical Faculty, University of Bonn, Venusberg-Campus 1, 53105 Bonn, Germany.

Email: cste@uni-bonn.de

Funding information

BMBF, Grant/Award Numbers: 01DN20001, 16GW0182; EU, Grant/Award Number: H2020-MSCA-ITN

Abstract

Extensive microglia reactivity has been well described in human and experimental temporal lobe epilepsy (TLE). To date, however, it is not clear whether and based on which molecular mechanisms microglia contribute to the development and progression of focal epilepsy. Astroglial gap junction coupled networks play an important role in regulating neuronal activity and loss of interastrocytic coupling causally contributes to TLE. Here, we show in the unilateral intracortical kainate (KA) mouse model of TLE that reactive microglia are primary producers of tumor necrosis factor (TNF) α and contribute to astrocyte dysfunction and severity of *status epilepticus* (SE). Immunohistochemical analyses revealed pronounced and persistent microglia reactivity, which already started 4 h after KA-induced SE. Partial depletion of microglia using a colony stimulating factor 1 receptor inhibitor prevented early astrocyte uncoupling and attenuated the severity of SE, but increased the mortality of epileptic mice following surgery. Using microglia-specific inducible TNF α knockout mice we identified microglia as the major source of TNF α during early epileptogenesis. Importantly, microglia-specific TNF α knockout prevented SE-induced gap junction uncoupling in astrocytes. Continuous telemetric EEG recordings revealed that during the first 4 weeks after SE induction, microglial TNF α did not significantly contribute to spontaneous generalized seizure activity. Moreover, the absence of microglial TNF α did not affect the development of hippocampal sclerosis but attenuated gliosis. Taken together, these data implicate reactive microglia in astrocyte dysfunction and network hyperexcitability after an epileptogenic insult.

KEYWORDS

astrocyte, gap junction coupling, hippocampal sclerosis, microglia, temporal lobe epilepsy, tumor necrosis factor alpha

This is an open access article under the terms of the [Creative Commons Attribution-NonCommercial-NoDerivs](https://creativecommons.org/licenses/by-nc-nd/4.0/) License, which permits use and distribution in any medium, provided the original work is properly cited, the use is non-commercial and no modifications or adaptations are made.

© 2022 The Authors. *GLIA* published by Wiley Periodicals LLC.

1 | INTRODUCTION

Accumulating clinical and experimental evidence indicates that neuroinflammation contributes to the pathophysiology of epilepsy (Aronica et al., 2017; Devinsky et al., 2013; Gershen et al., 2015; Löscher et al., 2020). Microglia are critical regulators of central nervous system (CNS) immunity and are highly reactive to various types of brain insults, including *status epilepticus* (SE), ischemia or infection (Eyo et al., 2014; Hanisch & Kettenmann, 2007; Qin et al., 2019; Rock et al., 2004). Importantly, there exist numerous reports of reactive microglia in both human and animal models of epilepsy (Broekaart et al., 2018; Feng et al., 2019; Hiragi et al., 2018; Morin-Bureau et al., 2018; Zattoni et al., 2011). In experimental temporal lobe epilepsy (TLE), microglia are characterized by an amoeboid morphology (De Simoni et al., 2000; Wyatt-Johnson et al., 2017), production of proinflammatory cytokines (Aronica et al., 2007; Benson et al., 2015; Sano et al., 2021; Varvel et al., 2016) as well as increased proliferation and enhanced K^+ conductance (Avignone et al., 2008; Feng et al., 2019). However, even though the link between reactive microglia and epilepsy is well documented, mechanistically the contribution of microglia to the pathophysiology of epilepsy is still incompletely understood.

A number of studies show that tumor necrosis factor alpha ($TNF\alpha$) transcript and protein levels increase rapidly in brain parenchyma and microglia following SE (Benson et al., 2015; De Simoni et al., 2000; Lehtimäki et al., 2003; Nikolic et al., 2018; Sano et al., 2021; Vezzani et al., 2002). Moreover, $TNF\alpha$ signaling increases seizure susceptibility (Patel et al., 2017; Probert et al., 1995; Rana & Musto, 2018; Riazzi et al., 2008; Weinberg et al., 2013). It remains unclear, however, whether microglia constitute the primary source of $TNF\alpha$ in experimental TLE, as other cells including astrocytes and infiltrating monocytes, are also immunocompetent (Devinsky et al., 2013; Vezzani et al., 2011). Previously, we have shown that disruption of astrocytic gap junction (GJ) coupling and concomitant impairments in extracellular K^+ buffering temporally precede neuronal cell death and spontaneous seizure development in a mouse model of kainate (KA)-induced TLE, pointing to a causal involvement in the genesis of the disease (Bedner et al., 2015). The seizure-induced decrease in coupling could be mimicked *in situ* by incubation of acute hippocampal slices with a combination of interleukin 1β (IL 1β) and $TNF\alpha$ (Bedner et al., 2015). Similarly, both treatment of cultured primary astrocytes with $TNF\alpha$ as well as co-culturing of astrocytes with activated microglia impair coupling efficiency (Haghikia et al., 2008; Mème et al., 2006). Together, these data suggest that microglial cytokines indirectly promote epileptogenesis, by reducing coupling efficiency and thus the K^+ and glutamate buffering capacity of astrocytes. In the present study, we therefore examined the contribution of reactive microglia and microglial $TNF\alpha$ to astrocyte GJ uncoupling and epileptogenesis in a mouse model of TLE. Pharmacological depletion of microglia using the colony-stimulating factor 1 receptor (CSF1R) inhibitor PLX5622 combined with microglia-specific inducible knock-out of $TNF\alpha$ were employed to assess the contribution of microglia to early astrocyte dysfunction and $TNF\alpha$ production following KA-

induced SE. Additionally, continuous telemetric electroencephalography (EEG) was combined with immunohistochemistry to investigate effects of $TNF\alpha$ depletion in microglia on acute and chronic epileptiform activity as well as the development of hippocampal sclerosis (HS).

2 | MATERIALS AND METHODS

2.1 | Animals

Male C57B6/J, FVB (Charles River, Sulzfeld, Germany) or GFAP-eGFP (Nolte et al., 2001) mice aged 90–120 days were used for the experiments. To study the effects of microglia specific knock-out of $TNF\alpha$ on epileptogenesis and astrocytic gap junction coupling, $Cx3cr1^{CreERT2}$ knock-in mice (Yona et al., 2013) were crossed with $TNF\alpha^{loxP/loxP}$ (Grievnikov et al., 2005) mice to yield $Cx3cr1^{CreERT2/+}-TNF\alpha^{loxP/loxP}$ and $Cx3cr1^{CreERT2/+}-TNF\alpha^{+/+}$ were used. Maintenance and handling of animals were performed according to EU and local governmental regulations. Experiments were approved by the North Rhine–Westphalia State Agency for Nature, Environment and Consumer Protection (approval number 84-02.04.2015.A393 and 81-02.04.2020.A420). All measures were taken to minimize the number of animals. Mice were kept under standard housing conditions (12 h/12 h dark–light cycle) with food and water provided *ad libitum*.

2.2 | Drugs

2.2.1 | Tamoxifen treatment

To induce site-specific recombination of loxP-flanked sequences, $Cx3cr1^{CreERT2/+}-TNF\alpha^{loxP/loxP}$ and $Cx3cr1^{CreERT2/+}-TNF\alpha^{+/+}$ mice received intraperitoneal (i.p.) injections of tamoxifen (Sigma-Aldrich, #T5648, Steinheim, Germany) dissolved in sunflower seed oil (Sigma-Aldrich, #88921) and EtOH at a ratio of 1:10. Mice were injected daily for 5 consecutive days receiving 2 mg per day of tamoxifen (100 μ l per mouse). A comparable treatment regimen has previously been shown to induce high site-specific recombination in the CNS of this Cre-mouse line (Goldmann et al., 2013). Mice were used for experiments ~30 days after tamoxifen administration in order to restrict Cre-mediated recombination to microglia (Parkhurst et al., 2013). Tamoxifen-injected $Cx3cr1^{CreERT2/+}-TNF\alpha^{+/+}$ mice served as the control group (CTRL).

2.2.2 | PLX5622 treatment

PLX5622 was provided by Plexikon Inc. (Berkeley, CA 94710, USA) and formulated in AIN-76A standard chow by Research Diets Inc. (New Brunswick, NJ 08901 USA) at 1200 ppm. Male FVB or C57B6J mice were fed with either a PLX5622-containing or AIN-76A control



diet for 7, 21, or 28 consecutive days before the start of the experiments. Twenty-one days of oral PLX5622 application have previously been shown to almost completely deplete IBA1⁺ microglia from the brain (Dagher et al., 2015). The diet was provided *ad libitum* and food intake was monitored by weighing the amount of diet consumed by the animals.

2.3 | Unilateral intracortical kainate injection and implantation of telemetric EEG transmitters

We employed the TLE-HS animal model as described previously (Bedner et al., 2015; Deshpande et al., 2020; Henning et al., 2021). Briefly, mice were anesthetized with a mixture of medetomidine (Cepetor, CP-Pharma, Burgdorf, Germany, 0.3 mg/kg, i.p.) and ketamine (Ketamidol, WDT, Garbsen, Germany, 40 mg/kg, i.p.) and placed into a stereotaxic frame equipped with a manual microinjection unit (David Kopf; Tujunga, CA, USA). A total volume of 70 nl of a 20 mM solution of KA (Tocris, Bristol, UK) dissolved in 0.9% sterile NaCl was stereotaxically injected into the neocortex just above the right dorsal hippocampus. The stereotaxic coordinates were: 2 mm posterior to bregma, 1.5 mm from midline, and 1.7 mm from the skull surface. Sham control mice received injections of 70 nl saline under the same conditions. Immediately after KA injection, two drill holes were made at 1 mm posterior to the injection site and 1.5 mm lateral from midline to insert two monopolar leads required for electrographic seizure detection. Telemetric transmitters (TA10EA-F20 or TA11ETA-F10; Data Sciences International (DSI), St. Paul, MN, USA) were implanted subcutaneously into the right abdominal region and the two monopolar leads were inserted ~1 mm deep into the cortex. Attached leads were fixed to the skull using superglue and covered with dental cement. The scalp incision was subsequently sutured and anesthesia stopped with atipamezol (Antisedan, Orion Pharma, Hamburg, Germany, 300 mg/kg, i.p.). To reduce pain, mice were injected with carprofen for 3 days (Rimadyl, Pfizer, Karlsruhe, Germany). Moreover, 0.25% Enrofloxacin (Baytril, Bayer, Leverkusen, Germany) was administered via drinking water to reduce the risk of infection. After surgery, mice were returned to clean cages and placed on individual radio receiving plates (RPC-1; Data Sciences International, New Brighton, MN, USA), which capture data signals from the transmitter and send them to a computer running Ponemah software (Version 5.2, Data Sciences International). EEG recordings (24 h/day, 7 days/week) were started directly after transmitter implantation and continued for 28 days after SE induction.

2.4 | EEG data analysis

EEG data was analyzed using NeuroScore (version 3.4.0) software (Data Sciences International) as described previously (Henning et al., 2021). Briefly, recordings were high pass filtered at 1 Hz and the number of seizures, their duration and spike numbers were determined using the spike train analysis tool implemented in NeuroScore

based on the following criteria: threshold value = $7.5 \times \text{SD}$ of the baseline (i.e., activity during artifact- and epileptiform-free epochs four weeks after SE) – 1000 μV , spike duration = 0.1–50 ms, spike interval = 0.1–2.5 s, minimum train duration = 30 s, train join interval = 1 s, minimum number of spikes = 50. The number of artifacts was minimized by repeating the spike train analysis with a threshold ranging from the maximum amplitude of actual epileptiform spikes (i.e., determined subjectively by manually scrolling through the EEG recording) – 1000 μV and subsequently subtracting that value from the value obtained during initial spike quantification (i.e., $7.5 \times \text{SD}$ of the baseline – 1000 μV). Fast Fourier transformation (FFT) was conducted to derive absolute δ (0.5–4 Hz), θ (4–8 Hz), α (8–13 Hz), β (13–30), and γ (30–50 Hz) power values, which were normalized to baseline activity prior to conducting statistics. The number of spontaneous generalized seizures during the chronic phase was determined manually from the EEG recordings by two experienced experimenters. Finally, to analyze EEG activity during SE in PLX5622 treated mice, spike number and EEG band power were normalized to the activity during the postictal state. For that, activity during at least five postictal periods lasting ~10 s was quantified. The spike threshold was set at $10 \times \text{SD}$ of baseline activity during the postictal state. All animals included in the study developed SE. Three animals (2 PLX and 1 control mice) were excluded from the analysis because the EEG signal was too noisy to allow accurate quantification of the baseline EEG activity.

2.5 | Whole-cell patch clamp and biocytin-filling of astrocytes

Mice were anesthetized with isoflurane (Piramal Healthcare, Morpeth, UK) and decapitated. Brains were quickly removed and 200 μm -thick coronal slices were cut on a vibratome (VT1000S, Leica Microsystems, Wetzlar, Germany) in ice cold preparation solution containing (in mM): 87 NaCl, 2.5 KCl, 1.25 NaH_2PO_4 , 25 NaHCO_3 , 7 MgCl_2 , 0.5 CaCl_2 , 25 glucose, 75 sucrose, equilibrated with carbogen to stabilize pH (5% CO_2 /95% O_2 , pH 7.4). After storage of slices (15 min, 35°C) in preparation solution, slices were transferred to a solution containing (in mM): 126 NaCl, 3 KCl, 2 MgSO_4 , 2 CaCl_2 , 10 glucose, 1.25 NaH_2PO_4 , 26 NaHCO_3 , gassed with carbogen (aCSF). To aid identification of astrocytes in the tissue, aCSF was supplemented with SR101 (1 μM , Sigma Aldrich, S7635, incubation 20 min, 35°C) (Kafitz et al., 2008). After SR101 staining, slices were transferred to aCSF and kept at room temperature (RT) for the duration of the experiments. For recordings, slices were transferred to a recording chamber and constantly perfused with aCSF. Patch pipettes fabricated from borosilicate capillaries with a resistance of 3–6 $\text{M}\Omega$ were filled with a solution containing (in mM): 130 K-gluconate, 1 MgCl_2 , 3 $\text{Na}_2\text{-ATP}$, 20 HEPES, 10 EGTA and biocytin (0.5%, Sigma Aldrich) (pH 7.2, 280–285 mOsm). To analyze gap junction coupling, whole-cell patch clamp recordings of SR101-positive astrocytes were performed during which astrocytes were filled with biocytin (20 min, RT). In addition to SR101 staining, astrocytes were identified by their characteristic morphology,

passive current–voltage relationship, low input resistance and a resting membrane potential close to the Nernst potential of K^+ . Current signals were amplified (EPC 8, HEKA Electronic, Lambrecht, Germany), filtered at 3 or 10 kHz, and sampled at 10 or 30 kHz (holding potential -80 mV). Online analysis was performed with TIDA 5.25 acquisition and analysis software for Windows (HEKA) and Igor Pro 6.37 software (WaveMetrics, Lake Oswego, OR, USA). Voltages were corrected for liquid junction potentials. Only recordings matching the following criteria were included in the analysis: (i) resting potential negative to -60 mV, (ii) membrane resistance ≤ 10 M Ω , and (iii) series resistance ≤ 20 M Ω . After the recording, slices containing a biocytin-filled astrocyte were stored in 4% paraformaldehyde (PFA)-containing phosphate buffered saline (PBS) overnight at 4°C and subsequently transferred into PBS and stored at 4°C until immunohistochemistry.

2.6 | Immunohistochemistry

2.6.1 | Tissue preparation

Animals were deeply anaesthetized by i.p. injection with 100–120 μl of a solution containing 40 mg/kg ketamine (WDT) and 0.3 mg/kg, medetomidine (CP-Pharma). After checking for hind paw reflexes, transcardial perfusion was applied with ice-cold PBS (30 ml) followed by 4% ice-cold PFA in PBS (30 ml). Brains were removed and stored for 24–48 h in 4% PFA-containing solution and subsequently stored in PBS at 4°C until slicing. Brains were cut into 40 μm thick coronal slices using a Leica VT1200S vibratome (Leica Microsystems).

2.6.2 | Antibody staining

Immunohistochemistry was performed using free-floating slices kept in 24-well plates. Slices from the dorsal hippocampus close to the KA injection site were used. For membrane permeabilization and blocking of unspecific epitopes, slices were incubated (1–2 h, RT) with 0.5% Triton X-100 (or 2% for staining of biocytin-filled astrocytes) and 10% normal goat or donkey serum (NGS, NDS) in PBS. Slices were subsequently incubated overnight with primary antibody solution containing PBS on a shaker at 4°C . The following primary antibodies were applied: rat anti-CD68 (1:200, BioRad Laboratories, MCA1957, Munich, Germany), rat anti-CD169 (1:400, BioRad Laboratories, MCA884), rabbit anti-GFAP (1:500, DAKO, Z0334, Hamburg, Germany), rabbit anti-IBA1 (1:400, Wako Chemicals, #019-19741, Neuss, Germany), mouse anti-NeuN (1:200, Merck Millipore, MAB377, Darmstadt, Germany), rabbit anti-Tmem119 (1:500, Abcam, ab209064), rabbit anti-TNFR1 (1:100, Abcam, ab19139, Berlin, Germany). On the following day, slices were washed three times with PBS for 5–10 min each and subsequently incubated with secondary antibodies conjugated with Alexa Fluor[®] 488, Alexa Fluor[®] 647, streptavidin-conjugated Alexa Fluor[®] 647 (1:500, 1:600 respectively, Invitrogen, Karlsruhe, Germany) or streptavidin-conjugated Cy3

antibody (1:300, Sigma Aldrich, S6402) in PBS (2% NGS, 1.5–2 h, RT). For staining of NeuN, slices were incubated with goat anti-mouse biotin (1:500, Dianova, AB_2338557, Hamburg, Germany) prior to incubation with streptavidin-conjugated Cy3 antibody (1 h, RT). After washing slices again three times with PBS (5–10 min), nuclear staining with Hoechst (1:200, diluted in dH_2O) was performed (10 min, RT). A final washing step ($3 \times$ PBS, 5 min each) was performed and slices were mounted with Aquapolymount (Polysciences, Heidelberg, Germany) on objective slides and covered with cover slips. Slides were stored at 4°C before confocal imaging.

2.6.3 | Confocal microscopy

A confocal laser scanning microscope (SP8, Leica, Hamburg, Germany) at 8 bit using $10\times$ (numerical aperture (NA): 0.4) $20\times$ (NA: 0.75), $40\times$ (NA: 1.1), and $63\times$ (NA: 1.2) objectives was used. Image resolution was set at 1024×1024 pixels recorded at a speed of 400 Hz, with a pinhole size of 1 airy unit (AU). Standard photomultiplier tubes or hybrid detectors were used for detection of fluorescent signals. Laser and detector settings were applied equally to all images acquired. Z-stacks were recorded at 0.36 μm (TNFR1), 0.42 μm (CD68), 1 μm (IBA1 & GFAP morphology, CD169), or 2 μm (GJ coupling & Hippocampal sclerosis) intervals.

2.7 | Quantification of immunostainings

2.7.1 | Microglial/macrophage morphology

Microglia/macrophage morphology was quantified based on IBA1 staining using the publicly available (<https://github.com/hansenjn/MotiQ>) plugin MotiQ for FIJI (Schindelin et al., 2012). Two to four IBA1⁺ cells per image were cropped out of 30 μm z-stacks ($40\times/1.1$ NA objective, region of interest (ROI): $242.42 \times 242.42 \times 30 \mu\text{m}^3$) from each condition to create single-cell images. Next, single-cell images were binarized by application of an automated intensity threshold (Otsu for KA experiments and Moments for PLX5622 experiments) to 0.5 scaled maximum intensity projections (MIPs) of the original image. Binary single-cell images were further filtered by removing all particles smaller than 100 voxels from the image. Finally, 3D reconstructions and skeletons were generated from which cell volume, average and total process length, ramification and polarity index were quantified and statistically compared between conditions. A Gauss filter ($\sigma = 2$) was applied prior to skeletonization. The ramification index indicates the complexity of the cell's shape using the following equation:

$$\text{Ramification index} = \frac{\text{cell surface area}}{4\pi \times \left(\frac{3 \times \text{cell volume}}{4\pi}\right)^{\frac{2}{3}}} \quad (1)$$

The polarity index was defined as:

$$\text{Polarity index} = \frac{\text{convex hull center} - \text{cell center}}{2 \times \sqrt[3]{\frac{3 \times \text{convex hull volume}}{4\pi}}} \quad (2)$$

and indicates the degree of unbalance in the distribution of processes emanating from the cell's soma (Fülle et al., 2018). The density of IBA1⁺ and CD169⁺ (ROI: 242.42 × 242.42 × 30–32 μm³) cells was quantified using the spot detection algorithm implemented in IMARIS 8.0 (Bitplane, Zurich, Switzerland).

2.7.2 | Microglia and astrocyte morphology and marker expression in PLX5622 experiments

The number of IBA1⁺ cells as well as the total volume occupied by the microglia-specific marker Tmem119 in PLX5622-treated FVB mice were determined in 3D images recorded using either a 10×/0.4 NA objective (IBA1; ROI: 969.70 × 969.70 × 15 μm³) or 40×/1.1 NA objective (Tmem119; ROI: 242.42 × 242.42 × 15–17 μm³) using the spot and surface detection algorithms implemented in IMARIS 8.0, respectively. Moreover, astrocyte morphology was determined based on GFAP staining in 3D images (63×/1.2 NA objective; ROI: 153.92 × 153.92 × 30 μm³) using the in-built Autopath algorithm implemented in IMARIS 8.0. Reconstruction parameters were kept identical across all images analyzed.

2.7.3 | Quantification of CD68 and IBA1 volumes

Custom-written macros in FIJI were used to determine the volume of CD68 and IBA1 signals occupied in each image (40×/1.1 NA objective; ROI: 242.42 × 242.42 × 20–22 μm³). Images were background subtracted (15 pixel rolling ball radius), median filtered (2 pixel radius) and subsequently binarized (Triangle for CD68 and Moments threshold for IBA1) after which the area occupied by the respective signal within each focal plane was quantified using the analyze particles function in FIJI. The obtained area values were subsequently summed up across all focal planes in order to obtain the total volume occupied by each signal.

2.7.4 | Colocalization of TNFR1 and GFAP

Colocalization analysis was performed with FIJI in TNFR1/GFAP double-stained hippocampal sections of KA-injected or control C57B6J mice. Images were recorded using a 63×/1.2 NA objective (ROI: 92.35 × 92.35 × 12 μm³). GFAP⁺ images were median filtered (3 pixel radius) and subsequently binarized (Triangle threshold). Image values of 0 and 1 were obtained by subtraction of the value 254 from the thresholded GFAP⁺ image. Next, the binary GFAP⁺ images and the TNFR1⁺ images were multiplied to derive the TNFR1 signal intensity in GFAP⁺ pixels. Signal intensities were

subsequently summed up across all focal planes to derive the total TNFR1 content in astrocytes. Cumulative TNFR1 signal intensity was divided by the total volume occupied by the GFAP signal to account for differences in GFAP expression between experimental conditions.

2.7.5 | Coupling efficiency of biocytin-filled astrocytes

Coupling efficiency was determined by manual counting of biocytin⁺ cells using the cell counter plugin implemented in FIJI and compared between injected (ipsilateral) and non-injected (contralateral) hemispheres. Another observer blinded to the experimental conditions recounted images of biocytin-filled astrocytes, and cell counts were subsequently averaged across both counts prior to statistical analysis.

2.7.6 | Hippocampal sclerosis

The extent of hippocampal sclerosis was estimated based on the quantification of four parameters: (i) the extent of granule cell dispersion (GCD) in the dentate gyrus (DG), (ii) the shrinkage of the CA1 *stratum radiatum*, (iii) the number of CA1 pyramidal neurons, and (iv) the extent of astrogliosis in CA1 *stratum radiatum*. GCD, *stratum radiatum* shrinkage and the number of CA1 pyramidal neurons were estimated in maximum intensity projections (MIPs) (ROI: 1163.64 × 1163.64 × 30–32 μm³). The extent of astrogliosis was measured in individually defined ROIs in CA1 *stratum radiatum* and subsequently normalized to ROI size. GCD quantification was performed as described previously (Deshpande et al., 2020; Henning et al., 2021). Briefly, GCL width was measured at four positions indicated as T1–T4. T1 and T2 were measured along a vertical line connecting the upper and lower cell layers of the DG, T3 and T4 at a distance halfway between the vertical line and the tip of the hilus. The average of the four values was used as an estimation of GCD. Shrinkage of the *stratum radiatum* was determined by drawing a vertical line connecting the pyramidal and molecular layer, above the highest point of the DG granule cell layer. The length of the vertical line served as an indication of the remaining width of the *stratum radiatum*. The extent of astrogliosis was measured by quantifying the area occupied by the GFAP signal in individual ROIs within all focal planes of each image. The total volume occupied by the GFAP signal was subsequently derived by summing up the area calculated across all focal planes and was normalized to the volume of the ROI prior to statistical analysis. Both GCD, *stratum radiatum* width and astrogliosis were quantified using FIJI software. The number of pyramidal neurons in the CA1 region was measured using the automated spot detection algorithm implemented in IMARIS8.0 within a 360 × 120 × 30 μm³ ROI placed within the CA1 pyramidal layer just above the highest point of the DG granule cell layer.

2.8 | Quantification of hippocampal TNF α concentrations

2.8.1 | Tissue preparation and biochemical extraction of hippocampal protein

Cx3cr1^{CreERT2/+}-TNF α ^{loxP/loxP} and Cx3cr1^{CreERT2/+}-TNF α ^{+/+} mice were transcardially perfused as described above. Dorsal hippocampi were quickly removed, weighed and flash frozen in liquid nitrogen before storage at -80°C until biochemical extraction. Frozen hippocampi were homogenized in homogenization buffer (1 \times PBS, 5 mM NaF, 20 mM pyrophosphate, 1 \times protease/phosphatase inhibitor (Cell Signaling, #5872, Frankfurt am Main, Germany)) using a Precellys[®] device (Bertin Instruments, Darmstadt, Germany) for 2 \times 15 s at 5000 rpm. Next, an equal volume of 2 \times RIPA buffer (50 mM Tris, 150 mM NaCl, 2% NP-40, 1% NaDOC, 0.2% SDS) was added to the sample, followed by sonication of the sample for 10 s and incubation on ice for 30 min. The homogenate was centrifuged for 30 min at 100,000g and the supernatant was collected. The total protein concentration in the supernatants was determined using a bicinchoninic acid (BCA) assay (Thermo Fisher Scientific, Bremen, Germany) according to the manufacturer's instructions.

2.8.2 | ELISA

For quantification of hippocampal TNF α concentrations an electrochemiluminescence ELISA (V-PLEX Mouse TNF- α Kit, K152QWD, MESO SCALE DIAGNOSTICS, LLC, Rockville, USA) was performed with a 1:1 sample dilution using the reagents supplied by the manufacturer and according to the manufacturer's instructions. Each sample was measured in duplicate and the average was normalized to the weight of hippocampal tissue and expressed as pg/mg tissue.

2.9 | Single-cell semiquantitative real time reverse transcription PCR

Single-cell transcript analysis was performed on astrocytes harvested from brain slices of the hippocampal CA1 region of KA-injected and non-injected C57B6J mice (Seifert et al., 2009). Astrocytes were identified by labeling with the fluorescent dye SR101 and based on electrophysiological characterization. Cells were aspirated into a patch pipette and expelled into reaction tubes filled with 3 μl DEPC-treated water, flash frozen in liquid nitrogen and stored at -20°C until the start of the RT-PCR. A reverse transcription reaction was started by adding 4.5 μl RT-mastermix containing RT-buffer (ThermoScientific), dNTPs (4 \times 250 μM , ThermoFisher), random hexamers (50 μM , Roche) RNasin (20 U, Promega), and Maxima H Minus reverse transcriptase (100 U, ThermoScientific) and incubated at 37°C for 1 h. Next, 40 μl of the mastermix were added to the RT product and a pre-amplification was performed for 20 cycles (denaturation at 94°C , 25 s; annealing at 51°C , 45 s; extension at 72°C , 25 s; final elongation

at 72°C , 7 min) with a thermocycler PTC-200 (MJ Research). The mastermix contained PCR buffer, MgCl_2 (2.5 mM), dNTPs (4 \times 50 μM), primers (200 nM each, Eurogentec), and 5 U Taq polymerase (Invitrogen). Thereafter, an aliquot of 1 μl was used as template for the real-time PCR using Takyon Mastermix (Eurogentec) or TaqMan universal PCR Mastermix for amplification of TNF α (Applied Biosystems), in a final volume of 12.5 μl . For detection and quantification of TNFR1, TNFR2, TNF α , and the reference genes GFAP and HPRT1, a Taqman primer/probe mix was used (Applied Biosystems). PCRs for the respective target and housekeeping genes were run in parallel wells for each sample as triplicates using a CFX384 Touch Real-Time PCR Detection System (BioRad Laboratories). Samples were incubated for 2 min at 50°C and after denaturation (10 min, 95°C), 50 cycles (denaturation at 95°C , 15 s; primer annealing and extension at 60°C , 60 s) were performed. The accumulation of the PCR product was detected by consecutively measuring the fluorescence intensity of the Taqman probe during each PCR cycle. The target gene/GFAP and target gene/HPRT1 expression ratios were determined by comparing C_T values of the target gene with those of the respective reference genes. The relative quantification of different genes was determined according to the following equation:

$$X_{\text{target}}/X_{\text{GFAP/HPRT1}} = E_{\text{GFAP/HPRT1}}^{\text{CT}_{\text{GFAP/HPRT1}}} / E_{\text{target}}^{\text{CT}_{\text{target}}} \quad (3)$$

yielding the gene ratio with X being the input copy number, E is the efficiency of amplification, and C_T is the cycle number at threshold detection. By quantification of target gene expression relative to GFAP or HPRT1, C_T was determined for each gene at the same fluorescence emission, R_n . The amplification efficiency was determined based on serial dilutions of mRNA and was 2.08 (HPRT1), 1.98 (GFAP), 2.03 (TNFR1), 2.02 (TNFR2), and 1.94 (TNF α). DEPC-water added to the RT-reaction served as a negative control.

2.10 | Statistical analysis

All statistical analyses were performed using R software (R Core Team, 2021, version 4.0.5, Austria) (R Core Team, 2021). Data are displayed as mean + standard deviation (SD) or as box plots representing median (line) and quartiles (25th and 75th percentile) with whiskers extending to the highest and lowest values within 1.5 times the interquartile range (IQR). Prior to statistical analysis, data were checked for normality by inspection of histograms and Q-Q plots as well as by applying a Shapiro-Wilk test. Levene's test was performed to check for homogeneity of variance between groups. In case of a significant deviation from normality, data were transformed according to Tukey's ladder of powers (Tukey, 1977) prior to conduction of statistical tests or by performing the appropriate non-parametric equivalent. For comparison of two independent groups, Student's t -test or Wilcoxon-rank sum test were used. More than two groups were compared with one-way analysis of variance (ANOVA) followed by post-hoc Tukey test or using Kruskal-Wallis test with Dunn's post-hoc test. p -Value

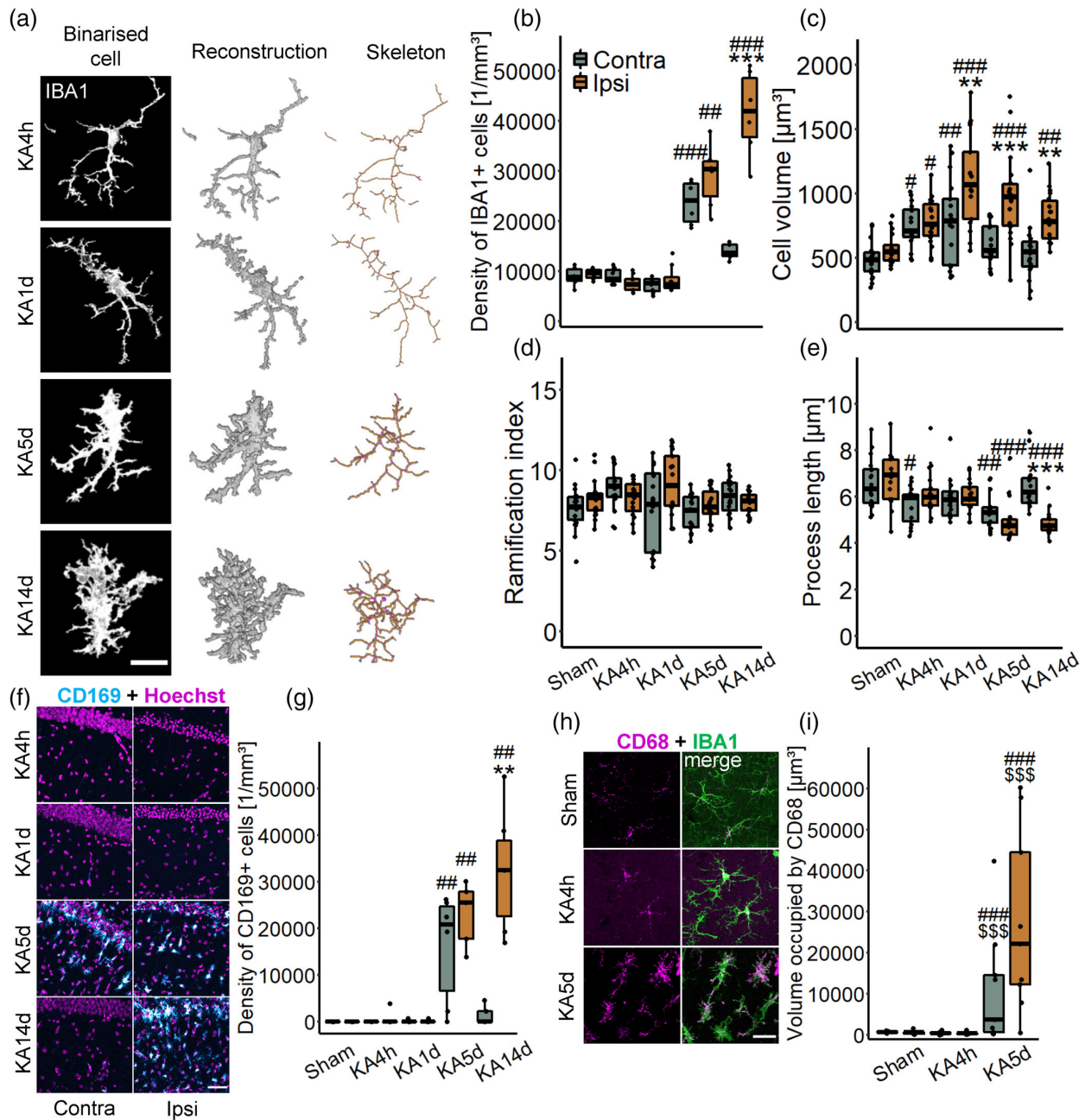


FIGURE 1 KA-induced TLE induces rapid microglia reactivity accompanied by delayed macrophage infiltration. (a) Representative images depicting the morphology of individual IBA1-positive cells in the ipsilateral hippocampal CA1 *stratum radiatum* of FVB mice at 4 h, 1, 5, and 14 days post SE induction. 3D reconstructions and skeletons were derived from the images to quantify the morphology of individual microglia/macrophages. Scale bar: 10 μm. (b–e) Quantitative analyses of density, volume, ramification index, and average process length of IBA1-positive cells indicate rapid and persistent activation of microglia/macrophages following KA-induced SE. $n = 15–20$ cells/condition, $N = 3$ mice/condition; two-way ANOVA; * versus contra, # versus sham. (f) Representative maximum intensity projection (MIPs) of CD169-positive macrophages (cyan) at 4 h, 5 days, and 14 days post SE induction. Scale bar: 50 μm. Images are background subtracted and brightness adjusted. (g) CD169 expression was increased in the hippocampal CA1 *stratum radiatum* during the latent and chronic periods, but not during SE. $n = 2–3$ slices/mouse, $N = 3$ mice/condition; two-way ANOVA; * versus contra, # versus sham. (h) Representative MIPs of a combined CD68 (magenta) and IBA1 (green) staining in the ipsilateral hippocampal CA1 *stratum radiatum* of sham- and KA-injected mice. Scale bar: 20 μm. Images depict a background subtracted and brightness adjusted region of interest (ROI) representative of the whole image. (i) CD68 expression was increased during the latent phase after KA-induced SE. $n = 3$ slices/mouse, $N = 3$ mice/condition; two-way ANOVA; # versus sham, \$ versus KA4h. Data are displayed as box plots representing median and quartiles. Black dots represent individual data points. ** $p < 0.01$, *** $p < 0.001$; # $p < 0.05$, ## $p < 0.01$, ### $p < 0.001$, \$\$\$ $p < 0.001$

adjustment for more than two groups was based either on Tukey's or the Benjamini–Hochberg method. For multifactorial data, two-way ANOVA or two-way aligned rank transform ANOVA (Wobbrock et al., 2011) were performed. Kaplan–Meier estimates were compared using a log-rank test and Fisher's exact test was used to analyze contingency tables. Differences between groups were considered statistically significant at $p < 0.05$. If not stated otherwise, “ n ” refers to the number of cells or slices, and “ N ” refers to the number of animals used.

3 | RESULTS

3.1 | Activation of innate immune cells in experimental TLE

Activation of microglial cells and invasion of neural tissue by blood-derived immune cells has been described in the sclerotic hippocampus of drug-resistant TLE patients and in various experimental epilepsy models (Broekaart et al., 2018; Di Nunzio et al., 2021; Feng et al., 2019; Morin-Brureau et al., 2018; Zattoni et al., 2011). In the unilateral intracortical KA mouse model of TLE with HS, which closely reproduces key features of the human condition, pronounced microgliosis was found in the chronically epileptic hippocampus (Deshpande et al., 2020). However, the time course of microglial activation during the early phase of epileptogenesis has not been studied in our model, and no information on immune cell infiltration is yet available. Here, we performed morphometric analysis of IBA1-immunolabeled cells in the hippocampal CA1 at different stages of KA-induced epileptogenesis to assess the temporal pattern of microglia activation. We focused on four different time points, representing the acute phase (i. e., before onset of neuronal death, 4 h post KA injection), the latent period (1 and 5 days) and the chronic phase (14 days) (Bedner et al., 2015). Microglial cell density, cell volume, branching index and average length of cell processes were quantified using 3D reconstructions and cytoskeletal predictions extracted from high-resolution confocal images (Figure 1a) and statistically compared between sham- and KA-injected mice as well as between the injected (ipsilateral) and non-injected (contralateral) hemispheres. The density of IBA1-positive cells remained unchanged 4 h and 1 day after KA injection, but increased markedly on the fifth day in the hippocampi of both hemispheres. While after two weeks innate immune cell density further increased on the ipsilateral side, it returned to baseline contralaterally (Figure 1b, see Table S2 for descriptive statistics of Figure 1). Hypertrophy of IBA1-positive cells was already detectable 4 h after KA injection (Figure 1c). Similar to the alterations in cell density, these changes, as well the reduction in process length (Figure 1e), were persistent ipsilaterally but transient on the contralateral side. However, ramification of IBA1-positive cells remained unchanged across all time points investigated (Figure 1d).

As not only microglia but also peripheral monocytes express IBA1, we next sought to determine to what extent the increased density of IBA1-positive cells resulted from microglial proliferation vs.

invasion of monocytes. For this purpose, we stained hippocampal slices from epileptic mice with the peripheral myeloid marker CD169 (Butovsky et al., 2012; Gao et al., 2015; Rice et al., 2015). CD169-positive cells were virtually absent 4 h and 1 day after KA, but abundant on both hemispheres after 5 days, and ipsilaterally after 14 days (Figure 1f,g). In order to test that in our model CD169 specifically labels peripheral monocytes, we performed double-staining of CD169 together with the microglia-specific marker Tmem119 (Bennett et al., 2016) 5 days post KA injection (Figure S1). Surprisingly, the staining revealed that a subset of CD169-positive cells also expressed Tmem119. Ipsilaterally, however, some CD169-positive cells were Tmem119-negative, which indicates monocyte infiltration.

To further characterize innate immune cell activation, we performed immunohistochemical staining for CD68, which is typically upregulated during inflammation by activated microglia/macrophages (Broekaart et al., 2018; Jurga et al., 2020). The resulting diffuse staining pattern (Figure 1h) made identification of individual cells and thus quantification of cell density difficult. Therefore, we determined the volume occupied by CD68 immunoreactivity in the hippocampal CA1 of sham- and KA-injected animals. Here, we observed a strong increase in immunoreactivity 5 days but not 4 h after KA injection, confirming that microglia/macrophages acquire a reactive phenotype after KA-induced SE (Figure 1i).

Taken together, these studies strongly suggest that hippocampal microglia become rapidly reactive following SE induction, even before the onset of neurodegeneration (Bedner et al., 2015). Ipsilaterally, the extent of innate immune cell activation gradually increased during the first two weeks of epileptogenesis. Transient microglial activation was also seen in the contralateral hippocampus.

3.2 | Microglia depletion prevents SE-induced GJ uncoupling

Loss of astrocytic GJ coupling is a characteristic feature of the sclerotic hippocampus in human and experimental TLE (Bedner et al., 2015). Our previous data suggest that the disruption of astrocyte coupling is mediated by microglia activation and release of pro-inflammatory cytokines (Bedner et al., 2015; Khan et al., 2016), although evidence for a causal relationship is still lacking. Thus, we employed the orally available CSF1R inhibitor PLX5622 (PLX) (Dagher et al., 2015) to deplete microglia from the brain prior to KA injection. Both non-injected and KA-injected (4 h post injection) FVB mice showed a 50%–60% reduction in IBA1-positive microglia in the hippocampus following 21 days of PLX treatment (non-injected: control diet $16,108 \pm 1660$ (mean \pm SD) vs. PLX 21 d 6586 ± 982 cells/mm³; KA-injected after 4 h: control diet $15,792 \pm 2168$ vs. PLX21d 7573 ± 952 cells/mm³) (Figure 2a,b). Extending PLX administration to 28 days slightly increased depletion efficacy, but was nonetheless not sufficient to completely abolish microglia in the hippocampus (Figure S2a, b). Moreover, the reduction in IBA1-positive microglia was similar after 7 and 21 days of PLX treatment, indicating rapid clearance of microglia from the brain (Figure S2b). Tmem119 immunostaining

confirmed these findings, demonstrating high but incomplete microglia depletion (~70%) in KA mice subjected to 21 days of PLX treatment (Figure S2c,d). The extent of microglia depletion after PLX treatment was similar in C57B6J and FVB mice (Figure S2e,f). Finally, quantification of the morphology of surviving microglia after PLX treatment revealed no significant cytoskeletal changes compared to mice receiving a control diet (Figure S2g–k). To summarize, these findings contrast previous reports demonstrating almost complete

removal of microglia from the brain after 3 weeks of continuous PLX treatment (Dagher et al., 2015). Nevertheless, our data show that CSF1R inhibition causes microglia depletion not only in the healthy but also the epileptic brain, making it a suitable approach to study the contribution of microglia to astrocyte dysfunction and epileptogenesis. Hence, in a next step we treated mice for 21 days with PLX prior to KA application and assessed GJ coupling 4 h later by biocytin filling of individual hippocampal CA1 *stratum radiatum* astrocytes. In the

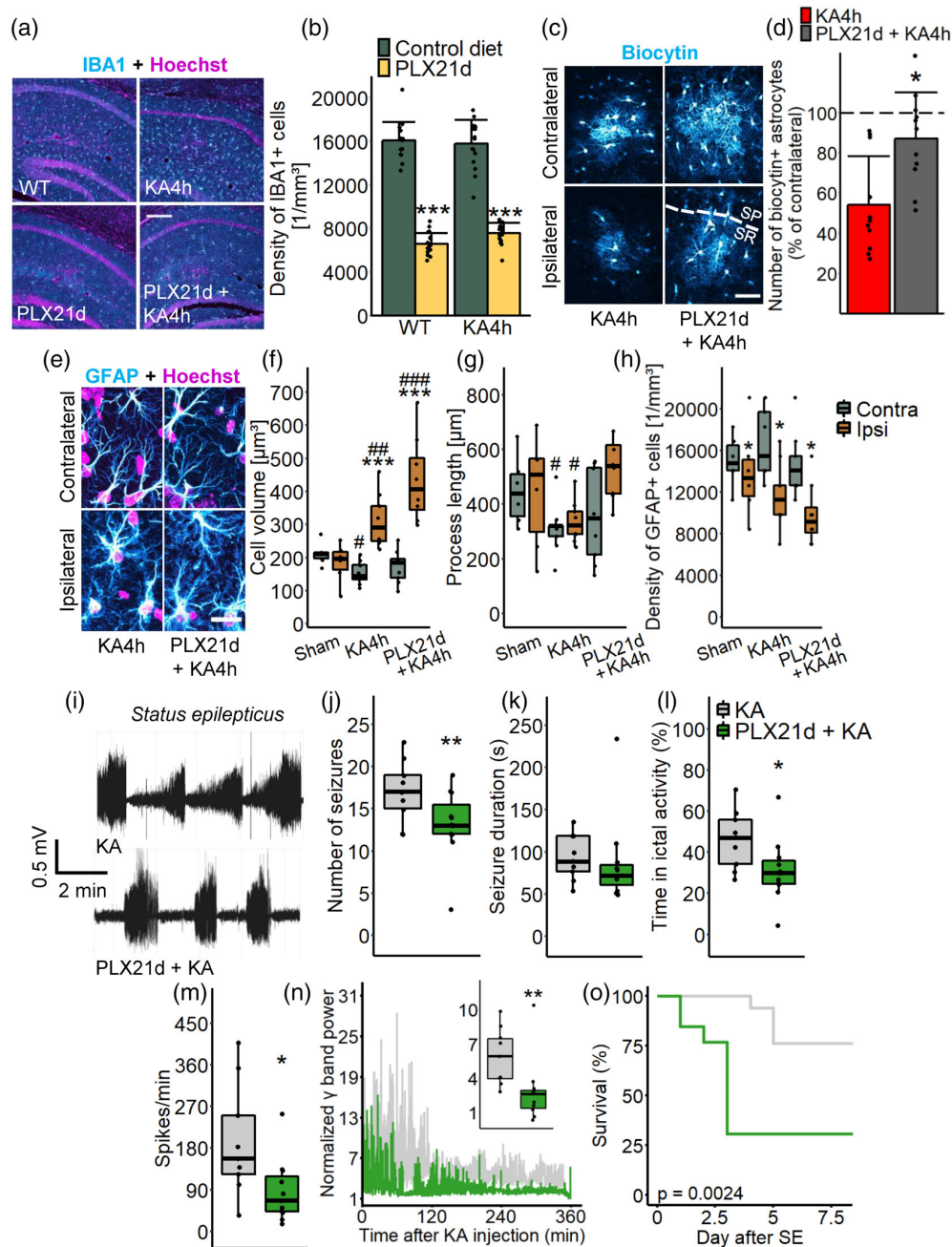


FIGURE 2 Legend on next page.

hippocampus of control mice, KA-induced SE led to a reduction of GJ coupling efficiency by about 50% at this time point (Bedner et al., 2015; Henning et al., 2021). Notably, PLX treatment and partial depletion of microglia completely prevented SE-induced uncoupling (KA 4 h: $54.14 \pm 24.31\%$ vs. PLX 21d + KA 4 h: $87.08 \pm 23.03\%$; percentage of coupled astrocytes ipsi- vs. contralaterally) (Figure 2c,d).

Alterations in GFAP expression and morphology are considered hallmarks of reactive astrocytes (Escartin et al., 2021). Moreover, pro-inflammatory cytokines released from microglia have been shown to induce astrogliosis (Liddel et al., 2017). To further elucidate the contribution of microglia to astrocyte reactivity during early KA-induced epileptogenesis, we characterized morphological features of GFAP-positive astrocytes in PLX-treated mice 4 h post KA injection in the CA1 *stratum radiatum*. Cell volume, total process length and cell density were quantified using 3D reconstructions derived from confocal images and compared between sham, KA and PLX21d + KA-treated mice (Figure 2e-h). The volume of GFAP-positive astrocytes was increased ipsilaterally and slightly decreased contralaterally, independent of whether mice were treated with PLX or not (Sham: ipsi 197, 164–218 vs. contra 212, 198–215 μm^3 ; KA 4 h: ipsi 291, 250–356 vs. contra 145, 135–178 μm^3 ; PLX 21 d + KA 4 h: ipsi 406, 345–501 vs. contra 184, 139–197 μm^3) (Figure 2f). The process lengths were reduced on both sides, an effect that could be prevented by PLX treatment (Sham: ipsi 508, 297–566 vs. contra 439, 356–508 μm ; KA 4 h: ipsi 322, 290–373 vs. contra 320, 282–321 μm ; PLX 21 d + KA 4 h: ipsi 538, 439–616 vs. contra 348, 216–532 μm) (Figure 2g). Consistent with our previously published data (Wu et al., 2021), the density of GFAP-positive cells was ipsilaterally decreased 4 h post KA, which was not prevented by PLX treatment (Figure 2h). A slight decrease in astrocyte density was also observed in the ipsilateral hippocampus of sham-injected mice (Sham: ipsi 13,352, 11,596–15,109 vs. contra 14,758, 14,055–16,515 cells/ mm^3 ; KA 4 h: ipsi 11,244, 9839–12,650 vs. contra 15,461, 14,055–19,677 cells/ mm^3 ; PLX 21 d + KA 4 h: ipsi 9136, 8082–10,541 vs. contra 14,055, 12,650–

15,461 cells/ mm^3) (Figure 2h). In conclusion, our data reveal that in addition to microglia, astrocytes become rapidly reactive following SE induction. However, partial microglia depletion only slightly affected the morphological alterations these cells underwent 4 h after onset of SE.

3.3 | Microglia depletion attenuates the severity of KA-induced SE but increases mortality

The protective effect of PLX treatment on astrocyte coupling prompted us to examine the consequences of microglia depletion on epileptogenesis in our TLE-HS model. As astrocyte uncoupling is thought to causally contribute to epileptogenesis (Bedner et al., 2015; Deshpande et al., 2020; Onodera et al., 2021), we hypothesized that PLX exerts antiepileptogenic effects in our model. A subset of mice was treated with PLX for 21 days and subsequently subjected to intracortical KA injection, which was immediately followed by implantation of telemetric EEG transmitters. A control group received standard chow prior to KA injection and transmitter implantation. We quantified the severity of SE, which in our model is manifested by a series of convulsive seizures (Figure 2i) lasting up to several hours. The number of seizures, their duration and the overall time spent in ictal activity was quantified during the first h of SE. Additionally, we counted the number of epileptic spikes during the first 6 h of recording and compared the spectral power in the γ range after fast Fourier transformation (FFT) of the EEG data. Baseline activity did not differ between groups ($p = 0.99$, independent samples t-test; data not shown). We detected significantly less seizures (KA: 17, 15–19 vs. PLX 21 d + KA: 13, 12–16 seizures) and a reduced time spent in ictal activity (KA: 47, 34–56 vs. PLX 21 d + KA: 30, 25%–36%) in PLX-treated compared to control mice during the first hour of KA-induced SE (Figure 2j,i) whereas seizure duration was not affected (KA: 89, 77–119 vs. PLX 21 d + KA: 71, 61–84 s) (Figure 2k). To further

FIGURE 2 Microglia depletion prevents astrocytic uncoupling and attenuates SE severity. (a) Representative MIPs of a combined IBA1 and Hoechst staining in the hippocampus of non-injected mice fed a control diet (non-injected), PLX-treated (PLX 21 days), KA-injected (KA 4 h) and PLX + KA-treated (PLX 21 days + KA 4 h) FVB mice. Scale bar: 200 μm . (b) The number of IBA1-positive cells was reduced by 50%–60% in the hippocampus of both, KA- and non-injected mice receiving PLX-diet (1200 mg/kg). $n = 3$ slices/mouse, $N = 3$ mice/condition; one-way ANOVA; * versus control diet. (c) Representative MIPs depicting biocytin-filled astrocytes labeled with streptavidin-conjugated Alexa Fluor[®] 647 in the ipsi- and contralateral hippocampal CA1 *stratum radiatum* region in KA-injected (KA 4 h) and PLX- + KA-treated (PLX 21 days + KA 4 h) FVB mice 4 h post KA injection. Images depict a background subtracted and brightness adjusted ROI representative of the whole coupling cloud. Scale bar: 50 μm . (d) Partial microglia depletion prevented GJ uncoupling of astrocytes during SE. $n = 11$ cells/condition, $N = 4$ mice; Independent samples t-test. The dashed line indicates the value of the contralateral hemisphere; * versus KA4h. (e) Representative MIPs of combined GFAP and Hoechst staining in the ipsi- and contralateral hippocampal CA1 *stratum radiatum* of mice with or without PLX pre-treatment, 4 h after KA injection. Scale bar: 20 μm . (f–h) Analyses of volume, total process length and density of GFAP-positive astrocytes revealed that microglia depletion only marginally affects astrogliosis. $n = 3$ slices/mouse, $N = 3$ mice/condition; two-way ANOVA; * versus contra, # versus sham. (i) Representative EEG traces during KA-induced SE in PLX-untreated (top) and PLX-treated (bottom) mice. (j–l) Number of seizures, seizure duration, and time spent in ictal activity during the first h of SE. PLX pre-treatment reduced number and time spent in seizures but not seizure duration. $N = 9$ KA and 11 PLX21d + KA mice; independent samples t-test; * versus KA. (m, n) The number of spikes per min as well as high frequency EEG activity ($\gamma = 30$ –50 Hz) were reduced in PLX-treated mice during the first 6 h after KA injection. $N = 9$ KA and 11 PLX21d + KA mice; Wilcoxon rank sum test; * versus KA. (o) Kaplan–Meier curve showing that the mortality was increased in PLX-treated compared to untreated mice following KA injection. $N = 17$ KA and 13 PLX21d + KA mice; log-rank test. Data are displayed as box plots representing median and quartiles, or as bar graphs with mean + SD. Black dots represent individual data points. SR, *stratum radiatum*; SP, *stratum pyramidale*. * $p < 0.05$; ** $p < 0.05$; *** $p < 0.001$; # $p < 0.05$; ## $p < 0.01$; ### $p < 0.001$

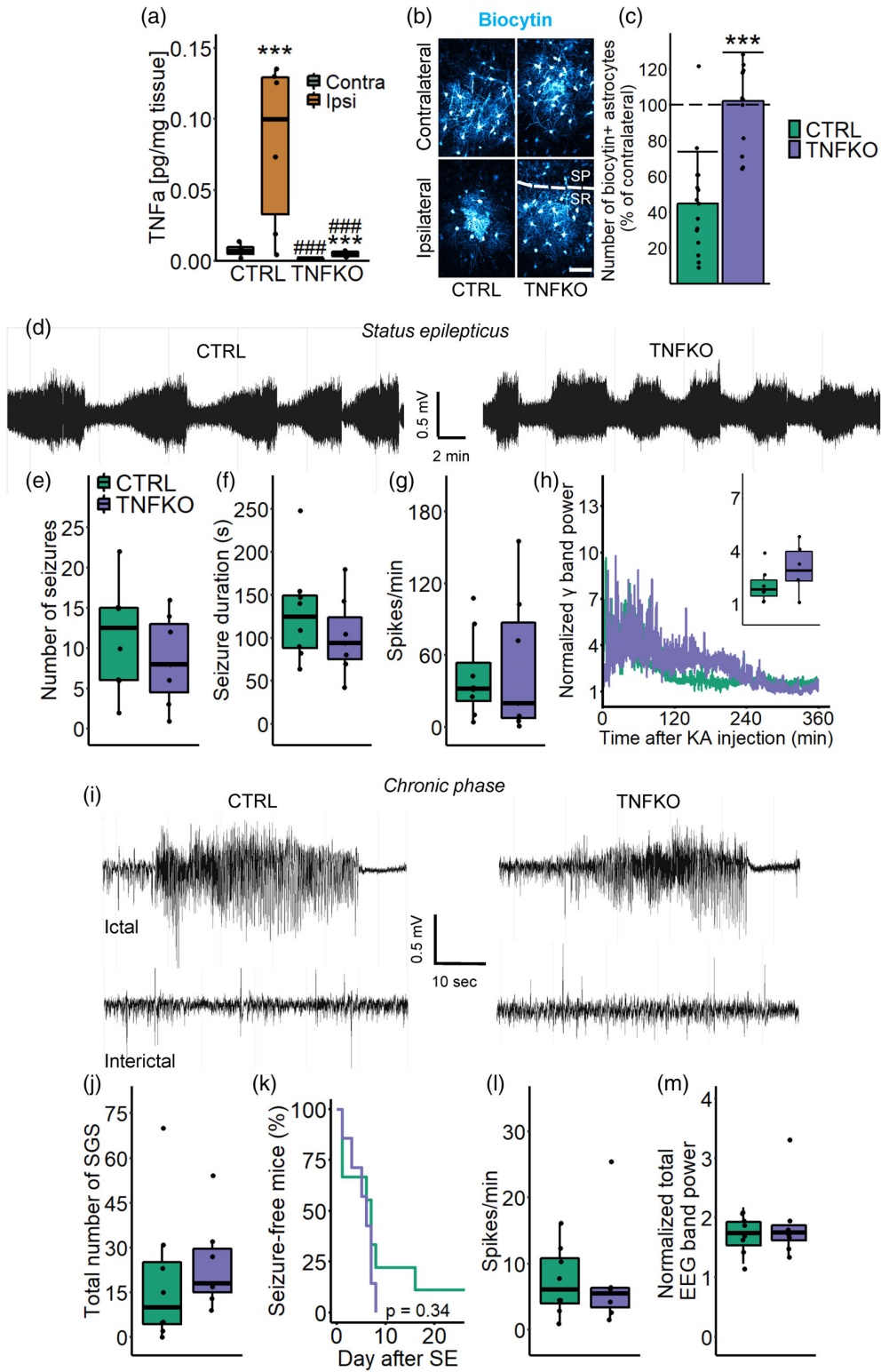


FIGURE 3 Legend on next page.

characterize SE, spike and spectral analyses were performed during an extended period of 6 h after SE induction. Both spike number (KA: 158, 124–251 vs. PLX 21 d + KA: 66, 43–119 spikes/min) and high-frequency activity in the γ range (KA: 5, 3.97–7.13 vs. PLX 21 d + KA: 2.6, 1.38–2.93) were significantly reduced in PLX-treated versus control mice (Figure 2m,n). Unexpectedly, PLX treatment significantly increased the mortality rate of KA injected mice (KA: 21.43% (3 of 14 mice) vs. PLX 21 d + KA: 69.23% (9 of 13 mice)) (Figure 2o), which made long-term investigations of the chronic phase impossible. Together, the data show that partial microglia depletion reduces the severity of KA-induced SE, implicating microglia as modulators of epileptiform activity.

3.4 | SE-induced uncoupling of astrocytes requires TNF α released from microglia

So far, our data (Figure 2) support a role for activated microglia in astrocyte uncoupling and ictogenesis following KA-induced SE, and we hypothesized that microglia exert their detrimental effects via the release of TNF α . To explore this hypothesis, we subjected microglia-specific and inducible TNF α knockout (TNFKO) mice to our TLE model and performed ELISA to quantify hippocampal TNF α concentrations 4 h post KA injection. TNF α levels were strongly increased in the ipsilateral hippocampus of heterozygous Cre-expressing control (CTRL) mice (ipsi 0.126, 0.074–0.13; contra 0.006, 0.005–0.009 pg/mg tissue) (Figure 3a). Although in TNFKO versus CTRL mice the ipsilateral TNF α level upon KA injection was markedly reduced, it was still higher than on the contralateral side (TNFKO: ipsi 0.005, 0.003–0.006; contra 0.001, 0.001–0.001 pg/mg tissue) (Figure 3a). Nevertheless, this ipsilateral reduction of TNF α in TNFKO mice was sufficient to completely prevent the 50% loss of astrocyte GJ coupling occurring in CTRL mice 4 h post KA injection (CTRL: 44.75 \pm 28.91% vs. TNFKO: 102 \pm 27.07%; percentage of coupled astrocytes ipsi- vs. contralaterally) (Figure 3b,c). Although single-cell transcript analysis did not detect significant changes in TNFR1 and TNFR2 mRNA expression

levels (Figure S3a,b), there was a significant increase in TNFR1 immunoreactivity in GFAP-positive astrocytes at both 4 h and 5 days post KA injection (Figure S3g,h). Collectively, these data provide evidence that during early epileptogenesis, microglia are a primary source of pro-inflammatory TNF α , which impairs astrocytic GJ coupling, probably via TNFR1 signaling.

3.5 | Microglia-specific reduction of TNF α does not affect KA-induced SE and subsequent generation of spontaneous seizure activity

Next, we used continuous EEG monitoring to address the question whether KA-induced SE and spontaneous seizure generation are affected in TNFKO mice over the first 4 weeks after KA injection. During the first hour of SE, neither the number of seizures (CTRL 12.5, 6–15 vs. TNFKO 8, 4.5–13 seizures) nor seizure duration (CTRL 125, 88–149 vs. TNFKO 94, 75–149 s) differed between genotypes (Figure 3e,f). During the first 6 h after KA injection the number of spikes (CTRL 11506, 7784–19,223 vs. TNFKO 7018, 2682–31,412 spikes/min) and high frequency EEG activity (CTRL 1.81, 1.44–2.35 vs. TNFKO 2.88, 2.3–3.97) were also similar (Figure 3g,h). Mortality was not different between both genotypes (data not shown). During the chronic phase (4 weeks post KA injection), the total number of spontaneous generalized seizures (SGS) did not differ between the genotypes (CTRL 10, 4.25–25 vs. TNFKO 18, 15–29.5 SGS) (Figure 3j). Likewise, the length of the latent phase was not influenced by the lack of microglial TNF α (CTRL 8.33 \pm 8.77 vs. TNFKO 5.29 \pm 2.5 days until first SGS) (Figure 3k). Finally, neither the total number of epileptic spikes per min (CTRL 6.25, 3.91–10.57 vs. TNFKO 3.78, 2.41–5.29 spikes/min) nor the total EEG band power (CTRL 1.75, 1.54–1.93 vs. TNFKO 1.75, 1.62–1.87) were different between experimental groups (Figure 3l,m). Taken together, these results indicate that the microglia-specific reduction of TNF α levels in TNFKO mice was insufficient to attenuate KA-induced SE or chronic seizure activity in our TLE model.

FIGURE 3 Reducing microglial TNF α prevented astrocytic uncoupling but did not attenuate seizure activity during SE and the chronic phase. (a) Tissue concentration of TNF α determined by ELISA was significantly increased 4 h after KA injection in the ipsi- versus contralateral dorsal hippocampus of both, Cx3cr1^{CreERT2/+}-TNF α ^{+/+} (CTRL) and Cx3cr1^{CreERT2/+}-TNF α ^{loxp/loxp} (TNFKO) mice, but the increase in TNFKO mice was significantly lower ($N = 5$ CTRL and 8 TNFKO mice; two-way ANOVA; * vs. ipsi, # vs. CTRL). (b) Representative MIPs depicting biocytin-positive astrocytes 4 h post KA injection in the ipsi- and contralateral hippocampal CA1 stratum radiatum of CTRL and TNFKO mice. Scale bar: 50 μ m. Images depict a background subtracted and brightness adjusted ROI representative of the whole coupling cloud. (c) Microglia-specific knockout of TNF α prevents uncoupling of astrocytes 4 h post KA injection. $n = 12$ –15 cells/condition, $N = 4$ –5 mice; Independent samples t -test. The dashed line indicates the value on the contralateral hemisphere; * versus CTRL. (d) Representative EEG traces during SE in TNFKO and CTRL mice. (e, f) No differences between groups regarding number and duration of seizures during the first h of SE were found. (g, h) Similarly, analyses of spike frequency and normalized γ band EEG activity during the first 6 h of EEG recording revealed no difference between genotypes (inset displays the median γ band activity over 6 h of SE). (i) Representative EEG traces (ictal activity, top; interictal, bottom) from TNFKO and CTRL mice during week 4 after KA injection. (j, k) Total number of SGS and the length of the latent phase did not differ between genotypes. (l, m) Spike frequency and normalized total EEG band power were similar in both groups. $N = 7$ TNFKO and 8 CTRL mice. Data are displayed as box plots representing median and quartiles and were analysed using either an independent samples t -test, a Wilcoxon rank sum test or a log-rank test. Black dots represent individual data points. SR, stratum radiatum; SP, stratum pyramidale. *** $p < 0.001$; ### $p < 0.001$

3.6 | Reduced TNF α release from microglia did not affect neurodegeneration but attenuated astro- and microgliosis in KA-induced TLE

Approximately two-thirds of patients with pharmacoresistant TLE exhibit HS, which is characterized by marked neurodegeneration, reactive astro- and microgliosis, and GCD (Aronica et al., 2007; Blümcke et al., 1999; Broekaart et al., 2018). These histopathological changes are well reproduced in our mouse model of TLE (Bedner et al., 2015; Deshpande et al., 2020). To determine whether reduction of microglial TNF α influences HS development, we immunostained hippocampal slices with antibodies against NeuN, GFAP, and Hoechst 4 weeks after epilepsy induction (Figure 4a). Hippocampal neurodegeneration, GCD and shrinkage of the CA1 *stratum radiatum* were similar in the hippocampus of KA-injected CTRL and TNFKO mice

(number of CA1 neurons: CTRL: ipsi 19, 9.5–24 vs. contra 71.5, 60–82.5; TNFKO: ipsi 25, 4–63 vs. contra 62, 53.5–74; *stratum radiatum* width: CTRL: ipsi 134.38, 84.81–147.92 vs. contra 185.4, 159.6–198.6 μ m; TNFKO: ipsi 112.50, 72.15–152.65 vs. contra 179.8, 167.8–194.5 μ m; GCD: CTRL: ipsi 78, 68.34–91.13 vs. contra 84.74, 71.33–99.85 μ m; TNFKO: ipsi 86.83, 83.17–121.63 vs. contra 82.43, 70.86–89.03 μ m) (Figure 4b–d). Next, the degree of astrogliosis in the hippocampal CA1 *stratum radiatum* based on the total volume occupied by the GFAP signal was quantified using a custom-written algorithm in FIJI. GFAP immunoreactivity was increased ipsi- vs. contralaterally in both genotypes, but this increase was less pronounced in TNFKO mice (CTRL (mean \pm SD): ipsi 4.5 \pm 1.35 vs. contra 3 \pm 1.21%; TNFKO: ipsi 3.87 \pm 1.65 vs. contra 2.33 \pm 0.91%) (Figure 4e). Finally, we determined the magnitude of microglia/macrophage activation by quantifying the volume occupied by IBA1-positive

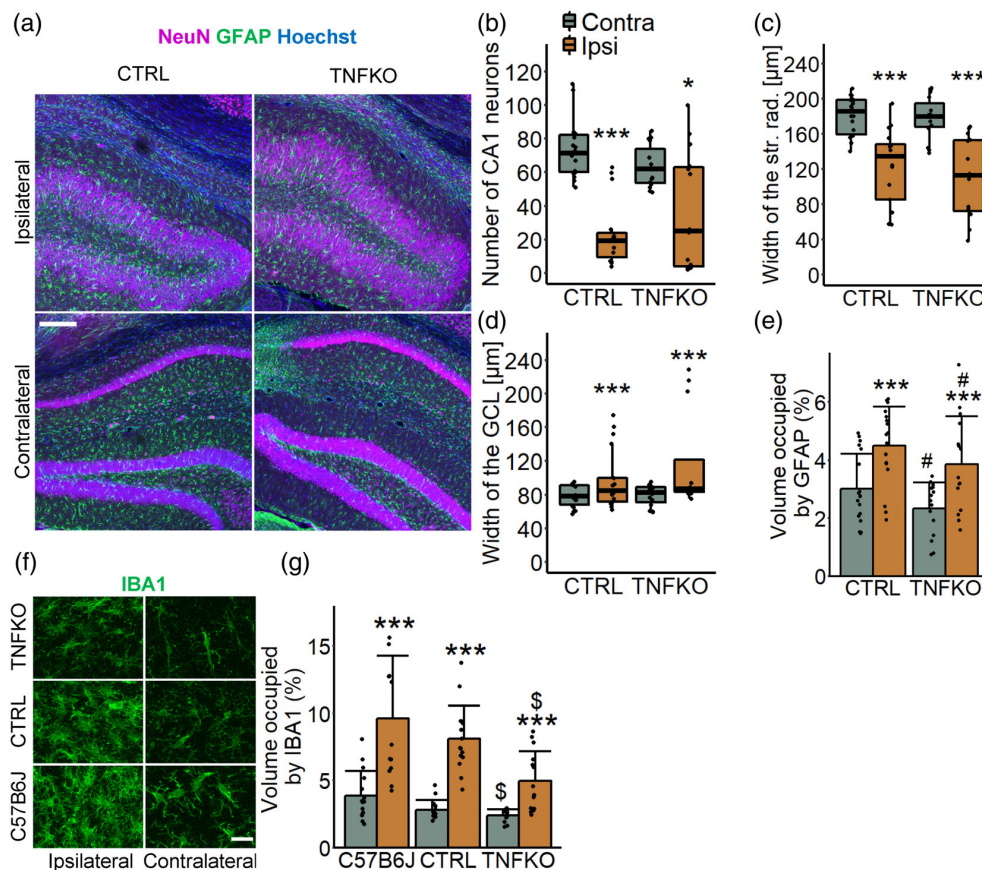


FIGURE 4 Microglia-specific reduction of TNF α attenuates astro- and microgliosis 4 weeks after KA-injection. (a) Representative MIPs of combined NeuN (magenta), GFAP (green), and Hoechst (blue) staining in ipsi- and contralateral hippocampal slices obtained 4 weeks after KA injection. Scale bar: 200 μ m. (b–e) KA-injected CTRL and TNFKO mice displayed similar pyramidal cell loss in the CA1 region, shrinkage of the *stratum radiatum* and GCD, while astrogliosis in the CA1 *stratum radiatum* was less pronounced both ipsi- and contralaterally in TNFKO mice. $n = 3$ slices/mouse, $N = 6$ CTRL and 5 TNFKO mice; * versus contra, # versus CTRL. (f) Representative MIPs of IBA1 staining in the ipsi- and contralateral hippocampal CA1 *stratum radiatum* from C57B6J, CTRL and TNFKO mice 4 weeks after KA injection. Scale bar: 20 μ m. (g) Microgliosis was present in all genotypes in the ipsilateral hippocampus, but overall reduced in KA-treated TNFKO compared to C57B6J mice. $n = 2$ –3 slices/mouse, $N = 5$ mice/condition; * versus ipsi; \$ versus C57B6J. Data are displayed as box plots representing median and quartiles or as bar graphs with mean \pm SD and were analysed using two-way ANOVA. Black dots represent individual data points. CA, cornu ammonis; str. rad., *stratum radiatum*; GCL, granule cell layer. *** $p < 0.001$; * $p < 0.05$; # $p < 0.05$; \$ $p < 0.05$

cells in the hippocampus of C57B6J, CTRL and TNFKO mice, 4 weeks post KA-induced SE (Figure 4f.g). The data revealed a pronounced increase in IBA1 immunoreactivity in ipsilateral hippocampi across all genotypes. While no differences were found in CTRL versus C57B6J and CTRL versus TNFKO mice, IBA1 immunoreactivity was significantly attenuated both ipsi- and contralaterally, in TNFKO compared to C57B6J mice (C57B6J: ipsi 9.60 ± 4.66 vs. contra $3.87 \pm 1.83\%$; CTRL: ipsi 8.11 ± 2.45 vs. contra $2.82 \pm 0.71\%$; TNFKO: ipsi 4.95 ± 2.24 vs. contra $2.41 \pm 0.45\%$) (Figure 4f.g). Thus, during the first 4 weeks of epileptogenesis, microglia-derived TNF α specifically promotes astrogliosis and innate immune cell activation while neurodegeneration and GCD are less sensitive.

4 | DISCUSSION

In the present study we show that microglia become rapidly and chronically activated in a mouse model closely resembling key features of human TLE (Bedner et al., 2015). By combining pharmacology and cell-type-specific gene knockout we identified microglia as major drivers of early TNF α production, severity of SE, reactive gliosis, and uncoupling of hippocampal astrocytes following KA injection. Microglia activation temporally preceded neuronal cell death and was also transiently detectable in the contralateral hippocampus, indicating that it was not a response to neurodegeneration, but rather a result of seizure activity *per se* (Bedner et al., 2015). Indeed, microglia register neuronal hyperactivity during KA-induced SE via a mechanism involving glutamate-dependent ATP release from neurons, which is sensed by microglial P2Y₁₂ receptors (Dissing-Olesen et al., 2014; Eyo et al., 2014). Our stereological analyses revealed a dramatic increase in the number of IBA1-positive cells during the latent and chronic phases of epilepsy. Moreover, the extent of innate immune cell activation gradually increased over time, which was indicated by the appearance of CD68, a marker of activated macrophages (Jurga et al., 2020). Both microglia and infiltrated monocytes jointly contribute to the pool of activated innate immune cells in experimental TLE (Feng et al., 2019; Käufer et al., 2018; Waltl, Käufer, Bröer, et al., 2018), and invasion of blood-borne monocytes exacerbates neurodegeneration, blood-brain barrier (BBB) breakdown and inflammation following SE (Varvel et al., 2016). Our data revealed the emergence of CD169-positive cells at later time points (i.e., 5 and 14 days post KA injection), indicating monocyte infiltration after KA injection. However, co-staining of CD169 with the microglia-specific marker Tmem119 at 5 days post KA injection questioned the specificity of CD169 as a marker of infiltrating monocytes. In support of this, reactive microglia have been shown to upregulate CD169 in other pathological conditions, such as following lipopolysaccharide (LPS) exposure and in experimental autoimmune encephalomyelitis (Bennett et al., 2016; Bogie et al., 2018). Nevertheless, it is possible that the CD169-positive/Tmem119-negative cells detected in the ipsilateral hippocampus are monocytes that have crossed the compromised BBB characteristic of our TLE model (Deshpande et al., 2017; Henning et al., 2021). Notably, the density of IBA1 and CD169 immunoreactive cells was also transiently increased

in the contralateral hippocampus. Whether contralateral innate immune cell activation contributes to the pathology of epilepsy remains to be established.

To study microglial contributions to epileptogenesis, we examined consequences of microglia depletion by applying the CSF1R inhibitor PLX5622 prior to KA injection. In contrast to previous observations (Basilico et al., 2022; Dagher et al., 2015), in the present study PLX only partially depleted microglia, regardless of the duration of application, mouse genotype or microglial markers employed. The morphology of PLX-resistant microglia remained unchanged. The reasons for the incomplete depletion remain unclear, as our mice had *ad libitum* access to the PLX-supplemented diet and readily consumed it (3–4 g/mouse/day). Nevertheless, this incomplete depletion was sufficient to completely prevent loss of astrocyte GJ coupling and to mitigate the severity of KA-induced SE. Together, these findings are consistent with our hypothesis that microglia indirectly promote epileptogenesis by decreasing GJ-mediated K⁺ and glutamate buffering capacity of astrocytes, and are in line with previous studies that have identified microglia as drivers of neuronal hyperactivity and seizures (Pascual et al., 2012; Riazzi et al., 2008; Rodgers et al., 2009). It should be noted, however, that other studies did not find evidence for a role of microglia in modulating KA- or pilocarpine- induced seizures (Altmann et al., 2022; Feng et al., 2019; Mirrione et al., 2010) or even reported increased SE severity after microglia depletion (Liu et al., 2020; Wu et al., 2020). Possible explanations underlying these discrepancies include differences between animal models and efficiency of microglia depletion.

Our stereological data revealed that astrocyte morphology changes are rapidly induced and occur in parallel with microglia activation upon SE induction. In addition, partial microglia depletion had only minor effects on astrocyte morphology changes during SE. This is in contrast to a previous study, showing that microglia activation precedes astrocyte reactivity and that depletion of microglia is sufficient to prevent morphological alterations of astrocytes after pilocarpine-induced SE (Sano et al., 2021). The lack of effect in the present study could be due to the incomplete depletion of microglia in our model. Alternatively, as astrocytes sense neuronal activity via a variety of ion channels and neurotransmitter receptors (Coulter & Steinhilber, 2015), astrocyte morphology changes in response to hyperactivity may be largely independent of inflammatory signaling by microglia.

To our surprise, microglia-depleted mice exhibited high mortality following KA-injection, a phenomenon that was also observed in other studies of SE- and infection-induced epilepsy (Sanchez et al., 2019; Waltl, Käufer, Gerhauser, et al., 2018; Wu et al., 2020). These studies showed that microglia depletion exacerbates neurodegeneration following an epileptogenic insult, indicating that microglia serve neuroprotective functions in epilepsy (Sanchez et al., 2019; Waltl et al., 2018; Wu et al., 2020). However, CSF1R is expressed in all myeloid cells of the body and CSF1R inhibition has been shown to reduce peripheral macrophage numbers (Green et al., 2020; Merry et al., 2020). Since macrophages play an important role in wound healing (Kim & Nair, 2019), reduced macrophage numbers following PLX treatment could have increased mortality due to impaired



regeneration after surgical EEG implantation. Thus, whether the increased mortality after microglia depletion in our model reflects a protective role of microglia in epilepsy or merely the peripheral side effects of blocking CSF1R, remains to be clarified. The observed increase in mortality after PLX treatment in our model nevertheless implies that microglia depletion does not represent a compelling strategy for the treatment of epilepsy and emphasizes the need for more targeted microglial manipulations in TLE.

The opposing effects of microglia depletion in our model prompted us to manipulate these cells in such a way that the antiepileptic aspects of PLX treatment are retained while simultaneously preserving essential functions of microglia for survival of the animals. We hypothesized that preventing the release of the pro-inflammatory cytokine TNF α from microglia could be a promising strategy, as the cytokine has previously been associated with both astrocyte reactivity and epilepsy (Liddel et al., 2017; Patel et al., 2017). Using microglia-specific inducible TNF α knockout mice, we identified microglia as the primary source of TNF α 4 h after KA injection. This finding is in line with studies demonstrating that microglia are major producers of TNF α following pilocarpine-induced SE (Sano et al., 2021; Wang et al., 2015). Importantly, reduction of TNF α in microglia prevented early astrocyte uncoupling, confirming that the loss of coupling in wild type mice after KA-induced SE (Bedner et al., 2015) depends on TNF α signaling. Our immunohistochemical analyses further revealed increased TNFR1 expression in astrocytes at 4 h and 5 days post KA injection, suggesting that microglial TNF α acts via TNFR1 to impair GJ coupling in astrocytes.

In contrast to our expectations, microglia-specific TNF α knock-out had no effects on SE or chronic epileptiform activity in our model. There are several possible explanations for this finding. First, it cannot be excluded that residual release of the cytokine still occurs in tamoxifen-treated TNFKO mice upon KA-induced SE and contributes to the ipsilateral increase we have observed, which might be sufficient to generate hyperactivity. Moreover, experimental data from various pathological conditions show that TNF α has antithetical effects depending on whether it signals via TNFR1 or TNFR2 (Balosso et al., 2005; Brambilla et al., 2011; Dong et al., 2016; Karamita et al., 2017; Patel et al., 2017; Weinberg et al., 2013). In the context of epilepsy, Balosso et al. (2005) demonstrated that the susceptibility to KA-induced acute seizures was reduced in mice lacking TNFR1 but increased in mice lacking TNFR2. Similarly, in a study by Patel et al. (2017) it was shown that combined knockout of TNFR1/TNFR2 decreased acute infection-induced seizures, while selective TNFR2 deletion led to exacerbation of seizures. Thus, it is possible that reduction of TNF α in microglia has no consequence on seizure activity in our model because deleterious and beneficial effects of TNF α signaling via TNFR1 and TNFR2 cancel out each other. While our data show that microglia are the primary source of TNF α released during SE, other immunocompetent cells might contribute to TNF α release at later stages of epileptogenesis, e.g. peripheral monocytes upon infiltration into the CNS. In the present study, TNF α reduction was

restricted to microglia by maintaining a sufficiently long interval between tamoxifen and KA injection, thus exploiting the much faster turnover rates of peripheral monocytes compared to microglia (Goldmann et al., 2013; Parkhurst et al., 2013). Conversely, shortening the interval between tamoxifen and KA injections would allow to investigate whether combined reduction of TNF α in microglia and peripheral monocytes attenuates seizure activity in our TLE model. The discrepancy between the data from our PLX and TNFKO experiments in terms of affecting SE severity might indicate that factors other than microglia-derived TNF α contribute to the susceptibility to KA-induced seizures. Indeed, microglia release several pro-inflammatory cytokines that modulate seizures, including interleukin (IL)-1 β (Vezzani et al., 1999, 2011). Additionally, a non-inflammatory reactive microglial state caused by genetic over-activation of mTOR and characterized by increased phagocytic activity has been shown to be sufficient to cause epileptic activity (Zhao et al., 2018). Thus, partial microglia depletion using PLX may have prevented phenotypic changes of microglia other than TNF α release, which might explain its seizure suppressing effects during KA-induced SE. The identification of microglia-derived factors underlying the beneficial effect of PLX on KA-induced seizures as seen in the present study requires further investigations.

In the present study microglia-specific TNF α knockout attenuated astrogliosis and immune cell activation, but did not attenuate neurodegeneration, GCD and *stratum radiatum* shrinkage during the chronic phase of epilepsy. Limited recombination efficiency or simultaneous modulation of TNFR1 and TNFR2 signaling may be responsible for the latter, as discussed above. For example, inhibition of TNFR1 was shown to ameliorate hippocampal cell death in KA-induced epilepsy (Weinberg et al., 2013), whereas increased neuronal loss occurred in mice lacking both TNFRs (Bruce et al., 1996). Thus, specifically targeting the TNF α -TNFR1 axis might represent a promising strategy to attenuate SE-induced neurodegeneration.

5 | CONCLUSION

The present study provides novel insights into the role of microglia reactivity and TNF α release in astrocyte dysfunction and epileptogenesis. During KA-induced SE, microglia become rapidly reactive and constitute a primary source of TNF α , which targets astrocytes, impairs GJ coupling and contributes to the development of TLE. The observations of the present study reveal additional mechanisms underlying inflammation-induced epileptogenesis and emphasize the importance of targeted anti-inflammatory treatments in TLE.

ACKNOWLEDGMENTS

The authors thank Francesco Santarelli for help with performing the TNF α ELISA. PLX5622 was provided under Materials Transfer Agreement by Plexikon Inc. (Berkeley, CA). Open Access funding enabled and organized by Projekt DEAL.

FUNDING INFORMATION

This research was supported by the EU (H2020-MSCA-ITN project 722053 EU-GliaPhD; to CS) and BMBF (16GW0182 CONNEXIN, 01DN20001 CONNEX; to CS).

CONFLICT OF INTEREST

The authors declare that they have no conflict of interest.

DATA AVAILABILITY STATEMENT

The data that support the findings of this study are available from the corresponding author upon reasonable request.

ORCID

Christian Steinhäuser  <https://orcid.org/0000-0003-2579-8357>

Peter Bedner  <https://orcid.org/0000-0003-0090-7553>

REFERENCES

- Altmann, A., Ryten, M., Di Nunzio, M., Ravizza, T., Tolomeo, D., Reynolds, R. H., Somani, A., Bacigaluppi, M., Iori, V., Micotti, E., Di Sapia, R., Cerovic, M., Palma, E., Ruffolo, G., Botía, J. A., Absil, J., Alhusaini, S., Alvim, M., Auvinen, P., ... Sisodiya, S. M. (2022). A systems-level analysis highlights microglial activation as a modifying factor in common epilepsies. *Neuropathology and Applied Neurobiology*, 48(1), e12758. <https://doi.org/10.1111/nan.12758>
- Aronica, E., Boer, K., van Vliet, E. A., Redeker, S., Baayen, J. C., Spliet, W. G. M., van Rijen, P. C., Troost, D., Lopes da Silva, F. H., Wadman, W. J., & Gorter, J. A. (2007). Complement activation in experimental and human temporal lobe epilepsy. *Neurobiology of Disease*, 26(3), 497–511. <https://doi.org/10.1016/j.nbd.2007.01.015>
- Aronica, E., Bauer, S., Bozzi, Y., Caleo, M., Dingledine, R., Gorter, J. A., Henshall, D. C., Kaufer, D., Koh, S., Löscher, W., Louboutin, J.-P., Mishto, M., Norwood, B. A., Palma, E., Poulter, M. O., Terrone, G., Vezzani, A., & Kaminski, R. M. (2017). Neuroinflammatory targets and treatments for epilepsy validated in experimental models. *Epilepsia*, 58, 27–38. <https://doi.org/10.1111/epi.13783>
- Avignone, E., Ulmann, L., Levavasseur, F., Rassendren, F., & Audinat, E. (2008). Status epilepticus induces a particular microglial activation state characterized by enhanced purinergic signaling. *Journal of Neuroscience*, 28(37), 9133–9144. <https://doi.org/10.1523/JNEUROSCI.1820-08.2008>
- Balosso, S., Ravizza, T., Perego, C., Peschon, J., Campbell, I. L., De Simoni, M. G., & Vezzani, A. (2005). Tumor necrosis factor- α inhibits seizures in mice via p75 receptors. *Annals of Neurology*, 57(6), 804–812. <https://doi.org/10.1002/ana.20480>
- Basilico, B., Ferrucci, L., Ratano, P., Golia, M. T., Grimaldi, A., Rosito, M., Ferretti, V., Reverte, I., Sanchini, C., Marrone, M. C., Giubettini, M., De Turris, V., Salerno, D., Garofalo, S., St-Pierre, M. K., Carrier, M., Renzi, M., Pagani, F., Modi, B., ... Ragozzino, D. (2022). Microglia control glutamatergic synapses in the adult mouse hippocampus. *Glia*, 70(1), 173–195. <https://doi.org/10.1002/glia.24101>
- Bedner, P., Dupper, A., Hüttmann, K., Müller, J., Herde, M. K., Dublin, P., Deshpande, T., Schramm, J., Häussler, C. A., Henneberger, C., Theis, M., & Steinhäuser, C. (2015). Astrocyte uncoupling as a cause of human temporal lobe epilepsy. *Brain*, 138(5), 1208–1222. <https://doi.org/10.1093/brain/awv067>
- Bennett, M. L., Bennett, F. C., Liddel, S. A., Ajami, B., Zamanian, J. L., Fernhoff, N. B., Mulinyawe, S. B., Bohlen, C. J., Adil, A., Tucker, A., Weissman, I. L., Chang, E. F., Li, G., Grant, G. A., Hayden Gephart, M. G., & Barres, B. A. (2016). New tools for studying microglia in the mouse and human CNS. *Proceedings of the National Academy of Sciences*, 113(12), E1738–E1746. <https://doi.org/10.1073/pnas.1525528113>
- Benson, M. J., Manzanero, S., & Borges, K. (2015). Complex alterations in microglial M1/M2 markers during the development of epilepsy in two mouse models. *Epilepsia*, 56(6), 895–905. <https://doi.org/10.1111/epi.12960>
- Blümcke, I., Beck, H., Lie, A. A., & Wiestler, O. D. (1999). Molecular neuropathology of human mesial temporal lobe epilepsy. *Epilepsy Research*, 36(2–3), 205–223. [https://doi.org/10.1016/S0920-1211\(99\)00052-2](https://doi.org/10.1016/S0920-1211(99)00052-2)
- Bogie, J. F., Boelen, E., Louagie, E., Delputte, P., Elewaut, D., van Horsen, J., Hendriks, J. J., & Hellings, N. (2018). CD169 is a marker for highly pathogenic phagocytes in multiple sclerosis. *Multiple Sclerosis Journal*, 24(3), 290–300. <https://doi.org/10.1177/1352458517698759>
- Brambilla, R., Ashbaugh, J. J., Magliozzi, R., Dellarole, A., Karmally, S., Szymkowski, D. E., & Bethea, J. R. (2011). Inhibition of soluble tumour necrosis factor is therapeutic in experimental autoimmune encephalomyelitis and promotes axon preservation and remyelination. *Brain*, 134(9), 2736–2754. <https://doi.org/10.1093/brain/awr199>
- Broekaart, D. W. M., Anink, J. J., Baayen, J. C., Idema, S., de Vries, H. E., Aronica, E., Gorter, J. J., & van Vliet, E. A. (2018). Activation of the innate immune system is evident throughout epileptogenesis and is associated with blood-brain barrier dysfunction and seizure progression. *Epilepsia*, 59(10), 1931–1944. <https://doi.org/10.1111/epi.14550>
- Bruce, A. J., Boling, W., Kindy, M. S., Peschon, J., Kraemer, P. J., Carpenter, M. K., Holtsberg, F. W., & Mattson, M. P. (1996). Altered neuronal and microglial responses to excitotoxic and ischemic brain injury in mice lacking TNF receptors. *Nature Medicine*, 2(7), 788–794. <https://doi.org/10.1038/nm0796-788>
- Butovsky, O., Siddiqui, S., Gabriely, G., Lanser, A. J., Dake, B., Murugaiyan, G., Doykan, C. E., Wu, P. M., Gali, R. R., Iyer, L. K., Lawson, R., Berry, J., Krichevsky, A. M., Cudkowicz, M. E., & Weiner, H. L. (2012). Modulating inflammatory monocytes with a unique microRNA gene signature ameliorates murine ALS. *Journal of Clinical Investigation*, 122(9), 3063–3087. <https://doi.org/10.1172/JCI62636>
- Coulter, D. A., & Steinhäuser, C. (2015). Role of Astrocytes in Epilepsy. *Cold Spring Harbor Perspectives in Medicine*, 5(3), a022434. <https://doi.org/10.1101/cshperspect.a022434>
- Dagher, N. N., Najafi, A. R., Kayala, K. M. N., Elmore, M. R. P., White, T. E., Medeiros, R., West, B. L., & Green, K. N. (2015). Colony-stimulating factor 1 receptor inhibition prevents microglial plaque association and improves cognition in 3xTg-AD mice. *Journal of Neuroinflammation*, 12(1), 139. <https://doi.org/10.1186/s12974-015-0366-9>
- De Simoni, M. G., Perego, C., Ravizza, T., Moneta, D., Conti, M., Marchesi, F., Garattini, S., & Vezzani, A. (2000). Inflammatory cytokines and related genes are induced in the rat hippocampus by limbic status epilepticus: Cytokines in status epilepticus. *European Journal of Neuroscience*, 12(7), 2623–2633. <https://doi.org/10.1046/j.1460-9568.2000.00140.x>
- Deshpande, T., Li, T., Henning, L., Wu, Z., Müller, J., Seifert, G., Steinhäuser, C., & Bedner, P. (2020). Constitutive deletion of astrocytic connexins aggravates kainate-induced epilepsy. *Glia*, 68, 2136–2147. <https://doi.org/10.1002/glia.23832>
- Deshpande, T., Li, T., Herde, M. K., Becker, A., Vatter, H., Schwarz, M. K., Henneberger, C., Steinhäuser, C., & Bedner, P. (2017). Subcellular reorganization and altered phosphorylation of the astrocytic gap junction protein connexin43 in human and experimental temporal lobe epilepsy. *Glia*, 65(11), 1809–1820. <https://doi.org/10.1002/glia.23196>
- Devinsky, O., Vezzani, A., Najjar, S., De Lanerolle, N. C., & Rogawski, M. A. (2013). Glia and epilepsy: Excitability and inflammation. *Trends in Neurosciences*, 36(3), 174–184. <https://doi.org/10.1016/j.tins.2012.11.008>
- Di Nunzio, M., Di Sapia, R., Sorrentino, D., Kebede, V., Cerovic, M., & Gullotta, G. S., Bacigaluppi, M., Audinat, E., Marchi, N., Ravizza, T., Vezzani, A. (2021). Microglia proliferation plays distinct roles in acquired epilepsy depending on disease stages. *Epilepsia*, 62(8), 1931–1945. <https://doi.org/10.1111/epi.16956>

- Dissing-Olesen, L., LeDue, J. M., Rungta, R. L., Hefendehl, J. K., Choi, H. B., & MacVicar, B. A. (2014). Activation of neuronal NMDA receptors triggers transient ATP-mediated microglial process outgrowth. *Journal of Neuroscience*, 34(32), 10511–10527. <https://doi.org/10.1523/JNEUROSCI.0405-14.2014>
- Dong, Y., Fischer, R., Naudé, P. J. W., Maier, O., Nyakas, C., Duffey, M., Van der Zee, E. A., Dekens, D., Douwenga, W., Herrmann, A., Guenzi, E., Kontermann, R. E., Pfizenmaier, K., & Eisel, U. L. M. (2016). Essential protective role of tumor necrosis factor receptor 2 in neurodegeneration. *Proceedings of the National Academy of Sciences*, 113(43), 12304–12309. <https://doi.org/10.1073/pnas.1605195113>
- Escartin, C., Galea, E., Lakatos, A., O'Callaghan, J. P., Petzold, G. C., Serrano-Pozo, A., Steinhäuser, C., Volterra, A., Carmignoto, G., Agarwal, A., Allen, N. J., Araque, A., Barbeito, L., Barzilai, A., Bergles, D. E., Bonvento, G., Butt, A. M., Chen, W.-T., Cohen-Salmon, M., ... Verkhratsky, A. (2021). Reactive astrocyte nomenclature, definitions, and future directions. *Nature Neuroscience*, 24(3), 312–325. <https://doi.org/10.1038/s41593-020-00783-4>
- Eyo, U. B., Peng, J., Swiatkowski, P., Mukherjee, A., Bispo, A., & Wu, L.-J. (2014). Neuronal hyperactivity recruits microglial processes via neuronal NMDA receptors and microglial P2Y12 receptors after status epilepticus. *Journal of Neuroscience*, 34(32), 10528–10540. <https://doi.org/10.1523/JNEUROSCI.0416-14.2014>
- Feng, L., Murugan, M., Bosco, D. B., Liu, Y., Peng, J., Worrell, G. A., Wang, H.-L., Ta, L. E., Richardson, J. R., Shen, Y., Wu, L. (2019). Microglial proliferation and monocyte infiltration contribute to microgliosis following status epilepticus. *Glia*, 67(8), 1434–1448. <https://doi.org/10.1002/glia.23616>
- Fülle, L., Offermann, N., Hansen, J. N., Breithausen, B., Erazo, A. B., Schanz, O., Radau, L., Gondorf, F., Knöpper, K., Alferink, J., Abdullah, Z., Neumann, H., Weighardt, H., Henneberger, C., & Förster, I. (2018). CCL17 exerts a neuroimmune modulatory function and is expressed in hippocampal neurons. *Glia*, 66(10), 2246–2261. <https://doi.org/10.1002/glia.23507>
- Gao, L., Brenner, D., Llorens-Bobadilla, E., Saiz-Castro, G., Frank, T., Wieghofer, P., Hill, O., Thiemann, M., Karray, S., Prinz, M., Weishaupt, J. H., & Martin-Villalba, A. (2015). Infiltration of circulating myeloid cells through CD95L contributes to neurodegeneration in mice. *Journal of Experimental Medicine*, 212(4), 469–480. <https://doi.org/10.1084/jem.20132423>
- Gershen, L. D., Zanotti-Fregonara, P., Dustin, I. H., Liow, J.-S., Hirvonen, J., Kreisl, W. C., Jenko, K. J., Inati, S. K., Fujita, M., Morse, C. L., Brouwer, C., Hong, J. S., Pike, V. W., Zoghbi, S. S., Innis, R. B., & Theodore, W. H. (2015). Neuroinflammation in temporal lobe epilepsy measured using positron emission tomographic imaging of translocator protein. *JAMA Neurology*, 72(8), 882–888. <https://doi.org/10.1001/jamaneurol.2015.0941>
- Goldmann, T., Wieghofer, P., Müller, P. F., Wolf, Y., Varol, D., Yona, S., Brendecke, S. M., Kierdorf, K., Staszewski, O., Datta, M., Luedde, T., Heikenwalder, M., Jung, S., & Prinz, M. (2013). A new type of microglia gene targeting shows TAK1 to be pivotal in CNS autoimmune inflammation. *Nature Neuroscience*, 16(11), 1618–1626. <https://doi.org/10.1038/nn.3531>
- Green, K. N., Craspe, J. D., & Hohsfield, L. A. (2020). To kill a microglia: A case for CSF1R inhibitors. *Trends in Immunology*, 41(9), 771–784. <https://doi.org/10.1016/j.it.2020.07.001>
- Grivennikov, S., Tumanov, A., Liepinsh, D., Kruglov, A., Marakusha, B., Shakhov, A., Murakami, T., Drutska, L. N., Förster, I., Clausen, B. E., Tassarollo, L., Ryffel, B., Kuprash, D. V., & Nedospasov, S. A. (2005). Distinct and nonredundant in vivo functions of TNF produced by T cells and macrophages/neutrophils protective and deleterious effects. *Immunity*, 22(1), 93–104. [https://doi.org/10.1016/S1074-7613\(04\)00379-6](https://doi.org/10.1016/S1074-7613(04)00379-6)
- Haghikia, A., Ladage, K., Lafênetre, P., Haghikia, A., Hinkerohe, D., Smikalla, D., Haase, C. G., Dermietzel, R., & Faustmann, P. M. (2008). Intracellular application of TNF-alpha impairs cell to cell communication via gap junctions in glioma cells. *Journal of Neuro-Oncology*, 86(2), 143–152. <https://doi.org/10.1007/s11060-007-9462-8>
- Hanisch, U.-K., & Kettenmann, H. (2007). Microglia: Active sensor and versatile effector cells in the normal and pathologic brain. *Nature Neuroscience*, 10(11), 1387–1394. <https://doi.org/10.1038/nn1997>
- Henning, L., Steinhäuser, C., & Bedner, P. (2021). Initiation of experimental temporal lobe epilepsy by early astrocyte uncoupling is independent of TGFβR1/ALK5 signaling. *Frontiers in Neurology*, 12, 660591. <https://doi.org/10.3389/fneur.2021.660591>
- Hiragi, T., Ikegaya, Y., & Koyama, R. (2018). Microglia after seizures and in epilepsy. *Cell*, 7(4), 26. <https://doi.org/10.3390/cells7040026>
- Jurga, A. M., Paleczna, M., & Kuter, K. Z. (2020). Overview of general and discriminating markers of differential microglia phenotypes. *Frontiers in Cellular Neuroscience*, 14, 198. <https://doi.org/10.3389/fncel.2020.00198>
- Kafitz, K. W., Meier, S. D., Stephan, J., & Rose, C. R. (2008). Developmental profile and properties of sulforhodamine 101–Labeled glial cells in acute brain slices of rat hippocampus. *Journal of Neuroscience Methods*, 169(1), 84–92. <https://doi.org/10.1016/j.jneumeth.2007.11.022>
- Karamita, M., Barnum, C., Möbius, W., Tansey, M. G., Szymkowski, D. E., Lassmann, H., & Probert, L. (2017). Therapeutic inhibition of soluble brain TNF promotes remyelination by increasing myelin phagocytosis by microglia. *JCI Insight*, 2(8), e87455. <https://doi.org/10.1172/jci.insight.87455>
- Käuffer, C., Chhatbar, C., Bröer, S., Walzl, I., Ghita, L., Gerhauser, I., Kalinke, U., & Löscher, W. (2018). Chemokine receptors CCR2 and CX3CR1 regulate viral encephalitis-induced hippocampal damage but not seizures. *Proceedings of the National Academy of Sciences*, 115(38), E8929–E8938. <https://doi.org/10.1073/pnas.1806754115>
- Khan, D., Dupper, A., Deshpande, T., Graan, P. N. E. D., Steinhäuser, C., & Bedner, P. (2016). Experimental febrile seizures impair interastrocytic gap junction coupling in juvenile mice: Astrocyte uncoupling by febrile seizures. *Journal of Neuroscience Research*, 94(9), 804–813. <https://doi.org/10.1002/jnr.23726>
- Kim, S. Y., & Nair, M. G. (2019). Macrophages in wound healing: Activation and plasticity. *Immunology & Cell Biology*, 97(3), 258–267. <https://doi.org/10.1111/imcb.12236>
- Lehtimäki, K. A., Peltola, J., Koskikallio, E., Keränen, T., & Honkaniemi, J. (2003). Expression of cytokines and cytokine receptors in the rat brain after kainic acid-induced seizures. *Molecular Brain Research*, 110(2), 253–260. [https://doi.org/10.1016/S0169-328X\(02\)00654-X](https://doi.org/10.1016/S0169-328X(02)00654-X)
- Liddel, S. A., Guttenplan, K. A., Clarke, L. E., Bennett, F. C., Bohlen, C. J., Schirmer, L., Bennett, M. L., Münch, A. E., Chung, W. S., Peterson, T. C., Wilton, D. K., Frouin, A., Napier, B. A., Panicker, N., Kumar, M., Buckwalter, M. S., Rowitch, D. H., Dawson, V. L., Dawson, T. M., ... Barres, B. A. (2017). Neurotoxic reactive astrocytes are induced by activated microglia. *Nature*, 541(7638), 481–487. <https://doi.org/10.1038/nature21029>
- Liu, M., Jiang, L., Wen, M., Ke, Y., Tong, X., Huang, W., & Chen, R. (2020). Microglia depletion exacerbates acute seizures and hippocampal neuronal degeneration in mouse models of epilepsy. *American Journal of Physiology-Cell Physiology*, 319(3), C605–C610. <https://doi.org/10.1152/ajpcell.00205.2020>
- Löscher, W., Potschka, H., Sisodiya, S. M., & Vezzani, A. (2020). Drug resistance in epilepsy: Clinical impact, potential mechanisms, and new innovative treatment options. *Pharmacological Reviews*, 72(3), 606–638. <https://doi.org/10.1124/pr.120.019539>
- Même, W., Calvo, C., Froger, N., Ezan, P., Amigou, E., Koulakoff, A., & Giaume, C. (2006). Proinflammatory cytokines released from microglia inhibit gap junctions in astrocytes: Potentiation by β-amyloid. *The FASEB Journal*, 20(3), 494–496. <https://doi.org/10.1096/fj.05-4297fje>
- Merry, T. L., Brooks, A. E. S., Masson, S. W., Adams, S. E., Jaiswal, J. K., Jamieson, S. M. F., & Shepherd, P. R. (2020). The CSF1 receptor inhibitor pexidartinib (PLX3397) reduces tissue macrophage levels without

- affecting glucose homeostasis in mice. *International Journal of Obesity*, 44(1), 245–253. <https://doi.org/10.1038/s41366-019-0355-7>
- Mirriore, M. M., Konomos, D. K., Gravanis, I., Dewey, S. L., Aguzzi, A., Heppner, F. L., & Tsirka, S. E. (2010). Microglial ablation and lipopolysaccharide preconditioning affects pilocarpine-induced seizures in mice. *Neurobiology of Disease*, 39(1), 85–97. <https://doi.org/10.1016/j.nbd.2010.04.001>
- Morin-Brureau, M., Milior, G., Royer, J., Chali, F., Le Duigou, C., Savary, E., Blugeon, C., Jourden, L., Akbar, D., Dupont, S., Navarro, V., Baulac, M., Bielle, F., Mathon, B., Clemenceau, S., & Miles, R. (2018). Microglial phenotypes in the human epileptic temporal lobe. *Brain*, 141(12), 3343–3360. <https://doi.org/10.1093/brain/awy276>
- Nikolic, L., Shen, W., Nobili, P., Virenque, A., Ulmann, L., & Audinat, E. (2018). Blocking TNF α -driven astrocyte purinergic signaling restores normal synaptic activity during epileptogenesis. *Glia*, 66(12), 2673–2683. <https://doi.org/10.1002/glia.23519>
- Nolte, C., Matyash, M., Pivneva, T., Schipke, C. G., Ohlemeyer, C., Hanisch, U. K., Kirchhoff, F., & Kettenmann, H. (2001) GFAP promoter-controlled EGFP expressing transgenic mice: a tool to visualize astrocytes and astrogliosis in living brain tissue. *Glia* 33(1):72–86.
- Onodera, M., Meyer, J., Furukawa, K., Hiraoka, Y., Aida, T., Tanaka, K., Rose, C. R., & Matsui, K. (2021). Exacerbation of epilepsy by astrocyte alkalization and gap junction uncoupling. *The Journal of Neuroscience*, 41(10), 2106–2118. <https://doi.org/10.1523/JNEUROSCI.2365-20.2020>
- Parkhurst, C. N., Yang, G., Ninan, I., Savas, J. N., Yates, J. R., Lafaille, J. J., Hempstead, B. L., Littman, D. R., & Gan, W.-B. (2013). Microglia promote learning-dependent synapse formation through brain-derived neurotrophic factor. *Cell*, 155(7), 1596–1609. <https://doi.org/10.1016/j.cell.2013.11.030>
- Pascual, O., Ben Achour, S., Rostaing, P., Triller, A., & Bessis, A. (2012). Microglia activation triggers astrocyte-mediated modulation of excitatory neurotransmission. *Proceedings of the National Academy of Sciences*, 109(4), E197–E205. <https://doi.org/10.1073/pnas.1111098109>
- Patel, D. C., Wallis, G., Dahle, E. J., McElroy, P. B., Thomson, K. E., Tesi, R. J., Szymkowski, D. E., West, P. J., Smeal, R. M., Patel, M., Fujinami, R. S., White, H. S., & Wilcox, K. S. (2017). Hippocampal TNF α signaling contributes to seizure generation in an infection-induced mouse model of limbic epilepsy. *Eneuro*, 4(2). <https://doi.org/10.1523/ENEURO.0105-17.2017>
- Probert, L., Akassoglou, K., Pasparakis, M., Kontogeorgos, G., & Kollias, G. (1995). Spontaneous inflammatory demyelinating disease in transgenic mice showing central nervous system-specific expression of tumor necrosis factor α . *Proceedings of the National Academy of Sciences*, 92, 11294–11298.
- Qin, C., Zhou, L.-Q., Ma, X.-T., Hu, Z.-W., Yang, S., Chen, M., Bosco, D. B., Wu, L.-J., & Tian, D.-S. (2019). Dual functions of microglia in ischemic stroke. *Neuroscience Bulletin*, 35(5), 921–933. <https://doi.org/10.1007/s12264-019-00388-3>
- R Core Team. (2021). R: A language and environment for statistical computing. 7 Feb 2022. <https://www.r-project.org/>.
- Rana, A., & Musto, A. E. (2018). The role of inflammation in the development of epilepsy. *Journal of Neuroinflammation*, 15(1), 144. <https://doi.org/10.1186/s12974-018-1192-7>
- Riaz, K., Galic, M. A., Kuzmiski, J. B., Ho, W., Sharkey, K. A., & Pittman, Q. J. (2008). Microglial activation and TNF production mediate altered CNS excitability following peripheral inflammation. *Proceedings of the National Academy of Sciences*, 105(44), 17151–17156. <https://doi.org/10.1073/pnas.0806682105>
- Rice, R. A., Spangenberg, E. E., Yamate-Morgan, H., Lee, R. J., Arora, R. P. S., Hernandez, M. X., Tenner, A. J., West, B. L., & Green, K. N. (2015). Elimination of microglia improves functional outcomes following extensive neuronal loss in the hippocampus. *Journal of Neuroscience*, 35(27), 9977–9989. <https://doi.org/10.1523/JNEUROSCI.0336-15.2015>
- Rock, R. B., Gekker, G., Hu, S., Sheng, W. S., Cheeran, M., Lokensgard, J. R., & Peterson, P. K. (2004). Role of microglia in central nervous system infections. *Clinical Microbiology Reviews*, 17(4), 942–964. <https://doi.org/10.1128/CMR.17.4.942-964.2004>
- Rodgers, K. M., Hutchinson, M. R., Northcutt, A., Maier, S. F., Watkins, L. R., & Barth, D. S. (2009). The cortical innate immune response increases local neuronal excitability leading to seizures. *Brain*, 132(9), 2478–2486. <https://doi.org/10.1093/brain/awp177>
- Sanchez, J. M. S., DePaula-Silva, A. B., Doty, D. J., Truong, A., Libbey, J. E., & Fujinami, R. S. (2019). Microglial cell depletion is fatal with low level picornavirus infection of the central nervous system. *Journal of Neurovirology*, 25(3), 415–421. <https://doi.org/10.1007/s13365-019-00740-3>
- Sano, F., Shigetomi, E., Shinozaki, Y., Tsuzukiyama, H., Saito, K., Mikoshiba, K., Horiuchi, H., Cheung, D. L., Nabekura, J., Sugita, K., Aihara, M., & Koizumi, S. (2021). Reactive astrocyte-driven epileptogenesis is induced by microglia initially activated following status epilepticus. *JCI Insight*, 6(9), e135391. <https://doi.org/10.1172/jci.insight.135391>
- Schindelin, J., Arganda-Carreras, I., Frise, E., Kaynig, V., Longair, M., Pietzsch, T., Preibisch, S., Rueden, C., Saalfeld, S., Schmid, B., Tinevez, J.-Y., White, D. J., Hartenstein, V., Eliceiri, K., Tomancak, P., & Cardona, A. (2012). Fiji: An open-source platform for biological-image analysis. *Nature Methods*, 9(7), 676–682. <https://doi.org/10.1038/nmeth.2019>
- Seifert, G., Huttmann, K., Binder, D. K., Hartmann, C., Wyczynski, A., Neusch, C., & Steinhauser, C. (2009). Analysis of astroglial K⁺ channel expression in the developing hippocampus reveals a predominant role of the Kir4.1 subunit. *Journal of Neuroscience*, 29(23), 7474–7488. <https://doi.org/10.1523/JNEUROSCI.3790-08.2009>
- Tukey, J. W. (1977). *Exploratory data analysis*. Addison-Wesley Pub. Co. http://archive.org/details/exploratorydata00tukey_0
- Varvel, N. H., Neher, J. J., Bosch, A., Wang, W., Ransohoff, R. M., Miller, R. J., & Dingledine, R. (2016). Infiltrating monocytes promote brain inflammation and exacerbate neuronal damage after status epilepticus. *Proceedings of the National Academy of Sciences*, 113(38), E5665–E5674. <https://doi.org/10.1073/pnas.1604263113>
- Vezzani, A., Conti, M., Luigi, A. D., Ravizza, T., Moneta, D., Marchesi, F., & Simoni, M. G. D. (1999). Interleukin-1 β immunoreactivity and microglia are enhanced in the rat hippocampus by focal kainate application: Functional evidence for enhancement of electrographic seizures. *The Journal of Neuroscience*, 19(12), 5065.
- Vezzani, A., French, J., Bartfai, T., & Baram, T. Z. (2011). The role of inflammation in epilepsy. *Nature Reviews Neurology*, 7(1), 31–40. <https://doi.org/10.1038/nrneuro.2010.178>
- Vezzani, A., Moneta, D., Richichi, C., Aliprandi, M., Burrows, S. J., Ravizza, T., Perego, C., & De Simoni, M. G. (2002). Functional role of inflammatory cytokines and anti-inflammatory molecules in seizures and epileptogenesis. *Epilepsia*, 43, 30–35. <https://doi.org/10.1046/j.1528-1157.43.s.5.14.x>
- Waltl, I., Käufer, C., Bröer, S., Chhatbar, C., Ghita, L., Gerhauser, I., Anjum, M., Kalinke, U., & Löscher, W. (2018). Macrophage depletion by liposome-encapsulated clodronate suppresses seizures but not hippocampal damage after acute viral encephalitis. *Neurobiology of Disease*, 110, 192–205. <https://doi.org/10.1016/j.nbd.2017.12.001>
- Waltl, I., Käufer, C., Gerhauser, I., Chhatbar, C., Ghita, L., Kalinke, U., & Löscher, W. (2018). Microglia have a protective role in viral encephalitis-induced seizure development and hippocampal damage. *Brain, Behavior, and Immunity*, 74, 186–204. <https://doi.org/10.1016/j.bbi.2018.09.006>
- Wang, N., Mi, X., Gao, B., Gu, J., Wang, W., Zhang, Y., & Wang, X. (2015). Minocycline inhibits brain inflammation and attenuates spontaneous recurrent seizures following pilocarpine-induced status epilepticus. *Neuroscience*, 287, 144–156. <https://doi.org/10.1016/j.neuroscience.2014.12.021>

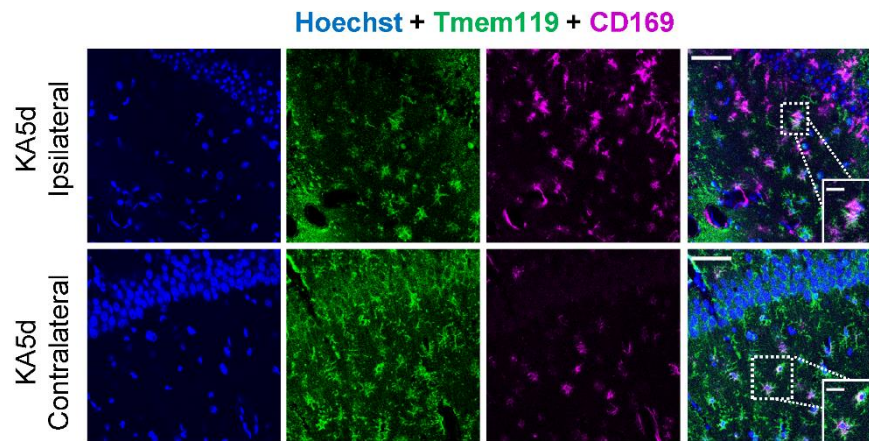


- Weinberg, M. S., Blake, B. L., & McCown, T. J. (2013). Opposing actions of hippocampus TNF α receptors on limbic seizure susceptibility. *Experimental Neurology*, 247, 429–437. <https://doi.org/10.1016/j.expneurol.2013.01.011>
- Wobbrock, J. O., Findlater, L., Gergle, D., & Higgins, J. J. (2011). The aligned rank transform for nonparametric factorial analyses using only anova procedures. In *Proceedings of the SIGCHI conference on human factors in computing systems*, pp. 143–146. Vancouver, BC, Canada: ACM. <https://doi.org/10.1145/1978942.1978963>.
- Wu, W., Li, Y., Wei, Y., Bosco, D. B., Xie, M., Zhao, M.-G., Richardson, J. R., & Wu, L.-J. (2020). Microglial depletion aggravates the severity of acute and chronic seizures in mice. *Brain, Behavior, and Immunity*, 89, 245–255. <https://doi.org/10.1016/j.bbi.2020.06.028>
- Wu, Z., Deshpande, T., Henning, L., Bedner, P., Seifert, G., & Steinhäuser, C. (2021). Cell death of hippocampal CA1 astrocytes during early epileptogenesis. *Epilepsia*, 62(7), 1569–1583. <https://doi.org/10.1111/epi.16910>
- Wyatt-Johnson, S. K., Herr, S. A., & Brewster, A. L. (2017). Status epilepticus triggers time-dependent alterations in microglia abundance and morphological phenotypes in the hippocampus. *Frontiers in Neurology*, 8, 700. <https://doi.org/10.3389/fneur.2017.00700>
- Yona, S., Kim, K.-W., Wolf, Y., Mildner, A., Varol, D., Breker, M., Strauss-Ayali, D., Viukov, S., Guillemins, M., Misharin, A., Hume, D. A., Perlman, H., Malissen, B., Zelzer, E., & Jung, S. (2013). Fate mapping reveals origins and dynamics of monocytes and tissue macrophages under homeostasis. *Immunity*, 38(1), 79–91. <https://doi.org/10.1016/j.immuni.2012.12.001>
- Zattoni, M., Mura, M. L., Deprez, F., Schwendener, R. A., Engelhardt, B., Frei, K., & Fritschy, J.-M. (2011). Brain infiltration of leukocytes contributes to the pathophysiology of temporal lobe epilepsy. *Journal of Neuroscience*, 31(11), 4037–4050. <https://doi.org/10.1523/JNEUROSCI.6210-10.2011>
- Zhao, X., Liao, Y., Morgan, S., Mathur, R., Feustel, P., Mazurkiewicz, J., Qian, J., Chang, J., Mathern, G. W., Adamo, M. A., Ritaccio, A. L., Gruenthal, M., Zhu, X., & Huang, Y. (2018). Noninflammatory changes of microglia are sufficient to cause epilepsy. *Cell Reports*, 22(8), 2080–2093. <https://doi.org/10.1016/j.celrep.2018.02.004>

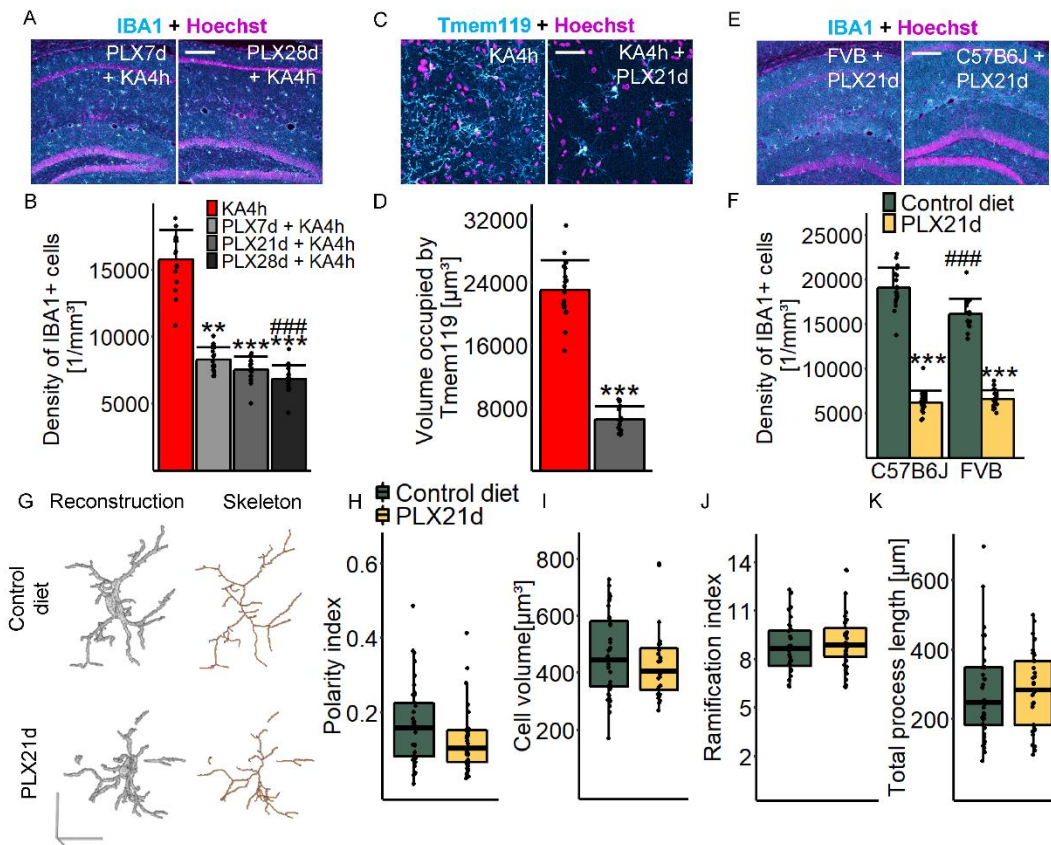
SUPPORTING INFORMATION

Additional supporting information can be found online in the Supporting Information section at the end of this article.

How to cite this article: Henning, L., Antony, H., Breuer, A., Müller, J., Seifert, G., Audinat, E., Singh, P., Brosseron, F., Heneka, M. T., Steinhäuser, C., & Bedner, P. (2023). Reactive microglia are the major source of tumor necrosis factor alpha and contribute to astrocyte dysfunction and acute seizures in experimental temporal lobe epilepsy. *Glia*, 71(2), 168–186. <https://doi.org/10.1002/glia.24265>

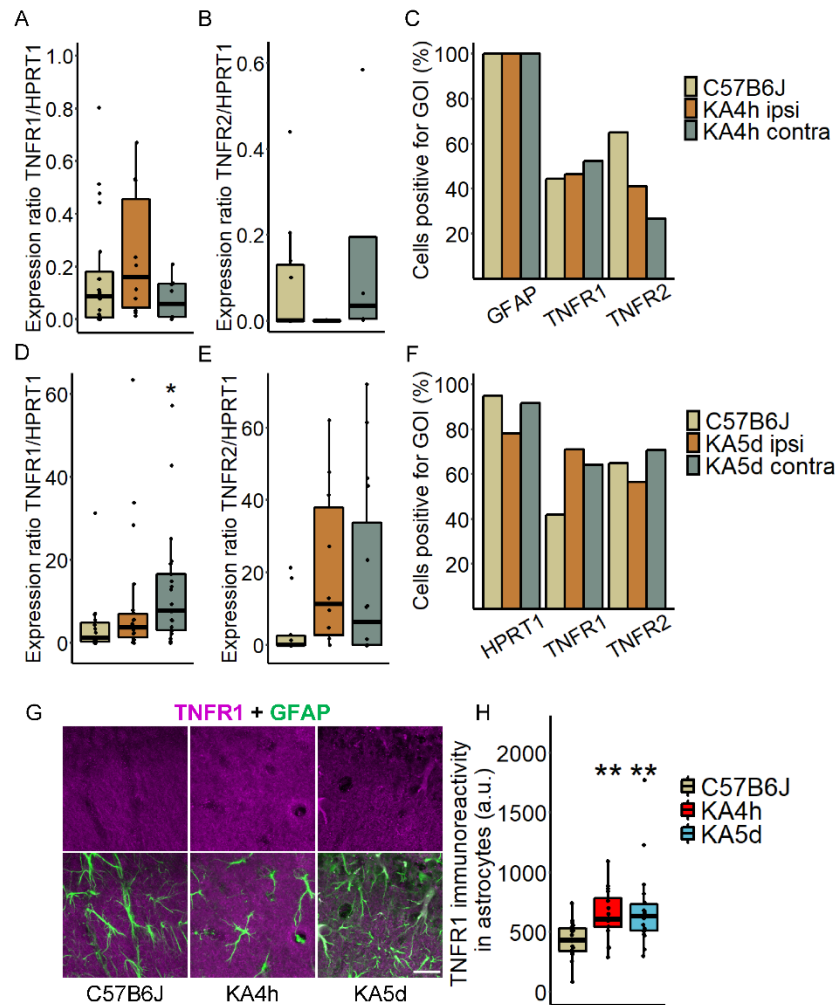


Supplementary Figure 1. CD169-positive cells partially co-express Tmem119 5 d post KA-induced SE. Representative images of a single focal plane of a combined Hoechst (blue), Tmem119 (green) and CD169 (magenta) staining in the hippocampal CA1 region of FVB mice. Scale bar: 50 μ m (Inset: 15 μ m). Images are background subtracted and brightness adjusted.



Supplementary Figure 2. CSF1R inhibition with PLX partially depletes microglia but has no influence on the morphology of surviving microglia. (A) Representative MIPs of combined IBA1 (cyan) and Hoechst (magenta) staining in the hippocampus of KA-injected FVB mice treated with PLX for 7, 21 or 28 d before SE induction. Scale bar: 200 μm . (B) IBA1 staining indicates partial microglia depletion regardless of the duration of PLX treatment at 4 h post KA injection, although 28 d was more effective than 7 d of PLX treatment (KA 4 h 13816 ± 1413 vs. PLX 7 d + KA 4 h 7326 ± 437 vs. PLX 21 d + KA 4 h 6696 ± 602 vs. PLX 28 d + KA 4 h 6063 ± 250 cells/mm³). $n = 2-3$ slices/mouse, $N = 3$ mice/condition; Kruskal-Wallis rank sum test followed by Dunn's post-hoc test; * vs. KA 4 h, # vs. PLX 7 d + KA 4 h. (C) Representative MIPs of combined Tmem119 (cyan) and Hoechst (magenta) staining in the CA1 *stratum radiatum*, 4 h after KA-injection of mice with or without 21 d of PLX pre-treatment. Scale bar: 50 μm . (D) 21 days of PLX pre-treatment reduced Tmem119 immunoreactivity by about 70% 4 h post KA injection (KA 4 h (mean + SD) $23017 + 3787$ vs. PLX 21 d + KA 4 h 6562 ± 1658 μm^3). $n = 2 - 3$ slices/mouse, $N = 3$ mice/condition; one-way ANOVA; * vs. KA 4 h. (E) Representative MIPs of combined IBA1 (cyan) and Hoechst (magenta) staining in the hippocampus of C57B6J and FVB mice receiving PLX for 21 d. Scale bar: 200 μm . (F) PLX-dependent microglia depletion was incomplete in both C57B16J and FVB mice. The density of

IBA1-positive cells was slightly lower in FVB vs. C57B6J mice fed a control diet (C57B6J: control diet 19060 ± 2265 vs. PLX 21 d 6209 ± 1289 ; FVB: control diet 16141 ± 1664 vs. PLX21d 6599 ± 984 cells/mm³). n = 3 slices/mouse, N = 3 mice/condition; two-way ANOVA; * vs. control diet, # vs. C57B6J. (G) 3D reconstruction and skeleton of IBA1-positive cells in the hippocampal CA1 *stratum radiatum* of mice treated either with control or PLX-containing diet for 21 d. Scale bar: 20 μ m. (H-K) Analyses of polarity, volume, ramification index and total process length of IBA1-positive cells revealed no differences between both groups (polarity (median, quartiles): control diet 0.159, 0.082-0.225 vs. PLX 21 d 0.104, 0.067-0.152; cell volume: control diet 444, 351-580 vs. PLX 21 d 406, 339-485 μ m³; ramification index: control diet 8.65, 7.56-9.73 vs. PLX 21 d 8.88, 8.13-9.88; process length: control diet 248, 183-350 vs. PLX 21 d 283, 183-368 μ m). n = 37 (control diet) and 36 (PLX 21 d) cells, N = 4 (control diet) and 3 (PLX 21 d) mice; Wilcoxon rank sum test or independent samples t-test. Data are displayed as mean + SD or as boxplots with median and quartiles. Black dots represent individual values. ** $p < 0.01$; *** $p < 0.001$; ### $p < 0.001$.



Supplementary Figure 3. Astrocytes upregulate TNFR1 in experimental TLE. (A, B) Normalized mRNA expression of TNFR1 and TNFR2 in astrocytes harvested from the hippocampal CA1 region was not different between non-injected and KA-injected C57B6J mice 4 h post KA injection (TNFR1/GFAP ratio: C57B6J 0.087, 0.006-0.18 vs. KA 4 h ipsi 0.161, 0.04-0.46 vs. KA 4 h contra 0.059, 0.009-0.14; TNFR2/GFAP ratio: C57B6J 0.0006, 0-0.13 vs. KA 4 h ipsi 0.0002, 0-0.0005 vs. KA 4 h contra 0.034, 0.004-0.194). TNFR1: n = 24 (C57B6J), 10 (KA 4 h ipsi), 8 (KA 4 h contra) cells; TNFR2: n = 10 (C57B6J), 6 (KA 4 h ipsi), 4 (KA 4 h contra) cells; Kruskal-Wallis rank sum test followed by Dunn's post-hoc test. (C) Percentage of cells that were positive for the gene of interest (GOI) in each experimental condition. Fisher's exact test with Benjamini-Hochberg adjusted multiple comparisons. (D, E) Normalized mRNA expression of TNFR1 and TNFR2 in astrocytes harvested from non-injected or KA-injected mice 5 d post injection. TNFR1 expression was significantly increased in astrocytes from the contralateral hippocampus while no difference was found for TNFR2

(TNFR1/HPRT1 ratio: C57B6J 1.1, 0.15-4.87 vs. KA 5 d ipsi 3.64, 1.23-6.86 vs. KA 5 d contra 7.65, 2.98-16.48; TNFR2/HPRT1 ratio: C57B6J 0.003, 0-2.57 vs. KA 5 d ipsi 11.38, 2.69-37.96 vs. KA 5 d contra 6.29, 0.02-33.76). TNFR1: n = 15 (C57B6J), 22 (KA 5 d ipsi), 21 (KA 5 d contra) cells; TNFR2: n = 10 (C57B6J), 10 (KA 5 d ipsi), 15 (KA 5 d contra) cells; Kruskal-Wallis rank sum test followed by Dunn's post-hoc test. * vs. C57B6J. (F) Percentage of cells that were positive for the GOI in each experimental condition. Fisher's exact test with Benjamini-Hochberg adjusted multiple comparisons. (G) Representative MIPs of combined TNFR1 (magenta) and GFAP (green) staining in the hippocampal CA1 region of C57B6J mice 4 h and 5 d post KA injection. Scale bar: 20 μ m. (H) TNFR1 expression was increased in astrocytes at 4 h and 5 d post KA injection (C57B6J 430, 341.28-532.67 vs. KA 4 h 606.4, 539-783.3 vs. KA 5 d 629.9, 511.9-730.7 a.u.). n = 3 slices/mouse, N = 3 mice/condition; Kruskal-Wallis rank sum test followed by Dunn's post-hoc test; * vs. C57B6J). Data are displayed as bar graphs or boxplots with median and quartiles. Black dots represent individual data points. * p < 0.05, ** p < 0.01.

4. Initiation of experimental temporal lobe epilepsy by early astrocyte uncoupling is independent of TGF β R1/ALK5 signaling

Lukas Henning, Christian Steinhäuser and Peter Bedner

The following chapter summarizes a research article that was published on 7th of May, 2021 in the journal *Frontiers in Neurology* (Volume 12) under the terms of the Creative Commons Attribution 4.0 International License (CC BY 4.0; <https://creativecommons.org/licenses/by/4.0/>). No changes to the original publication provided here were made. Copyright © 2021 Henning, Steinhäuser and Bedner. <https://doi.org/10.3389/fneur.2021.660591>

4.1 Summary of the publication

TLE and the brain insults that precede its development are closely related to BBB dysfunction (Greene et al., 2022; Milikovsky et al., 2019; van Vliet et al., 2007). Currently, however, it is not completely understood whether and how a compromised BBB contributes to the development and progression of epilepsy. Injection of the serum protein albumin into the brain is sufficient to cause epilepsy, suggesting that albumin mediates the pro-epileptic effects of a compromised BBB (Bar-Klein et al., 2014; Weissberg et al., 2015). Experimentally applied albumin is taken up by astrocytes *via* TGF β receptors, resulting in an abnormal molecular signature and impaired functionality of these cells (Bar-Klein et al., 2014; Braganza et al., 2012; Cacheaux et al., 2009; David et al., 2009; Ivens et al., 2007). In addition, observations from models of chemoconvulsant-induced epilepsy support the hypothesis that aberrant TGF β -signaling contributes to hyperexcitability and epilepsy (Greene et al., 2022; Tchekalarova et al., 2014; Zhang et al., 2019, 2020). Mechanistic insight for the link between albumin-induced TGF β signaling and seizures can be derived from a study demonstrating reduced astrocyte coupling efficiency following *intraventricular* albumin injection (Braganza et al., 2012), an important astrocyte homeostatic function assumed to causally contribute to epileptogenesis (Bedner et al., 2015; Wallraff et al., 2006). Based on these findings, here we employed the TGF β R1/ALK5 inhibitor IPW-5371 (Rabender et al., 2016) to examine whether aberrant albumin-induced TGF β R1/ALK5 signaling in astrocytes contributes to GJ uncoupling and epileptogenesis in a mouse model of MTLE-HS (Henning et al., 2021). Several experimental techniques including immunohistochemistry, intercellular tracer diffusion, and continuous telemetric EEG were combined to examine the consequences of inhibiting TGF β R1/ALK5

signaling during the acute/subacute phase of epileptogenesis on astrocyte uncoupling, seizure severity, and hippocampal degeneration in KA-induced epilepsy.

In line with previous findings (Greene et al., 2022; Munji et al., 2019; Zhang et al., 2019), KA-induced SE caused BBB disruption and albumin extravasation into the hippocampus. More specifically, albumin immunoreactivity was readily detectable in the injected vs. non-injected hippocampal CA1 region at 4 and 24 h post SE-induction, indicating rapid BBB opening in response to seizures. In contrast to our expectations, co-localization analysis of the astrocyte-specific cytoskeletal marker GFAP and albumin revealed only marginal albumin uptake into astrocytes during early epileptogenesis. Accordingly, application of the TGF β R1/ALK5 inhibitor IPW-5371 prior to SE induction did not prevent seizure-induced astrocyte uncoupling at the acute time point. Moreover, IPW-5371 pre-treatment slightly reduced epileptiform activity during the acute and chronic phases after KA administration, but did not affect the development of spontaneous recurrent seizures and HS (Henning et al., 2021).

Several important conclusions can be derived from the results of this study. First, we confirmed that BBB disruption and concomitant albumin leakage occur rapidly following KA-induced SE, indicating that albumin has the potential to contribute to the initiation of epilepsy. Second, in contrast to previous studies, we could not detect biologically relevant astrocytic albumin uptake, suggesting that albumin probably does not account for astrocyte uncoupling during KA-induced SE. This was confirmed by our finding that TGF β R1/ALK5 inhibition did not prevent astrocyte uncoupling, excluding aberrant TGF β signaling as the prime mediator of seizure-induced astrocyte uncoupling. Finally, the fact that early TGF β R1/ALK5 inhibition did only marginally affect epileptogenesis indicates that albumin-induced TGF β signaling during the early phase of epileptogenesis is not significantly involved in the development and progression of KA-induced epilepsy. Several considerations should be taken into account when interpreting the results of this study. First of all, we restricted our analyses to early time points after KA administration. It is possible that albumin uptake into astrocytes requires significantly more time, as the extracellular albumin concentration needs to achieve a certain threshold level to trigger uptake into astrocytes. Additionally, albumin could indirectly influence astrocytes, without the need for uptake and independently of TGF β signaling (Henning et al., 2021). Second, we did not examine whether downstream TGF β R1 signaling, such as Smad2 phosphorylation, occurred in astrocytes or any other CNS-resident cell population. Finally, prolonged TGF β R1/ALK5 inhibition may have been necessary to significantly alter the disease process, particularly in light of the fact that IPW-5371 remains only shortly active in the brain (Senatorov et al., 2019).

In conclusion, this study indicates that albumin-induced TGF β -signaling does not significantly contribute to dysfunctional astrocyte coupling and the consequential initiation of TLE.

4.2 Statement of contribution

Christian Steinhäuser and Peter Bedner conceived the project. Lukas Henning performed all immunohistochemical and tracer diffusion experiments, including preparation of necessary solutions and drug formulations. Surgical procedures to induce epilepsy including EEG transmitter transplantation were performed by Lukas Henning and Peter Bedner. Lukas Henning analyzed all imaging and electrophysiological data and established all necessary scripts and analysis pipelines. Similarly, all statistical analyses and visualizations were performed by Lukas Henning. All authors contributed to writing of the manuscript.

4.3 Publication

Henning, L., Steinhäuser, C., & Bedner, P. (2021). Initiation of Experimental Temporal Lobe Epilepsy by Early Astrocyte Uncoupling Is Independent of TGF β R1/ALK5 Signaling. *Frontiers in Neurology*, 12, 660591. <https://doi.org/10.3389/fneur.2021.660591>



Initiation of Experimental Temporal Lobe Epilepsy by Early Astrocyte Uncoupling Is Independent of TGF β R1/ALK5 Signaling

Lukas Henning, Christian Steinhäuser* and Peter Bedner*

Institute of Cellular Neurosciences, Medical Faculty, University of Bonn, Bonn, Germany

OPEN ACCESS

Edited by:

Esper A. Cavalheiro,
Federal University of São Paulo, Brazil

Reviewed by:

Ofer Prager,
Ben-Gurion University of the
Negev, Israel
Damir Janigro,
Case Western Reserve University,
United States

*Correspondence:

Christian Steinhäuser
cste@uni-bonn.de
Peter Bedner
peter.bedner@ukbonn.de

Specialty section:

This article was submitted to
Epilepsy,
a section of the journal
Frontiers in Neurology

Received: 29 January 2021

Accepted: 24 March 2021

Published: 07 May 2021

Citation:

Henning L, Steinhäuser C and
Bedner P (2021) Initiation of
Experimental Temporal Lobe Epilepsy
by Early Astrocyte Uncoupling Is
Independent of TGF β R1/ALK5
Signaling. *Front. Neurol.* 12:660591.
doi: 10.3389/fneur.2021.660591

Blood–brain barrier (BBB) dysfunction following brain insults has been associated with the development and progression of focal epilepsy, although the underlying molecular mechanisms are not fully elucidated yet. Activation of transforming growth factor beta (TGF β) signaling in astrocytes by extravasated albumin impairs the ability of astrocytes to properly interact with neurons, eventually leading to epileptiform activity. We used the unilateral intracortical kainate mouse model of temporal lobe epilepsy (TLE) with hippocampal sclerosis (HS) to gain further insights into the role of BBB leakage in *status epilepticus* (SE)-induced epileptogenesis. Immunohistochemical examination revealed pronounced albumin extravasation already 4 h after SE induction. Astrocytes were virtually devoid of albumin immunoreactivity (IR), indicating the lack of uptake by this time point. Inhibition of the TGF β pathway by the specific TGF β receptor 1 (TGF β R1) kinase inhibitor IPW-5371 did not prevent seizure-induced reduction of astrocytic gap junction coupling. Thus, loss of coupling, which is thought to play a causative role in triggering TLE-HS, is most likely not mediated by extravasated albumin. Continuous telemetric EEG recordings and video monitoring performed over a period of 4 weeks after epilepsy induction revealed that inhibition of the TGF β pathway during the initial phase of epileptogenesis slightly attenuated acute and chronic epileptiform activity, but did not reduce the extent of HS. Together, these data indicate that albumin extravasation due to increased BBB permeability and TGF β pathway activation during the first hours after SE induction are not significantly involved in initiating TLE.

Keywords: blood–brain barrier dysfunction, albumin extravasation, temporal lobe epilepsy, gap junctional coupling, astrocyte, transforming growth factor beta

KEY POINTS

- Strong albumin extravasation, but no astrocytic uptake, was detected 4 h after epilepsy induction.
- Seizure-induced reduction of astrocytic gap junction coupling was independent of TGF β R1/ALK5 signaling.
- Inhibition of TGF β R1/ALK5 signaling during early epileptogenesis slightly attenuated epileptiform activity but did not prevent the development of hippocampal sclerosis in experimental temporal lobe epilepsy.

INTRODUCTION

Epilepsy is often preceded by epileptogenic brain insults including traumatic brain injury, febrile seizures, or stroke (1–3). Impairment in blood–brain barrier (BBB) integrity is often associated with these insults and also occurs in the sclerotic hippocampus of patients with temporal lobe epilepsy (TLE) and corresponding animal models (4–7). Blood–brain barrier leakage leads to extravasation of the serum protein albumin into the brain parenchyma, which promotes epileptiform activity both *in situ* and *in vivo* (6, 8–10). Interestingly, serum albumin was proposed to be endocytosed into astrocytes *via* binding to transforming growth factor beta (TGF β) receptors and to activate TGF β signaling pathways (5, 6, 8). Albumin-induced TGF β signaling in astrocytes in turn provokes several physiological changes in these cells associated with the development of epilepsy, including excitatory synaptogenesis, impaired K⁺ and glutamate buffering, and production of pro-inflammatory cytokines (6, 11–13). Previously, we could demonstrate that disruption of astrocytic gap junction coupling and concomitant impairment of extracellular K⁺ buffering precede neuronal cell death in kainate-induced TLE, pointing toward a causative role in epileptogenesis (14). However, the underlying signaling pathway remains ill-defined. Interestingly, our previous work showed that albumin injected into the lateral ventricle is transported into hippocampal astrocytes leading to impaired astrocytic gap junction coupling 24 h after albumin injection (15). This was further supported by other findings demonstrating significant downregulation of transcripts for both astroglial gap junction-forming connexins, 24 h after albumin treatment in the rat brain (5, 11, 16). This suggests that albumin uptake into astrocytes promotes gap junction uncoupling *via* activation of TGF β signaling, leading to impaired spatial buffering of extracellular K⁺ and thereby promoting epileptic activity. To test this hypothesis, here we assessed in a mouse model of TLE whether aberrant albumin-mediated TGF β R1/ALK5 signaling upon kainate-induced *status epilepticus* (SE) induces astrocyte uncoupling and epileptogenesis. We took advantage of a novel TGF β R1 kinase inhibitor, IPW-5371, which effectively reduced TGF β signaling in the hippocampus of mice receiving intraventricular infusion of albumin (17). Immunohistochemistry, tracer diffusion studies, and continuous telemetric electroencephalography (EEG) were combined to assess the consequences of early inhibition of TGF β R1/ALK5 signaling on astrocytic coupling, seizure activity, and the development of HS.

MATERIALS AND METHODS

Animals

Male C57B6/J (Charles River, Sulzfeld, Germany, or bred in-house) mice aged 90–120 days were used for the experiments. Maintenance and handling of animals was performed according to local governmental regulations. Experiments were approved by the North Rhine–Westphalia State Agency for Nature, Environment and Consumer Protection (approval number 84-02.04.2015.A393). All measures were taken to minimize the number of animals used. Mice were kept under standard housing

conditions (12 h/12 h dark–light cycle) with food and water provided *ad libitum*.

Unilateral Intracortical Kainate Injection and Implantation of Telemetric Electroencephalography Transmitters

We employed the TLE-HS animal model as described previously (13, 18). Briefly, mice were anesthetized with a mixture of medetomidine (Cepetor, CP-Pharma, Burgdorf, Germany, 0.3 mg/kg, i.p.) and ketamine (Ketamidol, WDT, Garbsen, Germany, 40 mg/kg, i.p.) and placed into a stereotaxic frame equipped with a manual microinjection unit (TSE Systems GmbH, Bad Homburg, Germany). A total volume of 70 nl of a 20-mM solution of kainate (Tocris, Bristol, UK) in 0.9% sterile NaCl was stereotactically injected into the neocortex just above the right dorsal hippocampus. The stereotactic coordinates were 2 mm posterior to bregma, 1.5 mm from midline, and 1.7 mm from the skull surface. Sham control mice received injections of 70 nl saline under the same conditions. Directly after kainate injection, two drill holes were made at 1 mm posterior to the injection site and 1.5 mm lateral from midline for insertion of two monopolar leads required for electrographic seizure detection. Telemetric transmitters [TA10EA-F20 or TA11ETA-F10; Data Sciences International (DSI), St. Paul, MN, USA] were implanted subcutaneously into the right abdominal region, and both monopolar leads were inserted \sim 1 mm into the cortex. Attached leads were fixed to the skull using superglue and then covered with dental cement. Subsequently, the scalp incision was sutured and anesthesia stopped with atipamezol (Antisedan, Orion Pharma, Hamburg, Germany, 300 mg/kg, i.p.). To reduce pain, mice were injected for 3 days with carprofen (Rimadyl, Pfizer, Karlsruhe, Germany). Moreover, 0.25% enrofloxacin (Baytril, Bayer, Leverkusen, Germany) was administered *via* drinking water to reduce risk of infection. After surgery, mice were returned to clean cages and placed on individual radio receiving plates (RPC-1; Data Sciences International, New Brighton, MN, USA), which capture data signals from the transmitter and send them to a computer using the Ponemah software (Version 5.2, Data Sciences International) to convert the digital output of the receiver into a calibrated analog output. A video surveillance system (Bascom, Düsseldorf, Germany) was used to monitor behavioral seizure activity. Electroencephalography recordings (24 h/day, 7 days/week) were started immediately after transmitter implantation and continued for 28 days following the induction of SE.

Electroencephalography Analysis

Electroencephalography data were analyzed using NeuroScore (version 3.3.1) software (Data Sciences International) as described previously (19). Briefly, seizure frequency and duration as well as spike numbers was determined using the spike train analysis tool implemented in NeuroScore with the following criteria: threshold value = $7.5 \times$ SD of the baseline (i.e., activity during artifact- and epileptiform-free epochs) – 1,000 μ V, spike duration = 0.1–50 ms, spike interval = 0.1–2.5 s, minimum train duration = 30 s, train join interval = 1 s, and minimum

number of spikes = 50. Prior to spike analysis, recordings were high pass filtered at 1 Hz. Electroencephalography recordings were additionally verified by manual screening. Fast Fourier transformation (FFT) was performed to derive absolute δ (0.5–4 Hz), θ (4–8 Hz), α (8–13 Hz), β (13–30 Hz), and γ (30–50 Hz) power values during SE and the chronic phase, which were subsequently normalized to baseline activity prior to conducting statistics. The number of spontaneously generalized seizures during the chronic phase was determined manually by two experienced experimenters.

IPW-5371 Treatment

IPW-5371 was prepared as a suspension formulation (2 mg/ml IPW-5371 in 0.5% methylcellulose dissolved in 0.9% NaCl and Tween® 80) and applied once per 16–24 h and again ~15 min prior to kainate application (i.p. injection, 20 mg/kg). Daily i.p. injections of IPW-5371 at 20 mg/kg for 2 days effectively reduce TGF β signaling in the hippocampus of mice receiving intraventricular infusion of albumin (17). As a control, mice received vehicle (saline) injections under the same conditions.

Electrophysiology and Biocytin Loading of Astrocytes

Mice were anesthetized with isoflurane (Piramal Healthcare, Morpeth, UK) and decapitated. Next, brains were quickly removed and 200- μ m-thick coronal slices were cut on a vibratome (VT1000S, Leica, Wetzlar, Germany) in an ice-cold preparation solution containing the following (in mM): 87 NaCl, 2.5 KCl, 1.25 NaH₂PO₄, 25 NaHCO₃, 7 MgCl₂, 0.5 CaCl₂, 25 glucose, and 75 sucrose, equilibrated with carbogen (5% CO₂/95% O₂, pH 7.4). After storage of slices (15 min, 35°C) in preparation solution, the slices were transferred to a solution containing the following (in mM): 126 NaCl, 3 KCl, 2 MgSO₄, 2 CaCl₂, 10 glucose, 1.25 NaH₂PO₄, and 26 NaHCO₃ and gassed with carbogen to stabilize pH at 7.4 [artificial cerebrospinal fluid (aCSF)]. To aid in the identification of astrocytes in the tissue, aCSF was supplemented with SR101 (1 μ M, Sigma Aldrich, S7635, Steinheim, Germany; incubation 20 min, 35°C) (20). After SR101 staining, slices were transferred to aCSF and kept at room temperature (RT) for the duration of the experiments. For recordings, slices were transferred to a recording chamber and constantly perfused with aCSF. Patch pipettes fabricated from borosilicate capillaries with a resistance of 3–6 M Ω were filled with a solution containing the following (in mM): 130 K-gluconate, 1 MgCl₂, 3 Na₂-ATP, 20 HEPES, 10 EGTA, and biocytin (0.5%, Sigma Aldrich) (pH 7.2, 280–285 mOsm). For the analysis of gap junction coupling, whole-cell patch clamp recordings of SR101-positive astrocytes were performed during which astrocytes were filled with biocytin (20 min, RT). In addition to SR101 staining, astrocytes were identified by their characteristic morphology, small soma size, passive current-voltage relationship, and a resting membrane potential close to the Nernst potential for K⁺. Current signals were amplified (EPC 8, HEKA Electronic, Lambrecht, Germany), filtered at 3 or 10 kHz, and sampled at 10 or 30 kHz (holding potential –70 mV). Online analysis was performed with TIDA 5.25 acquisition and analysis software for Windows (HEKA) and Igor Pro

6.37 software (WaveMetrics, Lake Oswego, OR, USA). Voltages were corrected for liquid junction potentials. Only recordings matching the following criteria were included in the analysis: (i) resting potential negative to –60 mV, (ii) membrane resistance \leq 10 M Ω , and (iii) series resistance \leq 20 M Ω .

Immunohistochemistry

Tissue Preparation

Animals were deeply anesthetized by i.p. injection with 100–120 μ l of a solution containing 80 mg/kg ketamine (Ketamidol, WDT, Garbsen, Germany) and 1.2 mg/kg xylazine hydrochloride (Sigma-Aldrich). After checking for hind paw reflexes, transcatheterial perfusion was applied with ice-cold PBS (30 ml) followed by 4% ice-cold PFA in PBS (30 ml). Brains were removed and stored overnight in 4% PFA-containing solution and subsequently stored in PBS at 4°C until slicing. Brains were cut into 40- μ m-thick coronal slices using a Leica VT1200S vibratome (Leica Microsystems).

Staining

Immunohistochemistry was performed using free-floating slices kept in 24-well plates. Only slices from the dorsal hippocampus close to the injection site were used for staining. For membrane permeabilization and blocking of unspecific epitopes, slices were incubated (2 h, RT) with 0.5% Triton X-100 (or 2% for staining of biocytin-filled astrocytes) and 10% normal goat serum (NGS) in PBS. For immunostaining of albumin, no serum was applied during blocking and permeabilization steps. Slices were subsequently incubated overnight with primary antibody solution containing PBS on a shaker at 4°C. The following primary antibodies were applied: rabbit anti-GFAP (1:500, DAKO, Z0334, Hamburg, Germany), goat anti-albumin (1:200, Abcam, ab19194, Berlin, Germany), and mouse anti-NeuN (1:200, Merck Millipore, MAB377, Darmstadt, Germany). On the following day, slices were washed three times with PBS for 10 min each, followed by incubation with secondary antibodies conjugated with Alexa Fluor® 488, Alexa Fluor® 647, or streptavidin-conjugated Alexa Fluor® 647 (1:500 or 1:600, respectively, Invitrogen, Karlsruhe, Germany) in PBS (2% NGS, 1.5–2 h, RT). For staining of NeuN, slices were incubated with goat anti-mouse biotin (1:500, Dianova, AB_2338557, Hamburg, Germany) prior to incubation with streptavidin-conjugated Cy3 antibody (1:300, Sigma Aldrich, S6402; 1 h, RT). After washing the slices again three times with PBS (10 min), nuclear staining with Hoechst (1:200, diluted in dH₂O) was performed (10 min, RT). A final washing step (3 \times PBS, 5 min each) was performed and slices were mounted with Aqua-Poly/Mount (Polysciences, Heidelberg, Germany) on objective slides and covered with coverslips. Slides were stored at 4°C before confocal imaging.

Confocal Microscopy

Slides were imaged using a confocal laser scanning microscope (SP8, Leica, Hamburg, Germany) at 8 bit using 20 \times [numerical aperture (NA): 0.75], 40 \times (NA: 1.1), and 63 \times (NA: 1.2) objectives. Image resolution was set at 1,024 \times 1,024 pixels recorded at a speed of 400 Hz, with a pinhole size of 1 airy unit (AU) and a digital zoom of 1 (albumin extravasation), 1.2

(GJ coupling), or 2 (colocalization). Standard photomultiplier tubes were used for the detection of fluorescent signals. Laser and detector settings were applied equally to all images acquired. Z-stacks were taken at 2 μm (albumin extravasation and GJ coupling) or 0.3 μm (colocalization) intervals.

Quantification of Immunostainings

Immunohistochemical stainings were quantified either using Fiji/ImageJ (21) or Imaris 8.0 software (Bitplane, Zürich, Switzerland).

Albumin Extravasation

Albumin extravasation in the parenchyma was estimated by measuring the fluorescent intensity in the albumin channel in maximum intensity projections (MIP) using the image processing package Fiji. Initially, images were background subtracted using the rolling ball algorithm implemented in Fiji, with a radius set at 50 pixels (22). Albumin immunoreactivity (IR) was subsequently determined by quantifying the average pixel intensity in the albumin channel within the imaged field of view (290 \times 290 \times 20 μm).

Colocalization of Albumin and GFAP

Albumin content was quantified in albumin/GFAP double-stained hippocampal sections of C57B6J mice injected with kainate 4 h prior to brain perfusion. Images were analyzed equally applying a custom-written macro in Fiji software. Fluorescent intensity analysis was performed in regions of interest (ROIs) of 92 \times 92 \times 10 μm^3 . In a first step, the GFAP⁺ image was median filtered (5 pixel radius) and subsequently converted into a binary image applying the Triangle threshold algorithm implemented in Fiji (23). Next, the binary GFAP⁺ images and the albumin⁺ images were multiplied to derive albumin signal intensity in GFAP⁺ pixels. Within this multiplied image, the average pixel intensity value of albumin in GFAP⁺ pixels was measured and subsequently summed up across all focal plains to obtain albumin contents in GFAP⁺ cells. To determine albumin content in GFAP⁻ pixels, the GFAP image was preprocessed applying filtering and thresholding steps as described above. Next, the binarized GFAP⁺ image was subtracted from the albumin⁺ image to obtain albumin signal intensity in GFAP⁻ pixels. Average signal intensities were subsequently summed up across all focal plains for statistical comparison.

Coupling Efficiency in Biocytin-Filled Astrocytes

Coupling efficiency was determined by manual counting of biocytin⁺ cells using the cell counter plugin for Fiji and compared between injected (ipsilateral) and non-injected (contralateral) hemispheres. Another observer blinded to the experimental conditions recounted images of biocytin-filled astrocytes, and cell counts were subsequently averaged across both counts prior to statistical analysis.

Hippocampal Sclerosis

The extent of hippocampal sclerosis (HS) was estimated based on the quantification of three parameters: (i) extent of granule cell dispersion (GCD) in the dentate gyrus (DG), (ii) shrinkage of the CA1 *stratum radiatum*, and (iii) number of pyramidal

neurons in CA1 *stratum radiatum*. All three parameters were estimated in MIPs (1,163 \times 1,163 \times 40 μm^3). Granule cell dispersion quantification was performed as described previously (19). Briefly, GCL width was measured at four positions indicated as T1–T4. T1 and T2 were measured along a vertical line connecting the upper and lower cell layers of the DG, T3, and T4 at a distance halfway between the vertical line and the tip of the hilus. The average of the four values was used as an estimation of GCD. Shrinkage of the *stratum radiatum* was determined by drawing a vertical line connecting the pyramidal and molecular layer, above the peak of the DG granule cell layer. The length of the vertical line served as an indication of the remaining width of the *stratum radiatum*. Both GCL and *stratum radiatum* width were quantified using Fiji software. Finally, the number of pyramidal neurons in the CA1 region was quantified using the automated spot detection algorithm implemented in Imaris 8.0 within a 360 \times 120 \times 40- μm^3 ROI placed within the CA1 pyramidal layer just above the peak of the DG granule cell layer.

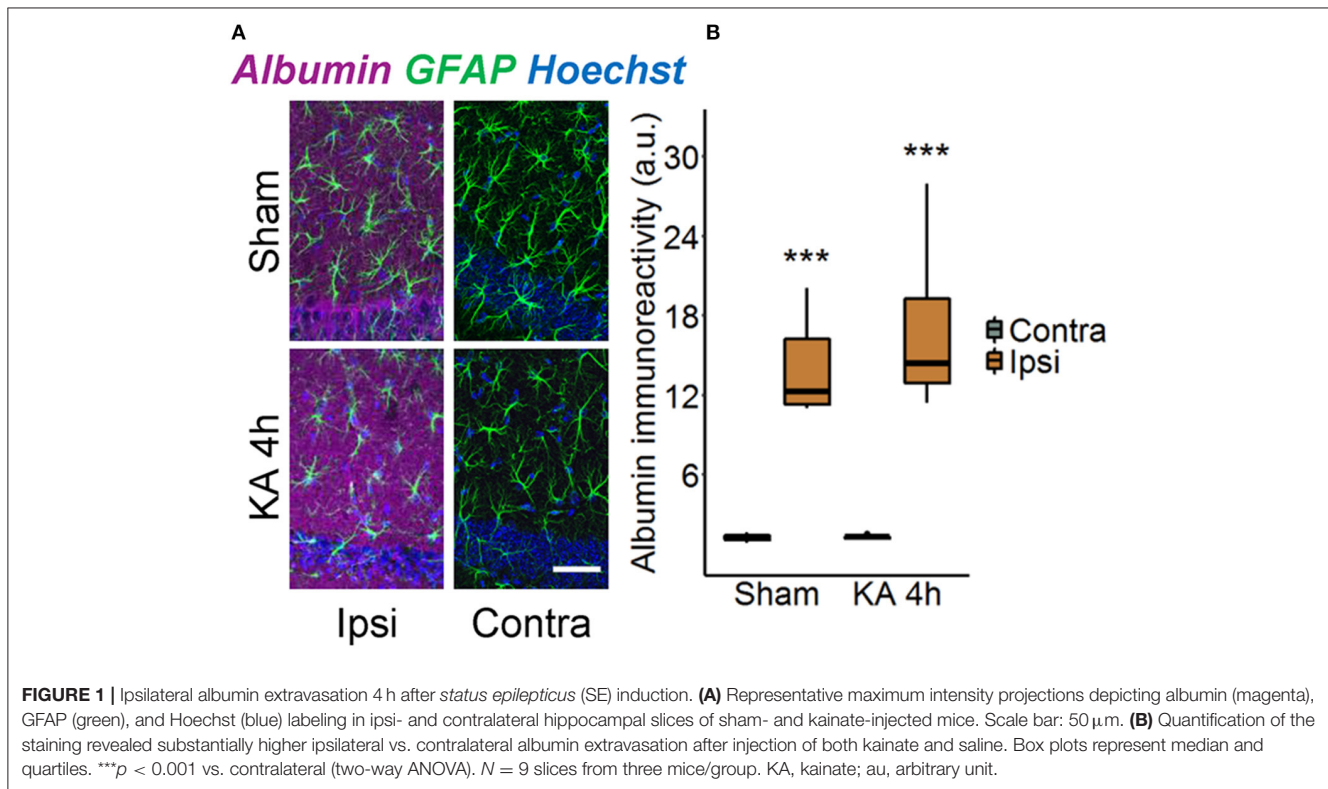
Statistical Analysis

Statistical analyses were performed using R software (R Core Team 2020, version 4.0.2, Austria) (24). Data are displayed as mean \pm SD or as box plots representing median (line) and quartiles (25th and 75th percentile) with whiskers extending to the highest and lowest values within 1.5 times the interquartile range (IQR). Prior to statistical analysis, data were checked for normality by inspection of histograms as well as by statistically testing for normality using a Shapiro–Wilk test. Levene's test was performed to check for homogeneity of variance between groups. In case of a significant deviation from normality, data were transformed according to Tukey's ladder of powers (25) prior to conduction of statistical tests or by performing the appropriate non-parametric test. For comparison of two groups, Student's *t*-test or Wilcoxon-rank sum test was used. More than two groups were compared with one-way analysis of variance (ANOVA) followed by *post-hoc* Tukey test or using Kruskal–Wallis test with Dunn's *post-hoc* test. For multifactorial data, two-way ANOVA was conducted. Kaplan–Meier estimates were compared using a log-rank test. Differences between means were considered significant at $p < 0.05$.

RESULTS

Strong Albumin Extravasation but Negligible Astrocytic Uptake 4 h After *status epilepticus* Induction

Disruption of the BBB accompanied by albumin extravasation occurs in human and experimental epilepsy, and there is growing evidence that this represents not only a pathological consequence but also a causative factor in epileptogenesis (26, 27). To shed further light on this important topic, we used an experimental mouse model, unilateral intracortical kainate injection, that closely mimics human TLE-HS in terms of seizure types, neuropathological changes, and pattern of epileptogenesis (14). In this model, we first examined the extent of albumin



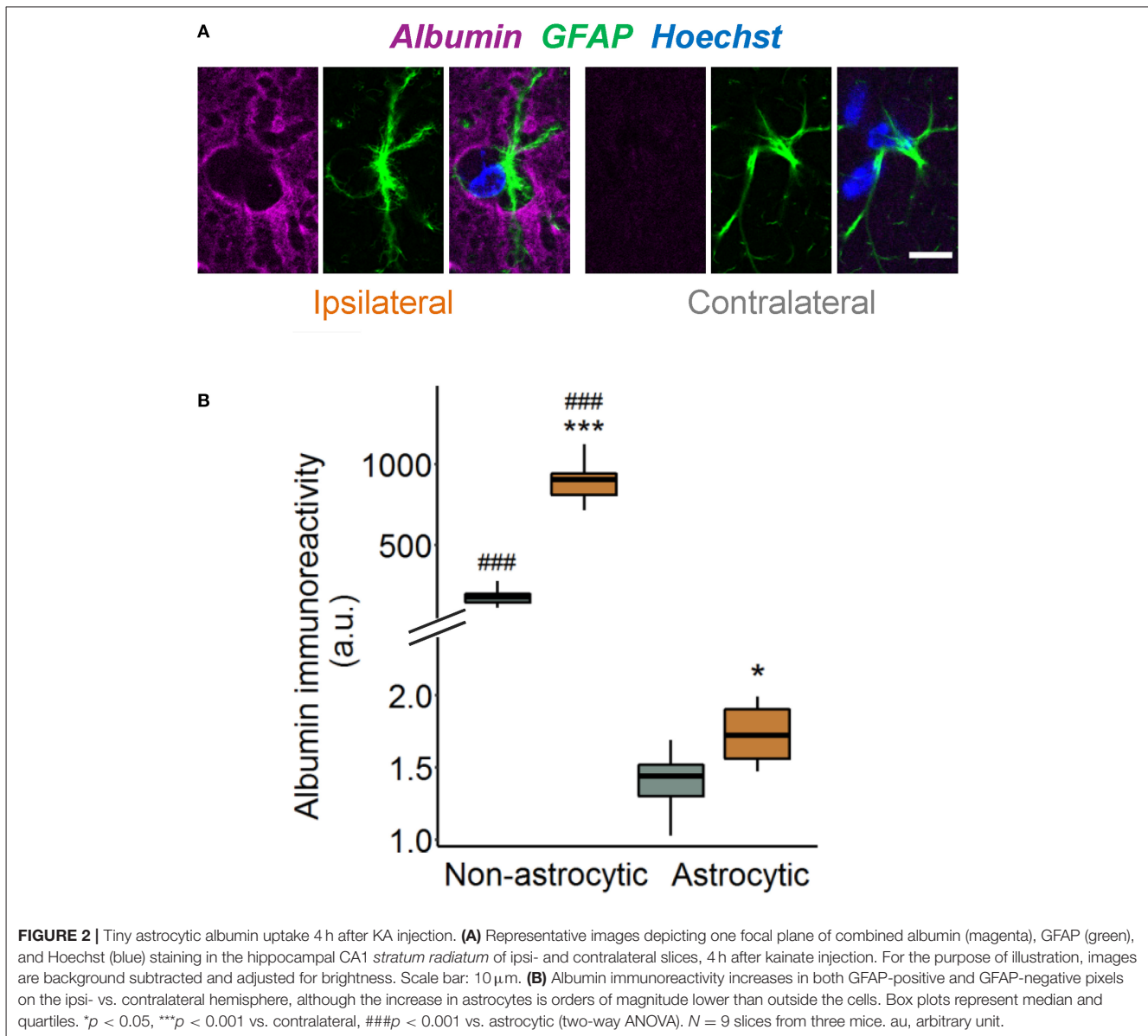
extravasation 4 h after kainate injection, a time point preceding neuronal cell death and the onset of spontaneous seizure activity (14). Immunohistochemical staining revealed strong extravascular albumin IR in the hippocampal CA1 region of the dorsal ipsilateral hippocampus (Figure 1, $p < 0.001$, two-way ANOVA). On the contralateral side, albumin was largely confined to blood vessels, indicating that BBB breakdown was restricted to the ipsilateral hippocampus. Surprisingly, we also detected a significant increase of albumin IR in the hippocampus of sham-injected mice. However, whereas albumin extravasation in epileptic mice persisted for months (26), it was a transient event in sham-injected mice and disappeared within 5 days after injection (data not shown).

Previous works demonstrated that TGF β receptor-mediated uptake of extravasated serum albumin into astrocytes is involved in epileptogenesis (6, 16). We therefore examined astrocytic albumin contents in albumin/GFAP double-stained hippocampal sections injected with kainate 4 h before (Figure 2A). Quantification revealed only faint albumin IR (<1%) in GFAP-positive compared with GFAP-negative pixels in the hippocampal CA1 region of both hemispheres (Figure 2B), indicating negligible astrocytic albumin uptake even in regions of high extravasation. Albumin IR was slightly higher in ipsilateral compared with contralateral astrocytes (Figure 2B, $p = 0.016$, two-way ANOVA), but because this effect was extremely small, its biological relevance is unclear. In conclusion, these results show that 4 h after epilepsy

induction, uptake of extravasated albumin by astrocytes is negligible.

Seizure-Induced Disruption of Astrocytic Coupling Is Independent of TGF β R1 Signaling

Disruption of astrocytic gap junctional communication is a characteristic feature of the sclerotic hippocampus of TLE patients and animal models. This astrocytic dysfunction and the consequential accumulation of extracellular K⁺ was detected already 4 h after intracortical kainate injection, leading to the suggestion that it plays a causative role in the pathogenesis of TLE (14). In another study, we demonstrated that intracerebroventricularly injected albumin is taken up by astrocytes and reduces their gap junctional coupling (15). Therefore, despite negligible astrocytic albumin uptake, the question arose whether activation of TGF β R1 by extravasated albumin mediates astrocyte uncoupling at this early stage of epileptogenesis. To address this question, we used a specific TGF β R1/ALK5 kinase inhibitor, IPW-5371, which has been shown to cross the BBB and to effectively reduce TGF β signaling (17). IPW-5371 was injected i.p. (20 mg/kg) 1 day and 15 min prior to kainate application, and gap junction coupling was assessed 4 h later by biocytin filling of individual hippocampal astrocytes. The results show that IPW-5371 pretreatment did not prevent seizure-induced astrocyte uncoupling (Figure 3).



Indeed, the number of biocytin-positive cells was reduced by 45% in the hippocampus of the injected hemisphere (ipsi 70 ± 26 vs. contra 128 ± 34 cells, mean \pm SD, $p = 0.0015$, independent samples t -test), which corresponds to data from epileptic mice with undisturbed TGF β R1 signaling (14). Thus, TGF β signaling appears not to be responsible for, or involved in, astrocyte uncoupling in experimental TLE.

IPW-5371 Pretreatment Slightly Attenuates Acute and Chronic Epileptiform Activity but Has no Effect on the Development of HS in Experimental TLE

Blood–brain barrier breakdown is implicated in the development of epilepsy through a mechanism involving astrocytic

TGF β R1/ALK5 signaling (6, 9, 16, 28). To gain a deeper insight into this relationship, we investigated consequences of TGF β R1 kinase inhibition during the initial phase of epileptogenesis on acute and chronic electrographic epileptiform activity and histopathological changes in our TLE model. Mice were injected with IPW-5371 as described above and implanted with telemetric transmitters directly after kainate injection. Electroencephalography recording and video monitoring were subsequently performed continuously (24 h/day) over a period of 4 weeks. Quantification of SE, which in our model is manifested by a series of convulsive seizures lasting up to 6 h, was performed in three different ways: (a) by examining the number and duration of seizures and time spent in ictal activity during the first hour of recording, (b) by counting the number of EEG spikes with amplitudes exceeding baseline

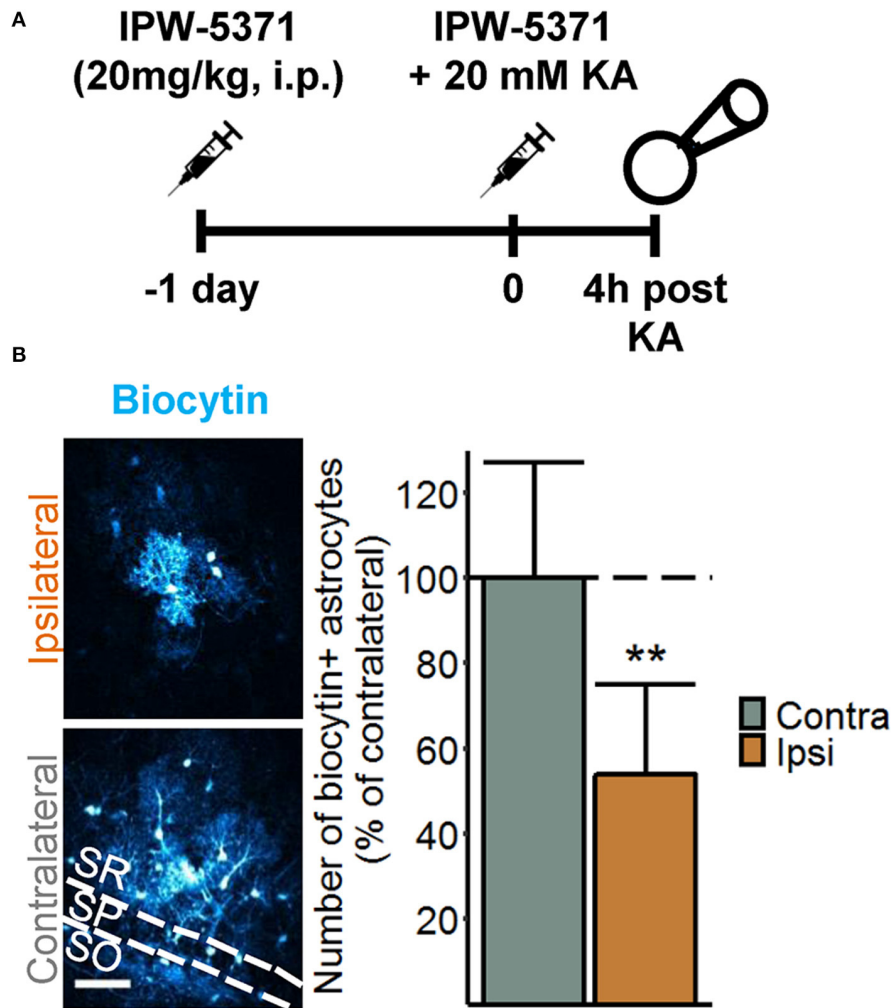
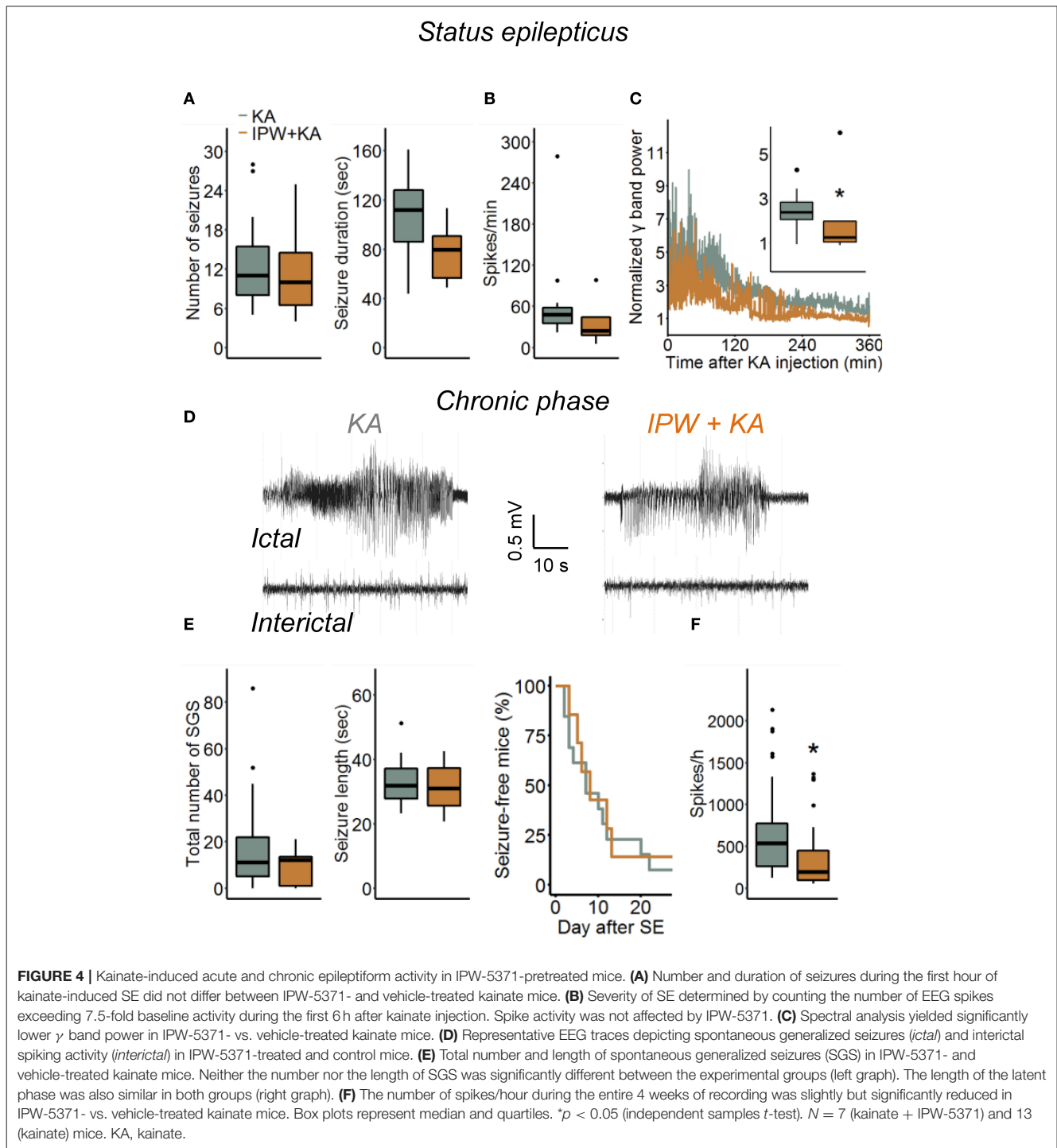


FIGURE 3 | Seizure-induced loss of astrocytic gap junctional communication is not mediated by TGFβR1 signaling. **(A)** Injection scheme for the biocytin diffusion studies. IPW-5371 was injected intraperitoneally (i.p.) once per day at 20 mg/kg for two consecutive days prior to SE induction via intracortical kainate injection. Four hours after kainate injection, animals were sacrificed and gap junctional coupling between hippocampal astrocytes was visualized by the intercellular spread of biocytin, which was included in the patch pipette solution during whole-cell patch clamp recordings (20 min). **(B)** Representative maximum intensity projections depicting biocytin-filled astrocytes labeled with streptavidin-conjugated AlexaFluor® (AF) 647 in hippocampal CA1 stratum radiatum of the ipsi- and contralateral hemispheres (left). Scale bar: 50 μm. The number of biocytin-positive astrocytes was significantly reduced on the ipsi- vs. contralateral hippocampus of IPW-5371-pretreated mice (right). Data represent mean ± SD. ***p* < 0.01 (independent samples *t*-test). *N* = 9 slices/condition from three mice. KA, kainate; SR, stratum radiatum; SP, stratum pyramidale; SO, stratum oriens.

activity at least 7.5-fold during the first 6 h of recording, and (c) by comparison of the spectral power in the γ range after FFT of the EEG data. Notably, activity during epileptiform-free periods did not differ between experimental groups (γ power baseline: kainate $2.72 \pm 1.36 \text{ nV}^2$ vs. IPW + kainate $3.38 \pm 0.97 \text{ nV}^2$, *p* = 0.29, independent samples *t*-test; $7.5 \times \text{SD}$ of baseline: kainate 196.61 ± 37.65 vs. IPW + kainate 222.75 ± 31.6 , *p* = 0.136, independent samples *t*-test). We found no differences between kainate mice treated with IPW-5371 or vehicle regarding the number of seizures or seizure duration within the first hour of SE (Figure 4A, *p* = 0.67 and *p* = 0.076, respectively, Mann-Whitney *U*-test). As mentioned earlier (19), this type of analysis is only

possible within the initial period of SE. For quantification of the entire SE, spike, and spectral analyses were extended to 6 h. While there was no difference in the number of spikes per minute during this period (*p* = 0.11, Mann-Whitney *U*-test), the normalized γ band power was significantly reduced in IPW-5371- vs. vehicle-treated kainate mice (Figures 4B,C, *p* = 0.037, Mann-Whitney *U*-test). These data indicated that TGFβR1 kinase inhibition interferes with acute seizure activity following kainate administration, specifically attenuating high-frequency activity in the γ range. The duration of the subsequent seizure-free (latent) phase was not influenced by IPW-5371 treatment (Figure 4A, right graph). Spontaneous generalized seizures



(Figure 4D) were seen in 92.3% (12 of 13) of vehicle-treated and 85.7% (6 of 7) of IPW-5371-treated kainate mice ($p = 0.73$, log-rank test). As shown in Figure 4E (left graph), the total number of spontaneous generalized seizures during the 4 weeks of recording hardly differed between the conditions ($p = 0.32$, Mann-Whitney U -test). Likewise, the duration of individual

generalized seizures was not different between the experimental groups (Figure 4E, right graph, $p = 0.6$, independent samples t -test). Importantly, during the entire recording period, the number of epileptic spikes per hour was significantly lower in the IPW-5371 group, indicating reduced total (e.g., ictal + interictal) activity (Figure 4F, $p = 0.023$, Mann-Whitney U -test). This

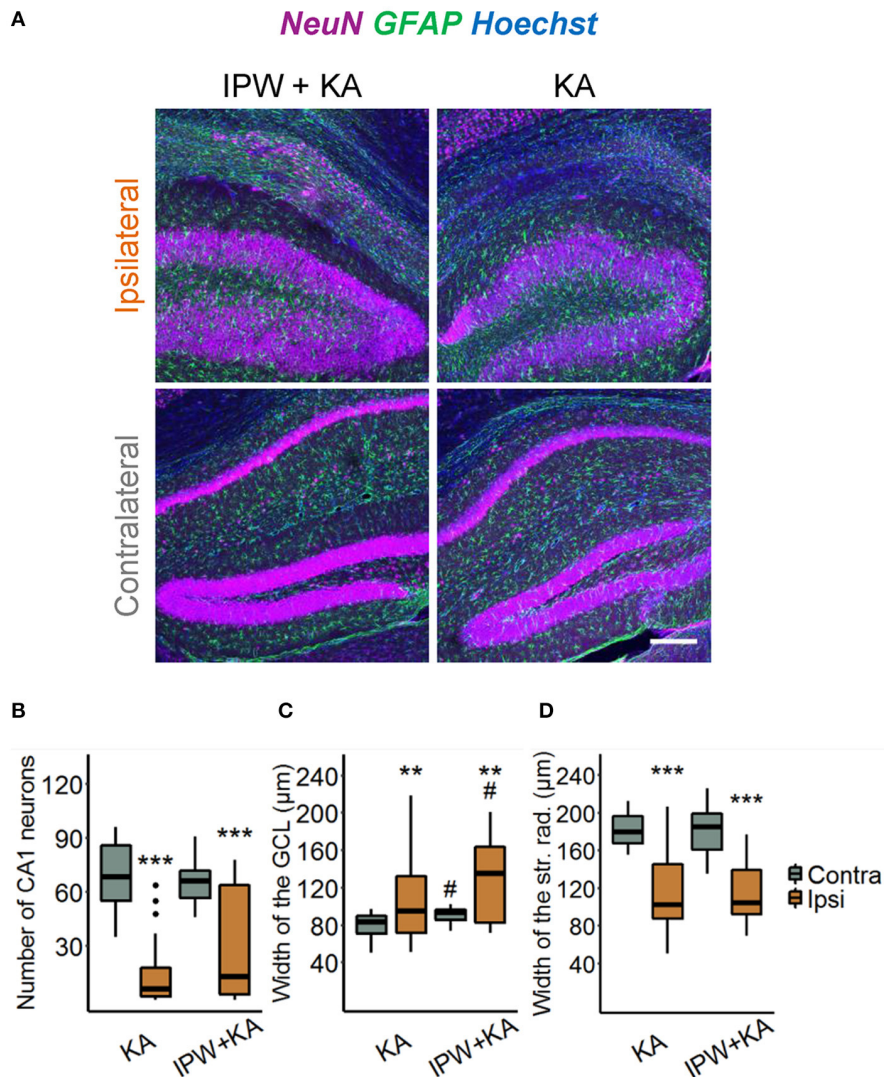


FIGURE 5 | IPW-5371 treatment has no effect on the development of HS in experimental TLE. **(A)** Representative maximum intensity projections of combined NeuN (magenta), GFAP (green), and Hoechst (blue) staining in ipsi- and contralateral hippocampal slices from IPW-5371- and vehicle-treated kainate mice 1 month after kainate injection. Scale bar: 200 μm . Hippocampi of both IPW-5371- and vehicle-treated kainate mice displayed similar **(B)** pyramidal cell loss in the CA1 region, **(C)** GCD in dentate gyrus, and **(D)** shrinkage of the CA1 *stratum radiatum*. Data display box plots representing median and quartiles. *** $p < 0.001$ vs. contralateral, ** $p < 0.01$, # $p < 0.05$ vs. control (two-way ANOVA). $N = 29\text{--}31$ slices from six animals/condition. CA, cornu ammonis; GCL, granule cell layer; str. rad., *stratum radiatum*.

finding was, however, not reflected by spectral analysis, since no difference was found in any of the frequency bands (data not shown). To assess a potential influence of the surgical procedure itself on seizure activity, brain activity was continuously EEG monitored for 9 days in a group of control mice that had received intracortical injection of 70 nl sterile NaCl (0.9%) instead of kainate. No seizures could be detected under these conditions ($n = 6$, data not shown).

We next explored the effect of IPW-5371 treatment on the development of HS. Hippocampal slices were stained with antibodies directed against NeuN, GFAP, and Hoechst 4 weeks after epilepsy induction (**Figure 5A**). Three hallmarks

of HS—degeneration of CA1 pyramidal neurons, shrinkage of the CA1 region, and GCD—were evaluated. The extent of neurodegeneration was determined by counting the number of NeuN-positive cells in an area of $360 \times 120 \times 40 \mu\text{m}^3$ within the CA1 *stratum pyramidale* underneath the injection side and at the same position on the contralateral side. The data show that the ipsilateral loss of NeuN-positive cells was similar in IPW-5371- vs. vehicle-treated kainate mice (19.69 ± 92.42 vs. $8.76 \pm 23.35\%$ of contralateral; $p < 0.001$, two-way ANOVA, **Figure 5B**). Likewise, neither GCD (148.69 ± 61.71 vs. $114.49 \pm 73.69\%$ of contralateral, $p = 0.0013$, two-way ANOVA) nor CA1 shrinkage (56.49 ± 25.41 vs. $56.86 \pm 32.17\%$ of contralateral, $p <$

0.001, two-way ANOVA) was attenuated by IPW-5371 treatment (Figures 5C,D). Unexpectedly, kainate mice pretreated with IPW-5371 displayed increased GCD compared with vehicle-treated kainate mice both ipsi- and contralaterally ($p = 0.014$, two-way ANOVA). Taken together, these data reveal that inhibition of the TGF β R1/ALK5 pathway with IPW-5371 slightly reduces acute and chronic kainate-induced epileptiform activity but does not prevent the development of HS.

DISCUSSION

Our data confirm that leakage of albumin through a compromised BBB represents an early event and possibly one of the causative factors in epileptogenesis. Indeed, prominent albumin IR is observed in the brain parenchyma as early as 4 h after SE induction, preceding most of the epilepsy-associated histopathological alterations in our experimental model (14). This result is not surprising, as it is known from various animal models of seizures and epilepsy that BBB opening occurs within a few minutes after seizure induction [for review, see (27, 29)]. Although previous work concluded that BBB leakage in epileptogenesis is transient and lasts only a few days, more recent studies observed the dysfunction also in chronic human and experimental epilepsy, indicating that it may also contribute to the progression of the disorder (5, 26, 29–33). In agreement with this view, we detected albumin extravasation also 5 days and 3 months after SE, triggered by intracortical kainate injection (26). A surprising finding of the present study was the relatively high hippocampal albumin extravasation in sham-injected mice. Apparently, in this model, initial BBB leakage is not solely evoked by kainate-induced seizure activity but may also be caused by the injection itself. Because in this model damage to the hippocampus is avoided by intracortical injections, the phenomenon may arise from local tissue pressure changes and/or inflammatory processes evoked by the injected saline. The fact that extravasated albumin was only transiently seen in sham controls indicates that seizure activity is a prerequisite for long-lasting BBB opening. On the other hand, these control experiments provide evidence that transient albumin extravasation is not sufficient to cause neuronal hyperactivity or neuronal damage, since we have never observed seizures or histopathological changes in sham-injected mice.

A number of reports have proposed that extravasated albumin exerts its epileptogenic effects by altering essential astrocytic functions, such as their ability to buffer K^+ and glutamate (11, 27, 34). Mechanistically, TGF β receptor-mediated albumin uptake into astrocytes was proposed to mediate changes in gene expression responsible for these functional alterations (6, 8, 9, 15). However, some studies reported proepileptic effects of extravasated or injected albumin in the absence of astrocytic albumin IR, raising the question of whether uptake is really required for the albumin effects (13, 35). Interestingly, despite the lack of astrocytic albumin, Bankstahl and colleagues observed reduced GFAP and AQP4 IR in albumin-positive hippocampal regions during the early phase of pilocarpine-triggered epileptogenesis, showing that

extravasated albumin can indeed influence astrocyte function without being taken up (35). Therefore, the lack of astrocytic albumin uptake found in our model does not exclude the possibility that albumin influences epileptogenesis *via* these cells.

Brain exposure to serum albumin impedes extracellular K^+ ($[K^+]_o$) buffering by reducing the expression of astrocytic inward rectifying K^+ channels (Kir 4.1) and gap junction proteins (6, 11, 15). According to the spatial K^+ buffering concept, excessive extracellular $[K^+]_o$ released during neuronal activity is passively taken up by astrocytes through Kir4.1 channels, and then redistributed through the gap junction-coupled astrocytic network to be released at regions of lower $[K^+]_o$ (36). Consequently, loss of Kir4.1 expression or astrocytic coupling would result in accumulation of $[K^+]_o$, neuronal depolarization, and a lowered threshold for seizure generation. We have previously demonstrated Kir4.1 downregulation in chronic human TLE (37, 38) as well as reduced astrocytic coupling and impaired K^+ clearance 4 h after SE induction in the intracortical kainate injection model of TLE (14). Since strong albumin extravasation was also found at this time point, it was reasonable to assume that albumin mediated the uncoupling. Our experiments with IPW-5371 do not support this hypothesis, although there is still the possibility that albumin affects coupling *via* a TGF β -independent pathway. Moreover, because we did not examine Kir4.1 expression in this study, we cannot rule out that impaired K^+ buffering in this model is mediated, at least in part, by albumin-induced downregulation of Kir4.1. Indeed, reduction of Kir4.1 expression may occur already 2 h after intracerebroventricular albumin injection (13), while downregulation of gap junction proteins and reduced interastrocytic coupling were demonstrated 24 h following exposure to albumin (11, 15). Disruption of astrocytic coupling in epileptogenesis is likely determined by different mechanisms at different time points during and after SE, and extravasated albumin may be involved at later time points of epileptogenesis.

Several studies provided convincing evidence that BBB leakiness contributes to epileptogenesis through albumin extravasation and activation of the TGF β pathway (6, 8, 9). This work revealed that albumin and TGF β R1 possess similar proepileptic effects that are prevented by TGF β pathway inhibition (9, 16). Our results show that early TGF β R1 inhibition only marginally affects the development of TLE, implying that BBB disruption and albumin extravasation over longer periods are required to crucially influence the process. Indeed, experimental opening of the BBB or albumin infusion over days was necessary to induce spontaneous seizures (6, 9, 10), while transient (short-term) hippocampal exposure to albumin, evoked by a single intracerebroventricular injection, was not sufficient to trigger seizures (13). According to its published pharmacokinetics, IPW-5371 effectively inhibits TGF β R1/ALK5 signaling for about 24 h (17). Future experiments are needed to reveal whether long-term inhibition (e.g., over the entire latency period, which lasts on average 5 days in this model) would completely suppress epileptogenesis. It must be stressed, however, that our data do not provide information about

whether TGF β signaling is activated by extravasated albumin and whether its proepileptic action is caused by changes in astrocytic function. Not only astrocytes but virtually all cell types in the brain, including neurons, microglia, and endothelial cells, produce TGF β and possess TGF β receptors (39). Our immunostaining indicated neuronal albumin uptake (at 24 h, but not yet 4 h post kainate, **Supplementary Figure 1**), an observation that matches several other studies (5, 13, 15, 40). Therefore, it would also be possible that albumin directly affects neuronal activity *via* TGF β signaling. Independent of this, extravasated albumin seems to affect neuronal excitability without influencing the strong histopathological alterations characteristic of HS. This result is consistent with previous research that found no evidence for albumin-induced neurodegeneration (10, 13, 34, 35). Unexpectedly, we observed even more pronounced GCD in IPW-5371-pretreated mice, both ipsi- and contralaterally. How TGF β R1 signaling regulates seizure-induced GCD remains to be elucidated in future experiments.

CONCLUSION

We show, in a mouse model closely resembling human TLE with HS, that albumin extravasation into the brain parenchyma arises very soon after SE induction. At this early stage, albumin is not yet taken up by astrocytes and uncoupling is not the result of albumin-stimulated TGF β R1/ALK5 signaling. Whether the latter is involved in the complete loss of coupling seen in chronic experimental and human epilepsy remains to be investigated. Inhibition of TGF β signaling during the first hours of kainate-induced SE only slightly affected epileptogenesis in our TLE model, suggesting that longer-lasting albumin extravasation is necessary to critically alter the pathological process. Our results provide new insights into the role of BBB dysfunction and the development of TLE, which may help in identifying new targets for antiepileptogenic strategies.

REFERENCES

- Shlosberg D, Benifla M, Kaufer D, Friedman A. Blood-brain barrier breakdown as a therapeutic target in traumatic brain injury. *Nat Rev Neurol*. (2010) 6:393–403. doi: 10.1038/nrneurol.2010.74
- Balami JS, Chen RL, Grunwald IQ, Buchan AM. Neurological complications of acute ischaemic stroke. *Lancet Neurol*. (2011) 10:357–71. doi: 10.1016/S1474-4422(10)70313-6
- Dubé CM, Brewster AL, Richichi C, Zha Q, Baram TZ. Fever, febrile seizures and epilepsy. *Trends Neurosci*. (2007) 30:490–6. doi: 10.1016/j.tins.2007.07.006
- Marchi N, Granata T, Ghosh C, Janigro D. Blood-brain barrier dysfunction and epilepsy: pathophysiologic role and therapeutic approaches: cerebrovascular determinants of seizure and epilepsy. *Epilepsia*. (2012) 53:1877–86. doi: 10.1111/j.1528-1167.2012.03637.x
- van Vliet EA, da Costa Araújo S, Redeker S, van Schaik R, Aronica E, Gorter JA. Blood-brain barrier leakage may lead to progression of temporal lobe epilepsy. *Brain*. (2007) 130:521–34. doi: 10.1093/brain/awl318

DATA AVAILABILITY STATEMENT

The original contributions presented in the study are included in the article/**Supplementary Material**, further inquiries can be directed to the corresponding author/s.

ETHICS STATEMENT

The animal study was reviewed and approved by North Rhine-Westphalia State Agency for Nature, Environment and Consumer Protection (approval number 84-02.04.2015.A393).

AUTHOR CONTRIBUTIONS

CS and PB designed and supervised the experiments, LH and PB performed and analyzed the experiments. All authors wrote the manuscript, contributed to the article, and approved the submitted version.

FUNDING

This work was supported by grants from the EU (H2020-MSCA-ITN project 722053 EU-GliaPhD) and BMBF (16GW0182 CONNEXIN, 01DN20001 CONNEX).

ACKNOWLEDGMENTS

We thank Anooshay Abid for the help in data analysis, Daniela Kaufer for stimulating ideas regarding the concept and comments on the final manuscript, and Barry Hart for providing IPW-5371 and for the final review of the manuscript.

SUPPLEMENTARY MATERIAL

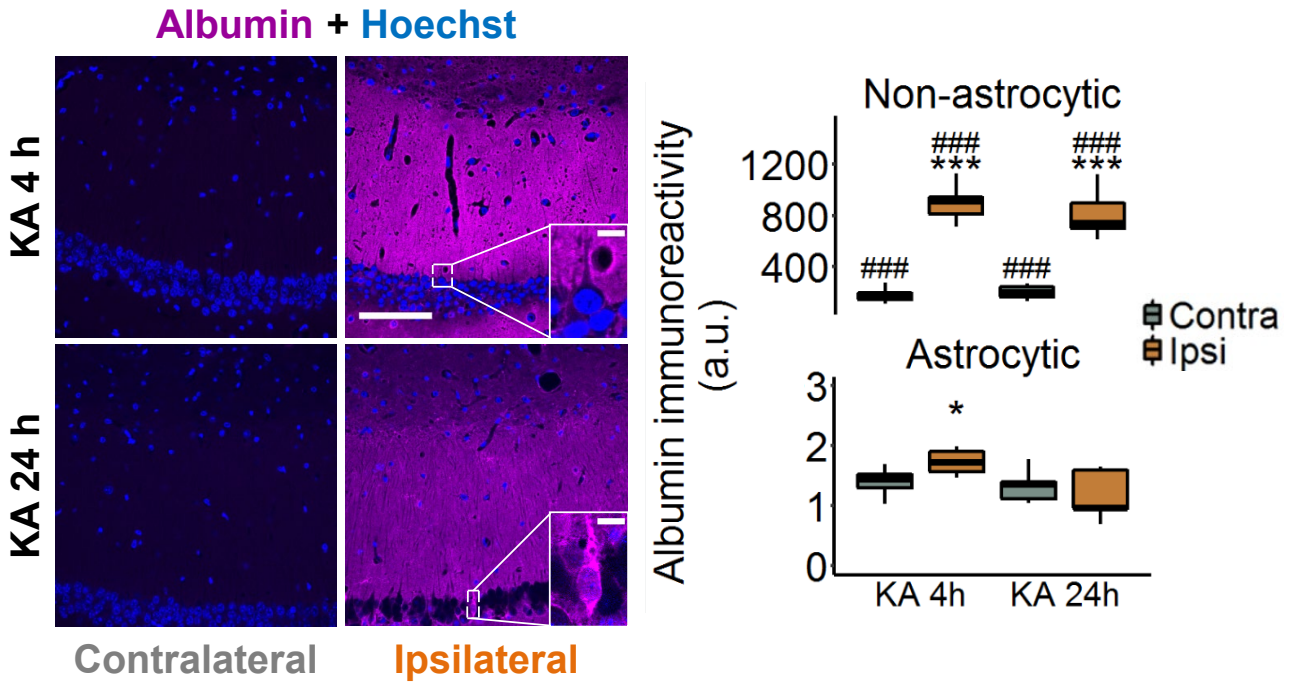
The Supplementary Material for this article can be found online at: <https://www.frontiersin.org/articles/10.3389/fneur.2021.660591/full#supplementary-material>

- Ivens S, Kaufer D, Flores LP, Bechmann I, Zumsteg D, Tomkins O, et al. TGF- β receptor-mediated albumin uptake into astrocytes is involved in neocortical epileptogenesis. *Brain*. (2007) 130:535–47. doi: 10.1093/brain/awl317
- Heinemann U, Gabriel S, Jauch R, Schulze K, Kivi A, Eilers A, et al. Alterations of glial cell function in temporal lobe epilepsy. *Epilepsia*. (2000) 41:S185–S189. doi: 10.1111/j.1528-1157.2000.tb01579.x
- Bar-Klein G, Cacheaux LP, Kamintsky L, Prager O, Weissberg I, Schoknecht K, et al. Losartan prevents acquired epilepsy via TGF- β signaling suppression. *Ann Neurol*. (2014) 75:864–75. doi: 10.1002/ana.24147
- Weissberg I, Wood L, Kamintsky L, Vazquez O, Milikovskiy DZ, Alexander A, et al. Albumin induces excitatory synaptogenesis through astrocytic TGF- β /ALK5 signaling in a model of acquired epilepsy following blood-brain barrier dysfunction. *Neurobiol Dis*. (2015) 78:115–25. doi: 10.1016/j.nbd.2015.02.029
- Seiffert E, Dreier JP, Ivens S, Bechmann I, Tomkins O, Heinemann U, et al. Lasting blood-brain barrier disruption induces epileptic focus in the rat somatosensory cortex. *J Neurosci*. (2004) 24:7829–36. doi: 10.1523/JNEUROSCI.1751-04.2004

11. David Y, Cacheaux LP, Ivens S, Lapolover E, Heinemann U, Kaufner D, et al. Astrocytic dysfunction in epileptogenesis: consequence of altered potassium and glutamate homeostasis? *J Neurosci.* (2009) 29:10588–99. doi: 10.1523/JNEUROSCI.2323-09.2009
12. Weissberg I, Reichert A, Heinemann U, Friedman A. Blood-brain barrier dysfunction in epileptogenesis of the temporal lobe. *Epilepsy Res Treat.* (2011) 2011:143908. doi: 10.1155/2011/143908
13. Frigerio F, Frasca A, Weissberg I, Parrella S, Friedman A, Vezzani A, et al. Long-lasting pro-ictogenic effects induced *in vivo* by rat brain exposure to serum albumin in the absence of concomitant pathology. *Epilepsia.* (2012) 53:1887–97. doi: 10.1111/j.1528-1167.2012.03666.x
14. Bedner P, Dupper A, Hüttmann K, Müller J, Herde MK, Dublin P, et al. Astrocyte uncoupling as a cause of human temporal lobe epilepsy. *Brain.* (2015) 138:1208–22. doi: 10.1093/brain/awv067
15. Braganza O, Bedner P, Hüttmann K, von Staden E, Friedman A, Seifert G, et al. Albumin is taken up by hippocampal NG2 cells and astrocytes and decreases gap junction coupling. *Epilepsia.* (2012) 53:1898–906. doi: 10.1111/j.1528-1167.2012.03665.x
16. Cacheaux LP, Ivens S, David Y, Lakhter AJ, Bar-Klein G, Shapira M, et al. Transcriptome profiling reveals TGF- β signaling involvement in epileptogenesis. *J Neurosci.* (2009) 29:8927–35. doi: 10.1523/JNEUROSCI.0430-09.2009
17. Senatorov VV, Friedman AR, Milikovskiy DZ, Ofer J, Saar-Ashkenazy R, Charbasha A, et al. Blood-brain barrier dysfunction in aging induces hyperactivation of TGF β signaling and chronic yet reversible neural dysfunction. *Sci Transl Med.* (2019) 11: doi: 10.1126/scitranslmed.aaw8283
18. Jefferys J, Steinhäuser C, Bedner P. Chemically-induced TLE models: topical application. *J Neurosci Methods.* (2016) 260:53–61. doi: 10.1016/j.jneumeth.2015.04.011
19. Deshpande T, Li T, Henning L, Wu Z, Müller J, Seifert G, et al. Constitutive deletion of astrocytic connexins aggravates kainate-induced epilepsy. *Glia.* (2020) 68: 2136–47. doi: 10.1002/glia.23832
20. Kafitz KW, Meier SD, Stephan J, Rose CR. Developmental profile and properties of sulforhodamine 101–Labeled glial cells in acute brain slices of rat hippocampus. *J Neurosci Methods.* (2008) 169:84–92. doi: 10.1016/j.jneumeth.2007.11.022
21. Schindelin J, Arganda-Carreras I, Frise E, Kaynig V, Longair M, Pietzsch T, et al. Fiji: an open-source platform for biological-image analysis. *Nat Methods.* (2012) 9:676–82. doi: 10.1038/nmeth.2019
22. Sternberg S. Biomedical image processing. *Computer.* (1983) 16:22–34.
23. Zack GW, Rogers WE, Latt SA. Automatic measurement of sister chromatid exchange frequency. *J Histochem Cytochem.* (1977) 25:741–53. doi: 10.1177/25.7.70454
24. R Core Team. *R: A Language and Environment for Statistical Computing.* R Foundation for Statistical Computing (2020). Available online at: <https://www.R-project.org/>
25. Tukey, JW. *Exploratory Data Analysis.* Reading, MA: Addison-Wesley Publishing Company (1977).
26. Deshpande T, Li T, Herde MK, Becker A, Vatter H, Schwarz MK, et al. Subcellular reorganization and altered phosphorylation of the astrocytic gap junction protein connexin43 in human and experimental temporal lobe epilepsy. *Glia.* (2017) 65:1809–20. doi: 10.1002/glia.23196
27. Löscher W, Friedman A. Structural, molecular, and functional alterations of the blood-brain barrier during epileptogenesis and epilepsy: a cause, consequence, or both? *Int J Mol Sci.* (2020) 21:591. doi: 10.3390/ijms21020591
28. Kim SY, Senatorov VV, Morrissey CS, Lippmann K, Vazquez O, Milikovskiy DZ, et al. TGF β signaling is associated with changes in inflammatory gene expression and perineuronal net degradation around inhibitory neurons following various neurological insults. *Sci Rep.* (2017) 7:7711. doi: 10.1038/s41598-017-07394-3
29. van Vliet EA, Aronica E, Gorter JA. Blood-brain barrier dysfunction, seizures and epilepsy. *Semin Cell Dev Biol.* (2015) 38:26–34. doi: 10.1016/j.semdb.2014.10.003
30. Pont F, Collet A, Lallemand G. Early and transient increase of rat hippocampal blood-brain barrier permeability to amino acids during kainic acid-induced seizures. *Neurosci Lett.* (1995) 184:52–4. doi: 10.1016/0304-3940(94)11166-G
31. Roch C, Leroy C, Nehlig A, Namer IJ. Magnetic resonance imaging in the study of the lithium-pilocarpine model of temporal lobe epilepsy in adult rats. *Epilepsia.* (2002) 43:325–5. doi: 10.1046/j.1528-1157.2002.11301.x
32. Nodde-Ekane XE, Hayward N, Gröhn O, Pitkänen A. Vascular changes in epilepsy: functional consequences and association with network plasticity in pilocarpine-induced experimental epilepsy. *Neuroscience.* (2010) 166:312–32. doi: 10.1016/j.neuroscience.2009.12.002
33. Gorter JA, van Vliet EA, Aronica E. Status epilepticus, blood-brain barrier disruption, inflammation, and epileptogenesis. *Epilepsy Behav.* (2015) 49:13–6. doi: 10.1016/j.yebeh.2015.04.047
34. Lapolover EG, Lippmann K, Salar S, Maslarova A, Dreier JP, Heinemann U, et al. Peri-infarct blood-brain barrier dysfunction facilitates induction of spreading depolarization associated with epileptiform discharges. *Neurobiol Dis.* (2012) 48:495–506. doi: 10.1016/j.nbd.2012.06.024
35. Bankstahl M, Breuer H, Leiter I, Märkel M, Bascuñana P, Michalski D, et al. Blood-Brain Barrier Leakage during Early Epileptogenesis Is Associated with Rapid Remodeling of the Neurovascular Unit. *eNeuro.* (2018) 5: doi: 10.1523/ENEURO.0123-18.2018
36. Orkand RK, Nicholls JG, Kuffler SW. Effect of nerve impulses on the membrane potential of glial cells in the central nervous system of amphibia. *J Neurophysiol.* (1966) 29:788–806. doi: 10.1152/jn.1966.29.4.788
37. Schröder W, Hinterkeuser S, Seifert G, Schramm J, Jabs R, Wilkin GP, et al. Functional and molecular properties of human astrocytes in acute hippocampal slices obtained from patients with temporal lobe epilepsy. *Epilepsia.* (2000) 41(Suppl 6):S181–4. doi: 10.1111/j.1528-1157.2000.tb01578.x
38. Hinterkeuser S, Schröder W, Hager G, Seifert G, Blümcke I, Elger CE, et al. Astrocytes in the hippocampus of patients with temporal lobe epilepsy display changes in potassium conductances. *Eur J Neurosci.* (2000) 12:2087–96. doi: 10.1046/j.1460-9568.2000.00104.x
39. Blobel GC, Schiemann WP, Lodish HF. Role of transforming growth factor β in human disease. *N Engl J Med.* (2000) 342:1350–8. doi: 10.1056/NEJM200005043421807
40. Rigau V, Morin M, Rousset M-C, de Bock F, Lebrun A, Coubes P, et al. Angiogenesis is associated with blood-brain barrier permeability in temporal lobe epilepsy. *Brain.* (2007) 130:1942–56. doi: 10.1093/brain/awm118

Conflict of Interest: The authors declare that the research was conducted in the absence of any commercial or financial relationships that could be construed as a potential conflict of interest.

Copyright © 2021 Henning, Steinhäuser and Bedner. This is an open-access article distributed under the terms of the Creative Commons Attribution License (CC BY). The use, distribution or reproduction in other forums is permitted, provided the original author(s) and the copyright owner(s) are credited and that the original publication in this journal is cited, in accordance with accepted academic practice. No use, distribution or reproduction is permitted which does not comply with these terms.



Supplementary Figure S1: Albumin is largely absent in astrocytes at 4 and 24 h post kainate, but appears to be taken up into ipsilateral CA1 pyramidal neurons, 24 h post kainate injection (*left panel, bottom right*). Scale bar: 100 μm (insets: 10 μm). * $P < 0.05$, *** $P < 0.001$ vs contralateral, ### $P < 0.001$ vs astrocytic (Two-way ANOVA).

5. Constitutive deletion of astrocytic connexins aggravates kainate-induced epilepsy

Tushar Deshpande, Tingsong Li, **Lukas Henning**, Zhou Wu, Julia Müller, Gerald Seifert, Christian Steinhäuser, Peter Bedner

The following chapter summarizes a research article that was published on 2nd of April, 2020 in the journal GLIA (Volume 68, Issue 10) under the terms of the Creative Commons Attribution 4.0 International License (CC BY 4.0; <https://creativecommons.org/licenses/by/4.0/>). No changes to the original publication provided here were made. © 2020 The Authors. GLIA published by Wiley Periodicals, Inc. <https://doi.org/10.1002/glia.23832>

5.1 Summary of the publication

The formation of large functional networks *via* pore-forming GJs allows for extensive intercellular communication between neighboring astrocytes (Giaume et al., 2021), which in turn has an important function in modulating the extracellular milieu and the synchronization of neuronal activity (Chever et al., 2016; Giaume et al., 2010). In contrast, the role of astroglial networks in the pathophysiology of epilepsy is less well understood. Our previous data demonstrate that a reduced astrocyte coupling efficiency and impaired K⁺ clearance precede neuronal death in experimental MTLE-HS, suggesting that dysfunctional GJ coupling causally contributes to the disease process (Bedner et al., 2015). Furthermore, slices from mice lacking the astroglial GJ-forming proteins Cx30 and C43 are characterized by spontaneous epileptiform events and a heightened sensitivity to epileptic stimuli (Wallraff et al., 2006), pointing towards a primarily pro-epileptic effect when interastrocytic coupling is impaired. However, data examining how the absence of astrocyte Cxs affects the development of chronic epilepsy is currently not available. To better understand the role of astroglial networks in the pathology of epilepsy, we took advantage of Cx DKO mice and subjected them to the KA model of MTLE-HS (Deshpande et al., 2020). We combined telemetric EEG to continuously monitor seizure activity following *intracortical* KA injection with immunohistochemical and microscopy techniques to examine the extent of HS, neuroinflammation and seizure-induced angio- and neurogenesis in DKO vs wild-type (WT) mice.

Our data revealed that DKO and WT mice were similarly susceptible to KA-induced SE, with somewhat more frequent but less durable acute seizures after KA-injection in DKO mice. Most

importantly, DKO mice displayed an increased number of spontaneous recurrent seizures as well as elevated spike frequency and spectral EEG power in the delta range (0.5 – 4 Hz) during the chronic phase of epilepsy. Although the extent of neuron loss in the CA1 pyramidal layer was similar between both genotypes, DKO exhibited less pronounced ipsilateral astrocyte reactivity in the hippocampal CA1 region and GCD in the DG one month post KA administration. Similarly, microglia reactivity and proliferation were attenuated in the ipsilateral CA1 region but not DG in DKO vs. WT mice. Finally, whereas seizure-induced neurogenesis was not affected by genetic deletion of astroglial Cxs, seizure-induced angiogenesis was significantly reduced in both the CA1 and DG of DKO vs. WT mice (Deshpande et al., 2020).

The results of this study show that loss of astroglial coupling exacerbates MTLE-HS pathology, largely confirming our hypothesis that the functional astroglial network primarily exerts antiepileptic functions. Indeed, chronic seizure activity was significantly increased in DKO mice demonstrating that the pro-convulsive effects of an impaired ionic buffering capacity of astrocytes outweigh the anticonvulsant potential of reduced metabolic supply to neurons, ultimately enhancing epileptiform activity. In contrast to our expectations, hippocampal neurodegeneration was not different between DKO and WT mice, suggesting that the increased seizure burden in DKO mice was a direct consequence of the loss of Cx channel functions and not mediated by more extensive neuronal loss. Moreover, the fact that the chronic seizure burden was increased in DKO mice although the extent of astro- and microgliosis as well as angiogenesis, phenomena suggested to be primarily pro-epileptic (Morin-Brureau et al., 2012; Robel et al., 2015; Sano et al., 2021), were less pronounced in DKO mice, further highlights the important role of dysfunctional astrocyte coupling in epileptogenesis. Of note, our data do not allow to derive definitive conclusions about the mechanisms underlying increased seizure activity in Cx-deficient mice. This is due to the fact that loss of functional GJ coupling between astrocytes not only impairs spatial K^+ buffering but also the redistribution of Na^+ and Ca^{2+} ions through the astrocytic network (Henneberger, 2017; Langer et al., 2012; Scemes & Giaume, 2006). Finally, several developmental side effects, such as white matter pathology (Lutz et al., 2009) and impaired glutamate uptake (Pannasch et al., 2011), have been identified in DKO mice, indicating the need for inducible Cx knock-out models.

Conclusively, this study provides evidence for an anti-epileptic role of the astrocyte GJ-coupled network, suggesting that treatments aiming to enhance GJ coupling in astrocytes might prove effective to mitigate the development and progression of epilepsy.

5.2 Statement of contribution



Christian Steinhäuser and Peter Bedner conceived the project. Tushar Deshpande, Tingsong Li and Zhou Wu performed immunohistochemical stainings, microscopy recordings and image analyses. Lukas Henning, Julia Müller and Peter Bedner performed all surgical procedures necessary for the experimental induction of epilepsy and EEG transmitter implantation. The analysis procedure for the EEG data was developed and conducted by Lukas Henning and Peter Bedner. Gerald Seifert took care of the breeding and genotyping of the animals. Statistical analyses were performed by Tushar Deshpande, Lukas Henning, Peter Bedner, Tingsong Li and Zhou Wu. Christian Steinhäuser, Peter Bedner and Tushar Deshpande wrote the manuscript.

5.3 Publication

Deshpande, T., Li, T., Henning, L., Wu, Z., Müller, J., Seifert, G., Steinhäuser, C., & Bedner, P. (2020). Constitutive deletion of astrocytic connexins aggravates kainate-induced epilepsy. *Glia*, 68(10), 2136–2147. <https://doi.org/10.1002/glia.23832>

RESEARCH ARTICLE

Constitutive deletion of astrocytic connexins aggravates kainate-induced epilepsy

Tushar Deshpande¹ | Tingsong Li² | Lukas Henning¹ | Zhou Wu¹ |
Julia Müller¹ | Gerald Seifert¹ | Christian Steinhäuser¹  | Peter Bedner¹ 

¹Institute of Cellular Neurosciences, Medical Faculty, University of Bonn, Bonn, Germany

²Department of Neurology, Children's Hospital of Chongqing Medical University, Chongqing, China

Correspondence

Peter Bedner, Institute of Cellular Neurosciences, Medical Faculty, University of Bonn, Venusberg-Campus 1, D-53127 Bonn, Germany.

Email: peter.bedner@ukb.uni-bonn.de

Present address

Tushar Deshpande, Institute of Physiological Chemistry and Pathobiochemistry, University of Muenster, Münster, Germany

Funding information

Bundesministerium für Bildung und Forschung, Grant/Award Number: 16GW0182
CONNEXIN; European Commission, Grant/Award Number: H2020-MSCA-ITN project 722053 EU-GliaPhD

Abstract

The astroglial gap junctional network formed by connexin (Cx) channels plays a central role in regulating neuronal activity and network synchronization. However, its involvement in the development and progression of epilepsy is not yet understood. Loss of interastrocytic gap junction (GJ) coupling has been observed in the sclerotic hippocampus of patients with mesial temporal lobe epilepsy (MTLE) and in mouse models of MTLE, leading to the suggestion that it plays a causative role in the pathogenesis. To further elucidate this clinically relevant question, we investigated consequences of astrocyte disconnection on the time course and severity of kainate-induced MTLE with hippocampal sclerosis (HS) by comparing mice deficient for astrocytic Cx proteins with wild-type mice (WT). Continuous telemetric EEG recordings and video monitoring performed over a period of 4 weeks after epilepsy induction revealed substantially higher seizure and interictal spike activity during the chronic phase in Cx deficient versus WT mice, while the severity of *status epilepticus* was not different. Immunohistochemical analysis showed that, despite the elevated chronic seizure activity, astrocyte disconnection did not aggravate the severity of HS. Indeed, the extent of CA1 pyramidal cell loss was similar between the experimental groups, while astrogliosis, granule cell dispersion, angiogenesis, and microglia activation were even reduced in Cx deficient as compared to WT mice. Interestingly, seizure-induced neurogenesis in the adult dentate gyrus was also independent of astrocytic Cxs. Together, our data indicate that constitutive loss of GJ coupling between astrocytes promotes neuronal hyperexcitability and attenuates seizure-induced histopathological outcomes.

KEYWORDS

astrocyte, gap junction channels, hippocampal sclerosis, neurogenesis, *status epilepticus*, temporal lobe epilepsy

1 | INTRODUCTION

The general ability of astrocytes to modulate neuronal function is well established while its specific involvement in the pathogenesis of neurological disorders is a matter of intense research. A striking feature of

astrocytes is their abundant intercellular connection via gap junction (GJ) channels, leading to the formation of large syncytium-like functional networks. Due to this network organization, astrocytes are in a position to effectively control and synchronize large neuronal assemblies, and it appears evident that impaired coupling has deleterious consequences on

This is an open access article under the terms of the Creative Commons Attribution License, which permits use, distribution and reproduction in any medium, provided the original work is properly cited.

© 2020 The Authors. *Glia* published by Wiley Periodicals, Inc.

brain functioning (Giaume, Koulakoff, Roux, Holcman, & Rouach, 2010). GJ channels are composed of a family of proteins called connexins (Cx). Six Cxs oligomerize into a hemichannel (connexon) and two connexons from adjacent cell membranes dock to form an intercellular GJ channel. In the hippocampus, the communication between astrocytes is mainly accomplished by Cx43 channels and only to a small extent by channels composed of Cx30 (Gosejacob et al., 2011). GJ channels are permeable to ions and small molecules up to 1 kDa, including second messengers, nucleotides, neurotransmitters, and energy metabolites (Giaume et al., 2010).

The role of astroglial networks in the pathophysiology of epilepsy is still debated (Boison & Steinhäuser, 2018; Steinhäuser, Seifert, & Bedner, 2012). On the one hand, astrocyte coupling limits neuronal excitability by clearance and redistribution of extracellular ions and neurotransmitters (Pannasch et al., 2011; Wallraff et al., 2006), while on the other hand astrocyte–astrocyte connections are required to maintain synaptic transmission by activity-dependent supply of energy metabolites from blood vessels to the firing neurons (Rouach, Koulakoff, Abudara, Willecke, & Giaume, 2008). Hence, in principle, the astroglial network exerts both proepileptic and antiepileptic effects. We have previously shown that the sclerotic hippocampus of patients with medically refractory mesial temporal lobe epilepsy (MTLE) is completely devoid of classical astrocytes and GJ coupling. The functional properties of human and murine astrocytes are strikingly similar (Bedner, Jabs, & Steinhäuser, 2019). In a mouse model of MTLE, we could demonstrate that astrocyte uncoupling and the consequential impairment of K^+ clearance temporally precede neuronal death and the onset of spontaneous seizure activity, pointing to a causative role of uncoupling in the genesis of MTLE (Bedner et al., 2015). In favor of a causative role is also the finding that transgenic mice with coupling-deficient astrocytes (Cx30^{-/-}; Cx43^{fl/fl}hGFAP-Cre mice; termed DKO mice) display disturbed K^+ and glutamate clearance as well as spontaneous epileptiform field potentials and a decreased threshold for evoking epileptiform activity in acute hippocampal slices (Pannasch et al., 2011; Wallraff et al., 2006). A recent study reported that DKO mice are less prone to pentylenetetrazole (PTZ)-induced hyperexcitability, leading to the speculation that specific blockade of astrocytic GJs could be of therapeutic benefit also in chronic seizures (Chever, Dossi, Pannasch, Derangeon, & Rouach, 2016). Hence, the data obtained from DKO mice so far are conflicting and do not allow firm conclusions on the role of the astroglial network in epilepsy. To shed more light on this issue, in the present study we examined the effects of Cx30 and Cx43 deletion in astrocytes on acute and chronic electrographic seizure activity as well as on the consequential morphological changes in a mouse model of MTLE with hippocampal sclerosis (HS).

2 | METHODS

2.1 | Animals

Maintenance and handling of animals was according to the local government regulations. Experiments were approved by the North

Rhine–Westphalia State Agency for Nature, Environment and Consumer Protection (approval numbers 84-02.04.2012.A212 and 84-02.04.2015.A393). All measures were taken to minimize the number of animals used. Mice were kept under standard housing conditions (12 hr/12 hr dark–light cycle, food, and water ad libitum). Male C57Bl6/J mice (Charles River, Sulzfeld, Germany) and transgenic mice lacking Cx30 and Cx43 in GFAP-positive cells (Cx30^{-/-}; Cx43^{fl/fl}hGFAP-Cre mice, Wallraff et al., 2006) aged 90–120 days were used for the experiments.

2.2 | Kainate injection and EEG recordings

We used the MTLE animal model previously established (Bedner et al., 2015). Briefly, mice were anesthetized with a mixture of medetomidine (Cepetor, CP-Pharma, Burgdorf, Germany, 0.3 mg/kg, i.p.) and ketamine (Ketamidol, WDT, Garbsen, Germany, 40 mg/kg, i.p.) and placed in a stereotaxic frame equipped with a manual microinjection unit (TSE Systems GmbH, Bad Homburg, Germany). A total volume of 70 μ l of a 20 mM solution of kainate (Tocris, Bristol, UK) in 0.9% sterile NaCl were stereotactically injected into the neocortex just above the right dorsal hippocampus. The stereotactic coordinates were 2 mm posterior to bregma, 1.5 mm from midline and 1.7 mm from the skull surface. Electrographic seizures were detected via skull surface electrodes implanted directly after kainate injection. Telemetric transmitters (TA10EA-F20, TA11ETA-F10; Data Sciences International, St. Paul, MN) were placed subcutaneously into the right abdominal region and the two monopolar leads were connected to stainless steel screws (length 2 mm; thread diameter 0.8 mm) positioned bilaterally 1.5 mm from the sagittal suture and 2 mm posterior to bregma. The attached leads were covered with dental cement, skin incisions sutured, and anesthesia stopped with atipamezole (Antisedan, Orion Pharma, Hamburg, Germany, 300 mg/kg, i.p.). To reduce pain, mice were subsequently injected for 3 days with carprofen (Rimadyl, Pfizer, Karlsruhe, Germany). Furthermore, 0.25% Enrofloxacin (Baytril, Bayer, Leverkusen, Germany) was administered via drinking water to reduce the risk of infection. Mice were then returned to clean cages and placed on individual radio receiving plates (RPC-1; Data Sciences International), which capture data signals from the transmitter and send them to a computer running Dataquest A.R.T. 4.00 Gold/Platinum software (Data Sciences International), which converts the digital output of the receiver into a calibrated analog output. A network-based video surveillance system (SeeTec, Philippsburg, Germany) was used to monitor behavioral seizure activity.

NeuroScore 3.2 software (Data Sciences International) was used for EEG analysis. Seizure frequency and duration were determined using the NeuroScore seizure detection module with the following parameters: threshold value = $10 \times SD$ of the baseline–1,000 μ V, spike duration = 0.05–50 ms, spike interval = 0.1–2.5 s, minimum train duration = 10 s, and minimum number of spikes per event = 50. All EEG recordings were

additionally verified by manual screening. Automated and manual EEG screening was always performed by two independent investigators, one of which was blinded to the experimental conditions. For spectral analysis, EEG data were subjected to fast Fourier transform (FFT) and the absolute power (i.e., the integral of the power values over the different frequency ranges expressed in μV^2) of the frequency bands δ (0.5–4 Hz), θ (4–8 Hz), α (8–13 Hz), β (13–30 Hz), and γ (30–50 Hz) were calculated in 10 s epochs for the entire 4 weeks of continuous EEG recording. The γ -band power during the first 6 hr of EEG recording was used for *status epilepticus* (SE) quantification, as the power in this frequency range is the most reliable and least artifact-prone indicator for SE severity (Lehmkuhle et al., 2009). In contrast, the interictal activity during the chronic phase is best reflected by the δ band power (Cohen, Navarro, Clemenceau, Baulac, & Miles, 2002; Putra et al., 2020), which was therefore determined in the third and fourth weeks. The calculated values were normalized to baseline activity, which was defined as the frequency power during several artifact- and epileptiform activity-free epochs (at least 10 min) within the last week of EEG recording. For spike analysis, EEG recordings were first high pass filtered at 1 Hz and then the number of EEG spikes exceeding 10-fold the SD of baseline activity was assessed using an automated spike detection protocol (NeuroScore). SD of baseline activity was calculated for every second of EEG recording during the above-mentioned epileptiform activity-free epochs.

2.3 | BrdU administration

Mice were given BrdU (1 mg/ml) through drinking water containing 1% sucrose for 14 days after kainate injection. BrdU administration was started 24 hr after kainate injection. From Day 16 after kainate injection, mice were given normal drinking water. On Day 30, anesthetized mice were perfused with PBS followed by 4% PFA. Brains from these mice were subsequently fixed in 4% PFA for 12–16 hr. The next day, brains were transferred in vials containing PBS and stored until further use. Brains were cut into 40 μm thick coronal sections with a vibratome. The sections were stored in PBS containing 0.01% sodium azide.

2.4 | Immunofluorescence staining

Sections were incubated with 2 N HCl for 30 min. After washing with PBS, remaining HCl in the sections was neutralized by incubating the sections in 0.1 M borate buffer for 10 min. After permeabilization and blocking (2 hr, room temperature) with 0.5% Triton X-100 and 10% normal goat serum (NGS) (or 10% normal donkey serum [NDS]) in PBS, the sections were incubated overnight (4°C) in 5% NGS (or NDS) in PBS containing 0.1% Triton X-100 and the following primary antibodies: rat anti-BrdU (AbD

Serotec, 1:500); goat anti-CD31 (R & D systems, 1:200); goat anti-GFAP (Abcam, 1:500); mouse anti-NeuN (Merck, 1:500); goat anti-doublecortin (DCX) (Santacruz Biotech, 1:100); rabbit anti-Iba1 (Dako, 1:1,000); rabbit anti-Prox1 (Chemicon, 1:2,500). After washing three times with PBS (5 min each), the sections were incubated with secondary antibodies conjugated with Alexa Fluor 488, Alexa Fluor 594 or Alexa Fluor 647 (Invitrogen, dilution 1:500 each) in PBS with 2% NGS (or 2% NDS) and 0.1% Triton X-100 for 1.5 hr at room temperature.

2.5 | Imaging and cell counting

A confocal laser-scanning microscope (Leica TCS SP8, Wetzlar, Germany) was used for image acquisition. For cell counting, images were taken at $\times 40$ magnification (stacks of eight image planes with optical thickness of 1 μm each) while for assessing granule cell dispersion (GCD), $\times 10$ magnification (stacks of three image planes with optical thickness of 8 μm) was used. Image resolution was 1,024 \times 1,024 pixels. Cell counting in the dentate gyrus (DG) and CA1 regions was performed in 290 \times 290 \times 4 μm^3 counting boxes. The first counting box in the DG was positioned 250 μm away from the tip of the granule cell layer (GCL) while the other two boxes were positioned over the two blades of the GCL, adjacent to the first box. In the CA1 region, the three boxes were placed one after another in a row. Cell numbers were averaged across boxes within the same region.

2.6 | Quantification of GCD, astrogliosis, microglial activation, and vascular density

For GCD quantification, a continuous line was drawn from the tip of the hilus till the bend of the upper blade (Figure 3a). Another, vertical line (dotted, d) was drawn at the end of the continuous line, connecting the upper and lower blades of the DG. GCL width was measured at four positions named T1–T4. T1 and T2 were measured along Line D, T3, and T4 at a distance halfway between Line D and the tip of the hilus. The average of the four values was used as an indicator of the extent of GCD. For assessing microglial activation, numbers of BrdU positive microglia and areas occupied by Iba1 staining were determined. The extent of astrogliosis was estimated by calculating the area occupied by GFAP immunoreactivity. A point counting method was used to quantify the vascular density (Rigau et al., 2007). The resulting parameter called “point count” is influenced not only by the number of vessels present in a given area but also by the size and tortuosity of the vessels. Briefly, a 5 \times 5 squares grid (edge length of one square 116.25 μm) was superposed onto the digitized image. The numbers of intersections made by blood vessels with this grid were counted. At least three sections were used per mouse. The point counts were first averaged across sections and then across mice.

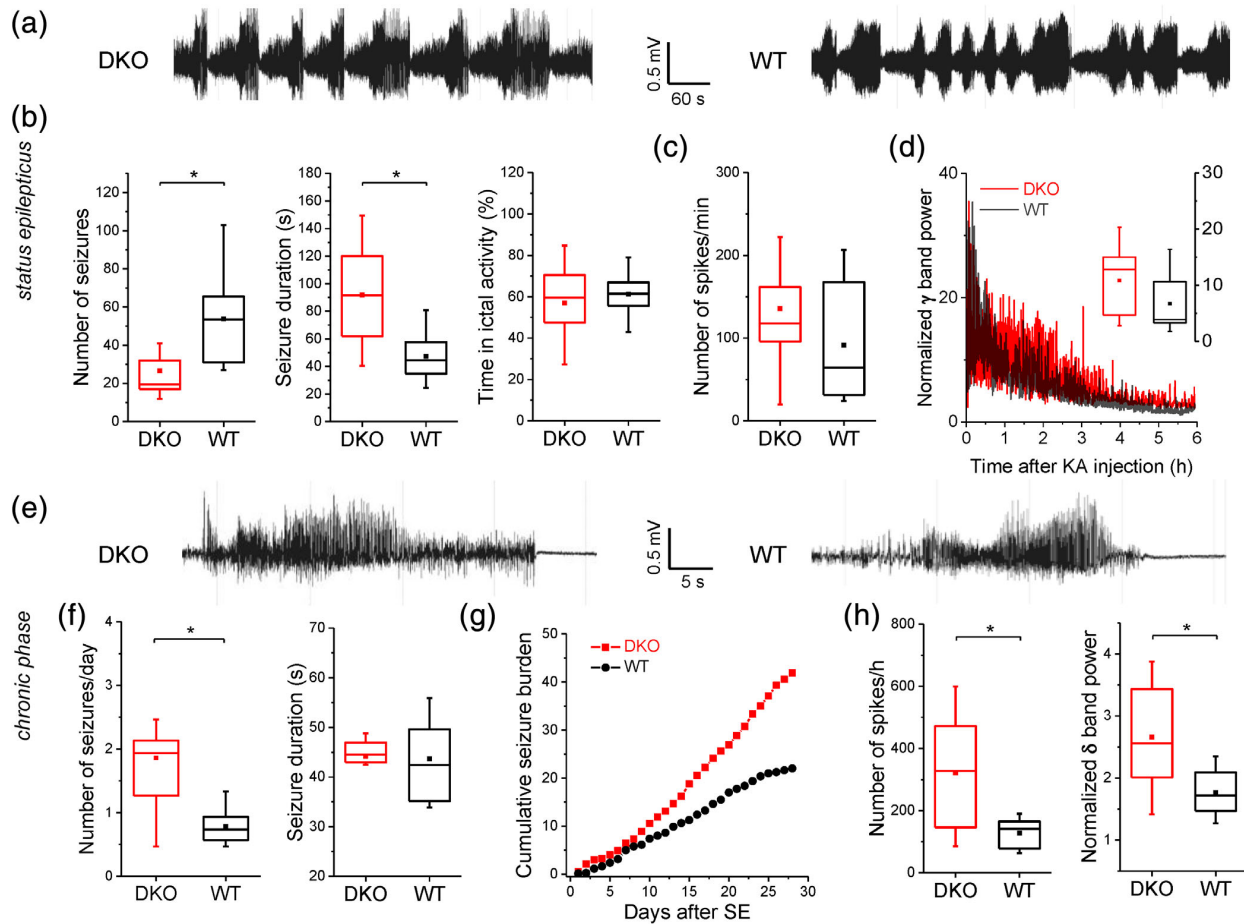


FIGURE 1 Kainate-induced seizure activity during *status epilepticus* (SE) and the chronic phase of epileptogenesis in DKO and wild-type (WT) mice. Kainate was stereotaxically injected into the deep layers of the neocortex above the right dorsal hippocampus. Electrographic seizures were continuously detected via cortical electrodes and telemetric transmitters. (a) Representative EEG traces recorded during SE in DKO and WT mice. (b) Quantification of number and duration of seizures, and total time spent in EEG seizures during the first hour after kainate injection. Seizures in DKO mice were of longer duration but less frequent. Total time spent in ictal activity was not different between DKO and WT mice. (c) The severity of SE was quantified by counting the number of EEG spikes exceeding at least tenfold baseline activity during the first 6 hr after kainate. No significant differences were observed between both genotypes. (d) Quantitative analysis of γ band EEG activity during SE in DKO and WT mice. γ band power was not influenced by the astrocytic uncoupling (inset, right). (e) Representative EEG traces recorded during spontaneous generalized seizures in DKO and WT mice. (f) Number and duration of spontaneous generalized seizures during the chronic phase (third and fourth weeks after kainate). Seizure frequency was significantly higher in DKO than in WT mice, while seizure duration was not different. (g) Averaged cumulative seizure burden in DKO and WT mice during the first 4 weeks after kainate injection. All values after Day 14 were significantly different between DKO and WT mice. (h) Spike frequency analysis detected significantly more spontaneous EEG spikes (exceeding at least tenfold baseline activity) during the third and fourth week post-SE, in DKO versus WT mice. Likewise, spectral analysis of spontaneous EEG activity during the same time period revealed higher δ band power in DKO mice. * $p < .05$ (t test). Boxes in box plots indicate interquartile range (IQR) with median (line) and mean (filled square); whiskers indicate $1.5 \times$ the IQR. $n = 9$ (DKO) and 8 (WT) animals [Color figure can be viewed at wileyonlinelibrary.com]

2.7 | Statistics

Data are given as mean \pm SD. Differences between groups were tested for significance using Student's t test or analysis of variance followed by Tukey's post hoc analysis. The level of significance was set at $p < .05$. Box plot data (Figure 1) are presented as Tukey boxes showing median (line), mean (filled square), and quartiles (25 and 75%; box). The whiskers extend to the highest and lowest values within 1.5 times interquartile range.

3 | RESULTS

3.1 | DKO mice exposed to the intracortical kainate model of MTLE-HS display unchanged overall SE severity but enhanced chronic seizure activity

To shed light on the role of astrocyte coupling in the development and progression of epilepsy, mice devoid of astrocytic GJ proteins



(DKO mice) were subjected to the unilateral intracortical kainate model of MTLE-HS. We have previously shown that this model reliably reproduces key morphological and functional features of chronic human MTLE with HS (Bedner et al., 2015). Continuous telemetric EEG recordings (24 hr/day for 4 weeks) and video monitoring were used to determine seizure activity during SE and the chronic phase. Kainate-induced SE was characterized by a series of generalized seizures lasting several hours (Figure 1a). For EEG quantification during SE, we examined the number and duration of seizures as well as the time spent in ictal activity during the first hour of recording. During this time window, an accurate determination of the duration of individual seizures was possible. The analysis revealed that in kainate-injected DKO mice, seizures during SE lasted significantly longer than in wild-type (WT) mice (91.8 ± 37.6 s vs. 47.4 ± 18.1 s, $p = .007$), but were less frequent (26.7 ± 15.5 seizures/hr vs. 53.7 ± 25.4 seizures/hr, $p = .01$). The total time spent in seizures was not different between genotypes (DKO: $57 \pm 17.7\%$; WT: $61.2 \pm 10.8\%$ of time, $p = .8$, Figure 1b).

Previous work has shown that SE in this MTLE model lasts about 4–5 hr (Bedner et al., 2015). To quantify total duration of SE, we counted during the first 6 hr of recording the number of EEG spikes with amplitudes exceeding baseline activity at least 7.5-fold. This analysis yielded no significant difference between kainate-injected DKO and WT mice (135.4 ± 86.6 spikes/min vs. 91.6 ± 69.8 spikes/min, $p = .3$, Figure 1c). Next, the same EEG data were subjected to spectral analysis using FFT and the power in the γ frequency range was compared. In accordance with spike frequency analysis, γ band power was not different between DKO and WT mice (10.8 ± 6.2 in DKO and 6.7 ± 5.2 in WT mice, $p = .2$, Figure 1d). Together, these findings indicate that astrocyte uncoupling affects the pattern of seizure activity during the initial phase of SE, but has no influence on overall SE severity.

All mice developed spontaneous generalized seizures after a latent period, the duration of which was not different between kainate-injected DKO and WT mice (3.75 ± 2.5 days vs. 3.62 ± 2 days, $p = .91$). Importantly, the frequency of spontaneous chronic seizures measured during the third and fourth week after epilepsy induction was more than twice as high in DKOs than in WT mice (1.9 ± 1.1 vs. 0.8 ± 0.3 seizures/day, $p = .02$, Figure 1e). Likewise, the cumulative number of chronic seizures over total recording time (44.1 ± 25.2 vs. 22.37 ± 9.8 seizures, $p = .03$, Figure 1g) was significantly higher in kainate-injected DKO mice. There was, however, no difference in the duration of spontaneous seizures between both genotypes (DKO: 47.4 ± 6.9 s vs. WT: 44.2 ± 7.4 s, $p = .4$, Figure 1g). Spike frequencies were assessed during the third and fourth weeks of recording. Considering amplitudes exceeding baseline activity at least tenfold revealed a significantly higher frequency of spontaneous EEG spikes in DKO mice (317.1 ± 185.6 spikes/hr vs. 127.6 ± 48.4 spikes/hr, $p = .01$). Likewise, spectral EEG analysis demonstrated higher δ band power (2.7 ± 0.9 vs. 1.8 ± 0.4 , $p = .02$, Figure 1h) in DKO than in WT mice, indicating increased interictal activity in the former. The power in the other frequency bands was not elevated in DKO mice. Irrespective of genotype, all seizures observed by video monitoring were severe convulsions with rearing and falling (Stage V seizures according to

Racine's classification, Racine, 1972), indicating that the severity of spontaneous chronic seizures was not influenced by the lack of GJ proteins. Together the data suggest that deletion of astrocytic Cxs exacerbates chronic seizure burden without affecting SE severity.

3.2 | Kainate-injected DKO mice show unaltered neurodegeneration but less pronounced astrogliosis and GCD

About two thirds of patients with pharmacoresistant MTLE display HS, characterized by prominent neuronal loss in the CA1 and CA4 regions, reactive astrogliosis and GCD (Blümcke, Beck, Lie, & Wiestler, 1999). These histopathological changes are well reproduced in our animal model (Bedner et al., 2015). To explore whether the lack of astrocytic Cxs influences the development of HS, we performed immunohistochemical analyses of hippocampal slices from DKO and WT animals, 1 month after kainate injection. First, we assessed the extent of neurodegeneration and astrogliosis by NeuN/GFAP/Hoechst triple staining (Figure 2a). For quantification, the number of NeuN-positive cells was counted in an area of $260 \times 260 \times 15 \mu\text{m}^3$ within the CA1 *stratum pyramidale* underneath the injection side (ipsilateral side) and at the same position on the contralateral side. Ipsilaterally, NeuN-positive cells were reduced by almost 90% in both kainate-injected DKO and WT mice (DKO: by $83.2 \pm 22.4\%$; WT: by $86 \pm 16.4\%$ $p = .86$, Figure 2b). No neurodegeneration could be detected in the CA3 *stratum pyramidale*, neither in DKO nor in WT mice (WT: 413 ± 45.1 vs. 358.3 ± 58.2 NeuN⁺ cells, $p = .14$; DKO: 358.3 ± 42.7 vs. 393 ± 49.1 NeuN⁺ cells, $p = .1$, $n = 3$ slices from three animals for each group; analyzed area $581.3 \times 581.3 \times 8 \mu\text{m}^3$, data not shown). In contrast, the area occupied by GFAP immunoreactivity, which reflects the extent of reactive astrogliosis, was significantly smaller in the ipsilateral CA1 *stratum radiatum* of DKO versus WT mice (DKO: $144.6 \pm 33\%$; WT: $196.7 \pm 31.6\%$, $p = .03$, Figure 2b).

Next we quantified seizure-induced GCD in DKO and WT mice, 1 month after SE, by determining the width of the GCL blades visualized by Prox1 staining (Figure 3a). Ipsilaterally, the width (average of T1–T4) was significantly increased, both in DKO and WT mice, when compared with the corresponding contralateral hippocampi. Notably, in DKO mice, the increase was less pronounced than in the WT ($157.90 \pm 29.63 \mu\text{m}$ vs. $219.47 \pm 7.66 \mu\text{m}$, $p = .03$) (Figure 3b). These data indicate that astrocytic Cxs influence seizure-induced GCD. However, earlier studies have demonstrated that the number of Prox1-positive cells in Cx-deficient mice (DKO and Cx43 KO mice) is reduced compared to WT mice, due to impaired adult neurogenesis in the subgranular zone (Kunze et al., 2009; Zhang et al., 2018). To investigate whether this phenomenon accounts for the differences in GCD upon kainate injection, we compared the width of the GCL blades in untreated (nonepileptic) DKO and WT mice. The results revealed thinner blades in DKO than in WT mice ($54.5 \pm 5.4 \mu\text{m}$ vs. $69.4 \pm 2.9 \mu\text{m}$, $p = .01$, Suppl. Figure S1). Thus, the lower GCD found ipsilaterally in kainate-injected DKO mice might simply be a consequence of the reduced number of Prox1-positive cells in this genotype.

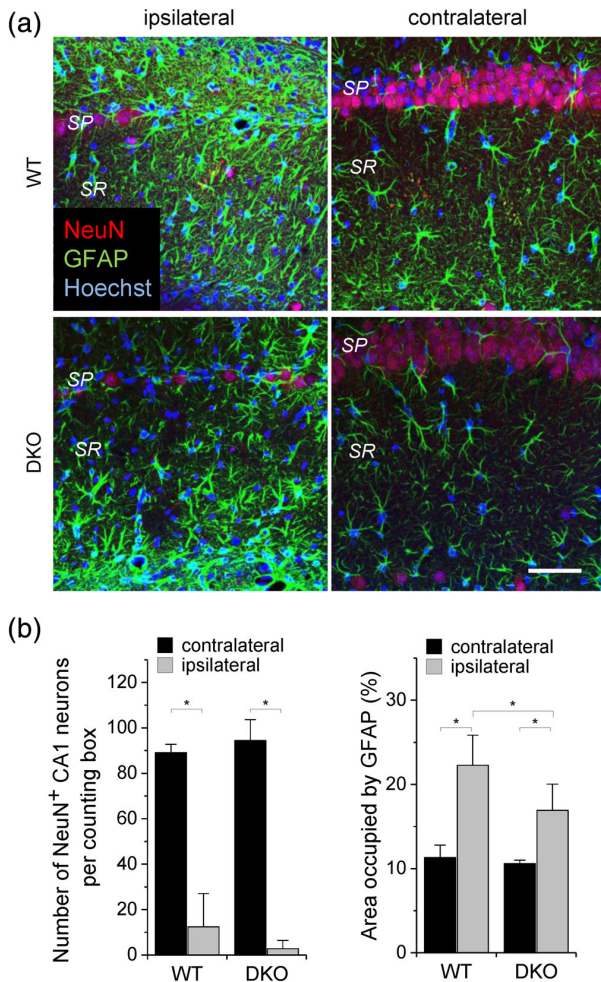


FIGURE 2 Loss of CA1 pyramidal neurons and reactive astrogliosis in DKO and wild-type (WT) mice in chronic mesial temporal lobe epilepsy. (a) NeuN (red)/GFAP (green)/Hoechst (blue) triple labeling in slices obtained from WT and DKO mice, 1 month after kainate injection. SP, stratum pyramidale; SR, stratum radiatum. Scale bar, 50 μm . (b) Quantification of the number of pyramidal neurons and GFAP immunoreactivity in an area of $260 \times 260 \times 15 \mu\text{m}^3$ within the CA1 subfield. The extent of astrogliosis, but not neurodegeneration, was reduced in DKO mice compared to WT mice. * $p < .05$ (analysis of variance [ANOVA] followed by post hoc Tukey's test). $n = 9$ slices from three animals per group [Color figure can be viewed at wileyonlinelibrary.com]

Taken together, immunohistochemical analyses indicated that, despite enhanced chronic seizure burden, deletion of astrocytic Cxs protects against the development of HS.

3.3 | Lower microglia activation in DKO mice 1 month after kainate injection

Activation of microglia is a primary inflammatory response to seizures (Eyo, Murugan, & Wu, 2017), which involves hypertrophy and process elongation of microglia and stimulation of proliferation (Avignone,

Lepleux, Angibaud, & Nägerl, 2015; Avignone, Ulmann, Levasseur, Rassendren, & Audinat, 2008). Using Iba1/BrdU double immunostaining, we assessed whether spontaneous chronic seizures differently affect microglia in DKO versus WT mice. One month after kainate injection, irrespective of genotype, the area occupied by microglia was increased ipsilaterally, both in the CA1 region and in the DG (Figure 4a,b,e, f). In the CA1 region, but not the DG, this increase was accompanied by a rise in the number of BrdU-positive Iba1 cells, indicating increased microglial proliferation (Figure 4a–d). Interestingly, microglial proliferation/activation in the ipsilateral CA1 region of DKO mice was lower than in WT mice, as indicated by the density of Iba1/BrdU-double-positive cells (76.8 ± 6.7 vs. 100 ± 11.1 per counting box, $p = .03$) and the area occupied by Iba1 immunoreactivity ($11,201.5 \pm 1,348 \mu\text{m}^2$ vs. $7,521.7 \pm 650.6 \mu\text{m}^2$, $p = .01$, Figure 4d,f). Together, these data indicate that astrocytic Cxs increase chronic seizure-induced microglial activation in the hippocampus.

3.4 | DKO mice have reduced seizure-induced angiogenesis

Angiogenesis is enhanced in epilepsy and it starts before the onset of spontaneous seizures (Newton, Girgenti, Collier, & Duman, 2006; Rigau et al., 2007). Endothelial cell proliferation is the hallmark of angiogenesis (Hellsten, Wennström, Bengzon, Mohapel, & Tingström, 2004). We used coimmunostaining of CD31 and BrdU to visualize newly generated endothelial cells. One month after kainate injection, the ipsilateral hippocampus displayed enhanced endothelial proliferation when compared with the corresponding contralateral side (Figure 5). In WT mice, the ipsilateral density of CD31/BrdU double-positive cells was more than threefold higher than contralaterally, both in the DG (14.66 ± 0.6 vs. 4.55 ± 2.7 cells per counting box, $p = .003$) and the CA1 region (19.1 ± 1.7 vs. 5.33 ± 2 cells per counting box, $p = .0008$, Figure 5). In DKO mice, the increase was less pronounced (DG, 8.3 ± 2.6 vs. 3.1 ± 0.8 cells per counting box, $p = .03$; CA1, 12.66 ± 2.6 vs. 5.33 ± 3.2 cells per counting box, $p = .04$, Figure 5). Importantly, the ipsilateral hippocampus of DKO mice showed a significantly lower density of CD31/BrdU double-positive cells compared to WT mice (Figure 5c,d). These data indicate that chronic seizure-induced endothelial cell proliferation is modulated by astrocytic Cxs. Next, we assessed vascular density using CD31 immunostaining. A point counting method was employed as reported previously (Rigau et al., 2007). In WT mice, a higher density of CD31-positive details was found on the ipsilateral versus contralateral side (ipsilateral: 81.55 ± 8.94 ; contralateral: 57.55 ± 6.40 , $p = .02$) while DKO mice were not affected (ipsilateral: 60.33 ± 1.76 ; contralateral: 50.55 ± 14.41 , $p = .3$, Figure 5e,f). This finding further supports an important role of astrocytic GJ proteins in chronic seizure-induced angiogenesis.

3.5 | Chronic seizure-induced neurogenesis is independent of astrocytic Cxs

While it is well established that seizures enhance adult hippocampal neurogenesis (e.g., Hüttmann et al., 2003), Kunze et al. (2009) showed that

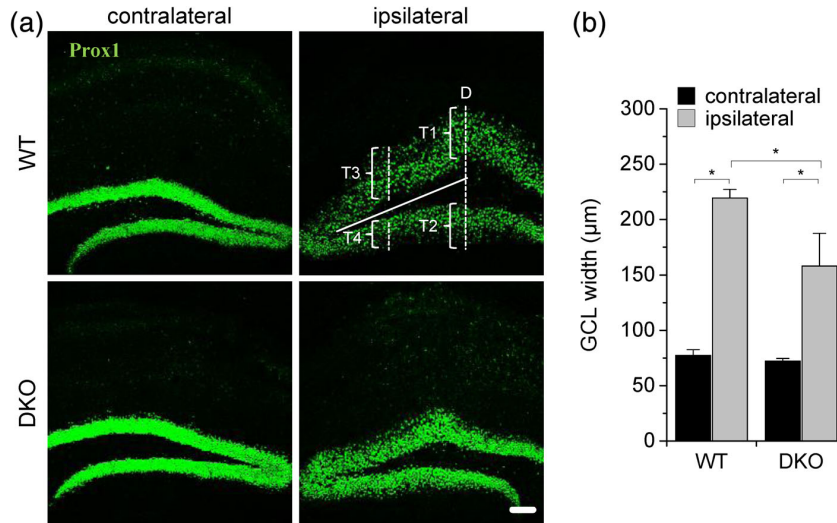


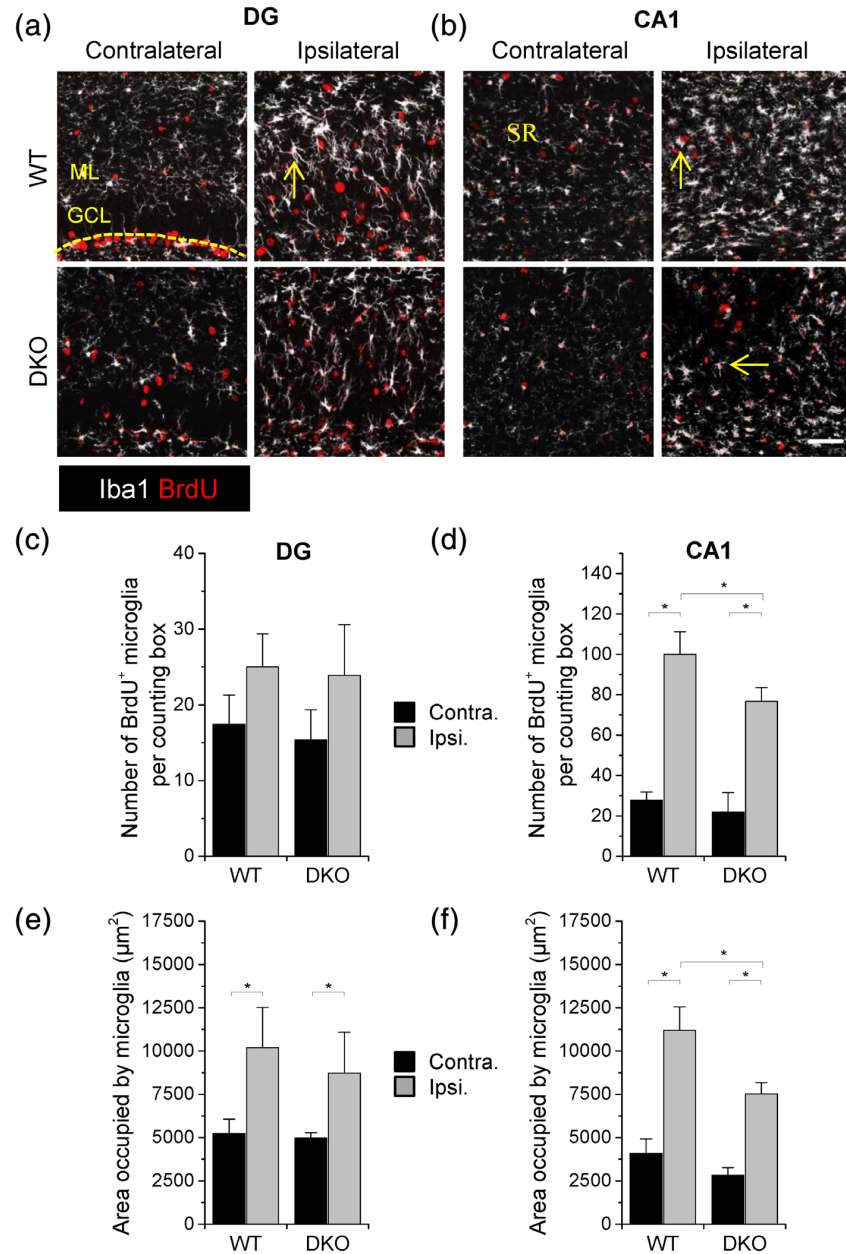
FIGURE 3 Seizure-induced granule cell dispersion (GCD) is attenuated in DKO mice. (a) Prox1 immunostaining, 1 month after kainate injection. Ipsilaterally, granule cells are dispersed in contrast to the compact cellular architecture in the contralateral hippocampus. T1–T4 indicate the positions of width evaluation of the granule cell layer (GCL), which were averaged to determine GCD. T1 and T2 are taken along Lines D, T3, and T4 at a distance halfway between Line D and the tip of the hilus. Scale bar, 100 μm . (b) Quantification of GCD 1 month after kainate using the average width of the GCL (μm). The ipsilateral width of the GCL significantly exceeded the contralateral side. GCD was less pronounced in DKO mice. * $p < .05$ (analysis of variance [ANOVA] followed by post hoc Tukey's test). $n = 9$ slices from three animals per group [Color figure can be viewed at wileyonlinelibrary.com]

under control (nonseizure) conditions, Cxs are essential for adult neurogenesis. However, it is not known whether seizure-induced neurogenesis is also influenced by Cxs. This question was addressed in DKO and WT mice, using triple labeling for Prox1, BrdU, and DCX (Figure 6a,b). Prox1 was used as a marker for mature granule cells, DCX to detect immature/newly born neurons and BrdU to label proliferating and newly generated cells. In agreement with previous findings, under control conditions (i.e., no kainate injection) neurogenesis was significantly impaired in DKO mice (DCX + BrdU, DKO: 1.3 ± 0.3 vs. WT: 2.6 ± 0.3 cells per counting box, $p = .008$; Prox1 + BrdU, DKO: 1.9 ± 0.4 vs. WT: 3.8 ± 0.4 cells per counting box, $p = .003$; Suppl. Figure S2). Next, kainate injections were performed and 1 month later, the sclerotic hippocampi located underneath the injection side were analyzed in DKO and WT mice. No DCX-positive or Prox1/BrdU-double-positive cells could be detected in that area, neither in DKO nor in WT mice (Figure 6a), showing that neurogenesis is completely absent in the dorsal ipsilateral DG. This finding is in agreement with earlier observations from the intrahippocampal kainate injection model of MTLE with HS (Häussler, Bielefeld, Froriep, Wolfart, & Haas, 2012). Similar to the latter study, we found strongly increased neurogenesis in the contralateral hippocampus. Although the number of DCX/BrdU- and Prox1/BrdU-positive cells was contralaterally higher in WT versus DKO mice (Figure 6c), the relative increase in seizure-induced neurogenesis was similar in both lines (DCX + BrdU, DKO: $612.7 \pm 243.6\%$ vs. WT: $582.9 \pm 124.8\%$, $p = .9$; Prox1 + BrdU, DKO: $634.6 \pm 335.7\%$ vs. WT: $684.9 \pm 139.9\%$, $p = .8$, Figure 6d). This implies that astrocytic Cxs are not involved in the seizure-induced increase of adult neurogenesis.

4 | DISCUSSION

We have previously shown that hippocampal astrocytes in human and experimental MTLE-HS lose coupling via GJ channels and that this uncoupling starts already before the onset of neurodegeneration and chronic seizure activity, hinting at a causative role in the initiation of MTLE (Bedner et al., 2015). The assumption that the astroglial network possesses antiepileptic properties is mainly based on the spatial K^+ buffering concept, according to which excessive extracellular K^+ released during neuronal activity is taken up by astrocytes, redistributed through the astrocytic network and released at regions of lower extracellular K^+ concentrations (Orkand, Nicholls, & Kuffler, 1966). According to this concept, loss of GJ-mediated coupling would result in accumulation of extracellular K^+ , neuronal depolarization and a lowered threshold for seizure generation. It would also depolarize astrocytes and reduce their glutamate uptake capacity, which again would promote seizure activity due to prolonged activation of excitatory synapses. Indeed, enhanced extracellular glutamate concentrations have been found in the cerebral fluid of MTLE patients (Cavus et al., 2005). However, the astroglial network has also been proposed to have proepileptic effects (Chever et al., 2016; Rouach et al., 2008). To elucidate consequences of astrocyte uncoupling on the development of chronic MTLE, we used transgenic mice lacking Cx30 and Cx43 in astrocytes. These mice are hyperexcitable in situ (Wallraff et al., 2006) but no spontaneous seizures or abnormal EEG activity was detected in vivo (Chever et al., 2016). We subjected DKO mice to our MTLE model and continuously assessed seizure activity over a period of 1 month. Despite a similar strength of kainate-induced SE in WT and DKO mice, on a long term, we observed a

FIGURE 4 Reduced microglial activation in DKO mice in chronic mesial temporal lobe epilepsy. (a,b) Iba1 (white) and BrdU (red) double immunostaining in the DG and CA1 region of wild-type (WT) and DKO mice, 1 month after kainate injection. Colocalization of BrdU with Iba1 indicates newly generated or proliferating microglia (examples indicated by arrows). Dashed-line demarcates the subgranular zone (SGZ) from the GCL. ML, molecular layer; SR, *stratum radiatum*. Scale bar, 50 μm . (c–d) Quantification of microglial activation 1 month after kainate by counting newly generated microglia and estimating the area occupied by Iba1 immunoreactivity in counting boxes ($290 \times 290 \times 8 \mu\text{m}^3$). (c,d) In both genotypes, ipsilaterally the density of BrdU-positive microglia was increased in the CA1 region, but not in the DG. This increase was significantly less in DKO versus WT mice. (e,f) The area occupied by Iba1 immunoreactivity was increased in the ipsilateral DG and CA1 region of both, DKO and WT mice. This increase was significantly less pronounced in the CA1 region of DKO mice. * $p < .05$ (analysis of variance [ANOVA] followed by post hoc Tukey's test). $n = 9$ slices from three animals per group [Color figure can be viewed at wileyonlinelibrary.com]



higher frequency of spontaneous generalized chronic seizures in mice lacking astrocytic Cxs, indicating an antiepileptic function of astrocyte coupling. One has of course to consider that astrocyte uncoupling in DKO mice differs from the acquired loss of coupling upon kainate injection or in human MTLE-HS. First, as Cx43 deletion in DKO mice occurs early in development (at around embryonic Day 13; Theis et al., 2003) and Cx30 is constitutively lacking, compensatory developmental changes are likely to occur. Indeed, astrocytic glutamate uptake, excitatory synaptic transmission and plasticity as well as adult neurogenesis in the DG are altered in these mice (Kunze et al., 2009; Pannasch et al., 2011; Pannasch et al., 2014). Second, DKO mice not only lack intercellular coupling but also the GJ proteins while in the

sclerotic hippocampus of human and experimental MTLE even increased Cx43 levels have been observed (Deshpande et al., 2017). Indeed, in our previous study, we found strong evidence that subcellular reorganization and augmented Cx43 phosphorylation (at Serine 255 and 368) account for the loss of coupling in human and experimental epilepsy (Deshpande et al., 2017). It is known that phosphorylation of Cx43 at these residues reduces intercellular coupling without compromising (GJ) or Cx hemichannel formation (Lampe et al., 2000; Thévenin et al., 2013; Warn-Cramer, Cottrell, Burt, & Lau, 1998). Thus, channel-independent effects of Cx proteins may influence synaptic transmission and seizure activity in WT but not in DKO mice (Pannasch et al., 2014; Pannasch, Dossi, Ezan, & Rouach, 2019).

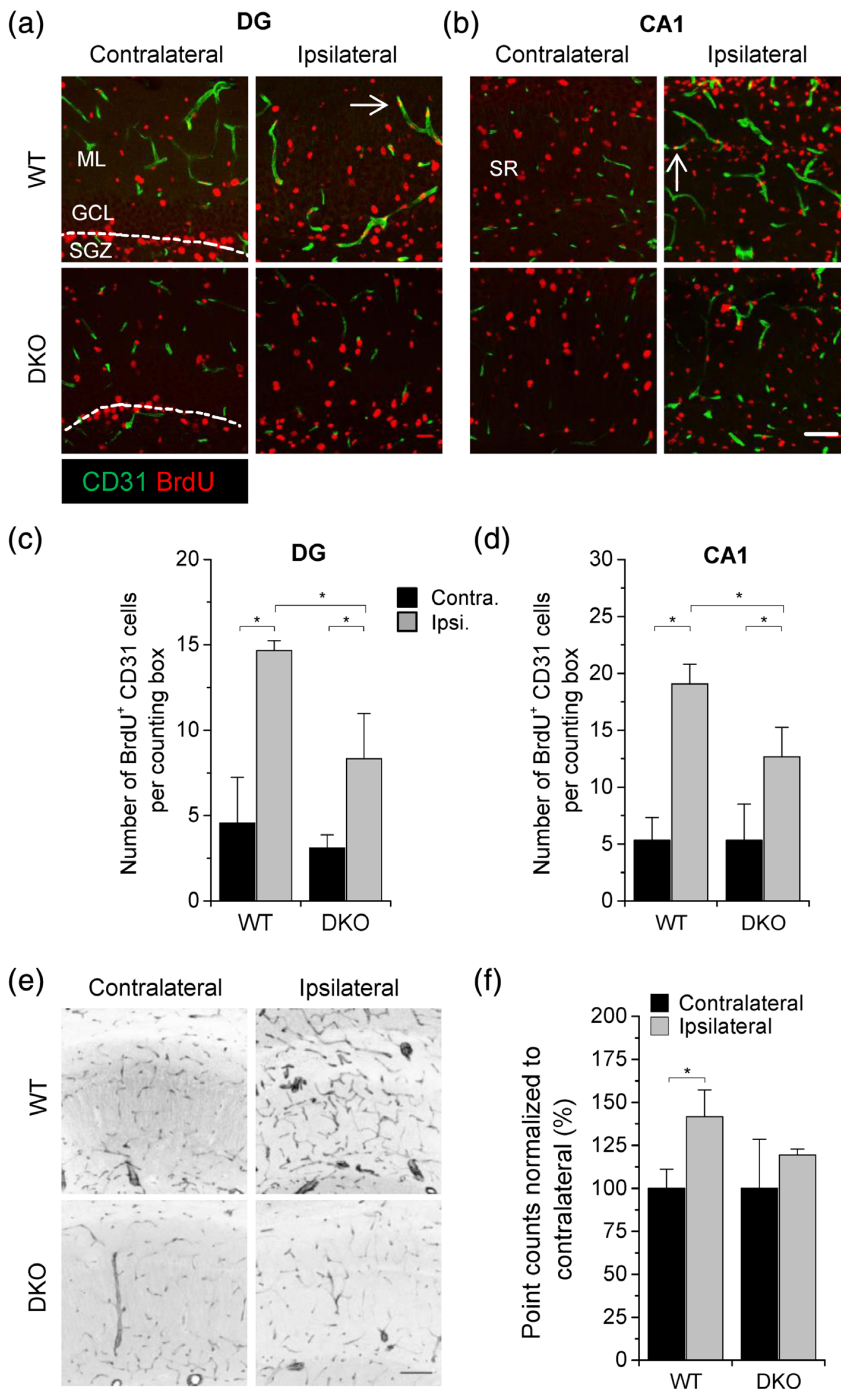
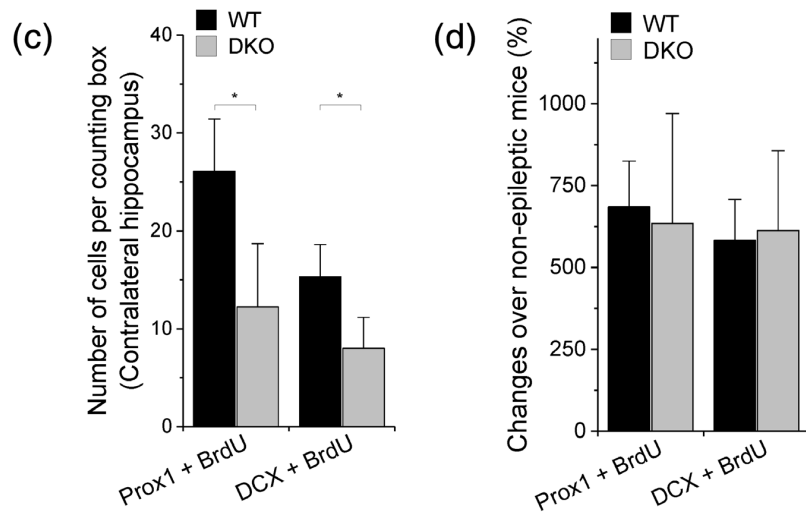
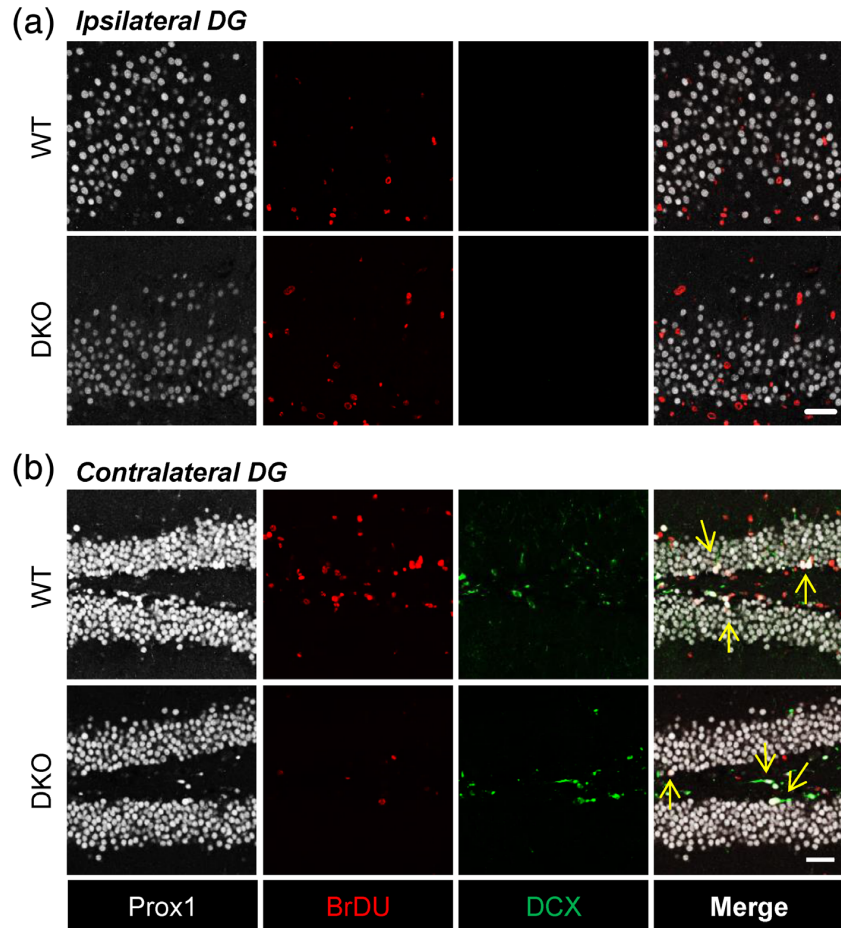


FIGURE 5 Reduced endothelial proliferation and vascular density in DKO mice in chronic mesial temporal lobe epilepsy. (a,b) CD31 (green) and BrdU (red) double immunostaining in the DG and CA1 region of wild-type (WT) and DKO mice 1 month after kainate injection. Colocalization of BrdU with CD31 indicates newly generated or proliferating endothelial cells (examples indicated by arrows). Dotted line demarcates the subgranular zone (SGZ) of the DG. ML, molecular layer; SR, *stratum radiatum*. Scale bar, 50 μ m. (c,d) Number of BrdU-positive CD31 cells per counting box ($290 \times 290 \times 8 \mu\text{m}^3$) in the DG (c) and CA1 region (d) 1 month after kainate. In both regions, the ipsilateral side showed more endothelial cell proliferation than the corresponding contralateral side. However, DKO mice showed less proliferation than WT mice, indicating a modulatory role of astrocytic Cxs on angiogenesis. (e) CD31 immunostaining in hippocampal slices, 1 month after kainate injection. CD31 delineates blood vessels. Scale bar, 100 μ m. (f) For quantification of vascular density 1 month after kainate, the “point counting method” was applied to confocal images from the CA1 region. The bar graphs show point counts normalized to the contralateral side. In WT mice, ipsilaterally the vascular density was 141.7% of the contralateral hippocampus. In DKO mice, this difference disappeared. * $p < .05$ (analysis of variance [ANOVA] followed by post hoc Tukey’s test). $n = 9$ slices from three animals per group and staining condition [Color figure can be viewed at wileyonlinelibrary.com]

Finally, one has to consider that astrocyte uncoupling in human and experimental MTLE is spatially restricted to the sclerotic area and the epileptic foci, while Cx deletion in DKO mice concerns the entire brain. Thus, lack of GJ proteins and hemichannels in DKO mice might partially counteract the proepileptic effect of uncoupling, which offers an explanation for the lack of seizures in untreated mice and the relatively moderate hyperexcitability found in acute brain slices obtained from these mice (Wallraff et al., 2006).

Applying our MTLE-HS model (Bedner et al., 2015), quantification of epileptic activity (time spent in ictal activity) during SE, that is, the first hours after kainate injection, revealed no significant difference between DKO and WT mice. Thus, it is unlikely that the higher number of subsequently developing spontaneous chronic seizures in DKO mice was simply a consequence of a more severe SE. In a recent study, i.p. injection of PTZ was used to investigate the role of astrocyte coupling in acute hyperexcitability (up to 30 min after injection).

FIGURE 6 Neurogenesis does not require astrocytic Cxs in chronic mesial temporal lobe epilepsy. (a,b) Prox1 (white), BrdU (red), and DCX (green) triple immunostaining in slices from wild-type (WT) and DKO mice, 1 month after kainate injection. BrdU was administered through drinking water till Day 14. (a) No DCX-positive cells were detected in the ipsilateral DG, irrespective of the genotype. Furthermore, no colocalization of Prox1 and BrdU was observed, confirming lack of newly born granule cells. Scale bar, 50 μ m. (b) Contralaterally, abundant DCX/BrdU and Prox1/BrdU colocalization was seen in both, DKO and WT mice. Arrows indicate newly born neurons, colabeled with all three markers. Scale bar, 50 μ m. (c,d) Quantification of Prox1/BrdU- and DCX/BrdU-double-positive cells 1 month after kainate, using counting boxes (290 \times 290 \times 4 μ m³) positioned 250 μ m away from the outermost margin of the GCL flexure, oriented perpendicularly to the longitudinal axis of the GCL. Although the density of Prox1/BrdU- and DCX/BrdU-positive cells was significantly lower in DKO mice, the relative increase of these values in the epileptic versus nonepileptic condition was similar in both genotypes. * $p < .05$ (t test). n.s., not significant. $n = 9$ slices from three animals per group [Color figure can be viewed at wileyonlinelibrary.com]



In this model, more but shorter seizures were observed in DKO mice (Chever et al., 2016). The present study did not intend to analyze the mechanisms of SE generation, but addressed the consequences of astrocyte Cx deficiency on epileptogenesis post-SE, that is, development and progression of spontaneous chronic seizures. By exerting a similar acute seizure burden in DKO and WT mice, we consider our

model well suited to investigate the role of the astroglial coupling network on the pathogenesis of MTL.

Despite the higher frequency of spontaneous chronic seizures, the extent of neurodegeneration was not significantly different between Cx-deficient and WT mice. Given the important role of the astroglial network in glutamate and K⁺ buffering as well as in the



efficient supply of energetic metabolites one would expect exacerbated neurodegeneration in DKO mice. In line with this assumption, Cx43 KO mice exhibited larger infarct volumes after induced ischemia (Nakase, Fushiki, & Naus, 2003; Siushansian, Bechberger, Cechetto, Hachinski, & Naus, 2001). On the other hand, several studies indicated that astrocyte GJ channels mediate propagation and amplification of cell injury by allowing intercellular diffusion of toxic/stress molecules (Frantseva, Kokarotseva, & Perez Velazquez, 2002; Lin et al., 1998). Possibly, these two opposite effects of astrocyte uncoupling compensate each other in our experimental approach. The immunohistochemical analyses further revealed attenuated astrogliosis, microglial activation, and angiogenesis in Cx-deficient mice. These phenomena might be attributed to the lack of Cx hemichannels, which were thought to be involved in the regulation of microglial chemotaxis and process elongation via release of ATP (Davalos et al., 2005). Furthermore, elevated ATP levels amplify inflammation through NALP3 inflammasome activation not only in microglia but also in other brain cell types (Bours, Dagnelie, Giuliani, Wesselius, & Di Virgilio, 2011; Zhou, Green, Bennet, Gunn, & Davidson, 2019). The limited inflammatory responses in DKO mice in turn could be responsible for the attenuated astrogliosis and angiogenesis, as the mutual influence of these processes is well-documented (Jackson, Seed, Kircher, Willoughby, & Winkler, 1997; Sofroniew & Vinters, 2010).

Another point to consider is that the cortical electrodes used in this study are not appropriate for detection of focal seizure activity within the hippocampus. The frequency of such seizures may differ from those recorded in the cortex and may correlate with the extent of histopathological alterations. Further studies, for instance using hippocampal depth electrodes, are required to elucidate this question.

Previous work of our group demonstrated that GJ channel-dependent functions of Cx43 (but not of Cx30) are involved in the regulation of adult neurogenesis in the DG. Indeed, in DKO as well as in Cx43 KO mice proliferation and the number of radial glia-like cells were substantially reduced (Kunze et al., 2009; Zhang et al., 2018), indicating that intercellular transfer of molecules through Cx43 GJ channels is necessary for proper neurogenesis. In the present study, we found that chronic seizures similarly potentiate adult neurogenesis in WT and DKO mice, suggesting that physiological and chronic seizure-induced neurogenesis are differentially regulated.

Collectively, the present data provide new insights as to how astrocyte GJ proteins and channels may contribute to the development of chronic epilepsy. The finding that DKO mice display a higher frequency of spontaneous generalized chronic seizures supports the view that loss of astrocyte coupling as observed in human and experimental MTLE-HS represents a crucial event in the pathogenesis of the disease. Molecules specifically acting as GJ activators and restoring astrocyte coupling in the epileptic brain might therefore allow for the development of new therapeutic approaches.

ACKNOWLEDGMENTS

Work of the authors is currently supported by grants from the EU (H2020-MSCA-ITN project 722053 EU-GliaPhD) and BMBF (16GW0182 CONNEXIN).

CONFLICT OF INTEREST

The authors declare no potential conflict of interest.

DATA AVAILABILITY STATEMENT

The data that support the findings of this study are available from the corresponding author upon reasonable request.

ORCID

Christian Steinhäuser  <https://orcid.org/0000-0003-2579-8357>

Peter Bedner  <https://orcid.org/0000-0003-0090-7553>

REFERENCES

- Avignone, E., Lepleux, M., Angibaud, J., & Nägerl, U. V. (2015). Altered morphological dynamics of activated microglia after induction of status epilepticus. *Journal of Neuroinflammation*, 12(1), 202. <https://doi.org/10.1186/s12974-015-0421-6>
- Avignone, E., Ulmann, L., Levavasseur, F., Rassendren, F., & Audinat, E. (2008). Status epilepticus induces a particular microglial activation state characterized by enhanced purinergic signaling. *Journal of Neuroscience*, 28(37), 9133–9144. <https://doi.org/10.1523/JNEUROSCI.1820-08.2008>
- Bedner, P., Dupper, A., Hüttmann, K., Müller, J., Herde, M. K., Dublin, P., ... Steinhäuser, C. (2015). Astrocyte uncoupling as a cause of human temporal lobe epilepsy. *Brain*, 138(5), 1208–1222. <https://doi.org/10.1093/brain/awv067>
- Bedner, P., Jabs, R., & Steinhäuser, C. (2019). Properties of human astrocytes and NG2 glia. *Glia*, 68, 756–767. <https://doi.org/10.1002/glia.23725>
- Blümcke, I., Beck, H., Lie, A. A., & Wiestler, O. D. (1999). Molecular neuropathology of human mesial temporal lobe epilepsy. *Epilepsy Research*, 36(2), 205–223. [https://doi.org/10.1016/S0920-1211\(99\)00052-2](https://doi.org/10.1016/S0920-1211(99)00052-2)
- Boison, D., & Steinhäuser, C. (2018). Epilepsy and astrocyte energy metabolism. *Glia*, 66(6), 1235–1243. <https://doi.org/10.1002/glia.23247>
- Bours, M. J. L., Dagnelie, P. C., Giuliani, A. L., Wesselius, A., & di Virgilio, F. (2011). P2 receptors and extracellular ATP: A novel homeostatic pathway in inflammation. *Frontiers in Bioscience (Scholar Edition)*, 3, 1443–1456. <https://doi.org/10.2741/235>
- Cavus, I., Kasoff, W. S., Cassaday, M. P., Jacob, R., Gueorguieva, R., Sherwin, R. S., ... Abi-Saab, W. M. (2005). Extracellular metabolites in the cortex and hippocampus of epileptic patients. *Annals of Neurology*, 57(2), 226–235. <https://doi.org/10.1002/ana.20380>
- Chever, O., Dossi, E., Pannasch, U., Derangeon, M., & Rouach, N. (2016). Astroglial networks promote neuronal coordination. *Science Signaling*, 9(410), ra6–ra6. <https://doi.org/10.1126/scisignal.aad3066>
- Cohen, I., Navarro, V., Clemenceau, S., Baulac, M., & Miles, R. (2002). On the origin of interictal activity in human temporal lobe epilepsy in vitro. *Science*, 298(5597), 1418–1421. <https://doi.org/10.1126/science.1076510>
- Davalos, D., Grutzendler, J., Yang, G., Kim, J. V., Zuo, Y., Jung, S., ... Gan, W.-B. (2005). ATP mediates rapid microglial response to local brain injury in vivo. *Nature Neuroscience*, 8(6), 752–758. <https://doi.org/10.1038/nn1472>
- Deshpande, T., Li, T., Herde, M. K., Becker, A., Vatter, H., Schwarz, M. K., ... Bedner, P. (2017). Subcellular reorganization and altered phosphorylation of the astrocytic gap junction protein connexin43 in human and experimental temporal lobe epilepsy. *Glia*, 65(11), 1809–1820. <https://doi.org/10.1002/glia.23196>
- Eyo, U. B., Murugan, M., & Wu, L.-J. (2017). Microglia-neuron communication in epilepsy. *Glia*, 65(1), 5–18. <https://doi.org/10.1002/glia.23006>
- Frantseva, M. V., Kokarotseva, L., & Perez Velazquez, J. L. (2002). Ischemia-induced brain damage depends on specific gap-junctional coupling. *Journal of Cerebral Blood Flow and Metabolism*, 22(4), 453–462. <https://doi.org/10.1097/00004647-200204000-00009>

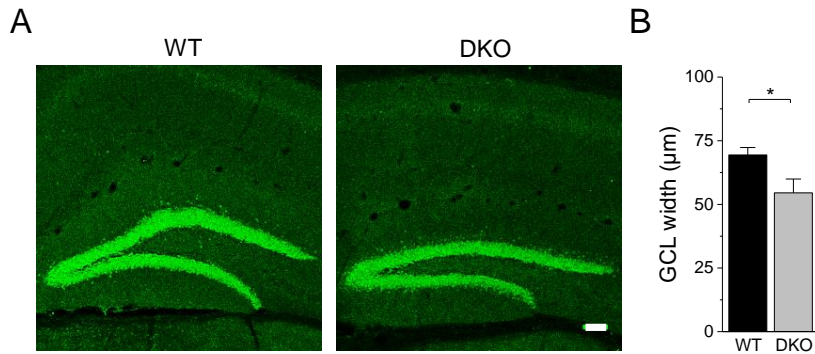
- Giaume, C., Koulakoff, A., Roux, L., Holcman, D., & Rouach, N. (2010). Astroglial networks: A step further in neuroglial and gliovascular interactions. *Nature Reviews Neuroscience*, 11(2), 87–99. <https://doi.org/10.1038/nrn2757>
- Gosejacob, D., Dublin, P., Bedner, P., Hüttmann, K., Zhang, J., Tress, O., ... Theis, M. (2011). Role of astroglial connexin30 in hippocampal gap junction coupling. *Glia*, 59(3), 511–519. <https://doi.org/10.1002/glia.21120>
- Häussler, U., Bielefeld, L., Froriep, U. P., Wolfart, J., & Haas, C. A. (2012). Septotemporal position in the hippocampal formation determines epileptic and neurogenic activity in temporal lobe epilepsy. *Cerebral Cortex*, 22(1), 26–36. <https://doi.org/10.1093/cercor/bhr054>
- Hellsten, J., Wennström, M., Bengzon, J., Mohapel, P., & Tingström, A. (2004). Electroconvulsive seizures induce endothelial cell proliferation in adult rat hippocampus. *Biological Psychiatry*, 55(4), 420–427. <https://doi.org/10.1016/j.biopsych.2003.08.013>
- Hüttmann, K., Sadgrove, M., Wallraff, A., Hinterkeuser, S., Kirchhoff, F., Steinhäuser, C., & Gray, W. P. (2003). Seizures preferentially stimulate proliferation of radial glia-like astrocytes in the adult dentate gyrus: Functional and immunocytochemical analysis. *European Journal of Neuroscience*, 18(10), 2769–2778. <https://doi.org/10.1111/j.1460-9568.2003.03002.x>
- Jackson, J. R., Seed, M. P., Kircher, C. H., Willoughby, D. A., & Winkler, J. D. (1997). The codependence of angiogenesis and chronic inflammation. *The FASEB Journal*, 11(6), 457–465. <https://doi.org/10.1096/fasebj.11.6.9194526>
- Kunze, A., Congreso, M. R., Hartmann, C., Wallraff-Beck, A., Hüttmann, K., Bedner, P., ... Steinhäuser, C. (2009). Connexin expression by radial glia-like cells is required for neurogenesis in the adult dentate gyrus. *Proceedings of the National Academy of Sciences of the United States of America*, 106(27), 11336–11341. <https://doi.org/10.1073/pnas.0813160106>
- Lampe, P. D., TenBroek, E. M., Burt, J. M., Kurata, W. E., Johnson, R. G., & Lau, A. F. (2000). Phosphorylation of connexin43 on serine368 by protein kinase C regulates gap junctional communication. *Journal of Cell Biology*, 149(7), 1503–1512. <https://doi.org/10.1083/jcb.149.7.1503>
- Lehmkuhle, M. J., Thomson, K. E., Scheerlinck, P., Pouliot, W., Greger, B., & Dudek, F. E. (2009). A simple quantitative method for analyzing electrographic status epilepticus in rats. *Journal of Neurophysiology*, 101(3), 1660–1670. <https://doi.org/10.1152/jn.91062.2008>
- Lin, J. H.-C., Weigel, H., Cotrina, M. L., Liu, S., Bueno, E., Hansen, A. J., ... Nedergaard, M. (1998). Gap-junction-mediated propagation and amplification of cell injury. *Nature Neuroscience*, 1(6), 494–500. <https://doi.org/10.1038/2210>
- Nakase, T., Fushiki, S., & Naus, C. C. G. (2003). Astrocytic gap junctions composed of connexin 43 reduce apoptotic neuronal damage in cerebral ischemia. *Stroke*, 34(8), 1987–1993. <https://doi.org/10.1161/01.STR.0000079814.72027.34>
- Newton, S. S., Girgenti, M. J., Collier, E. F., & Duman, R. S. (2006). Electroconvulsive seizure increases adult hippocampal angiogenesis in rats. *European Journal of Neuroscience*, 24(3), 819–828. <https://doi.org/10.1111/j.1460-9568.2006.04958.x>
- Orkand, R. K., Nicholls, J. G., & Kuffler, S. W. (1966). Effect of nerve impulses on the membrane potential of glial cells in the central nervous system of amphibia. *Journal of Neurophysiology*, 29(4), 788–806. <https://doi.org/10.1152/jn.1966.29.4.788>
- Pannasch, U., Dossi, E., Ezan, P., & Rouach, N. (2019). Astroglial Cx30 sustains neuronal population bursts independently of gap-junction mediated biochemical coupling. *Glia*, 67(6), 1104–1112. <https://doi.org/10.1002/glia.23591>
- Pannasch, U., Freche, D., Dallérac, G., Ghézali, G., Escartin, C., Ezan, P., ... Rouach, N. (2014). Connexin 30 sets synaptic strength by controlling astroglial synapse invasion. *Nature Neuroscience*, 17(4), 549–558. <https://doi.org/10.1038/nn.3662>
- Pannasch, U., Vargová, L., Reingruber, J., Ezan, P., Holcman, D., Giaume, C., ... Rouach, N. (2011). Astroglial networks scale synaptic activity and plasticity. *Proceedings of the National Academy of Sciences of the United States of America*, 108(20), 8467–8472. <https://doi.org/10.1073/pnas.1016650108>
- Putra, M., Sharma, S., Gage, M., Gasser, G., Hinojo-Perez, A., Olson, A., ... Thippeswamy, T. (2020). Inducible nitric oxide synthase inhibitor, 1400W, mitigates DFP-induced long-term neurotoxicity in the rat model. *Neurobiology of Disease*, 133, 104443. <https://doi.org/10.1016/j.nbd.2019.03.031>
- Racine, R. J. (1972). Modification of seizure activity by electrical stimulation: II. Motor seizure. *Electroencephalography and Clinical Neurophysiology*, 32(3), 281–294. [https://doi.org/10.1016/0013-4694\(72\)90177-0](https://doi.org/10.1016/0013-4694(72)90177-0)
- Rigau, V., Morin, M., Rousset, M.-C., de Bock, F., Lebrun, A., Coubes, P., ... Lerner-Natoli, M. (2007). Angiogenesis is associated with blood-brain barrier permeability in temporal lobe epilepsy. *Brain: A Journal of Neurology*, 130(Pt. 7), 1942–1956. <https://doi.org/10.1093/brain/awm118>
- Rouach, N., Koulakoff, A., Abudara, V., Willecke, K., & Giaume, C. (2008). Astroglial metabolic networks sustain hippocampal synaptic transmission. *Science*, 322(5907), 1551–1555. <https://doi.org/10.1126/science.1164022>
- Siushansian, R., Bechberger, J. F., Cechetto, D. F., Hachinski, V. C., & Naus, C. C. (2001). Connexin43 null mutation increases infarct size after stroke. *The Journal of Comparative Neurology*, 440(4), 387–394. <https://doi.org/10.1002/cne.1392>
- Sofroniew, M. V., & Vinters, H. V. (2010). Astrocytes: Biology and pathology. *Acta Neuropathologica*, 119(1), 7–35. <https://doi.org/10.1007/s00401-009-0619-8>
- Steinhäuser, C., Seifert, G., & Bedner, P. (2012). Astrocyte dysfunction in temporal lobe epilepsy: K⁺ channels and gap junction coupling. *Glia*, 60(8), 1192–1202. <https://doi.org/10.1002/glia.22313>
- Theis, M., Jauch, R., Zhuo, L., Speidel, D., Wallraff, A., Döring, B., ... Willecke, K. (2003). Accelerated hippocampal spreading depression and enhanced locomotory activity in mice with astrocyte-directed inactivation of connexin43. *The Journal of Neuroscience: The Official Journal of the Society for Neuroscience*, 23(3), 766–776.
- Thévenin, A. F., Kowal, T. J., Fong, J. T., Kells, R. M., Fisher, C. G., & Falk, M. M. (2013). Proteins and mechanisms regulating gap-junction assembly, internalization, and degradation. *Physiology*, 28(2), 93–116. <https://doi.org/10.1152/physiol.00038.2012>
- Wallraff, A., Köhling, R., Heinemann, U., Theis, M., Willecke, K., & Steinhäuser, C. (2006). The impact of astrocytic gap junctional coupling on potassium buffering in the hippocampus. *Journal of Neuroscience*, 26(20), 5438–5447. <https://doi.org/10.1523/JNEUROSCI.0037-06.2006>
- Warn-Cramer, B. J., Cottrell, G. T., Burt, J. M., & Lau, A. F. (1998). Regulation of connexin-43 gap junctional intercellular communication by mitogen-activated protein kinase. *Journal of Biological Chemistry*, 273(15), 9188–9196. <https://doi.org/10.1074/jbc.273.15.9188>
- Zhang, J., Griemsmann, S., Wu, Z., Dobrowolski, R., Willecke, K., Theis, M., ... Bedner, P. (2018). Connexin43, but not connexin30, contributes to adult neurogenesis in the dentate gyrus. *Brain Research Bulletin*, 136, 91–100. <https://doi.org/10.1016/j.brainresbull.2017.07.001>
- Zhou, K. Q., Green, C. R., Bennet, L., Gunn, A. J., & Davidson, J. O. (2019). The role of connexin and pannexin channels in perinatal brain injury and inflammation. *Frontiers in Physiology*, 10, 141. <https://doi.org/10.3389/fphys.2019.00141>

SUPPORTING INFORMATION

Additional supporting information may be found online in the Supporting Information section at the end of this article.

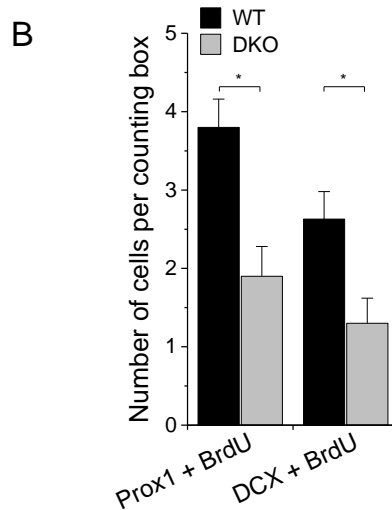
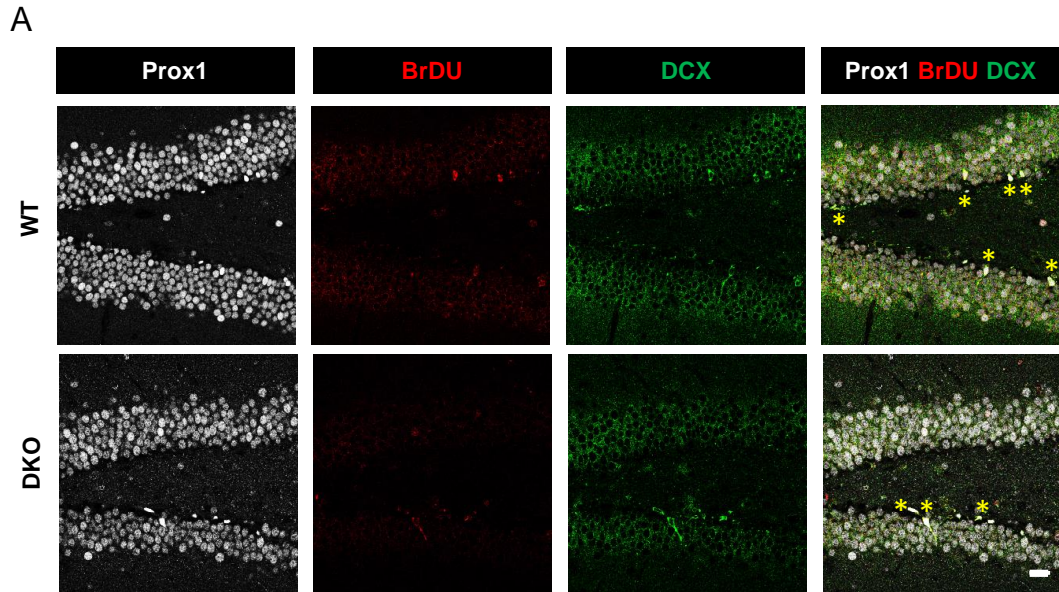
How to cite this article: Deshpande T, Li T, Henning L, et al. Constitutive deletion of astrocytic connexins aggravates kainate-induced epilepsy. *Glia*. 2020;68:2136–2147. <https://doi.org/10.1002/glia.23832>

Supp. Figure 1



Supplemental Figure 1: Reduced GCL width in non-epileptic DKO mice. A) Prox1 immunostaining of granule cells in the DG of WT and DKO mice. The width of the GCL was determined as described in Fig. 3. Scale bar, 100 µm. B) Data were averaged and compared between WT and DKO mice. The bar graphs reveal slimmer GCL blades in DKO mice. * $p < 0.01$, $n = 3$.

Supp. Figure 2



Supplemental Figure 2: Basal adult neurogenesis is substantially reduced in DKO mice. (A) Prox1 (white), BrdU (red) and DCX (green) immunostaining in the DG of WT and DKO mice. BrdU was administered through the drinking water for 14 days and mice were sacrificed 28 days after onset of BrdU administration. Asterisks indicate cells co-localizing BrdU and DCX. Almost all of the BrdU- or DCX-positive cells were also Prox1-positive. (B) Quantification of the number of Prox1/BrdU- and DCX/BrdU double-positive cells in counting boxes ($290 \times 290 \times 4 \mu\text{m}^3$) positioned $250 \mu\text{m}$ away from the outermost margin of the GCL flexure, perpendicularly to the longitudinal axis of the GCL. The density of Prox1/BrdU- and DCX/BrdU-positive cells was significantly lower in DKO mice, indicating reduced basal neurogenesis. $n = 3$, $*p < 0.01$

6. Discussion

The present study examined the role of astrocyte and BBB dysfunction as well as microglia-mediated immunity in experimental MTLE-HS. More specifically, this thesis comprises three publications dealing with separate but interlinked questions: I) what is the contribution of reactive microglia to the production of TNF α , astrocyte dysfunction and epileptogenesis in MTLE-HS; II) does albumin-induced TGF β signaling account for astrocyte GJ uncoupling and thereby contribute to epileptogenesis and III) what are the consequences of a dysfunctional astroglial GJ-coupled network for the development and progression of MTLE-HS.

In the following section, the major findings of this study and their implications for our understanding of epilepsy will be discussed.

A major aim of this PhD thesis was to decipher the upstream molecular mechanisms that promote astrocytic GJ uncoupling in KA-induced MTLE-HS. Previously, we could show that TNF α , which impairs astrocyte GJ coupling *in vitro* (Haghikia et al., 2008), increases rapidly in the injected hippocampus in response to *intracortical* KA-induced SE (Müller, 2018). However, a dysfunctional BBB and extravasation of serum albumin into the brain parenchyma have also been implicated in astrocyte GJ uncoupling and epileptogenesis (Braganza et al., 2012; Cacheaux et al., 2009; David et al., 2009; Ivens et al., 2007; Weissberg et al., 2015). Which of these two target mechanisms is actually responsible for the loss of astrocyte GJ coupling in the *intracortical* KA model of MTLE-HS has not yet been fully established. The results presented here help to clarify this question in several ways: In chapter 3 we could identify microglia as the major source of the pro-inflammatory cytokine TNF α during the acute phase of KA-induced MTLE-HS. This result corroborates previous findings demonstrating that microglia contribute to TNF α production in experimental epilepsy (Benson et al., 2015; Sano et al., 2021; Wang et al., 2015). Most importantly, we could show that microglia-derived TNF α is primarily responsible for astrocyte GJ uncoupling during early epileptogenesis. In fact, both partial microglia depletion as well as microglia-specific knock-out of TNF α prevented seizure-induced uncoupling after KA-injection. At the same time, the data presented in chapter 4 reveal that albumin-induced TGF β R1/ALK5 signaling is not involved in astrocyte uncoupling following KA-induced SE. First, we did not find evidence for biologically relevant albumin uptake into astrocytes at 4 and 24 h after KA administration. Second, pre-treatment with the TGF β R1/ALK5 inhibitor IPW5371, which has previously been shown to pass the BBB (Senatorov et al., 2019), did not prevent astrocyte uncoupling. Taken together, these data

convincingly demonstrate that microglia-derived TNF α , but not albumin-induced TGF β signaling is primarily responsible for loss of functional coupling between astrocytes during the early stages of experimental MTLE-HS.

Some considerations should be taken into account when interpreting the results of chapter 3 and 4. First, BBB dysfunction and pro-inflammatory cytokine release are not necessarily independent phenomena. For example, pro-inflammatory TNF α has been shown to impair BBB integrity (Chen et al., 2019; Cheng et al., 2018; Huang et al., 2022; Librizzi et al., 2012; Nishioku et al., 2010; Weinberg et al., 2013). However, disruption of the sTNF α /TNFR1 signaling pathway using a dominant-negative sTNF α inhibitor did not affect the extent of albumin extravasation 4 h post KA injection (unpublished data). Moreover, as direct inhibition of TGF β R1/ALK5 activation, which is supposed to occur as a consequence of albumin extravasation, did not prevent seizure-induced GJ uncoupling, it is unlikely that the detrimental effect of microglial TNF α on astrocytic GJ coupling is mediated by a compromised BBB. Alternatively, serum-derived proteins could induce microglial reactivity and TNF α release. Indeed, experimental BBB disruption and albumin application have been shown to cause neuroinflammation and glial reactivity (Cacheaux et al., 2009; David et al., 2009; Frigerio et al., 2012; Ralay Ranaivo & Wainwright, 2010). However, several mechanisms potentially contribute to microglia reactivity in epilepsy. For example, microglia can directly sense neuronal hyperactivity during SE through a mechanism involving glutamate-dependent ATP release from neurons, which activates microglial P2Y12 receptors (Eyo et al., 2014). Thus, future studies will need to investigate the potential interplay between BBB breakdown and microglia reactivity in epilepsy.

Second, we have not assessed whether microglia contribute to TNF α production also at later stages of epileptogenesis. Indeed, our previous data show that ipsilateral TNF α levels remain significantly elevated at 24 h post KA-induced SE (Müller, 2018). Single-cell gene expression data further revealed increased TNF α mRNA expression in astrocytes 5 d post KA injection (unpublished data). This suggests that cytokine release occurs in waves, possibly due to the emergence of spontaneous seizures at later time points, and that other immunocompetent cells contribute to TNF α production during the latent phase of epilepsy. Moreover, the infiltration of peripheral macrophages could lead to another peak in TNF α tissue concentrations (Varvel et al., 2016). Finally, we cannot rule out a contribution of aberrant albumin-induced TGF β R1/ALK5 signaling to astrocyte dysfunction and epileptogenesis at later stages of the disease, especially because extravasated albumin persists in the brain until the chronic phase of

epilepsy (Deshpande et al., 2017). For example, losartan, an angiotensin II type 1 receptor inhibitor that also interferes with TGF β signaling in the brain (Bar-Klein et al., 2014), has been shown to decrease chronic seizure burden as well as hippocampal neurodegeneration and behavioral impairments when administered chronically after the induction of KA-induced SE (Tchekalarova et al., 2014). Indeed, TGF β R1/ALK5 inhibition mildly affected chronic epileptiform activity in our model, an effect that could potentially be enhanced with prolonged pharmacological treatment.

To our surprise, although genetic deletion of microglial TNF α completely prevented seizure-induced GJ uncoupling, it did neither affect acute nor chronic seizure burden in our model. The lack of effect could be explained by the previously reported antagonistic effects of TNFR1 vs TNFR2 signaling in experimental epilepsy (Balosso et al., 2005; Patel et al., 2017; Weinberg et al., 2013). Further support for this hypothesis derives from previous data demonstrating that blocking sTNF α /TNFR1 signaling using the dominant-negative sTNF α inhibitor XPro1595 (Steed et al., 2003) prior to *intracortical* KA application completely abrogates epileptogenesis (Müller, 2018). Moreover, gene expression and immunohistochemistry data further revealed upregulation of TNFR1 in astrocytes, indicating that aberrant sTNF α /TNFR1 signaling underlies compromised astrocyte GJ coupling and epileptogenesis in our MTLE-HS model (Henning et al., 2022). Collectively, these data suggest that pharmacotherapies specifically targeting TNFR1 signaling to restore essential astrocyte functions could prove valuable for the treatment of MTLE-HS.

The need for highly specific microglial manipulation in epilepsy is further supported by our finding that although partial pharmacological microglial depletion resulted in reduced acute seizure activity it also increased mortality after KA-induced SE. These data suggest that microglia also serve protective roles in epilepsy. Indeed, microglia depletion has been shown to increase mortality, seizure severity and neurodegeneration in other studies of SE- and infection-induced epilepsy (Sanchez et al., 2019; Waltl, Käufer, Gerhauser, et al., 2018; Wu et al., 2020). Moreover, microglia have been suggested to confine neuronal hyperactivity. For example, microglia suppress excessive neuronal excitation by a negative feedback mechanism involving microglial ATP-to-adenosine conversion and neuronal A $_1$ R activation (Badimon et al., 2020). Additionally, knock-out of G $_i$ -protein-coupled receptors in microglia leads to the development of spontaneous seizures and increases the susceptibility to pilocarpine-induced seizures (Merlini et al., 2021). Taken together, targeted manipulations that reprogram microglia

towards an anti-epileptic phenotype are necessary to prevent loss of essential microglial functions important for brain homeostasis and survival in epilepsy (Fumagalli et al., 2018).

Chapter 3 and 4 of this work uncovered the molecular mechanisms underlying astrocyte dysfunction in experimental MTLE-HS, identifying TNF α derived from reactive microglia as the key mediator of seizure-induced astrocyte GJ uncoupling. However, due to its involvement in both ion buffering and metabolic supply to neurons, the astroglial network exhibits both anti- as well as pro-epileptic potential (Chever et al., 2016; Pannasch et al., 2011; Rouach et al., 2008; Wallraff et al., 2006). Therefore, another aim of this work was to better understand the consequences of dysfunctional astrocyte GJ coupling for the development and progression of experimental epilepsy. The data provided in chapter 5 demonstrate that constitutive deletion of astroglial Cxs exacerbates MTLE-HS pathology, suggesting that the pro-convulsive effects of a dysfunctional astroglial network override its anti-convulsant potential. This result is in line with other findings demonstrating that loss of functional astrocyte coupling promotes epileptic activity. For example, hippocampal slices from mice lacking both astroglial Cxs have been shown to be hyperexcitable (Pannasch et al., 2011; Wallraff et al., 2006). Moreover, a recent study demonstrates that preventing alkalization-induced impairments in astrocyte GJ coupling mitigates kindling-induced epileptiform activity (Onodera et al., 2021). Interestingly, pharmacological blockade of astrocyte GJs was found to be insufficient to cause epileptiform activity (Bazzigaluppi et al., 2017). Furthermore, in a recent study altered excitability but no spontaneous seizures were observed in mice with inducible deletion of astroglial Cx30 and Cx43 (Hösli et al., 2022). Similarly, we did not observe spontaneous seizures in our Cx DKO mice, in the absence of KA (Deshpande et al., 2020). However, these studies have several limitations, as pharmacological GJ blockers possess a number of side effects and conditional knock-out of astroglial Cxs in Hösli et al. (2022) was incomplete. Collectively, these data suggest that loss of functional astrocyte coupling exacerbates epileptogenesis in response to an epileptogenic stimulus, but is probably not *per se* sufficient to cause epilepsy.

The data presented here do not allow to derive definitive conclusions about the mechanism by which a perturbed astroglial network aggravates epilepsy. Nevertheless, some potential mechanisms should be discussed. Most importantly, loss of functional astrocyte coupling has been proposed to impair spatial K⁺ buffering, leading to net accumulation of extracellular K⁺ (Kofuji & Newman, 2004; Steinhäuser et al., 2012). According to the ‘K⁺ accumulation hypothesis’ (Fertziger & Ranck, 1970), an increased [K⁺]_o promotes neuronal excitability due to a depolarizing shift in the equilibrium potential for K⁺, which further enhances neuronal

activity and may eventually culminate in the development of seizures (Bazzigaluppi et al., 2017). Spatial K^+ buffering by astroglial networks in turn has been proposed to prevent excessive neuronal depolarization due to redistribution of extracellular K^+ to distant sites (Steinhäuser et al., 2012). Whether astroglial networks contribute to spatial K^+ buffering is controversially discussed, however. Pharmacological blockade of astrocyte GJs *in vivo* has been shown to cause elevated K^+ concentrations in the somatosensory cortex of mice (Bazzigaluppi et al., 2017). Moreover, impaired K^+ clearance was detected in hippocampal slices of mice lacking astroglial Cxs (Pannasch et al., 2011; Wallraff et al., 2006). However, in Wallraff et al. (2006) maximal stimulation intensities were required to detect differences in extracellular K^+ concentrations between DKO and WT mice. Similarly, recent studies suggest that the contribution of astrocyte GJ coupling to K^+ buffering is restricted to pathologically large K^+ elevations in the CNS (Breithausen et al., 2020; EbrahimAmini et al., 2021). For example, pharmacological blockade of the GJ coupled network modulates the amplitude and spread of extracellular K^+ transients in response to high concentrations of focally applied KCl in the neocortex *in vivo* (EbrahimAmini et al., 2021). Similarly, Breithausen et al. (2020) reported that GJ blockade increased the amplitude of extracellular K^+ transients only if the K^+ concentration was experimentally increased to > 10 mM *in situ*. Importantly, however, K^+ concentrations have been shown to exceed 10 mM during epileptiform activity (Bazzigaluppi et al., 2017; Heinemann et al., 1977; Sybert & Ward, 1974) and seizure activity disrupts the astrocyte GJ coupled network (Onodera et al., 2021; Wang et al., 2020). Therefore, these results suggest that a dysfunctional GJ-coupled network could exacerbate seizures due to impaired spatial buffering of extracellular K^+ . Of note, loss of astrocyte GJ coupling could exert pro-epileptic effects independent of dysfunctional K^+ buffering. As mentioned in chapter 5, astrocyte GJ-coupled networks are involved in the redistribution of Na^+ and Ca^{2+} ions (Henneberger, 2017; Langer et al., 2012; Scemes & Giaume, 2006). For example, impaired GJ coupling could promote accumulation of intracellular Na^+ in astrocytes, leading to a reduced driving force for uptake of extracellular glutamate and thus increased excitatory neurotransmission (Rose et al., 2018). Likewise, increased intracellular Na^+ causes reversal of the Na^+/Ca^{2+} exchanger (NCX), leading to Ca^{2+} entry into astrocytes which could lead to aberrant gliotransmission (Henneberger, 2017). Moreover, channel-independent effects of astrocyte Cxs have been described. For example, Cx30 controls the intrusion of astroglial processes into the synaptic cleft, thereby indirectly modulating glutamate transport and excitatory synaptic transmission (Pannasch et al., 2014). Thus, loss of astroglial Cxs in DKO mice could affect epileptic activity in several ways, independently of impaired K^+ homeostasis.

7. Conclusions

The present doctoral thesis addressed the molecular pathways underlying an impaired astroglial GJ-coupled network in MTLE-HS and its contribution to the initiation of the disorder. Interastrocytic GJ-coupling enables spatial redistribution of extracellular K^+ , which is particularly relevant during pathological conditions characterized by large and localized extracellular K^+ increases (Breithausen et al., 2020; EbrahimAmini et al., 2021). However, the contribution of this particular astrocyte dysfunction to the development and progression of epilepsy was not yet fully understood, as astrocyte networks possess both pro- as well as anti-epileptic potential (Chever et al., 2016; Rouach et al., 2008; Wallraff et al., 2006). Based on genetic deletion of astroglial Cx30 and Cx43 this work demonstrates an overall anti-epileptic role of the astrocyte network, as loss of astroglial Cxs led to exacerbation of epilepsy in a well-established mouse model of MTLE-HS. This finding therefore extends our previous work showing that astrocytes in human and experimental MTLE rapidly lose their ability to form GJ coupled networks (Bedner et al., 2015), and provides direct evidence that dysfunctional interastrocytic GJ-coupling aggravates the pathology of epilepsy.

In addition, chapter 3 and 4 of this thesis aimed to identify more precisely the molecular pathways underlying dysfunctional GJ coupling in hippocampal astrocytes during epileptogenesis. Both microglia-derived $TNF\alpha$ as well as albumin-induced $TGF\beta$ signaling in astrocytes were equally plausible candidates to account for the impaired astrocytic coupling efficiency in epileptic tissue (Bedner et al., 2015; Braganza et al., 2012; Cacheaux et al., 2009; Haghikia et al., 2008). Therefore, we directly compared the evidence for $TGF\beta$ - vs. $TNF\alpha$ -induced astrocyte uncoupling in a mouse model of MTLE-HS. The results show that microglia-derived $TNF\alpha$ but not albumin-induced $TGF\beta$ signaling is the major factor responsible for astrocyte GJ uncoupling during early epileptogenesis. More specifically, we identified reactive microglia as the major initiators of a detrimental neuroinflammatory cascade, in which aberrant release of pro-inflammatory $TNF\alpha$ leads to astrocyte network dysfunction and impaired ion homeostasis, thereby promoting neuronal hyperexcitability (Figure 9). In conclusion, this work highlights glial dysfunction and neuroinflammation as important targets for the development of novel anti-epileptogenic drugs.

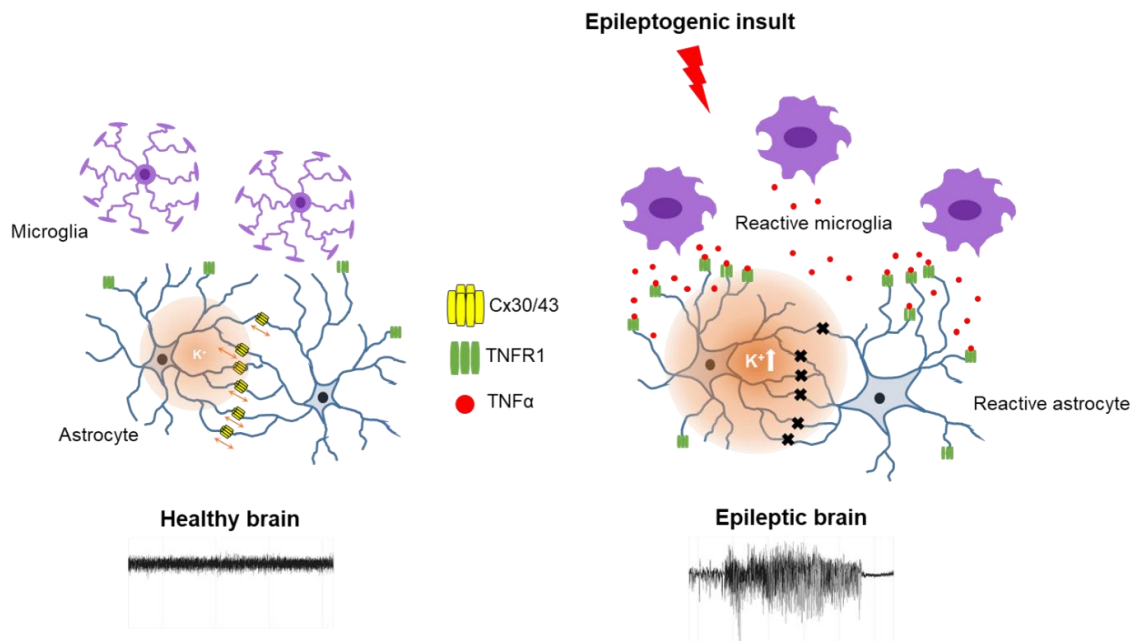


Figure 9. Reactive microglia-derived TNF α impairs astrocyte GJ coupling and K⁺ homeostasis, exacerbating the pathology of epilepsy. In this model, epileptogenic brain insults, including SE, lead to rapid astro- and microglial reactivity. Reactive microglia release high amounts of the pro-inflammatory cytokine TNF α , which acts *via* TNFR1 on astrocytes to impair interastrocytic GJ coupling and spatial K⁺ buffering. As a consequence, extracellular K⁺ accumulates locally and increases neuronal excitability, ultimately promoting the development of spontaneous seizures.

8. Perspective

The results presented here suggest that targeted manipulation of TNF α /TNFR1 signaling, instead of global TNF α inhibition, is necessary to achieve an antiepileptogenic treatment effect. Indeed, our previous work already identified the promising treatment potential of XPro1595, a dominant-negative and BBB-permeable sTNF α inhibitor, in the *intracortical* KA model of MTLE-HS (Müller, 2018). Future studies should extend on that by investigating the antiepileptogenic potential of XPro1595 also in other epilepsy models, such as the pilocarpine model of MTLE-HS. If successful, clinical trials could be initiated to examine the efficacy and tolerability of XPro1595 in the context of human epilepsy. Moreover, co-administration of a TNFR2-specific agonist, such as EHD2–scTNFR2 (Dong et al., 2016), together with XPro1595, would allow to investigate whether concomitant stimulation of TNFR2 signaling amplifies the antiepileptogenic effects of TNFR1 antagonism in epilepsy (Müller, 2018).

According to our current understanding, TNF α exerts a pro-convulsive role by impairing essential astrocyte functions through TNFR1 signaling (Müller, 2018). However, TNF α has several neuromodulatory effects (McCoy & Tansey, 2008; Santello & Volterra, 2012). Future studies should therefore more closely investigate the role of astroglial TNFR1-signaling in

epileptogenesis. To this end, mice with astrocyte-specific and inducible TNFR1 deletion will help to substantiate our hypothesis that astroglial TNFR1 activation is primarily responsible for the pro-epileptogenic effects of aberrant TNF α signaling in epilepsy. Finally, more data regarding the dynamics and origin of TNF α at various stages of epileptogenesis is required. For example, our microglia-specific TNF α knock-out mice could help to clarify whether microglia contribute to TNF α production also at later stages of epilepsy.

Alternatively, pharmacological preservation of a high astroglial coupling efficiency may represent a novel and effective treatment option in epilepsy. Indeed, BBB-permeable Cx43-specific GJ-enhancers have already been developed (Butera et al., 2009; Wang et al., 2018). However, Cx43 activators could exert undesirable side effects, as Cx43 is strongly expressed in cardiomyocytes in the heart (De Vuyst et al., 2011). Therefore, Cx43 modulators need to be modified to ensure specificity towards astrocytic Cxs (Müller, 2018). Recently developed cellular assays will be helpful to identify novel Cx GJ modulators (Danish et al., 2021). In experimental epilepsy, astrocyte-specific overexpression of Cx43 represents another possibility to examine the anti-epileptic potential of enhancing GJ-mediated interastrocytic communication. Stable Cre-inducible overexpression of Cx43 has already been demonstrated in embryonic stem cells, allowing to generate transgenic mice for astrocyte-specific overexpression of Cx43 (Niemann et al., 2022). Conversely, subjecting inducible astrocyte-specific Cx30 and 43 knock-out mice (Hösli et al., 2022) to *intracortical* KA injection would allow to overcome some of the limitations associated with the use of our constitutive DKO mice and to provide further insight into the role of astrocyte networks in epileptogenesis.

Summary of the thesis

The major aim of the present cumulative doctoral thesis was to examine the contribution of astrocyte network dysfunction and microglia-mediated neuroinflammation to the development and progression of temporal lobe epilepsy. More specifically, this thesis is divided into three chapters that address separate but interconnected objectives: I) to define the contribution of reactive microglia to the production of neuroinflammatory TNF α , astrocyte dysfunction and epileptogenesis; II) to examine the consequences of seizure-induced BBB dysfunction and albumin-induced TGF β signaling for astroglial network function and epilepsy development and III) to evaluate the role of a dysfunctional astroglial network in epileptogenesis. In order to tackle these research questions, we employed a mouse model of MTLE-HS, which has previously been shown to recapitulate key features of the pathology (Bedner et al., 2015).

First, the results summarized in chapter 3 of this thesis demonstrate that microglia-derived TNF α is rapidly released following an epileptogenic brain insult in mice and is the major factor responsible for astrocyte uncoupling during early epileptogenesis in our model. In contrast to our expectations, however, microglia-specific TNF α knock-out did not affect seizure burden and histopathological changes in mice, which could be explained by the previously reported opposing effects of TNFR1 vs. TNFR2 signaling (Patel et al., 2017; Weinberg et al., 2013). Second, the publication presented in chapter 4 of this thesis shows that pharmacological inhibition of TGF β R1/ALK5 signaling does not prevent astrocyte uncoupling and only marginally affects epileptogenesis in our MTLE-HS model. Together, the data presented in both chapters strongly indicate that pro-inflammatory TNF α , but not albumin-induced TGF β signaling is primarily responsible for dysfunctional astrocyte communication during early epileptogenesis. Therefore, targeted manipulation of TNF α /TNFR1 signaling could represent a novel antiepileptogenic treatment strategy, as already indicated by our previous findings (Müller, 2018). Finally, chapter 5 of this thesis addressed the long-standing question whether a dysfunctional astrocyte network exerts primarily pro- or anti-epileptic effects. Based on genetic deletion of the astroglial GJ-forming proteins Cx30 and Cx43, the data in chapter 5 demonstrate an overall pro-epileptic effect of a dysfunctional astrocyte network, identifying it as a driver of epileptogenesis. Collectively, the data of this doctoral thesis indicate astrocyte network dysfunction and impaired ion homeostasis due to aberrant TNF α signaling as a major contributing factor to epileptogenesis and as a promising target for the development of antiepileptogenic drugs.

References

- Al Rihani, S. B., Darakjian, L. I., Deodhar, M., Dow, P., Turgeon, J., & Michaud, V. (2021). Disease-Induced Modulation of Drug Transporters at the Blood–Brain Barrier Level. *International Journal of Molecular Sciences*, *22*(7), 3742. <https://doi.org/10.3390/ijms22073742>
- Altmann, A., Ryten, M., Di Nunzio, M., Ravizza, T., Tolomeo, D., Reynolds, R. H., Somani, A., Bacigaluppi, M., Iori, V., Micotti, E., Di Sapia, R., Cerovic, M., Palma, E., Ruffolo, G., Botía, J. A., Absil, J., Alhusaini, S., Alvim, M. K. M., Auvinen, P., ... Sisodiya, S. M. (2022). A systems-level analysis highlights microglial activation as a modifying factor in common epilepsies. *Neuropathology and Applied Neurobiology*, *48*(1), e12758. <https://doi.org/10.1111/nan.12758>
- Alvestad, S., Hammer, J., Hoddevik, E. H., Skare, Ø., Sonnewald, U., Amiry-Moghaddam, M., & Ottersen, O. P. (2013). Mislocalization of AQP4 precedes chronic seizures in the kainate model of temporal lobe epilepsy. *Epilepsy Research*, *105*(1–2), 30–41. <https://doi.org/10.1016/j.eplepsyres.2013.01.006>
- Anders, S., Minge, D., Griemsmann, S., Herde, M. K., Steinhäuser, C., & Henneberger, C. (2014). Spatial properties of astrocyte gap junction coupling in the rat hippocampus. *Philosophical Transactions of the Royal Society B: Biological Sciences*, *369*(1654), 20130600. <https://doi.org/10.1098/rstb.2013.0600>
- Androsova, G., Krause, R., Borghei, M., Wassenaar, M., Auce, P., Avbersek, A., Becker, F., Berghuis, B., Campbell, E., Coppola, A., Francis, B., Wolking, S., Cavalleri, G. L., Craig, J., Delanty, N., Koeleman, B. P. C., Kunz, W. S., Lerche, H., Marson, A. G., ... the EpiPGX Consortium. (2017). Comparative effectiveness of antiepileptic drugs in patients with mesial temporal lobe epilepsy with hippocampal sclerosis. *Epilepsia*, *58*(10), 1734–1741. <https://doi.org/10.1111/epi.13871>

- Araque, A., Carmignoto, G., Haydon, P. G., Oliet, S. H. R., Robitaille, R., & Volterra, A. (2014). Gliotransmitters Travel in Time and Space. *Neuron*, *81*(4), 728–739. <https://doi.org/10.1016/j.neuron.2014.02.007>
- Araque, A., Parpura, V., Sanzgiri, R. P., & Haydon, P. G. (1999). Tripartite synapses: Glia, the unacknowledged partner. *Trends in Neurosciences*, *22*(5), 208–215. [https://doi.org/10.1016/S0166-2236\(98\)01349-6](https://doi.org/10.1016/S0166-2236(98)01349-6)
- Aronica, E., Bauer, S., Bozzi, Y., Caleo, M., Dingledine, R., Gorter, J. A., Henshall, D. C., Kaufer, D., Koh, S., Löscher, W., Louboutin, J.-P., Mishto, M., Norwood, B. A., Palma, E., Poulter, M. O., Terrone, G., Vezzani, A., & Kaminski, R. M. (2017). Neuroinflammatory targets and treatments for epilepsy validated in experimental models. *Epilepsia*, *58*, 27–38. <https://doi.org/10.1111/epi.13783>
- Aronica, E., Boer, K., van Vliet, E. A., Redeker, S., Baayen, J. C., Spliet, W. G. M., van Rijen, P. C., Troost, D., Lopes da Silva, F. H., Wadman, W. J., & Gorter, J. A. (2007). Complement activation in experimental and human temporal lobe epilepsy. *Neurobiology of Disease*, *26*(3), 497–511. <https://doi.org/10.1016/j.nbd.2007.01.015>
- Aronica, E., Zurolo, E., Iyer, A., de Groot, M., Anink, J., Carbonell, C., van Vliet, E. A., Baayen, J. C., Boison, D., & Gorter, J. A. (2011). Upregulation of adenosine kinase in astrocytes in experimental and human temporal lobe epilepsy: ADK, Astrocytes, and TLE. *Epilepsia*, *52*(9), 1645–1655. <https://doi.org/10.1111/j.1528-1167.2011.03115.x>
- Aulická, S., Česká, K., Šána, J., Siegl, F., Brichtová, E., Ošlejšková, H., Hermanová, M., Hendrych, M., Michu, E. P., Brázdil, M., Slabý, O., & Nestrašil, I. (2022). Cytokine-chemokine profiles in the hippocampus of patients with mesial temporal lobe epilepsy and hippocampal sclerosis. *Epilepsy Research*, *180*, 106858. <https://doi.org/10.1016/j.eplepsyres.2022.106858>
- Avignone, E., Ulmann, L., Levavasseur, F., Rassendren, F., & Audinat, E. (2008). Status Epilepticus Induces a Particular Microglial Activation State Characterized by

- Enhanced Purinergic Signaling. *Journal of Neuroscience*, 28(37), 9133–9144.
<https://doi.org/10.1523/JNEUROSCI.1820-08.2008>
- Badimon, A., Strasburger, H. J., Ayata, P., Chen, X., Nair, A., Ikegami, A., Hwang, P., Chan, A. T., Graves, S. M., Uweru, J. O., Ledderose, C., Kutlu, M. G., Wheeler, M. A., Kahan, A., Ishikawa, M., Wang, Y.-C., Loh, Y.-H. E., Jiang, J. X., Surmeier, D. J., ... Schaefer, A. (2020). Negative feedback control of neuronal activity by microglia. *Nature*, 586(7829), 417–423. <https://doi.org/10.1038/s41586-020-2777-8>
- Balosso, S., Ravizza, T., Perego, C., Peschon, J., Campbell, I. L., De Simoni, M. G., & Vezzani, A. (2005). Tumor necrosis factor- α inhibits seizures in mice via p75 receptors. *Annals of Neurology*, 57(6), 804–812. <https://doi.org/10.1002/ana.20480>
- Bankstahl, M., Breuer, H., Leiter, I., Märkel, M., Bascuñana, P., Michalski, D., Bengel, F. M., Löscher, W., Meier, M., Bankstahl, J. P., & Härtig, W. (2018). Blood–Brain Barrier Leakage during Early Epileptogenesis Is Associated with Rapid Remodeling of the Neurovascular Unit. *Eneuro*, 5(3), ENEURO.0123-18.2018.
<https://doi.org/10.1523/ENEURO.0123-18.2018>
- Bar-Klein, G., Cacheaux, L. P., Kamintsky, L., Prager, O., Weissberg, I., Schoknecht, K., Cheng, P., Kim, S. Y., Wood, L., Heinemann, U., Kaufer, D., & Friedman, A. (2014). Losartan prevents acquired epilepsy via TGF- β signaling suppression: Astrocytic TGF- β and Epilepsy. *Annals of Neurology*, 75(6), 864–875.
<https://doi.org/10.1002/ana.24147>
- Basilico, B., Ferrucci, L., Ratano, P., Golia, M. T., Grimaldi, A., Rosito, M., Ferretti, V., Reverte, I., Sanchini, C., Marrone, M. C., Giubettini, M., De Turris, V., Salerno, D., Garofalo, S., St-Pierre, M., Carrier, M., Renzi, M., Pagani, F., Modi, B., ... Ragozzino, D. (2022). Microglia control glutamatergic synapses in the adult mouse hippocampus. *Glia*, 70(1), 173–195. <https://doi.org/10.1002/glia.24101>

- Bauer, K. Fr., & Leonhardt, H. (1955). Zur Kenntnis der Blut-Gehirnschranke. Cardiazolschock und Schrankenzusammenbruch. *Archiv für Psychiatrie und Nervenkrankheiten Vereinigt mit Zeitschrift für die Gesamte Neurologie und Psychiatrie*, 193(1), 68–77. <https://doi.org/10.1007/BF00352637>
- Bauer, K. Fr., & Leonhardt, H. (1956). A contribution to the pathological physiology of the blood-brain-barrier. Megaphen stabilises the blood-brain-barrier. *The Journal of Comparative Neurology*, 106(2), 363–370. <https://doi.org/10.1002/cne.901060207>
- Bazzigaluppi, P., Weisspapir, I., Stefanovic, B., Leybaert, L., & Carlen, P. L. (2017). Astrocytic gap junction blockade markedly increases extracellular potassium without causing seizures in the mouse neocortex. *Neurobiology of Disease*, 101, 1–7. <https://doi.org/10.1016/j.nbd.2016.12.017>
- Beattie, E. C., Stellwagen, D., Morishita, W., Bresnahan, J. C., Ha, B. K., Von Zastrow, M., Beattie, M. S., & Malenka, R. C. (2002). Control of Synaptic Strength by Glial TNF α . *Science*, 295(5563), 2282–2285. <https://doi.org/10.1126/science.1067859>
- Becker, A. J. (2018). Review: Animal models of acquired epilepsy: insights into mechanisms of human epileptogenesis. *Neuropathology and Applied Neurobiology*, 44(1), 112–129. <https://doi.org/10.1111/nan.12451>
- Bedner, P., Dupper, A., Hüttmann, K., Müller, J., Herde, M. K., Dublin, P., Deshpande, T., Schramm, J., Häussler, U., Haas, C. A., Henneberger, C., Theis, M., & Steinhäuser, C. (2015). Astrocyte uncoupling as a cause of human temporal lobe epilepsy. *Brain*, 138(5), 1208–1222. <https://doi.org/10.1093/brain/awv067>
- Ben-Ari, Y., & Cossart, R. (2000). Kainate, a double agent that generates seizures: Two decades of progress. *Trends in Neurosciences*, 23(11), 580–587. [https://doi.org/10.1016/S0166-2236\(00\)01659-3](https://doi.org/10.1016/S0166-2236(00)01659-3)

- Benson, M. J., Manzanero, S., & Borges, K. (2015). Complex alterations in microglial M1/M2 markers during the development of epilepsy in two mouse models. *Epilepsia*, 56(6), 895–905. <https://doi.org/10.1111/epi.12960>
- Binder, D. K., & Steinhäuser, C. (2006). Functional changes in astroglial cells in epilepsy. *Glia*, 54(5), 358–368. <https://doi.org/10.1002/glia.20394>
- Blümcke, I., Thom, M., Aronica, E., Armstrong, D. D., Bartolomei, F., Bernasconi, A., Bernasconi, N., Bien, C. G., Cendes, F., Coras, R., Cross, J. H., Jacques, T. S., Kahane, P., Mathern, G. W., Miyata, H., Moshé, S. L., Oz, B., Özkara, Ç., Perucca, E., ... Spreafico, R. (2013). International consensus classification of hippocampal sclerosis in temporal lobe epilepsy: A Task Force report from the ILAE Commission on Diagnostic Methods. *Epilepsia*, 54(7), 1315–1329. <https://doi.org/10.1111/epi.12220>
- Boche, D., Perry, V. H., & Nicoll, J. A. R. (2013). Review: Activation patterns of microglia and their identification in the human brain: Microglia in human brain. *Neuropathology and Applied Neurobiology*, 39(1), 3–18. <https://doi.org/10.1111/nan.12011>
- Bouilleret, V., Ridoux, V., Depaulis, A., Marescaux, C., Nehlig, A., & Le Gal La Salle, G. (1999). Recurrent seizures and hippocampal sclerosis following intrahippocampal kainate injection in adult mice: Electroencephalography, histopathology and synaptic reorganization similar to mesial temporal lobe epilepsy. *Neuroscience*, 89(3), 717–729. [https://doi.org/10.1016/S0306-4522\(98\)00401-1](https://doi.org/10.1016/S0306-4522(98)00401-1)
- Braganza, O., Bedner, P., Hüttmann, K., von Staden, E., Friedman, A., Seifert, G., & Steinhäuser, C. (2012). Albumin is taken up by hippocampal NG2 cells and astrocytes and decreases gap junction coupling. *Epilepsia*, 53(11), 1898–1906. <https://doi.org/10.1111/j.1528-1167.2012.03665.x>
- Brambilla, R., Ashbaugh, J. J., Magliozzi, R., Dellarole, A., Karmally, S., Szymkowski, D. E., & Bethea, J. R. (2011). Inhibition of soluble tumour necrosis factor is therapeutic in

- experimental autoimmune encephalomyelitis and promotes axon preservation and remyelination. *Brain*, 134(9), 2736–2754. <https://doi.org/10.1093/brain/awr199>
- Breithausen, B. (2020). *Control of ion and neurotransmitter homeostasis by hippocampal astroglial networks* [Doctoral dissertation, Rheinische Friedrich-Wilhelms-Universität Bonn]. Universitäts- und Landesbibliothek Bonn. <https://bonndoc.ulb.uni-bonn.de/xmlui/handle/20.500.11811/8847>
- Breithausen, B., Kautzmann, S., Boehlen, A., Steinhäuser, C., & Henneberger, C. (2020). Limited contribution of astroglial gap junction coupling to buffering of extracellular K⁺ in CA1 stratum radiatum. *Glia*, 68(5), 918–931. <https://doi.org/10.1002/glia.23751>
- Brenner, D., Blaser, H., & Mak, T. W. (2015). Regulation of tumour necrosis factor signalling: Live or let die. *Nature Reviews Immunology*, 15(6), 362–374. <https://doi.org/10.1038/nri3834>
- Briellmann, R. S., Kalnins, R. M., Berkovic, S. F., & Jackson, G. D. (2002). Hippocampal pathology in refractory temporal lobe epilepsy: T2-weighted signal change reflects dentate gliosis. *Neurology*, 58(2), 265–271. <https://doi.org/10.1212/WNL.58.2.265>
- Broekaart, D. W. M., Anink, J. J., Baayen, J. C., Idema, S., de Vries, H. E., Aronica, E., Gorter, J. A., & van Vliet, E. A. (2018). Activation of the innate immune system is evident throughout epileptogenesis and is associated with blood-brain barrier dysfunction and seizure progression. *Epilepsia*, 59(10), 1931–1944. <https://doi.org/10.1111/epi.14550>
- Bushong, E. A., Martone, M. E., Jones, Y. Z., & Ellisman, M. H. (2002). Protoplasmic Astrocytes in CA1 Stratum Radiatum Occupy Separate Anatomical Domains. *The Journal of Neuroscience*, 22(1), 183–192. <https://doi.org/10.1523/JNEUROSCI.22-01-00183.2002>
- Butera, J. A., Larsen, B. D., Hennan, J. K., Kerns, E., Di, L., Alimardanov, A., Swillo, R. E., Morgan, G. A., Liu, K., Wang, Q., Rossman, E. I., Unwalla, R., McDonald, L.,

- Huselton, C., & Petersen, J. S. (2009). Discovery of (2*S*,4*R*)-1-(2-Aminoacetyl)-4-benzamidopyrrolidine-2-carboxylic Acid Hydrochloride (GAP-134)¹³, an Orally Active Small Molecule Gap-Junction Modifier for the Treatment of Atrial Fibrillation. *Journal of Medicinal Chemistry*, *52*(4), 908–911. <https://doi.org/10.1021/jm801558d>
- Cacheaux, L. P., Ivens, S., David, Y., Lakhter, A. J., Bar-Klein, G., Shapira, M., Heinemann, U., Friedman, A., & Kaufer, D. (2009). Transcriptome Profiling Reveals TGF-Signaling Involvement in Epileptogenesis. *Journal of Neuroscience*, *29*(28), 8927–8935. <https://doi.org/10.1523/JNEUROSCI.0430-09.2009>
- Chen, A.-Q., Fang, Z., Chen, X.-L., Yang, S., Zhou, Y.-F., Mao, L., Xia, Y.-P., Jin, H.-J., Li, Y.-N., You, M.-F., Wang, X.-X., Lei, H., He, Q.-W., & Hu, B. (2019). Microglia-derived TNF- α mediates endothelial necroptosis aggravating blood brain-barrier disruption after ischemic stroke. *Cell Death & Disease*, *10*(7), 487. <https://doi.org/10.1038/s41419-019-1716-9>
- Cheng, Y., Desse, S., Martinez, A., Worthen, R. J., Jope, R. S., & Beurel, E. (2018). TNF α disrupts blood brain barrier integrity to maintain prolonged depressive-like behavior in mice. *Brain, Behavior, and Immunity*, *69*, 556–567. <https://doi.org/10.1016/j.bbi.2018.02.003>
- Cheung, G., Bataveljic, D., Visser, J., Kumar, N., Moulard, J., Dallérac, G., Mozheiko, D., Rollenhagen, A., Ezan, P., Mongin, C., Chever, O., Bemelmans, A.-P., Lübke, J., Leray, I., & Rouach, N. (2022). Physiological synaptic activity and recognition memory require astroglial glutamine. *Nature Communications*, *13*(1), 753. <https://doi.org/10.1038/s41467-022-28331-7>
- Cheung, G., Chever, O., & Rouach, N. (2014). Connexons and pannexons: Newcomers in neurophysiology. *Frontiers in Cellular Neuroscience*, *8*, 348. <https://doi.org/10.3389/fncel.2014.00348>

- Chever, O., Dossi, E., Pannasch, U., Derangeon, M., & Rouach, N. (2016). Astroglial networks promote neuronal coordination. *Science Signaling*, *9*(410).
<https://doi.org/10.1126/scisignal.aad3066>
- Clarkson, C., Smeal, R. M., Hasenoehrl, M. G., White, J. A., Rubio, M. E., & Wilcox, K. S. (2020). Ultrastructural and functional changes at the tripartite synapse during epileptogenesis in a model of temporal lobe epilepsy. *Experimental Neurology*, *326*, 113196. <https://doi.org/10.1016/j.expneurol.2020.113196>
- Conte, G., Parras, A., Alves, M., Ollà, I., De Diego-Garcia, L., Beamer, E., Alalqam, R., Ocampo, A., Mendez, R., Henshall, D. C., Lucas, J. J., & Engel, T. (2020). High concordance between hippocampal transcriptome of the mouse intra-amygdala kainic acid model and human temporal lobe epilepsy. *Epilepsia*, *61*(12), 2795–2810.
<https://doi.org/10.1111/epi.16714>
- Crespel, A., Coubes, P., Rousset, M.-C., Brana, C., Rougier, A., Rondouin, G., Bockaert, J., Baldy-Moulinier, M., & Lerner-Natoli, M. (2002). Inflammatory reactions in human medial temporal lobe epilepsy with hippocampal sclerosis. *Brain Research*, *952*(2), 159–169. [https://doi.org/10.1016/S0006-8993\(02\)03050-0](https://doi.org/10.1016/S0006-8993(02)03050-0)
- Dallérac, G., Zapata, J., & Rouach, N. (2018). Versatile control of synaptic circuits by astrocytes: Where, when and how? *Nature Reviews Neuroscience*, *19*(12), 729–743.
<https://doi.org/10.1038/s41583-018-0080-6>
- Daneman, R., & Prat, A. (2015). The Blood–Brain Barrier. *Cold Spring Harbor Perspectives in Biology*, *7*(1), a020412. <https://doi.org/10.1101/cshperspect.a020412>
- Danish, A., Gedschold, R., Hinz, S., Schiedel, A. C., Thimm, D., Bedner, P., Steinhäuser, C., & Müller, C. E. (2021). A Cellular Assay for the Identification and Characterization of Connexin Gap Junction Modulators. *International Journal of Molecular Sciences*, *22*(3), 1417. <https://doi.org/10.3390/ijms22031417>

- Davalos, D., Grutzendler, J., Yang, G., Kim, J. V., Zuo, Y., Jung, S., Littman, D. R., Dustin, M. L., & Gan, W.-B. (2005). ATP mediates rapid microglial response to local brain injury in vivo. *Nature Neuroscience*, 8(6), 752–758. <https://doi.org/10.1038/nn1472>
- David, Y., Cacheaux, L. P., Ivens, S., Lamilover, E., Heinemann, U., Kaufer, D., & Friedman, A. (2009). Astrocytic Dysfunction in Epileptogenesis: Consequence of Altered Potassium and Glutamate Homeostasis? *Journal of Neuroscience*, 29(34), 10588–10599. <https://doi.org/10.1523/JNEUROSCI.2323-09.2009>
- De Simoni, M. G., Perego, C., Ravizza, T., Moneta, D., Conti, M., Marchesi, F., De Luigi, A., Garattini, S., & Vezzani, A. (2000). Inflammatory cytokines and related genes are induced in the rat hippocampus by limbic status epilepticus: Cytokines in status epilepticus. *European Journal of Neuroscience*, 12(7), 2623–2633. <https://doi.org/10.1046/j.1460-9568.2000.00140.x>
- De Vuyst, E., Boengler, K., Antoons, G., Sipido, K. R., Schulz, R., & Leybaert, L. (2011). Pharmacological modulation of connexin-formed channels in cardiac pathophysiology: Connexins and ischaemic cardiac failure. *British Journal of Pharmacology*, 163(3), 469–483. <https://doi.org/10.1111/j.1476-5381.2011.01244.x>
- Deshpande, T. (2017). *Unravelling mechanisms causing astrocytic uncoupling in epilepsy* [Doctoral dissertation, Rheinische Friedrich-Wilhelms-Universität Bonn].
Universitäts- und Landesbibliothek Bonn. <https://bonndoc.ulb.uni-bonn.de/xmlui/handle/20.500.11811/7262>
- Deshpande, T., Li, T., Henning, L., Wu, Z., Müller, J., Seifert, G., Steinhäuser, C., & Bedner, P. (2020). Constitutive deletion of astrocytic connexins aggravates kainate-induced epilepsy. *Glia*, 68(10), 2136–2147. <https://doi.org/10.1002/glia.23832>
- Deshpande, T., Li, T., Herde, M. K., Becker, A., Vatter, H., Schwarz, M. K., Henneberger, C., Steinhäuser, C., & Bedner, P. (2017). Subcellular reorganization and altered phosphorylation of the astrocytic gap junction protein connexin43 in human and

- experimental temporal lobe epilepsy. *Glia*, 65(11), 1809–1820.
<https://doi.org/10.1002/glia.23196>
- Devinsky, O., Vezzani, A., Najjar, S., De Lanerolle, N. C., & Rogawski, M. A. (2013). Glia and epilepsy: Excitability and inflammation. *Trends in Neurosciences*, 36(3), 174–184. <https://doi.org/10.1016/j.tins.2012.11.008>
- Di Nunzio, M., Di Sapia, R., Sorrentino, D., Kebede, V., Cerovic, M., Gullotta, G. S., Bacigaluppi, M., Audinat, E., Marchi, N., Ravizza, T., & Vezzani, A. (2021). Microglia proliferation plays distinct roles in acquired epilepsy depending on disease stages. *Epilepsia*, 62(8), 1931–1945. <https://doi.org/10.1111/epi.16956>
- Dissing-Olesen, L., LeDue, J. M., Rungta, R. L., Hefendehl, J. K., Choi, H. B., & MacVicar, B. A. (2014). Activation of Neuronal NMDA Receptors Triggers Transient ATP-Mediated Microglial Process Outgrowth. *Journal of Neuroscience*, 34(32), 10511–10527. <https://doi.org/10.1523/JNEUROSCI.0405-14.2014>
- Dong, Y., Fischer, R., Naudé, P. J. W., Maier, O., Nyakas, C., Duffey, M., Van der Zee, E. A., Dekens, D., Douwenga, W., Herrmann, A., Guenzi, E., Kontermann, R. E., Pfizenmaier, K., & Eisel, U. L. M. (2016). Essential protective role of tumor necrosis factor receptor 2 in neurodegeneration. *Proceedings of the National Academy of Sciences*, 113(43), 12304–12309. <https://doi.org/10.1073/pnas.1605195113>
- Dubé, C. M., Brewster, A. L., Richichi, C., Zha, Q., & Baram, T. Z. (2007). Fever, febrile seizures and epilepsy. *Trends in Neurosciences*, 30(10), 490–496.
<https://doi.org/10.1016/j.tins.2007.07.006>
- EbrahimAmini, A., Bazzigaluppi, P., Aquilino, M. S., Stefanovic, B., & Carlen, P. L. (2021). Neocortical in vivo focal and spreading potassium responses and the influence of astrocytic gap junctional coupling. *Neurobiology of Disease*, 147, 105160.
<https://doi.org/10.1016/j.nbd.2020.105160>

- Eid, T., Lee, T.-S. W., Thomas, M. J., Amiry-Moghaddam, M., Bjørnsen, L. P., Spencer, D. D., Agre, P., Ottersen, O. P., & de Lanerolle, N. C. (2005). Loss of perivascular aquaporin 4 may underlie deficient water and K⁺ homeostasis in the human epileptogenic hippocampus. *Proceedings of the National Academy of Sciences*, *102*(4), 1193–1198. <https://doi.org/10.1073/pnas.0409308102>
- Eid, T., Thomas, M., Spencer, D., Rundén-Pran, E., Lai, J., Malthankar, G., Kim, J., Danbolt, N., Ottersen, O., & de Lanerolle, N. (2004). Loss of glutamine synthetase in the human epileptogenic hippocampus: Possible mechanism for raised extracellular glutamate in mesial temporal lobe epilepsy. *The Lancet*, *363*(9402), 28–37. [https://doi.org/10.1016/S0140-6736\(03\)15166-5](https://doi.org/10.1016/S0140-6736(03)15166-5)
- Escartin, C., Galea, E., Lakatos, A., O’Callaghan, J. P., Petzold, G. C., Serrano-Pozo, A., Steinhäuser, C., Volterra, A., Carmignoto, G., Agarwal, A., Allen, N. J., Araque, A., Barbeito, L., Barzilai, A., Bergles, D. E., Bonvento, G., Butt, A. M., Chen, W.-T., Cohen-Salmon, M., ... Verkhratsky, A. (2021). Reactive astrocyte nomenclature, definitions, and future directions. *Nature Neuroscience*, *24*(3), 312–325. <https://doi.org/10.1038/s41593-020-00783-4>
- Escartin, C., Guillemaud, O., & Carrillo-de Sauvage, M. (2019). Questions and (some) answers on reactive astrocytes. *Glia*, *67*(12), 2221–2247. <https://doi.org/10.1002/glia.23687>
- Eyo, U. B., Murugan, M., & Wu, L.-J. (2017). Microglia-Neuron Communication in Epilepsy: Microglia in Epilepsy. *Glia*, *65*(1), 5–18. <https://doi.org/10.1002/glia.23006>
- Eyo, U. B., Peng, J., Swiatkowski, P., Mukherjee, A., Bispo, A., & Wu, L.-J. (2014). Neuronal Hyperactivity Recruits Microglial Processes via Neuronal NMDA Receptors and Microglial P2Y₁₂ Receptors after Status Epilepticus. *Journal of Neuroscience*, *34*(32), 10528–10540. <https://doi.org/10.1523/JNEUROSCI.0416-14.2014>

- Faustman, D., & Davis, M. (2010). TNF receptor 2 pathway: Drug target for autoimmune diseases. *Nature Reviews Drug Discovery*, *9*(6), 482–493.
<https://doi.org/10.1038/nrd3030>
- Faustmann, P. M., Haase, C. G., Romberg, S., Hinkerohe, D., Szlachta, D., Smikalla, D., Krause, D., & Dermietzel, R. (2003). Microglia activation influences dye coupling and Cx43 expression of the astrocytic network. *Glia*, *42*(2), 101–108.
<https://doi.org/10.1002/glia.10141>
- Feng, L., Murugan, M., Bosco, D. B., Liu, Y., Peng, J., Worrell, G. A., Wang, H., Ta, L. E., Richardson, J. R., Shen, Y., & Wu, L. (2019). Microglial proliferation and monocyte infiltration contribute to microgliosis following status epilepticus. *Glia*, *67*(8), 1434–1448. <https://doi.org/10.1002/glia.23616>
- Fertziger, A. P., & Ranck, J. B. J. (1970). Potassium accumulation in interstitial space during epileptiform seizures. *Experimental Neurology*, *26*(3), 571–585.
<http://deepblue.lib.umich.edu/handle/2027.42/32795>
- Fisher, R. S., Acevedo, C., Arzimanoglou, A., Bogacz, A., Cross, J. H., Elger, C. E., Engel, J., Forsgren, L., French, J. A., Glynn, M., Hesdorffer, D. C., Lee, B. I., Mathern, G. W., Moshé, S. L., Perucca, E., Scheffer, I. E., Tomson, T., Watanabe, M., & Wiebe, S. (2014). ILAE Official Report: A practical clinical definition of epilepsy. *Epilepsia*, *55*(4), 475–482. <https://doi.org/10.1111/epi.12550>
- Freitas-Andrade, M., Wang, N., Bechberger, J. F., De Bock, M., Lampe, P. D., Leybaert, L., & Naus, C. C. (2019). Targeting MAPK phosphorylation of Connexin43 provides neuroprotection in stroke. *Journal of Experimental Medicine*, *216*(4), 916–935.
<https://doi.org/10.1084/jem.20171452>
- French, J. A., Williamson, P. D., Thadani, V. M., Darcey, T. M., Mattson, R. H., Spencer, S. S., & Spencer, D. D. (1993). Characteristics of medial temporal lobe epilepsy: I.

- Results of history and physical examination. *Annals of Neurology*, 34(6), 774–780.
<https://doi.org/10.1002/ana.410340604>
- Frigerio, F., Frasca, A., Weissberg, I., Parrella, S., Friedman, A., Vezzani, A., & Noe', F. M. (2012). Long-lasting pro-ictogenic effects induced in vivo by rat brain exposure to serum albumin in the absence of concomitant pathology: *Albumin and Brain Excitability*. *Epilepsia*, 53(11), 1887–1897. <https://doi.org/10.1111/j.1528-1167.2012.03666.x>
- Fumagalli, M., Lombardi, M., Gressens, P., & Verderio, C. (2018). How to reprogram microglia toward beneficial functions: How to reprogram microglia toward beneficial functions. *Glia*, 66(12), 2531–2549. <https://doi.org/10.1002/glia.23484>
- Galanopoulou, A. S., Löscher, W., Lubbers, L., O'Brien, T. J., Staley, K., Vezzani, A., D'Ambrosio, R., White, H. S., Sontheimer, H., Wolf, J. A., Twyman, R., Whittemore, V., Wilcox, K. S., & Klein, B. (2021). Antiepileptogenesis and disease modification: Progress, challenges, and the path forward—Report of the Preclinical Working Group of the 2018 NINDS-sponsored antiepileptogenesis and disease modification workshop. *Epilepsia Open*, 6(2), 276–296. <https://doi.org/10.1002/epi4.12490>
- Garrido-Mesa, N., Zarzuelo, A., & Gálvez, J. (2013). Minocycline: Far beyond an antibiotic: Minocycline: far beyond an antibiotic. *British Journal of Pharmacology*, 169(2), 337–352. <https://doi.org/10.1111/bph.12139>
- Gershen, L. D., Zanotti-Fregonara, P., Dustin, I. H., Liow, J.-S., Hirvonen, J., Kreisl, W. C., Jenko, K. J., Inati, S. K., Fujita, M., Morse, C. L., Brouwer, C., Hong, J. S., Pike, V. W., Zoghbi, S. S., Innis, R. B., & Theodore, W. H. (2015). Neuroinflammation in Temporal Lobe Epilepsy Measured Using Positron Emission Tomographic Imaging of Translocator Protein. *JAMA Neurology*, 72(8), 882.
<https://doi.org/10.1001/jamaneurol.2015.0941>

- Giaume, C., Koulakoff, A., Roux, L., Holcman, D., & Rouach, N. (2010). Astroglial networks: A step further in neuroglial and gliovascular interactions. *Nature Reviews Neuroscience*, *11*(2), 87–99. <https://doi.org/10.1038/nrn2757>
- Giaume, C., Naus, C. C., Sáez, J. C., & Leybaert, L. (2021). Glial Connexins and Pannexins in the Healthy and Diseased Brain. *Physiological Reviews*, *101*(1), 93–145. <https://doi.org/10.1152/physrev.00043.2018>
- Gosejacob, D., Dublin, P., Bedner, P., Hüttmann, K., Zhang, J., Tress, O., Willecke, K., Pfrieger, F., Steinhäuser, C., & Theis, M. (2011). Role of astroglial connexin30 in hippocampal gap junction coupling. *Glia*, *59*(3), 511–519. <https://doi.org/10.1002/glia.21120>
- Gouder, N. (2004). Overexpression of Adenosine Kinase in Epileptic Hippocampus Contributes to Epileptogenesis. *Journal of Neuroscience*, *24*(3), 692–701. <https://doi.org/10.1523/JNEUROSCI.4781-03.2004>
- Green, K. N., Crapser, J. D., & Hohsfield, L. A. (2020). To Kill a Microglia: A Case for CSF1R Inhibitors. *Trends in Immunology*, *41*(9), 771–784. <https://doi.org/10.1016/j.it.2020.07.001>
- Greene, C., Hanley, N., Reschke, C. R., Reddy, A., Mäe, M. A., Connolly, R., Behan, C., O’Keeffe, E., Bolger, I., Hudson, N., Delaney, C., Farrell, M. A., O’Brien, D. F., Cryan, J., Brett, F. M., Beausang, A., Betsholtz, C., Henshall, D. C., Doherty, C. P., & Campbell, M. (2022). Microvascular stabilization via blood-brain barrier regulation prevents seizure activity. *Nature Communications*, *13*(1), 2003. <https://doi.org/10.1038/s41467-022-29657-y>
- Haghikia, A., Ladage, K., Lafênetre, P., Haghikia, A., Hinkerohe, D., Smikalla, D., Haase, C. G., Dermietzel, R., & Faustmann, P. M. (2008). Intracellular application of TNF-alpha impairs cell to cell communication via gap junctions in glioma cells. *Journal of Neuro-Oncology*, *86*(2), 143–152. <https://doi.org/10.1007/s11060-007-9462-8>

- Hall, C. N., Reynell, C., Gesslein, B., Hamilton, N. B., Mishra, A., Sutherland, B. A., O'Farrell, F. M., Buchan, A. M., Lauritzen, M., & Attwell, D. (2014). Capillary pericytes regulate cerebral blood flow in health and disease. *Nature*, *508*(7494), 55–60. <https://doi.org/10.1038/nature13165>
- Hammer, J., Alvestad, S., Osen, K. K., Skare, Ø., Sonnewald, U., & Ottersen, O. P. (2008). Expression of glutamine synthetase and glutamate dehydrogenase in the latent phase and chronic phase in the kainate model of temporal lobe epilepsy. *Glia*, *56*(8), 856–868. <https://doi.org/10.1002/glia.20659>
- Hanisch, U.-K., & Kettenmann, H. (2007). Microglia: Active sensor and versatile effector cells in the normal and pathologic brain. *Nature Neuroscience*, *10*(11), 1387–1394. <https://doi.org/10.1038/nn1997>
- Harms, A., S., Cao, S., Rowse, A., L., Thome, A., D., Xinru, L., Mangieri, L., R., Cron, R., Q., Shacka, J., J., Raman, C., & Standaert, D., G. (2013). MHCII Is Required for α -Synuclein-Induced Activation of Microglia, CD4 T Cell Proliferation, and Dopaminergic Neurodegeneration. *The Journal of Neuroscience*, *33*(23), 9592–9600. <https://doi.org/10.1523/JNEUROSCI.5610-12.2013>
- Haynes, S. E., Hollopeter, G., Yang, G., Kurpius, D., Dailey, M. E., Gan, W.-B., & Julius, D. (2006). The P2Y₁₂ receptor regulates microglial activation by extracellular nucleotides. *Nature Neuroscience*, *9*(12), 1512–1519. <https://doi.org/10.1038/nn1805>
- Heinemann, U., Lux, H. D., & Gutnick, M. J. (1977). Extracellular free calcium and potassium during paroxysmal activity in the cerebral cortex of the cat. *Experimental Brain Research*, *27*(3), 237-243. <https://doi.org/10.1007/BF00235500>
- Heneka, M. T., Kummer, M. P., & Latz, E. (2014). Innate immune activation in neurodegenerative disease. *Nature Reviews Immunology*, *14*(7), 463–477. <https://doi.org/10.1038/nri3705>

- Heneka, M. T., Kummer, M. P., Stutz, A., Delekate, A., Schwartz, S., Vieira-Saecker, A., Griep, A., Axt, D., Remus, A., Tzeng, T.-C., Gelpi, E., Halle, A., Korte, M., Latz, E., & Golenbock, D. T. (2013). NLRP3 is activated in Alzheimer's disease and contributes to pathology in APP/PS1 mice. *Nature*, *493*(7434), 674–678. <https://doi.org/10.1038/nature11729>
- Henneberger, C. (2017). Does rapid and physiological astrocyte-neuron signalling amplify epileptic activity?: Do astrocytes amplify epileptic activity? *The Journal of Physiology*, *595*(6), 1917–1927. <https://doi.org/10.1113/JP271958>
- Henneberger, C., Papouin, T., Oliet, S. H. R., & Rusakov, D. A. (2010). Long-term potentiation depends on release of d-serine from astrocytes. *Nature*, *463*(7278), 232–236. <https://doi.org/10.1038/nature08673>
- Henning, L., Antony, H., Breuer, A., Müller, J., Seifert, G., Audinat, E., Singh, P., Brosseron, F., Heneka, M. T., Steinhäuser, C., & Bedner, P. (2022). Reactive microglia are the major source of tumor necrosis factor alpha and contribute to astrocyte dysfunction and acute seizures in experimental temporal lobe epilepsy. *Glia*. Advance online publication. <https://doi.org/10.1002/glia.24265>
- Henning, L., Steinhäuser, C., & Bedner, P. (2021). Initiation of Experimental Temporal Lobe Epilepsy by Early Astrocyte Uncoupling Is Independent of TGFβR1/ALK5 Signaling. *Frontiers in Neurology*, *12*, 660591. <https://doi.org/10.3389/fneur.2021.660591>
- Hertz, L., Xu, J., Song, D., Yan, E., Gu, L., & Peng, L. (2013). Astrocytic and neuronal accumulation of elevated extracellular K⁺ with a 2/3 K⁺/Na⁺ flux ratio—Consequences for energy metabolism, osmolarity and higher brain function. *Frontiers in Computational Neuroscience*, *7*, 114. <https://doi.org/10.3389/fncom.2013.00114>
- Hickman, S. E., Kingery, N. D., Ohsumi, T. K., Borowsky, M. L., Wang, L., Means, T. K., & El Khoury, J. (2013). The microglial sensome revealed by direct RNA sequencing. *Nature Neuroscience*, *16*(12), 1896–1905. <https://doi.org/10.1038/nn.3554>

- Hinterkeuser, S., Schröder, W., Hager, G., Seifert, G., Blümcke, I., Elger, C. E., Schramm, J., & Steinhäuser, C. (2000). Astrocytes in the hippocampus of patients with temporal lobe epilepsy display changes in potassium conductances: Patch-clamp analysis of astrocytes in human brain. *European Journal of Neuroscience*, *12*(6), 2087–2096. <https://doi.org/10.1046/j.1460-9568.2000.00104.x>
- Hol, E. M., & Pekny, M. (2015). Glial fibrillary acidic protein (GFAP) and the astrocyte intermediate filament system in diseases of the central nervous system. *Current Opinion in Cell Biology*, *32*, 121–130. <https://doi.org/10.1016/j.ceb.2015.02.004>
- Hösli, L., Binini, N., Ferrari, K. D., Thieren, L., Looser, Z. J., Zuend, M., Zanker, H. S., Berry, S., Holub, M., Möbius, W., Ruhwedel, T., Nave, K.-A., Giaume, C., Weber, B., & Saab, A. S. (2022). Decoupling astrocytes in adult mice impairs synaptic plasticity and spatial learning. *Cell Reports*, *38*(10), 110484. <https://doi.org/10.1016/j.celrep.2022.110484>
- Huang, W.-Y., Lai, Y.-L., Liu, K.-H., Lin, S., Chen, H.-Y., Liang, C.-H., Wu, H.-M., & Hsu, K.-S. (2022). TNF α -mediated necroptosis in brain endothelial cells as a potential mechanism of increased seizure susceptibility in mice following systemic inflammation. *Journal of Neuroinflammation*, *19*(1), 29. <https://doi.org/10.1186/s12974-022-02406-0>
- Iadecola, C. (2004). Neurovascular regulation in the normal brain and in Alzheimer's disease. *Nature Reviews Neuroscience*, *5*(5), 347–360. <https://doi.org/10.1038/nrn1387>
- Ivens, S., Kaufer, D., Flores, L. P., Bechmann, I., Zumsteg, D., Tomkins, O., Seiffert, E., Heinemann, U., & Friedman, A. (2007). TGF- receptor-mediated albumin uptake into astrocytes is involved in neocortical epileptogenesis. *Brain*, *130*(2), 535–547. <https://doi.org/10.1093/brain/awl317>
- Janigro, D., & Walker, M. C. (2014). What Non-neuronal Mechanisms Should Be Studied to Understand Epileptic Seizures? In H. E. Scharfman & P. S. Buckmaster (Hrsg.), *Issues*

- in Clinical Epileptology: A View from the Bench* (Bd. 813, S. 253–264). Springer Netherlands. https://doi.org/10.1007/978-94-017-8914-1_20
- Jefferys, J., Steinhäuser, C., & Bedner, P. (2016). Chemically-induced TLE models: Topical application. *Journal of Neuroscience Methods*, *260*, 53–61. <https://doi.org/10.1016/j.jneumeth.2015.04.011>
- Jurga, A. M., Paleczna, M., & Kuter, K. Z. (2020). Overview of General and Discriminating Markers of Differential Microglia Phenotypes. *Frontiers in Cellular Neuroscience*, *14*, 198. <https://doi.org/10.3389/fncel.2020.00198>
- Kanner, A. M., & Bicchi, M. M. (2022). Antiseizure Medications for Adults With Epilepsy: A Review. *JAMA*, *327*(13), 1269. <https://doi.org/10.1001/jama.2022.3880>
- Käufer, C., Chhatbar, C., Bröer, S., Walzl, I., Ghita, L., Gerhauser, I., Kalinke, U., & Löscher, W. (2018). Chemokine receptors CCR2 and CX3CR1 regulate viral encephalitis-induced hippocampal damage but not seizures. *Proceedings of the National Academy of Sciences*, *115*(38). <https://doi.org/10.1073/pnas.1806754115>
- Khakh, B. S., & Sofroniew, M. V. (2015). Diversity of astrocyte functions and phenotypes in neural circuits. *Nature Neuroscience*, *18*(7), 942–952. <https://doi.org/10.1038/nn.4043>
- Kirkman, N. J., Libbey, J. E., Wilcox, K. S., White, H. S., & Fujinami, R. S. (2010). Innate but not adaptive immune responses contribute to behavioral seizures following viral infection. *Epilepsia*, *51*(3), 454–464. <https://doi.org/10.1111/j.1528-1167.2009.02390.x>
- Kobayashi, K., Imagama, S., Ohgomori, T., Hirano, K., Uchimura, K., Sakamoto, K., Hirakawa, A., Takeuchi, H., Suzumura, A., Ishiguro, N., & Kadomatsu, K. (2013). Minocycline selectively inhibits M1 polarization of microglia. *Cell Death & Disease*, *4*(3), e525–e525. <https://doi.org/10.1038/cddis.2013.54>
- Kofuji, P., & Newman, E. A. (2004). Potassium buffering in the central nervous system. *Neuroscience*, *129*(4), 1043–1054. <https://doi.org/10.1016/j.neuroscience.2004.06.008>

- Kramer, K., Schaudien, D., Eisel, U. L. M., Herzog, S., Richt, J. A., Baumgärtner, W., & Herden, C. (2012). TNF-Overexpression in Borna Disease Virus-Infected Mouse Brains Triggers Inflammatory Reaction and Epileptic Seizures. *PLoS ONE*, 7(7), e41476. <https://doi.org/10.1371/journal.pone.0041476>
- Lachos, J., Zattoni, M., Wieser, H.-G., Fritschy, J.-M., Langmann, T., Schmitz, G., Errede, M., Virgintino, D., Yonekawa, Y., & Frei, K. (2011). Characterization of the Gene Expression Profile of Human Hippocampus in Mesial Temporal Lobe Epilepsy with Hippocampal Sclerosis. *Epilepsy Research and Treatment*, 2011, 1–11. <https://doi.org/10.1155/2011/758407>
- Langer, J., Stephan, J., Theis, M., & Rose, C. R. (2012). Gap junctions mediate intercellular spread of sodium between hippocampal astrocytes in situ. *Glia*, 60(2), 239–252. <https://doi.org/10.1002/glia.21259>
- Lehtimäki, K. A., Peltola, J., Koskikallio, E., Keränen, T., & Honkaniemi, J. (2003). Expression of cytokines and cytokine receptors in the rat brain after kainic acid-induced seizures. *Molecular Brain Research*, 110(2), 253–260. [https://doi.org/10.1016/S0169-328X\(02\)00654-X](https://doi.org/10.1016/S0169-328X(02)00654-X)
- Li, Q., & Barres, B. A. (2018). Microglia and macrophages in brain homeostasis and disease. *Nature Reviews Immunology*, 18(4), 225–242. <https://doi.org/10.1038/nri.2017.125>
- Librizzi, L., Noè, F., Vezzani, A., de Curtis, M., & Ravizza, T. (2012). Seizure-induced brain-borne inflammation sustains seizure recurrence and blood–brain barrier damage. *Annals of Neurology*, 72(1), 82–90. <https://doi.org/10.1002/ana.23567>
- Liddel, S. A., & Barres, B. A. (2017). Reactive Astrocytes: Production, Function, and Therapeutic Potential. *Immunity*, 46(6), 957–967. <https://doi.org/10.1016/j.immuni.2017.06.006>
- Liddel, S. A., Guttenplan, K. A., Clarke, L. E., Bennett, F. C., Bohlen, C. J., Schirmer, L., Bennett, M. L., Münch, A. E., Chung, W.-S., Peterson, T. C., Wilton, D. K., Frouin,

- A., Napier, B. A., Panicker, N., Kumar, M., Buckwalter, M. S., Rowitch, D. H., Dawson, V. L., Dawson, T. M., ... Barres, B. A. (2017). Neurotoxic reactive astrocytes are induced by activated microglia. *Nature*, *541*(7638), 481–487.
<https://doi.org/10.1038/nature21029>
- Lieberman, A. P., Pitha, P. M., Shin, H. S., & Shin, M. L. (1989). Production of tumor necrosis factor and other cytokines by astrocytes stimulated with lipopolysaccharide or a neurotropic virus. *Proceedings of the National Academy of Sciences*, *86*(16), 6348-6352. <https://doi.org/10.1073/pnas.86.16.6348>
- Liu, J. Y. W., Dzurova, N., Al-Kaaby, B., Mills, K., Sisodiya, S. M., & Thom, M. (2020). Granule Cell Dispersion in Human Temporal Lobe Epilepsy: Proteomics Investigation of Neurodevelopmental Migratory Pathways. *Frontiers in Cellular Neuroscience*, *14*, 53. <https://doi.org/10.3389/fncel.2020.00053>
- Löscher, W., & Brandt, C. (2010). Prevention or Modification of Epileptogenesis after Brain Insults: Experimental Approaches and Translational Research. *Pharmacological Reviews*, *62*(4), 668–700. <https://doi.org/10.1124/pr.110.003046>
- Löscher, W., & Friedman, A. (2020). Structural, Molecular, and Functional Alterations of the Blood-Brain Barrier during Epileptogenesis and Epilepsy: A Cause, Consequence, or Both? *International Journal of Molecular Sciences*, *21*(2), 591.
<https://doi.org/10.3390/ijms21020591>
- Löscher, W., Klitgaard, H., Twyman, R. E., & Schmidt, D. (2013). New avenues for anti-epileptic drug discovery and development. *Nature Reviews Drug Discovery*, *12*(10), 757–776. <https://doi.org/10.1038/nrd4126>
- Löscher, W., Potschka, H., Sisodiya, S. M., & Vezzani, A. (2020). Drug Resistance in Epilepsy: Clinical Impact, Potential Mechanisms, and New Innovative Treatment Options. *Pharmacological Reviews*, *72*(3), 606–638.
<https://doi.org/10.1124/pr.120.019539>

- Lutz, S. E., Zhao, Y., Gulinello, M., Lee, S. C., Raine, C. S., & Brosnan, C. F. (2009). Deletion of Astrocyte Connexins 43 and 30 Leads to a Dysmyelinating Phenotype and Hippocampal CA1 Vacuolation. *Journal of Neuroscience*, *29*(24), 7743–7752. <https://doi.org/10.1523/JNEUROSCI.0341-09.2009>
- Ma, B., Buckalew, R., Du, Y., Kiyoshi, C. M., Alford, C. C., Wang, W., McTigue, D. M., Enyeart, J. J., Terman, D., & Zhou, M. (2016). Gap junction coupling confers isopotentiality on astrocyte syncytium. *Glia*, *64*(2), 214–226. <https://doi.org/10.1002/glia.22924>
- Madry, C., Kyrargyri, V., Arancibia-Cárcamo, I. L., Jolivet, R., Kohsaka, S., Bryan, R. M., & Attwell, D. (2018). Microglial Ramification, Surveillance, and Interleukin-1 β Release Are Regulated by the Two-Pore Domain K⁺ Channel THIK-1. *Neuron*, *97*(2), 299–312. <https://doi.org/10.1016/j.neuron.2017.12.002>
- Mantovani, A., Sica, A., & Locati, M. (2005). Macrophage Polarization Comes of Age. *Immunity*, *23*(4), 344–346. <https://doi.org/10.1016/j.immuni.2005.10.001>
- Marchi, N., Betto, G., Fazio, V., Fan, Q., Ghosh, C., Machado, A., & Janigro, D. (2009). Blood-brain barrier damage and brain penetration of antiepileptic drugs: Role of serum proteins and brain edema. *Epilepsia*, *50*(4), 664–677. <https://doi.org/10.1111/j.1528-1167.2008.01989.x>
- Márquez-Rosado, L., Solan, J. L., Dunn, C. A., Norris, R. P., & Lampe, P. D. (2012). Connexin43 phosphorylation in brain, cardiac, endothelial and epithelial tissues. *Biochimica et Biophysica Acta (BBA) - Biomembranes*, *1818*(8), 1985–1992. <https://doi.org/10.1016/j.bbamem.2011.07.028>
- McCoy, M. K., & Tansey, M. G. (2008). TNF signaling inhibition in the CNS: Implications for normal brain function and neurodegenerative disease. *Journal of Neuroinflammation*, *5*(1), 1–13. <https://doi.org/10.1186/1742-2094-5-45>

- Même, W., Calvo, C., Froger, N., Ezan, P., Amigou, E., Koulakoff, A., & Giaume, C. (2006). Proinflammatory cytokines released from microglia inhibit gap junctions in astrocytes: Potentiation by β -amyloid. *The FASEB Journal*, *20*(3), 494–496.
<https://doi.org/10.1096/fj.05-4297fje>
- Merlini, M., Rafalski, V. A., Ma, K., Kim, K.-Y., Bushong, E. A., Rios Coronado, P. E., Yan, Z., Mendiola, A. S., Sozmen, E. G., Ryu, J. K., Haberl, M. G., Madany, M., Sampson, D. N., Petersen, M. A., Bardehle, S., Tognatta, R., Dean, T., Acevedo, R. M., Cabriga, B., ... Akassoglou, K. (2021). Microglial Gi-dependent dynamics regulate brain network hyperexcitability. *Nature Neuroscience*, *24*(1), 19–23.
<https://doi.org/10.1038/s41593-020-00756-7>
- Merlot, A. M., Kalinowski, D. S., & Richardson, D. R. (2014). Unraveling the mysteries of serum albumin—more than just a serum protein. *Frontiers in Physiology*, *5*, 299.
<https://doi.org/10.3389/fphys.2014.00299>
- Merry, T. L., Brooks, A. E. S., Masson, S. W., Adams, S. E., Jaiswal, J. K., Jamieson, S. M. F., & Shepherd, P. R. (2020). The CSF1 receptor inhibitor pexidartinib (PLX3397) reduces tissue macrophage levels without affecting glucose homeostasis in mice. *International Journal of Obesity*, *44*(1), 245–253. <https://doi.org/10.1038/s41366-019-0355-7>
- Mihály, A., & Bozóky, B. (1984). Immunohistochemical localization of extravasated serum albumin in the hippocampus of human subjects with partial and generalized epilepsies and epileptiform convulsions. *Acta Neuropathologica*, *65*(1), 25–34.
<https://doi.org/10.1007/BF00689824>
- Milikovsky, D. Z., Ofer, J., Senatorov, V. V., Friedman, A. R., Prager, O., Sheintuch, L., Elazari, N., Veksler, R., Zelig, D., Weissberg, I., Bar-Klein, G., Swissa, E., Hanael, E., Ben-Arie, G., Schefenbauer, O., Kamintsky, L., Saar-Ashkenazy, R., Shelef, I., Shamir, M. H., ... Friedman, A. (2019). Paroxysmal slow cortical activity in

- Alzheimer's disease and epilepsy is associated with blood-brain barrier dysfunction. *Science Translational Medicine*, *11*(521), eaaw8954.
<https://doi.org/10.1126/scitranslmed.aaw8954>
- Minami, M., Kuraishi, Y., & Satoh, M. (1991). Effects of kainic acid on messenger RNA levels of IL-1 β , IL-6, TNF α and LIF in the rat brain. *Biochemical and Biophysical Research Communications*, *176*(2), 593-598. [https://doi.org/10.1016/S0006-291X\(05\)80225-6](https://doi.org/10.1016/S0006-291X(05)80225-6)
- Mishra, A., Reynolds, J. P., Chen, Y., Gourine, A. V., Rusakov, D. A., & Attwell, D. (2016). Astrocytes mediate neurovascular signaling to capillary pericytes but not to arterioles. *Nature Neuroscience*, *19*(12), 1619–1627. <https://doi.org/10.1038/nn.4428>
- Morin-Brureau, M., Milior, G., Royer, J., Chali, F., Le Duigou, C., Savary, E., Blugeon, C., Jourden, L., Akbar, D., Dupont, S., Navarro, V., Baulac, M., Bielle, F., Mathon, B., Clemenceau, S., & Miles, R. (2018). Microglial phenotypes in the human epileptic temporal lobe. *Brain*, *141*(12), 3343–3360. <https://doi.org/10.1093/brain/awy276>
- Morin-Brureau, M., Rigau, V., & Lerner-Natoli, M. (2012). Why and how to target angiogenesis in focal epilepsies. *Epilepsia*, *53*(6), 64–68.
<https://doi.org/10.1111/j.1528-1167.2012.03705.x>
- Müller, J. (2018). *Preservation of Astrocytic Coupling Prevents Epileptogenesis* [Doctoral dissertation, Rheinische Friedrich-Wilhelms-Universität Bonn]. Universitäts- und Landesbibliothek Bonn. <https://bonndoc.ulb.uni-bonn.de/xmlui/handle/20.500.11811/7647>
- Munji, R. N., Soung, A. L., Weiner, G. A., Sohet, F., Semple, B. D., Trivedi, A., Gimlin, K., Kotoda, M., Korai, M., Aydin, S., Batugal, A., Cabangcala, A. C., Schupp, P. G., Oldham, M. C., Hashimoto, T., Noble-Haeusslein, L. J., & Daneman, R. (2019). Profiling the mouse brain endothelial transcriptome in health and disease models

- reveals a core blood–brain barrier dysfunction module. *Nature Neuroscience*, 22(11), 1892–1902. <https://doi.org/10.1038/s41593-019-0497-x>
- Nedergaard, M., Ransom, B., & Goldman, S. A. (2003). New roles for astrocytes: Redefining the functional architecture of the brain. *Trends in Neurosciences*, 26(10), 523–530. <https://doi.org/10.1016/j.tins.2003.08.008>
- Newman, E. A., Frambach, D. A., & Odette, L. L. (1984). Control of Extracellular Potassium Levels by Retinal Glial Cell K⁺ Siphoning. *Science*, 225(4667), 1174–1175. <https://doi.org/10.1126/science.6474173>
- Niemann, P., Schiffer, M., Malan, D., Grünberg, S., Roell, W., Geisen, C., & Fleischmann, B. K. (2022). Generation and Characterization of an Inducible Cx43 Overexpression System in Mouse Embryonic Stem Cells. *Cells*, 11(4), 694. <https://doi.org/10.3390/cells11040694>
- Nikolic, L., Shen, W., Nobili, P., Virenque, A., Ulmann, L., & Audinat, E. (2018). Blocking TNF α -driven astrocyte purinergic signaling restores normal synaptic activity during epileptogenesis. *Glia*, 66(12), 2673–2683. <https://doi.org/10.1002/glia.23519>
- Nimmerjahn, A., Kirchhoff, F., & Helmchen, F. (2005). Resting Microglial Cells Are Highly Dynamic Surveillants of Brain Parenchyma in Vivo. *Science*, 308(5726), 1314–1318. DOI: 10.1126/science.1110647
- Nishioku, T., Matsumoto, J., Dohgu, S., Sumi, N., Miyao, K., Takata, F., Shuto, H., Yamauchi, A., & Kataoka, Y. (2010). Tumor Necrosis Factor- α Mediates the Blood–Brain Barrier Dysfunction Induced by Activated Microglia in Mouse Brain Microvascular Endothelial Cells. *Journal of Pharmacological Sciences*, 112(2), 251–254. <https://doi.org/10.1254/jphs.09292SC>
- Nitsch, C., & Klatzo, I. (1983). Regional patterns of blood-brain barrier breakdown during epileptiform seizures induced by various convulsive agents. *Journal of the*

Neurological Sciences, 59(3), 305–322. [https://doi.org/10.1016/0022-510X\(83\)90016-](https://doi.org/10.1016/0022-510X(83)90016-3)

3

- Oberheim, N. A., Goldman, S. A., & Nedergaard, M. (2012). Heterogeneity of Astrocytic Form and Function. In: Milner, R. (Hrsg.), *Astrocytes. Methods in Molecular Biology*, 814. Humana Press. https://doi.org/10.1007/978-1-61779-452-0_3
- Obermeier, B., Daneman, R., & Ransohoff, R. M. (2013). Development, maintenance and disruption of the blood-brain barrier. *Nature Medicine*, 19(12), 1584–1596. <https://doi.org/10.1038/nm.3407>
- Onodera, M., Meyer, J., Furukawa, K., Hiraoka, Y., Aida, T., Tanaka, K., Tanaka, K. F., Rose, C. R., & Matsui, K. (2021). Exacerbation of Epilepsy by Astrocyte Alkalization and Gap Junction Uncoupling. *The Journal of Neuroscience*, 41(10), 2106–2118. <https://doi.org/10.1523/JNEUROSCI.2365-20.2020>
- Orkand, R. K., Nicholls, J. G., & Kuffler, S. W. (1966). Effect of nerve impulses on the membrane potential of glial cells in the central nervous system of amphibia. *Journal of Neurophysiology*, 29(4), 788–806. <https://doi.org/10.1152/jn.1966.29.4.788>
- Ortinski, P. I., Dong, J., Mungenast, A., Yue, C., Takano, H., Watson, D. J., Haydon, P. G., & Coulter, D. A. (2010). Selective induction of astrocytic gliosis generates deficits in neuronal inhibition. *Nature Neuroscience*, 13(5), 584–591. <https://doi.org/10.1038/nn.2535>
- Pannasch, U., Freche, D., Dallérac, G., Ghézali, G., Escartin, C., Ezan, P., Cohen-Salmon, M., Benchenane, K., Abudara, V., Dufour, A., Lübke, J. H. R., Déglon, N., Knott, G., Holcman, D., & Rouach, N. (2014). Connexin 30 sets synaptic strength by controlling astroglial synapse invasion. *Nature Neuroscience*, 17(4), 549–558. <https://doi.org/10.1038/nn.3662>

- Pannasch, U., & Rouach, N. (2013). Emerging role for astroglial networks in information processing: From synapse to behavior. *Trends in Neurosciences*, *36*(7), 405–417. <https://doi.org/10.1016/j.tins.2013.04.004>
- Pannasch, U., Vargová, L., Reingruber, J., Ezan, P., Holcman, D., Giaume, C., Syková, E., & Rouach, N. (2011). Astroglial networks scale synaptic activity and plasticity. *Proceedings of the National Academy of Sciences*, *108*(20), 8467–8472. <https://doi.org/10.1073/pnas.1016650108>
- Paolicelli, R. C., Bolasco, G., Pagani, F., Maggi, L., Scianni, M., Panzanelli, P., Giustetto, M., Ferreira, T. A., Guiducci, E., Dumas, L., Ragozzino, D., & Gross, C. T. (2011). Synaptic Pruning by Microglia Is Necessary for Normal Brain Development. *Science*, *333*(6048), 1456–1458. <https://doi.org/10.1126/science.1202529>
- Parker, E., Aboghazleh, R., Mumby, G., Veksler, R., Ofer, J., Newton, J., Smith, R., Kamintsky, L., Jones, C. M. A., O’Keeffe, E., Kelly, E., Doelle, K., Roach, I., Yang, L. T., Moradi, P., Lin, J. M., Gleason, A. J., Atkinson, C., Bowen, C., ... Friedman, A. (2022). Concussion susceptibility is mediated by spreading depolarization-induced neurovascular dysfunction. *Brain*, *145*(6), 2049–2063. <https://doi.org/10.1093/brain/awab450>
- Parkhurst, C. N., Yang, G., Ninan, I., Savas, J. N., Yates, J. R., Lafaille, J. J., Hempstead, B. L., Littman, D. R., & Gan, W.-B. (2013). Microglia Promote Learning-Dependent Synapse Formation through Brain-Derived Neurotrophic Factor. *Cell*, *155*(7), 1596–1609. <https://doi.org/10.1016/j.cell.2013.11.030>
- Passlick, S., Rose, C. R., Petzold, G. C., & Henneberger, C. (2021). Disruption of Glutamate Transport and Homeostasis by Acute Metabolic Stress. *Frontiers in Cellular Neuroscience*, *15*, 637784. <https://doi.org/10.3389/fncel.2021.637784>

- Patel, D. C., Tewari, B. P., Chaunsali, L., & Sontheimer, H. (2019). Neuron–glia interactions in the pathophysiology of epilepsy. *Nature Reviews Neuroscience*, *20*(5), 282–297. <https://doi.org/10.1038/s41583-019-0126-4>
- Patel, D. C., Wallis, G., Dahle, E. J., McElroy, P. B., Thomson, K. E., Tesi, R. J., Szymkowski, D. E., West, P. J., Smeal, R. M., Patel, M., Fujinami, R. S., White, H. S., & Wilcox, K. S. (2017). Hippocampal TNF α Signaling Contributes to Seizure Generation in an Infection-Induced Mouse Model of Limbic Epilepsy. *Eneuro*, *4*(2), ENEURO.0105-17.2017. <https://doi.org/10.1523/ENEURO.0105-17.2017>
- Pekny, M., & Wilhelmsson, U. (2006). GFAP and Astrocyte Intermediate Filaments. In A. Lajtha & R. Lim (Hrsg.), *Handbook of Neurochemistry and Molecular Neurobiology: Neuroactive Proteins and Peptides* (S. 289–314). Springer, Boston, MA, US. https://doi.org/10.1007/978-0-387-30381-9_14
- Pellerin, L., & Magistretti, P. J. (1994). Glutamate uptake into astrocytes stimulates aerobic glycolysis: A mechanism coupling neuronal activity to glucose utilization. *Proceedings of the National Academy of Sciences*, *91*(22), 10625–10629. <https://doi.org/10.1073/pnas.91.22.10625>
- Perea, G., Navarrete, M., & Araque, A. (2009). Tripartite synapses: Astrocytes process and control synaptic information. *Trends in Neurosciences*, *32*(8), 421–431. <https://doi.org/10.1016/j.tins.2009.05.001>
- Pernhorst, K., Herms, S., Hoffmann, P., Cichon, S., Schulz, H., Sander, T., Schoch, S., Becker, A. J., & Grote, A. (2013). TLR4, ATF-3 and IL8 inflammation mediator expression correlates with seizure frequency in human epileptic brain tissue. *Seizure*, *22*(8), 675–678. <https://doi.org/10.1016/j.seizure.2013.04.023>
- Perucca, E., Brodie, M. J., Kwan, P., & Tomson, T. (2020). 30 years of second-generation antiseizure medications: Impact and future perspectives. *The Lancet Neurology*, *19*(6), 544–556. [https://doi.org/10.1016/S1474-4422\(20\)30035-1](https://doi.org/10.1016/S1474-4422(20)30035-1)

- Philippot, C., Griemsmann, S., Jabs, R., Seifert, G., Kettenmann, H., & Steinhäuser, C. (2021). Astrocytes and oligodendrocytes in the thalamus jointly maintain synaptic activity by supplying metabolites. *Cell Reports*, *34*(3), 108642. <https://doi.org/10.1016/j.celrep.2020.108642>
- Pitkänen, A. (2010). Therapeutic approaches to epileptogenesis-Hope on the horizon: Treatment of Epileptogenesis. *Epilepsia*, *51*, 2–17. <https://doi.org/10.1111/j.1528-1167.2010.02602.x>
- Pitkänen, A., & Engel, J. (2014). Past and Present Definitions of Epileptogenesis and Its Biomarkers. *Neurotherapeutics*, *11*(2), 231–241. <https://doi.org/10.1007/s13311-014-0257-2>
- Pitsch, J., Kuehn, J. C., Gnatkovsky, V., Müller, J. A., van Loo, K. M. J., de Curtis, M., Vatter, H., Schoch, S., Elger, C. E., & Becker, A. J. (2019). Anti-epileptogenic and Anti-convulsive Effects of Fingolimod in Experimental Temporal Lobe Epilepsy. *Molecular Neurobiology*, *56*(3), 1825–1840. <https://doi.org/10.1007/s12035-018-1181-y>
- Prager, O., Kamintsky, L., Hasam-Henderson, L. A., Schoknecht, K., Wuntke, V., Papageorgiou, I., Swolinsky, J., Muoio, V., Bar-Klein, G., Vazana, U., Heinemann, U., Friedman, A., & Kovács, R. (2019). Seizure-induced microvascular injury is associated with impaired neurovascular coupling and blood–brain barrier dysfunction. *Epilepsia*, *60*(2), 322–336. <https://doi.org/10.1111/epi.14631>
- Prinz, M., Jung, S., & Priller, J. (2019). Microglia Biology: One Century of Evolving Concepts. *Cell*, *179*(2), 292–311. <https://doi.org/10.1016/j.cell.2019.08.053>
- Probert, L., Akassoglou, K., Pasparakis, M., Kontogeorgost, G., & Kollias, G. (1995). Spontaneous inflammatory demyelinating disease in transgenic mice showing central nervous system-specific expression of tumor necrosis factor α . *Proceedings of the*

National Academy of Sciences, 92(24), 11294–11298.

<https://doi.org/10.1073/pnas.92.24.11294>

Proper, E. A., Hoogland, G., Kappen, S. M., Jansen, G. H., Rensen, M. G. A., Schrama, L. H., van Veelen, C. W. M., van Rijen, P. C., van Nieuwenhuizen, O., Gispen, W. H., & de Graan, P. N. E. (2002). Distribution of glutamate transporters in the hippocampus of patients with pharmaco-resistant temporal lobe epilepsy. *Brain*, 125(1), 32–43.

<https://doi.org/10.1093/brain/awf001>

Qin, C., Zhou, L.-Q., Ma, X.-T., Hu, Z.-W., Yang, S., Chen, M., Bosco, D. B., Wu, L.-J., & Tian, D.-S. (2019). Dual Functions of Microglia in Ischemic Stroke. *Neuroscience Bulletin*, 35(5), 921–933. <https://doi.org/10.1007/s12264-019-00388-3>

Rabender, C., Mezzaroma, E., Mauro, A. G., Mullangi, R., Abbate, A., Anscher, M., Hart, B., & Mikkelsen, R. (2016). IPW-5371 Proves Effective as a Radiation Countermeasure by Mitigating Radiation-Induced Late Effects. *Radiation Research*, 186(5), 478–488.

<https://doi.org/10.1667/RR14403.2>

Ralay Ranaivo, H., & Wainwright, M. S. (2010). Albumin activates astrocytes and microglia through mitogen-activated protein kinase pathways. *Brain Research*, 1313, 222–231.

<https://doi.org/10.1016/j.brainres.2009.11.063>

Rana, A., & Musto, A. E. (2018). The role of inflammation in the development of epilepsy.

Journal of Neuroinflammation, 15(1), 144. <https://doi.org/10.1186/s12974-018-1192-7>

Rappold, P. M., Lynd-Balta, E., & Joseph, S. A. (2006). P2X7 receptor immunoreactive profile confined to resting and activated microglia in the epileptic brain. *Brain Research*, 1089(1), 171–178.

<https://doi.org/10.1016/j.brainres.2006.03.040>

Rayaprolu, S., Mullen, B., Baker, M., Lynch, T., Finger, E., Seeley, W. W., Hatanpaa, K. J., Lomen-Hoerth, C., Kertesz, A., Bigio, E. H., Lippa, C., Josephs, K. A., Knopman, D. S., White, C. L., Caselli, R., Mackenzie, I. R., Miller, B. L., Boczarska-Jedynak, M., Opala, G., ... Ross, O. A. (2013). TREM2 in neurodegeneration: Evidence for

- association of the p.R47H variant with frontotemporal dementia and Parkinson's disease. *Molecular Neurodegeneration*, 8(1), 19. <https://doi.org/10.1186/1750-1326-8-19>
- Rempe, R. G., Hartz, A. M. S., Soldner, E. L. B., Sokola, B. S., Alluri, S. R., Abner, E. L., Kryscio, R. J., Pekcec, A., Schlichtiger, J., & Bauer, B. (2018). Matrix Metalloproteinase-Mediated Blood-Brain Barrier Dysfunction in Epilepsy. *The Journal of Neuroscience*, 38(18), 4301–4315. <https://doi.org/10.1523/JNEUROSCI.2751-17.2018>
- Robel, S., Buckingham, S. C., Boni, J. L., Campbell, S. L., Danbolt, N. C., Riedemann, T., Sutor, B., & Sontheimer, H. (2015). Reactive Astrogliosis Causes the Development of Spontaneous Seizures. *Journal of Neuroscience*, 35(8), 3330–3345. <https://doi.org/10.1523/JNEUROSCI.1574-14.2015>
- Rock, R. B., Gekker, G., Hu, S., Sheng, W. S., Cheeran, M., Lokensgard, J. R., & Peterson, P. K. (2004). Role of Microglia in Central Nervous System Infections. *Clinical Microbiology Reviews*, 17(4), 942–964. <https://doi.org/10.1128/CMR.17.4.942-964.2004>
- Rose, C. R., Felix, L., Zeug, A., Dietrich, D., Reiner, A., & Henneberger, C. (2018). Astroglial Glutamate Signaling and Uptake in the Hippocampus. *Frontiers in Molecular Neuroscience*, 10, 451. <https://doi.org/10.3389/fnmol.2017.00451>
- Rouach, N., Koulakoff, A., Abudara, V., Willecke, K., & Giaume, C. (2008). Astroglial Metabolic Networks Sustain Hippocampal Synaptic Transmission. *Science*, 322(5907), 1551–1555. <https://doi.org/10.1126/science.1164022>
- Rüber, T., David, B., Lüchters, G., Nass, R. D., Friedman, A., Surges, R., Stöcker, T., Weber, B., Deichmann, R., Schlaug, G., Hattingen, E., & Elger, C. E. (2018). Evidence for peri-ictal blood–brain barrier dysfunction in patients with epilepsy. *Brain*, 141(10), 2952–2965. <https://doi.org/10.1093/brain/awy242>

- Rusina, E., Bernard, C., & Williamson, A. (2021). The Kainic Acid Models of Temporal Lobe Epilepsy. *Eneuro*, 8(2). <https://doi.org/10.1523/ENEURO.0337-20.2021>
- Salar, S., Maslarova, A., Lippmann, K., Nichtweiss, J., Weissberg, I., Sheintuch, L., Kunz, W. S., Shorer, Z., Friedman, A., & Heinemann, U. (2014). Blood-brain barrier dysfunction can contribute to pharmacoresistance of seizures. *Epilepsia*, 55(8), 1255–1263. <https://doi.org/10.1111/epi.12713>
- Sanchez, J. M. S., DePaula-Silva, A. B., Doty, D. J., Truong, A., Libbey, J. E., & Fujinami, R. S. (2019). Microglial cell depletion is fatal with low level picornavirus infection of the central nervous system. *Journal of NeuroVirology*, 25(3), 415–421. <https://doi.org/10.1007/s13365-019-00740-3>
- Sano, F., Shigetomi, E., Shinozaki, Y., Tsuzuki-yama, H., Saito, K., Mikoshiba, K., Horiuchi, H., Cheung, D. L., Nabekura, J., Sugita, K., Aihara, M., & Koizumi, S. (2021). Reactive astrocyte-driven epileptogenesis is induced by microglia initially activated following status epilepticus. *JCI Insight*, 6(9), e135391. <https://doi.org/10.1172/jci.insight.135391>
- Santello, M., Bezzi, P., & Volterra, A. (2011). TNF α Controls Glutamatergic Gliotransmission in the Hippocampal Dentate Gyrus. *Neuron*, 69(5), 988–1001. <https://doi.org/10.1016/j.neuron.2011.02.003>
- Santello, M., Toni, N., & Volterra, A. (2019). Astrocyte function from information processing to cognition and cognitive impairment. *Nature Neuroscience*, 22(2), 154–166. <https://doi.org/10.1038/s41593-018-0325-8>
- Santello, M., & Volterra, A. (2012). TNF α in synaptic function: Switching gears. *Trends in Neurosciences*, 35(10), 638–647. <https://doi.org/10.1016/j.tins.2012.06.001>
- Scemes, E., & Giaume, C. (2006). Astrocyte calcium waves: What they are and what they do. *Glia*, 54(7), 716–725. <https://doi.org/10.1002/glia.20374>

- Schafer, D. P., Lehrman, E. K., Kautzman, A. G., Koyama, R., Mardinly, A. R., Yamasaki, R., Ransohoff, R. M., Greenberg, M. E., Barres, B. A., & Stevens, B. (2012). Microglia Sculpt Postnatal Neural Circuits in an Activity and Complement-Dependent Manner. *Neuron*, *74*(4), 691–705. <https://doi.org/10.1016/j.neuron.2012.03.026>
- Scheffer, I. E., Berkovic, S., Capovilla, G., Connolly, M. B., French, J., Guilhoto, L., Hirsch, E., Jain, S., Mathern, G. W., Moshé, S. L., Nordli, D. R., Perucca, E., Tomson, T., Wiebe, S., Zhang, Y., & Zuberi, S. M. (2017). ILAE classification of the epilepsies: Position paper of the ILAE Commission for Classification and Terminology. *Epilepsia*, *58*(4), 512–521. <https://doi.org/10.1111/epi.13709>
- Seiffert, E. (2004). Lasting Blood-Brain Barrier Disruption Induces Epileptic Focus in the Rat Somatosensory Cortex. *Journal of Neuroscience*, *24*(36), 7829–7836. <https://doi.org/10.1523/JNEUROSCI.1751-04.2004>
- Senatorov, V. V., Friedman, A. R., Milikovsky, D. Z., Ofer, J., Saar-Ashkenazy, R., Charbash, A., Jahan, N., Chin, G., Mihaly, E., Lin, J. M., Ramsay, H. J., Moghbel, A., Preininger, M. K., Eddings, C. R., Harrison, H. V., Patel, R., Shen, Y., Ghanim, H., Sheng, H., ... Kaufer, D. (2019). Blood-brain barrier dysfunction in aging induces hyperactivation of TGF β signaling and chronic yet reversible neural dysfunction. *Science Translational Medicine*, *11*(521), eaaw8283. <https://doi.org/10.1126/scitranslmed.aaw8283>
- Shapiro, L. A., Wang, L., & Ribak, C. E. (2008). Rapid astrocyte and microglial activation following pilocarpine-induced seizures in rats: Rapid Seizure-induced Glial Activation. *Epilepsia*, *49*, 33–41. <https://doi.org/10.1111/j.1528-1167.2008.01491.x>
- Shlosberg, D., Benifla, M., Kaufer, D., & Friedman, A. (2010). Blood–brain barrier breakdown as a therapeutic target in traumatic brain injury. *Nature Reviews Neurology*, *6*(7), 393–403. <https://doi.org/10.1038/nrneurol.2010.74>

- Sierra, A., Paolicelli, R. C., & Kettenmann, H. (2019). Cien Años de Microglía: Milestones in a Century of Microglial Research. *Trends in Neurosciences*, *42*(11), 778–792.
<https://doi.org/10.1016/j.tins.2019.09.004>
- Solan, J. L., & Lampe, P. D. (2020). Src Regulation of Cx43 Phosphorylation and Gap Junction Turnover. *Biomolecules*, *10*(12), 1596.
<https://doi.org/10.3390/biom10121596>
- Srivastava, P. K., van Eyll, J., Godard, P., Mazzuferi, M., Delahaye-Duriez, A., Van Steenwinckel, J., Gressens, P., Danis, B., Vandenplas, C., Foerch, P., Leclercq, K., Mairet-Coello, G., Cardenas, A., Vanclef, F., Laaniste, L., Niespodziany, I., Keaney, J., Gasser, J., Gillet, G., ... Johnson, M. R. (2018). A systems-level framework for drug discovery identifies Csf1R as an anti-epileptic drug target. *Nature Communications*, *9*(1), 3561. <https://doi.org/10.1038/s41467-018-06008-4>
- Steed, P. M., Tansey, M. G., Zalevsky, J., Zhukovsky, E. A., Desjarlais, J. R., Szymkowski, D. E., Abbott, C., Carmichael, D., Chan, C., Cherry, L., Cheung, P., Chirino, A. J., Chung, H. H., Doberstein, S. K., Eivazi, A., Filikov, A. V., Gao, S. X., Hubert, R. S., Hwang, M., ... Dahiyat, B. I. (2003). Inactivation of TNF Signaling by Rationally Designed Dominant-Negative TNF Variants. *Science*, *301*(5641), 1895–1898.
<https://doi.org/10.1126/science.1081297>
- Steinhäuser, C., Seifert, G., & Bedner, P. (2012). Astrocyte dysfunction in temporal lobe epilepsy: K⁺ channels and gap junction coupling. *Glia*, *60*(8), 1192–1202.
<https://doi.org/10.1002/glia.22313>
- Stephan, J., Eitelmann, S., & Zhou, M. (2021). Approaches to Study Gap Junctional Coupling. *Frontiers in Cellular Neuroscience*, *15*, 640406.
<https://doi.org/10.3389/fncel.2021.640406>
- Stevens, B., Allen, N. J., Vazquez, L. E., Howell, G. R., Christopherson, K. S., Nouri, N., Micheva, K. D., Mehalow, A. K., Huberman, A. D., Stafford, B., Sher, A., Litke, A.

- M., Lambris, J. D., Smith, S. J., John, S. W. M., & Barres, B. A. (2007). The Classical Complement Cascade Mediates CNS Synapse Elimination. *Cell*, *131*(6), 1164–1178.
<https://doi.org/10.1016/j.cell.2007.10.036>
- Sun, W., Cornwell, A., Li, J., Peng, S., Osorio, M. J., Aalling, N., Wang, S., Benraiss, A., Lou, N., Goldman, S. A., & Nedergaard, M. (2017). SOX9 Is an Astrocyte-Specific Nuclear Marker in the Adult Brain Outside the Neurogenic Regions. *The Journal of Neuroscience*, *37*(17), 4493–4507. <https://doi.org/10.1523/JNEUROSCI.3199-16.2017>
- Swamy, M., Yusof, W. R. W., Sirajudeen, K. N. S., Mustapha, Z., & Govindasamy, C. (2011). Decreased glutamine synthetase, increased citrulline–nitric oxide cycle activities, and oxidative stress in different regions of brain in epilepsy rat model. *Journal of Physiology and Biochemistry*, *67*(1), 105–113.
<https://doi.org/10.1007/s13105-010-0054-2>
- Sweeney, M. D., Zhao, Z., Montagne, A., Nelson, A. R., & Zlokovic, B. V. (2019). Blood-Brain Barrier: From Physiology to Disease and Back. *Physiological Reviews*, *99*(1), 21–78. <https://doi.org/10.1152/physrev.00050.2017>
- Sypert, G. W., & Ward, A. A. (1974). Changes in extracellular potassium activity during neocortical propagated seizures. *Experimental Neurology*, *45*(1), 19–41.
[https://doi.org/10.1016/0014-4886\(74\)90097-1](https://doi.org/10.1016/0014-4886(74)90097-1)
- Tatum IV, W. O. (2012). Mesial Temporal Lobe Epilepsy. *Journal of Clinical Neurophysiology*, *29*(5), 356-365. doi: 10.1097/WNP.0b013e31826b3ab7
- Tchekalarova, J. D., Ivanova, N. M., Pechlivanova, D. M., Atanasova, D., Lazarov, N., Kortenska, L., Mitreva, R., Lozanov, V., & Stoynev, A. (2014). Antiepileptogenic and neuroprotective effects of losartan in kainate model of temporal lobe epilepsy. *Pharmacology Biochemistry and Behavior*, *127*, 27–36.
<https://doi.org/10.1016/j.pbb.2014.10.005>

- Therajaran, P., Hamilton, J. A., O'Brien, T. J., Jones, N. C., & Ali, I. (2020). Microglial polarization in posttraumatic epilepsy: Potential mechanism and treatment opportunity. *Epilepsia*, *61*(2), 203–215. <https://doi.org/10.1111/epi.16424>
- Thévenin, A. F., Kowal, T. J., Fong, J. T., Kells, R. M., Fisher, C. G., & Falk, M. M. (2013). Proteins and Mechanisms Regulating Gap-Junction Assembly, Internalization, and Degradation. *Physiology*, *28*(2), 93–116. <https://doi.org/10.1152/physiol.00038.2012>
- Thom, M. (2014). Review: Hippocampal sclerosis in epilepsy: a neuropathology review: Hippocampal sclerosis in epilepsy. *Neuropathology and Applied Neurobiology*, *40*(5), 520–543. <https://doi.org/10.1111/nan.12150>
- Tremblay, M.-È., Lowery, R. L., & Majewska, A. K. (2010). Microglial Interactions with Synapses Are Modulated by Visual Experience. *PLoS Biology*, *8*(11), e1000527. <https://doi.org/10.1371/journal.pbio.1000527>
- Vainchtein, I. D., Chin, G., Cho, F. S., Kelley, K. W., Miller, J. G., Chien, E. C., Liddelow, S. A., Nguyen, P. T., Nakao-Inoue, H., Dorman, L. C., Akil, O., Joshita, S., Barres, B. A., Paz, J. T., Molofsky, A. B., & Molofsky, A. V. (2018). Astrocyte-derived interleukin-33 promotes microglial synapse engulfment and neural circuit development. *Science*, *359*(6381), 1269–1273. <https://doi.org/10.1126/science.aal3589>
- van Gassen, K. L. I., de Wit, M., Koerkamp, M. J. A. G., Rensen, M. G. A., van Rijen, P. C., Holstege, F. C. P., Lindhout, D., & de Graan, P. N. E. (2008). Possible role of the innate immunity in temporal lobe epilepsy. *Epilepsia*, *49*(6), 1055–1065. <https://doi.org/10.1111/j.1528-1167.2007.01470.x>
- van Vliet, E. A., Aronica, E., & Gorter, J. A. (2015). Blood–brain barrier dysfunction, seizures and epilepsy. *Seminars in Cell & Developmental Biology*, *38*, 26–34. <https://doi.org/10.1016/j.semcdb.2014.10.003>

- van Vliet, E. A., da Costa Araujo, S., Redeker, S., van Schaik, R., Aronica, E., & Gorter, J. A. (2007). Blood-brain barrier leakage may lead to progression of temporal lobe epilepsy. *Brain*, *130*(2), 521–534. <https://doi.org/10.1093/brain/awl318>
- Varvel, N. H., Neher, J. J., Bosch, A., Wang, W., Ransohoff, R. M., Miller, R. J., & Dingledine, R. (2016). Infiltrating monocytes promote brain inflammation and exacerbate neuronal damage after status epilepticus. *Proceedings of the National Academy of Sciences*, *113*(38), E5665–E5674. <https://doi.org/10.1073/pnas.1604263113>
- Verkhatsky, A., Ho, M. S., Zorec, R., & Parpura, V. (Hrsg.). (2019). *Neuroglia in Neurodegenerative Diseases* (Bd. 1175). Springer Singapore. <https://doi.org/10.1007/978-981-13-9913-8>
- Verkhatsky, A., & Nedergaard, M. (2018). Physiology of Astroglia. *Physiol Rev*, *98*(1), 239–389. doi: 10.1152/physrev.00042.2016
- Vezzani, A., Conti, M., Luigi, A. D., Ravizza, T., Moneta, D., Marchesi, F., & Simoni, M. G. D. (1999). Interleukin-1 β Immunoreactivity and Microglia Are Enhanced in the Rat Hippocampus by Focal Kainate Application: Functional Evidence for Enhancement of Electrographic Seizures. *The Journal of Neuroscience*, *19*(12), 5054–65. doi: 10.1523/JNEUROSCI.19-12-05054.1999
- Vezzani, A., French, J., Bartfai, T., & Baram, T. Z. (2011). The role of inflammation in epilepsy. *Nature Reviews Neurology*, *7*(1), 31–40. <https://doi.org/10.1038/nrneurol.2010.178>
- Vezzani, A., Moneta, D., Richichi, C., Aliprandi, M., Burrows, S. J., Ravizza, T., Perego, C., & De Simoni, M. G. (2002). Functional Role of Inflammatory Cytokines and Antiinflammatory Molecules in Seizures and Epileptogenesis. *Epilepsia*, *43*, 30–35. <https://doi.org/10.1046/j.1528-1157.43.s.5.14.x>

- Virchow, R. (2010). *Die Cellularpathologie in ihrer Begründung auf physiologische und pathologische Gewebelehre*. Philipps-Universität Marburg.
<https://doi.org/10.17192/eb2010.0274> (Original work published 1858)
- Virchow, R. (2013). *Gesammelte Abhandlungen zur wissenschaftlichen Medicin: Mit 3 Tafeln und 45 Holzschnitten*. Philipps-Universität Marburg.
<https://doi.org/10.17192/eb2013.0012> (Original work published 1856)
- Wallraff, A., Köhling, R., Heinemann, U., Theis, M., Willecke, K., & Steinhäuser, C. (2006). The Impact of Astrocytic Gap Junctional Coupling on Potassium Buffering in the Hippocampus. *Journal of Neuroscience*, *26*(20), 5438–5447.
<https://doi.org/10.1523/JNEUROSCI.0037-06.2006>
- Waltl, I., Käufer, C., Bröer, S., Chhatbar, C., Ghita, L., Gerhauser, I., Anjum, M., Kalinke, U., & Löscher, W. (2018). Macrophage depletion by liposome-encapsulated clodronate suppresses seizures but not hippocampal damage after acute viral encephalitis. *Neurobiology of Disease*, *110*, 192–205. <https://doi.org/10.1016/j.nbd.2017.12.001>
- Waltl, I., Käufer, C., Gerhauser, I., Chhatbar, C., Ghita, L., Kalinke, U., & Löscher, W. (2018). Microglia have a protective role in viral encephalitis-induced seizure development and hippocampal damage. *Brain, Behavior, and Immunity*, *74*, 186–204.
<https://doi.org/10.1016/j.bbi.2018.09.006>
- Wang, J. S. H., Freitas-Andrade, M., Bechberger, J. F., Naus, C. C., Yeung, K. K.-C., & Whitehead, S. N. (2018). Matrix-assisted laser desorption/ionization imaging mass spectrometry of intraperitoneally injected danegaptide (ZP1609) for treatment of stroke-reperfusion injury in mice. *Rapid Communications in Mass Spectrometry*, *32*(12), 951–958. <https://doi.org/10.1002/rcm.8115>
- Wang, N., Mi, X., Gao, B., Gu, J., Wang, W., Zhang, Y., & Wang, X. (2015). Minocycline inhibits brain inflammation and attenuates spontaneous recurrent seizures following

- pilocarpine-induced status epilepticus. *Neuroscience*, 287, 144–156.
<https://doi.org/10.1016/j.neuroscience.2014.12.021>
- Wang, Q., Wang, W., Aten, S., Kiyoshi, C. M., Du, Y., & Zhou, M. (2020). Epileptiform Neuronal Discharges Impair Astrocyte Syncytial Isopotentiality in Acute Hippocampal Slices. *Brain Sciences*, 10(4), 208.
<https://doi.org/10.3390/brainsci10040208>
- Weinberg, M. S., Blake, B. L., & McCown, T. J. (2013). Opposing actions of hippocampus TNF α receptors on limbic seizure susceptibility. *Experimental Neurology*, 247, 429–437. <https://doi.org/10.1016/j.expneurol.2013.01.011>
- Weissberg, I., Wood, L., Kamintsky, L., Vazquez, O., Milikovsky, D. Z., Alexander, A., Oppenheim, H., Ardizzone, C., Becker, A., Frigerio, F., Vezzani, A., Buckwalter, M. S., Huguenard, J. R., Friedman, A., & Kaufer, D. (2015). Albumin induces excitatory synaptogenesis through astrocytic TGF- β /ALK5 signaling in a model of acquired epilepsy following blood–brain barrier dysfunction. *Neurobiology of Disease*, 78, 115–125. <https://doi.org/10.1016/j.nbd.2015.02.029>
- Wilhelmsson, U., Bushong, E. A., Price, D. L., Smarr, B. L., Phung, V., Terada, M., Ellisman, M. H., & Pekny, M. (2006). Redefining the concept of reactive astrocytes as cells that remain within their unique domains upon reaction to injury. *Proceedings of the National Academy of Sciences*, 103(46), 17513–17518.
<https://doi.org/10.1073/pnas.0602841103>
- Wu, W., Li, Y., Wei, Y., Bosco, D. B., Xie, M., Zhao, M.-G., Richardson, J. R., & Wu, L.-J. (2020). Microglial depletion aggravates the severity of acute and chronic seizures in mice. *Brain, Behavior, and Immunity*, 89, 245–255.
<https://doi.org/10.1016/j.bbi.2020.06.028>

- Wu, Y., Dissing-Olesen, L., MacVicar, B. A., & Stevens, B. (2015). Microglia: Dynamic Mediators of Synapse Development and Plasticity. *Trends in Immunology*, *36*(10), 605–613. <https://doi.org/10.1016/j.it.2015.08.008>
- Wyatt-Johnson, S. K., Sommer, A. L., Shim, K. Y., & Brewster, A. L. (2021). Suppression of Microgliosis With the Colony-Stimulating Factor 1 Receptor Inhibitor PLX3397 Does Not Attenuate Memory Defects During Epileptogenesis in the Rat. *Frontiers in Neurology*, *12*, 651096. <https://doi.org/10.3389/fneur.2021.651096>
- Yamamoto, A., Schindler, C. K., Murphy, B. M., Bellver-Estelles, C., So, N. K., Taki, W., Meller, R., Simon, R. P., & Henshall, D. C. (2006). Evidence of tumor necrosis factor receptor 1 signaling in human temporal lobe epilepsy. *Experimental Neurology*, *202*(2), 410–420. <https://doi.org/10.1016/j.expneurol.2006.07.003>
- Zattoni, M., Mura, M. L., Deprez, F., Schwendener, R. A., Engelhardt, B., Frei, K., & Fritschy, J.-M. (2011). Brain Infiltration of Leukocytes Contributes to the Pathophysiology of Temporal Lobe Epilepsy. *Journal of Neuroscience*, *31*(11), 4037–4050. <https://doi.org/10.1523/JNEUROSCI.6210-10.2011>
- Zhang, B., Gaiteri, C., Bodea, L.-G., Wang, Z., McElwee, J., Podtelezchnikov, A. A., Zhang, C., Xie, T., Tran, L., Dobrin, R., Fluder, E., Clurman, B., Melquist, S., Narayanan, M., Suver, C., Shah, H., Mahajan, M., Gillis, T., Mysore, J., ... Emilsson, V. (2013). Integrated Systems Approach Identifies Genetic Nodes and Networks in Late-Onset Alzheimer's Disease. *Cell*, *153*(3), 707–720. <https://doi.org/10.1016/j.cell.2013.03.030>
- Zhang, Y., & Barres, B. A. (2010). Astrocyte heterogeneity: An underappreciated topic in neurobiology. *Current Opinion in Neurobiology*, *20*(5), 588–594. <https://doi.org/10.1016/j.conb.2010.06.005>
- Zhang, Y., Zhang, M., Zhu, W., Pan, X., Wang, Q., Gao, X., Wang, C., Zhang, X., Liu, Y., Li, S., & Sun, H. (2020). Role of Elevated Thrombospondin-1 in Kainic Acid-Induced

Status Epilepticus. *Neuroscience Bulletin*, 36(3), 263–276.

<https://doi.org/10.1007/s12264-019-00437-x>

Zhang, Y., Zhu, W., Yu, H., Yu, J., Zhang, M., Pan, X., Gao, X., Wang, Q., & Sun, H. (2019).

P2Y4/TSP-1/TGF- β 1/pSmad2/3 pathway contributes to acute generalized seizures induced by kainic acid. *Brain Research Bulletin*, 149, 106–119.

<https://doi.org/10.1016/j.brainresbull.2019.04.004>

Zhao, X., Liao, Y., Morgan, S., Mathur, R., Feustel, P., Mazurkiewicz, J., Qian, J., Chang, J.,

Mathern, G. W., Adamo, M. A., Ritaccio, A. L., Gruenthal, M., Zhu, X., & Huang, Y. (2018). Noninflammatory Changes of Microglia Are Sufficient to Cause Epilepsy.

Cell Reports, 22(8), 2080–2093. <https://doi.org/10.1016/j.celrep.2018.02.004>

Zhao, Z., Nelson, A. R., Betsholtz, C., & Zlokovic, B. V. (2015). Establishment and

Dysfunction of the Blood-Brain Barrier. *Cell*, 163(5), 1064–1078.

<https://doi.org/10.1016/j.cell.2015.10.067>

Zonta, M., Angulo, M. C., Gobbo, S., Rosengarten, B., Hossmann, K.-A., Pozzan, T., &

Carmignoto, G. (2003). Neuron-to-astrocyte signaling is central to the dynamic control of brain microcirculation. *Nature Neuroscience*, 6(1), 43–50.

<https://doi.org/10.1038/nn980>

List of figures

Figure 1. Different subtypes of MTLE-HS according to the ILAE consensus classification.....	3
Figure 2. Overview of TNFR1 (p55) and TNFR2 (p75) signaling pathways	6
Figure 3. Astrocytes are characterized by morphological heterogeneity and occupy distinct non-overlapping territories.	8
Figure 4. Structural composition of gap junction channels	11
Figure 5. Spatial K⁺ buffering in astroglial networks.....	12
Figure 6. Reactive hippocampal astrocytes.....	13
Figure 7. Morphological and molecular alterations of microglia in response to seizure activity	19
Figure 8. Structural components and epilepsy-associated alterations of the BBB.....	21
Figure 9. Reactive microglia-derived TNFα impairs astrocyte GJ coupling and K⁺ homeostasis, exacerbating the pathology of epilepsy	93